Craniofacial growth and development

in modern humans and Neanderthals

Candidate: Federica Landi

Supervisor: Prof. Paul O'Higgins

Submission for the degree of PhD in Human Sciences

Hull York Medical School

Submission date 31/07/2020

A mamma, papa', Lorenzo, Sofia e Rinaldo

Ad Alessio

Ad Antonio

Abstract

This thesis assesses craniofacial growth, development and the dynamics of developmental interactions among cranial regions in modern humans and Neanderthals. To these ends, virtual segmentation, landmarking and Geometric Morphometrics (GM) are applied to an ontogenetic series of the whole crania of 68 *H. sapiens* and 12 *H. neanderthalensis*. First, the ontogenetic shape and form changes in the cranial vault, base and face are explored, and the locations and magnitudes of these changes are discussed. Secondly, allometric scaling is tested for differences among different age classes in the three regions of the cranium. In addition, the degree of covariation among these and how it changes over time is investigated.

The study then focuses on interactions among facial regions. First, similar analyses as those used in the study of the cranium are applied to compare growth, development and covariation among parts of the face in different age classes. Additionally, a sample of 227 modern humans from 0 to 6 years of age is analysed using path analysis, to investigate the cascade of interactions and relative contributions of soft tissue and skeletal elements to the overall growth and development of the face. Last, the facial morphology of *H. sapiens* is compared to that of *H. neanderthalensis* and their ontogenetic trajectories are tested for divergence. Novel method registration-free colour maps are used to visualise regional changes during growth and development and to compare the morphologies of the two species. Covariation among facial elements is also compared to assess potential differences in developmental interactions. In modern humans, the results show that allometry and covariation change significantly among age classes and between cranial regions during ontogeny and that covariation is stronger in younger subadults than in older subadults and adults. Among modern humans, significantly divergent trajectories are observed between age classes during ontogeny in all three cranial regions. In the modern human face, allometric scaling also differs among age stages in each region. Interestingly, covariation among facial regions becomes progressively non-significant with time, with the exception of those including the nose and maxilla. Path analysis in modern humans shows a large contribution of the proxy used for nasal septum to the overall facial development. Soft tissues contribute only locally to the development of some skeletal elements of the face. Major aspects of the differences between adult

modern humans and Neanderthals are already present in the youngest individuals. However, additional differences arise through differences in the degree of change in facial size and significantly divergent allometric trajectories. Analyses of covariation among Neanderthal facial regions suffer from small sample size but, where significant, suggest that the interactions among cranial components are similar to those in modern humans, with some differences.

List of contents

Abstract 3

List of contents 5

Acknowledgements 8

Author's declaration 9

1.0 Introduction 9

1.0.1 The study of the face from an ontogenetic perspective 12

1.0.2 Skeletal anatomy of the skull 13

1.0.3 Cranial vault anatomy, function and development 13

1.0.4 Cranial base anatomy, function and development 17

1.1 Facial anatomy, ontogeny and evolution 20

1.1.1 Prenatal and postnatal development of the facial complex 24

1.1.2 Hypotheses concerning the ontogeny of the face in *H. sapiens* and *H. neanderthalensis* 28

1.1.3 Modularity and integration of the facial complex 30

1.1.4 Embryological development of the nasal septum 36

1.1.5 Postnatal growth, development and integration of the nasal septum 39

1.1.6 Maxillary sinuses in facial ontogeny 45

1.1.6.1 Form and function of paranasal sinuses 45

1.1.6.2 Prenatal and postnatal development of maxillary sinuses 46

1.1.6.3 Maxillary sinuses: evolutionary history and variation 51

1.1.7 Evolutionary hypotheses on facial differences between *H. sapiens* and *H. Neanderthalensis* 54

1.1.8 Objectives and hypotheses 57

2.0 Materials and methods 60

2.1 The modern human sample 60

2.2 The Neanderthal sample 61

2.3 Semi-automatic and automatic segmentation of 3D surfaces 62

2.4 Geometric Morphometrics 65
2.4.1 Quantification of morphology and analyses of variation 65
2.4.2 Generalised Procrustes Analysis 67
2.4.3 Landmark and semilandmark configuration used in the study 68
2.4.4 Intraobserver error and missing data 75
2.4.5 Sliding semilandmarks 77
2.4.6 Thin plate splines, transformation grids and warping 79
2.5 Multivariate statistical methods 82
2.5.1 Principal Component Analysis 82
2.5.2 Multivariate regression 83
2.5.3 Partial Least Squares analysis 83
2.6 Path analysis 85
3.0 Research and results 88
3.1 Covariation and correlation in the human cranium: a 3D morphometric study of the interactions between cranial base, cranial vault and facial complex during ontogeny 88
3.1.1 The importance of cranial element interactions 88
3.1.2 Modules and regions of the cranium 88
3.1.3 Hypotheses on craniofacial growth and development 90
3.1.4 The hypotheses 94
3.1.5 Material and methods 95
3.1.5.1 The sample 95
3.1.5.2 The dataset 95
3.1.5.3 Statistical analyses 96
3.1.6 Results 98
3.1.7 Discussion 115
3.1.7.1 Summary of the key findings 115
3.1.7.2 The cranium and its regions: the cranial vault, base and face 117
3.1.7.2.1 Cranial ontogeny and allometric trends 117
3.1.7.2.2. Cranial vault, base and face ontogeny and allometric trends 119

3.1.7.2.3 Partial least squares analysis: the cranial vault, base and facial blocks 121
3.1.8 Conclusions 123
3.2 Growth, development and covariation of the facial elements in modern humans 124
3.2.1 Ontogenetic interactions between facial elements 124
3.2.2 The hypotheses 124
3.2.3 Materials and methods 129
3.2.3.1 The sample 129
3.2.3.2 The dataset 129
3.2.3.3 Statistical analyses 131
3.2.4 Results 132
3.2.5 Discussion 143
3.2.6 Conclusions 148
3.3 Path Analyses applied to growth models: contribution of skeletal and soft-tissue matrices to facial ontogeny 151
3.3.1 Background 151
3.3.2 Path analysis in literature 152
3.3.3 The hypotheses 154
3.3.4 Material and methods 160
3.3.4.1 The explanation of the paths 160
3.3.4.2 The sample 161
3.3.4.3 Skeletal measurements 162
3.3.4.4 Soft tissue measurements 163
3.3.4.5 Statistical analyses 171
3.3.5 Results 172
3.3.5.1 Skeletal measurements 172
3.3.5.2 Soft and skeletal measurements 179
3.3.6 Discussion and Conclusions 182
3.4 The facial ontogeny of *H. neanderthalensis* and *H. sapiens* 187
3.4.1 Ontogenetic trajectories in Neanderthals and modern humans 187

3.4.2 Covariation patterns in Neanderthal and modern humans 189

3.4.3 The hypotheses 190

3.4.4 Material and methods 191

3.4.4.1 The sample 191

3.4.4.2 The dataset 191

3.4.4.3 Statistical analyses 194

3.4.5 Results 197

3.4.6 Discussion and conclusions 209

4.0 General discussion and conclusions 213

4.1 Synthesis of key findings 213

4.2 Limitations of the present study and implications for future research 218

5.0 Supplementary Material 220

6.0 Bibliography 230

Acknowledgements

Thanks to Prof O'Higgins for being my mentor. Thanks to Dr Fitton, Dr Cox and Dr Cobb for their feedback and suggestions on this body of work and to the whole HYMS team for being welcoming and friendly. Thanks to Dr Barraclough for collecting the data on soft tissues for Chapter 3.3. Thanks to Dr Evteev for allowing access to a large body of CT-scans of newborns and infants. Thanks to Prof. Manzi for his precious feedback on the project and for allowing access to the CT-scans of Neanderthal fossil specimens. Thanks to Dr Gunz, Prof Maureille, Prof Hublin for allowing the study of the fossil material. Thanks to Dr Profico, Dr Buzi and Dr Veneziano for their constant feedback and suggestions on the R coding. Thanks to my colleague Emily Hunter for her emotional support.

Author's declaration

I confirm that this work is original and that if any passage(s) or diagram(s) have been copied from academic papers, books, internet or any other sources these are clearly identified by the use of quotation marks and the reference(s) is fully cited. I certify that, other than where indicated, this is my own work and does not breach the regulations of HYMS, the University of Hull or the University of York regarding plagiarism or academic conduct in examinations. I have read the HYMS Code of Practice on Academic Misconduct, and state that this piece of work is my own and does not contain any unacknowledged work from any other sources.

1.0 Introduction

The facial complex hosts important sensory organs and structures of great functional relevance such as our visual, respiratory and masticatory systems. Together, all its components form a developmental unit that is morphologically connected to and influenced by the shape and orientation of adjacent cranial elements, namely the cranial base and cranial vault.

Evolutionary changes in the face occurred constantly in the hominin lineage, driven by biomechanical, environmental or structural needs. Therefore, the developmental investigation of the morphology of the face must take into account its ontogeny, its relationship within the skull, together with its changes during the evolution of the hominin lineage. In this framework, the main questions to be answered are: is facial reduction in *Homo sapiens* a structural consequence of changes in other cranial regions? Or is it an independent change driven by environmental or biomechanical pressures acting (or acting less) on the face itself? Which are the evolutionary pressures and developmental constraints and interactions that drive the so-called "facial reduction" in *H. sapiens* compared to the heavily built facial complex of *Homo neanderthalensis*?

This project aims to describe the growth and developmental changes that underlie differences in the face throughout the evolution of late Pleistocene *Homo* and modern humans. The ultimate goal of this project is to determine how the different midfacial regions evolved and developed and how they interact with each other and with more distant regions during growth and development in both *H. sapiens* and *H. neanderthalensis*.

The first chapter presents a critical approach to the literature review of the anatomy, evolution, function and variation of the cranium and the face with the aim of developing testable hypotheses concerning facial morphogenesis in Neanderthals and modern humans. The anatomy of the cranium is described, with a focus on each of its regions and their reciprocal anatomical relationships. The review summarises the literature about the interactions among skull regions during ontogeny in Neanderthals and modern humans. In relation to growth and development, the Functional Matrix and the Nasal Septum theories are described, and their strengths and weaknesses examined. State-of-the-art studies of integration and modularity between the face and the cranium are discussed. Furthermore, previous studies of sinus anatomy, function and variability are reviewed with the aim of elucidating their ontogeny in relation to that of the face. Finally, various

hypotheses raised to explain the differences in the facial complex among *H. sapiens* and *H. neanderthalensis* are reviewed and discussed.

In the second chapter, the materials and methods adopted in the work are presented. Virtual acquisition and segmentation of the materials are discussed. Geometric morphometric (GM) methodological tools used in this thesis are described. The preparation of data is discussed, such as landmarking and estimation of missing landmarks. The latter is performed by comparing and testing different statistical approaches. Subsequently, the GM method of semilandmark sliding is thoroughly described and tested for replicability among different software tools. The statistical analyses performed in the thesis are then described and discussed, with a focus on Generalised Procrustes Analysis (GPA), Principal Component Analysis (PCA), partial least squares (PLS) and path analysis.

The third chapter presents the results of this work divided into sections.

Section 3.1 analyses patterns of growth and development of the skull in modern humans. Modern human skull variance and morphological changes during ontogeny are described in terms of direction and magnitude. Shape and size changes over time are described for the cranial base, vault and face; differences in timing and mode of development as well as developmental integration among cranial regions during ontogeny are investigated.

Section 3.2 explores facial patterns of covariation and allometric development during ontogeny in modern humans, analysing the regions of the orbit, zygomatico-maxilla, palate, nasal cavity and maxillary sinuses. The influence of size on shape and the integration among facial regions is compared in younger subadults, older subadults and adults.

Section 3.3 explores the hierarchical interactions among facial elements in infants from 0 to 6 years old and analyses the relative contribution of the soft and hard tissue components to the overall facial growth and development during early ontogeny.

In section 3.4, the facial ontogenetic development is compared between Neanderthals and modern humans. Neanderthal ontogenetic facial shape variations are explored and compared with what is observed in modern humans. Divergence of ontogenetic facial trajectories between *H. sapiens* and *H. neanderthalensis* is tested. Covariation among facial regions is compared between the two species.

Chapter four concludes the thesis by summarising the major findings and discussing them in light of the literature about facial morphology and ontogeny in modern humans and Neanderthals. Future work and the points yet to be clarified are discussed.

1.0.1 The study of the face from an ontogenetic perspective

The facial region shows considerable variation among living and extinct hominins. Such variation is determined by genetics and natural selection, constrained by phylogeny and influenced by non-genetic stimuli throughout life (Martinez-Abadias et al., 2009). All these factors manifest themselves through differences or similarities in patterns of growth and development between species during ontogeny. It has been shown how changes in these patterns between species, although defined prenatally, are often emphasised during the postnatal period, and that even within a species, differences in the timing and mode of development of different cranial parts among populations lead to diverse adult morphologies (Viðarsdóttir et al., 2002; Cobb and O'Higgins, 2004). Therefore, by looking at craniofacial patterns of growth and development in terms of hierarchies, degrees of interaction and variability, it is possible to investigate if and how these patterns are preserved or changed among phylogenetically closely related species. Furthermore, by studying facial ontogeny we come to understand the processes and mechanisms that underlie inter-adult diversity.

The use of geometric morphometric techniques to investigate hominin facial morphology has a long history (Bookstein, 1998; O'Higgins, 2000; Bastir et al., 2007; Ponce de Leon and Zollikofer, 2001; Viðarsdóttir et al., 2002; Mitteroecker and Gunz, 2009; Evteev et al., 2014). These methods, applied to the study of cranial morphology, led to the formulation of evolutionary hypotheses about morphological variations between species through functional adaptations to factors such as climate, diet or social requirements (Wang et al., 2010; Noback et al., 2011; Evteev et al., 2014; Marquez et al., 2014; De Azevedo et al., 2017; Godinho et al., 2018; Wroe et al., 2018), as well as providing non-adaptive explanations, such as the diversification of morphology by genetic drift (Weaver et al.,2007; Ackermann and Cheverud, 2004; Buck et al., 2018). However, due to the lack of

data, most studies have focused on the external morphology of adult specimens. Although several recent studies examined the relationships between internal (such as the nasal passages, paranasal sinuses and orbits) and external cranial regions (Holton et al., 2018; Godinho and O'Higgins, 2018), little is known about how these covary during ontogeny in hominins and how they contribute to differences in growth and development between species.

1.0.2 Skeletal anatomy of the skull

Understanding the patterns of cranial bone formation, accretion, interaction and remodelling is essential to formulate hypotheses concerning the mechanisms by which growth and development of the hominin skull are regulated. Such hypotheses are formulated and tested in this thesis in Sections 3.1 to 3.4. Therefore, in Chapter 1, the developmental anatomy of the human skull and what is known about developmental interactions and their role in integrating development is reviewed.

The skull incorporates diverse structures that serve different functions; *e.g.* supporting and housing the brain and sense organs, feeding and breathing (O'Higgins and Cohn, 2000; O'Higgins et al., 2006).

The human skull can be divided into three cranial regions: the cranial vault, formed from intramembranous bone of paraxial mesodermal and neural crest origin; the basicranium, formed from endochondral bone of neural crest origin; and the viscerocranium, formed from intramembranous bone of neural crest origin. During growth and development, these anatomical regions meet and form the skull, a single morphogenetic unit and a highly functionally integrated structure (Bruner, 2007).

1.0.3 Cranial vault anatomy, function and development

The cranial vault is a domed bony structure that forms a protective case around the brain and is made up of the frontal bone, the greater wings of the sphenoid, the two parietals, the two temporals and the occipital bone. The vault is anteriorly articulated with the face through the frontal bone and the frontal torus (Bruner, 2007). Laterally, the greater wings of the sphenoid and the temporal plate form the lateral wall of the vault, while the zygomatic process of the temporal bone connects the lateral wall to the anterior zygomatic bone. The squamous part of the occipital bone constitutes the posterior part of the cranial vault, while the rest of the occipital forms part of the cranial base.

The main function of the cranial vault is to support the brain during its growth and development. Changes in brain size during growth affect skull morphology. Notably, the ossification of the intramembranous calvarial bones depends on the presence of the brain during foetal development; in its absence (anencephaly), no bony calvarium forms (Sperber et al., 2010). The subordinate and supportive role of the cranial vault is also evident when looking at changes in brain size during evolution and development, always followed by coordinated changes in neurocranial size and shape (Lieberman, 2011; Richtsmeier et al., 2006; Weickenmeier et al., 2017).

The bones of the cranial vault form by intramembranous ossification of the mesenchymal tissue surrounding the developing brain during the foetal period, with centres of ossification first appearing at approximately the $7^{th} – 8^{th}$ weeks in utero (Jin et al., 2016).

It is worth remembering that in intramembranous ossification, mesenchymal cells differentiate into osteoblasts, forming a centre of ossification. This contrasts with endochondral ossification, in which mesenchymal cells differentiate into chondroblasts, forming a cartilaginous matrix of glycoproteins, creating a cartilage model of the future bone. Once it has mineralized, the osteoid matrix forms a collar of periosteal bone surrounding the cartilage. Invasion and replacement of the cartilage model by bone completes the process (Karaplis, 2008).

At birth, the infant cranium has a large and bulbous calvarium and a relatively small face, which constitutes one-eighth of the neonatal cranial volume. By adulthood, the facial skeleton accounts for approximately half of the overall cranium (Enlow, 1990), due to the different growth patterns of the skull regions (Figure 1.1, Bastir et al., 2006).

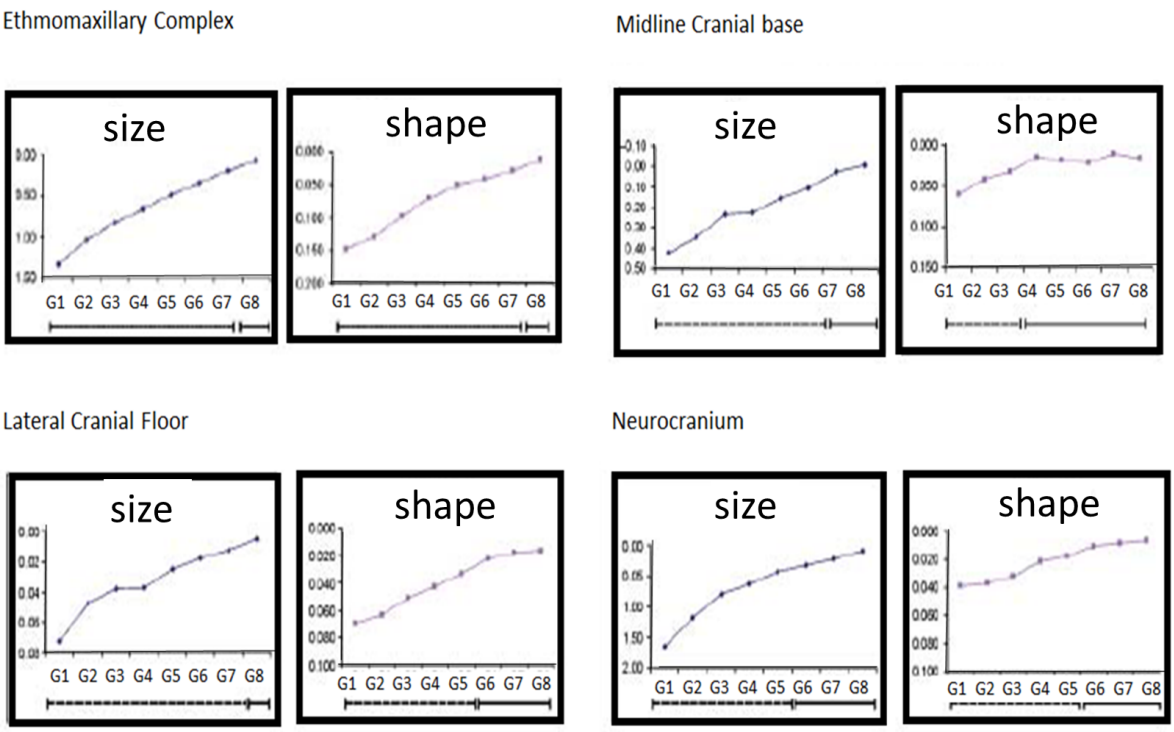

Figure 1.1. Spatiotemporal patterns of maturation of cranial elements (Bastir et al., 2006). Age categories are: G1 2–3 years, G2 4–5 years, G3 6–7 years, G4 8–9 years, G5 10–11 years, G6 12–13 years, G7 16–17 years, G8 18 and more.

Indeed, the facial skeleton undergoes rapid growth during infancy and childhood while growth of the calvarium slows considerably after the fourth year (Enlow and Moyers, 1982).

Cranial vault sutures, which are periosteum-lined fibrous joints, separate the individual bones and provide sites of growth. The major sutures of the cranial vault include the following: metopic suture (where the two frontal bony plates meet), coronal suture (where each frontal bone plate meets with a parietal bone plate), the sagittal suture (where the two parietal bone plates meet) and the lambdoid suture (where both parietal bones meet the occipital bone).

In a newborn skull, fontanelles are found where sutures will merge (Figure 1.2). These temporary discontinuities between the bones of the calvarium aid the passage of the head through the birth canal at childbirth and, with sutures, permit an increase in the size of the neurocranium to match brain growth after birth. All the fontanelles are closed by

the age of 18 months. Nonetheless, the proper fusion of the sutures occurs much later: the metopic suture is usually obliterated by 7 years of age (although in 15% of the individuals remains unfused), while the sagittal, coronal, and lambdoidal suture fusion happens much later in life within a wide age range (Sahni, and Jit, 2005).

Sutures were once (Sicher and DuBrul, 1949), but are no longer (Koski, 1968; Opperman, 2000), thought to be primary drivers of growth (growth centres with intrinsic growth potential); the current interpretation is that they act as growth sites (Opperman, 2000), meaning that bone formation happens at the edge of the bone front but it is stimulated by forces external to the suture itself. However, there is debate about what elements drive and regulate growth at the sutures (Moss and Young, 1960; Scott, 1956; Precious and Delaire, 1987; Mooney et al., 1989; Mays, 2012; Hall and Precious, 2013; Goergen et al., 2017). Indeed, although it is generally thought that bone growth at the cranial and facial sutures occurs when the ossifying fronts are gradually forced apart, the potential roles of elements such as the brain, dura mater, nasal cartilage, orbits and oral capsule as principal driving forces are, as yet, not fully understood (Opperman et al., 2005, see discussion on the potential facial pacemakers of the nasal cartilage, orbits and oral capsule in Section 1.1.5).

A study has examined intramembranous bone growth at cranial vault sutures by artificially creating a mechanical force and applying it to the head of anaesthetised rabbits using strain gauges (Kopher and Mao, 2003). The study observed that micro-compression and micro-tension both produce sutural growth, thus challenging the precept that compression would lead to resorption activity at suture sites, while tension would lead to formation, and suggesting that the effect of mechanical loads, cartilage and organ growth on cranial sutures is still poorly understood. Another study (Opperman et al., 2005) suggests that after the sutures fuse, further growth and development depend on surface deposition and resorption (remodelling), so braincase growth would shift from the sutures to the bone surfaces.

Indeed, while evidence shows that brain growth stimulates the development of the braincase during prenatal and early postnatal phases (Richtsmeier and Flaherty, 2013), other elements and factors not yet clarified act on the remodelling of the cranial vault during ontogeny.

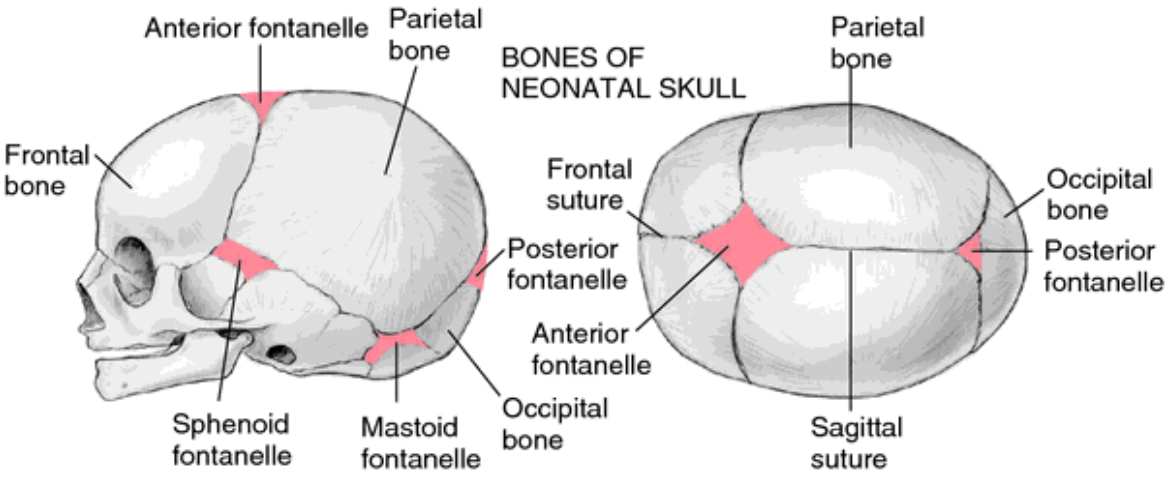

Figure 1.2. Newly born skull anatomy with fontanelle evidenced (Sperber et al., 2010).

1.0.4 Cranial base anatomy, function and development

The basicranium or cranial base supports the brain and, with the calvarium, completes the neurocranium (Figure 1.3). It is made up of five bones: the ethmoid, sphenoid, occipital, frontal and temporal. Postnatally, the cranial base is the first element of the skull to reach maturity in shape and size (Bastir et al., 2006), thus setting the spatial conditions for the other cranial regions to grow, develop and integrate (Enlow and Hans, 1996; Lieberman et al., 2000; Kuroe et al., 2004). Structurally, the cranial base supports the growth of the brain, the articulation of the mandible and shares important bony elements with the facial complex. In addition, the opening of the foramen magnum and other foramina along the cranial base allow the cranium to be connected to the vertebral column and permit the passage of neural and circulatory connections between the brain, the face and the post-cranium (Nie, 2005).

The cranial base region can be divided morphologically and functionally into anterior middle and posterior cranial fossae, separated by bony ridges. This division into separate fossae has been used by researchers to investigate the behaviour of the cranial base

during ontogeny and its relationship with the cranial vault and facial regions during hominin evolution (Rhoton, 2002; Bastir and Rosas, 2005; Bastir et al., 2008; Gkantidis and Halazonetis, 2011; Bastir and Rosas, 2016). Indeed, numerous studies suggest that the elements of the cranial base that contribute to the anterior and middle cranial fossae are highly developmentally integrated with the face (Lieberman et al., 2000; Bastir, and Rosas, 2006; Neaux et al., 2013). In fact, the anterior cranial fossa forms the roof of the orbits and contains the cribriform plate of the ethmoid bone, while the middle fossa lies directly behind the orbits and the midface. Thus, spatial modifications of these components likely have consequences for the spatial arrangement of some facial components (Enlow, 1966, 1990; Bastir and Rosas, 2005; Bastir et al., 2008; Bastir and Rosas, 2016). Furthermore, the cranial base is linked functionally to the cranial vault because of their shared role in sustaining the brain. The anterior cranial fossa accommodates the frontal lobes of the brain, while the middle fossa hosts the temporal lobes and the posterior cranial fossa supports the occipital lobes. A further connection between base and vault is formed by the occipital bone, which contributes to the posterior cranial fossa and the posterior part of the vault (Bruner et al., 2015).

Prenatally, the base of the skull appears at the second month of embryonic life as a narrow cartilaginous platform (endochondral ossification) ventrally disposed over the cerebral mass (but the conversion of the ectomeninx mesenchyme into cartilage has already begun by the 6th week). At this stage, the anterior portion consists of an aggregation of cells from the ectodermic neural crest while the posterior portion is made of cartilaginous mesodermal cells. The spheno-occipital synchondrosis (the cartilaginous joint between the two bones) underlines this subdivision, separating two areas that are embryologically distinct (Jeffery and Spoor, 2004).

During the 2nd and 3rd postnatal year, the occipital squama joins the exoccipital region (external surface around the *foramen magnum*) at the posterior intraoccipital synchondrosis. The exoccipital region joins the basioccipital area at the anterior intraoccipital synchrondroses, which are found within the condyles.Around the year of 5, these synchondroses will no longer be present. Postnatally, the endocranial surfaces of the occipital bone are predominantly resorptive, and the ectocranial surfaces are depository, resulting in relative downward displacement of the floor of the posterior cranial fossa to accommodate the enlarging brain (Arat et al., 2010).

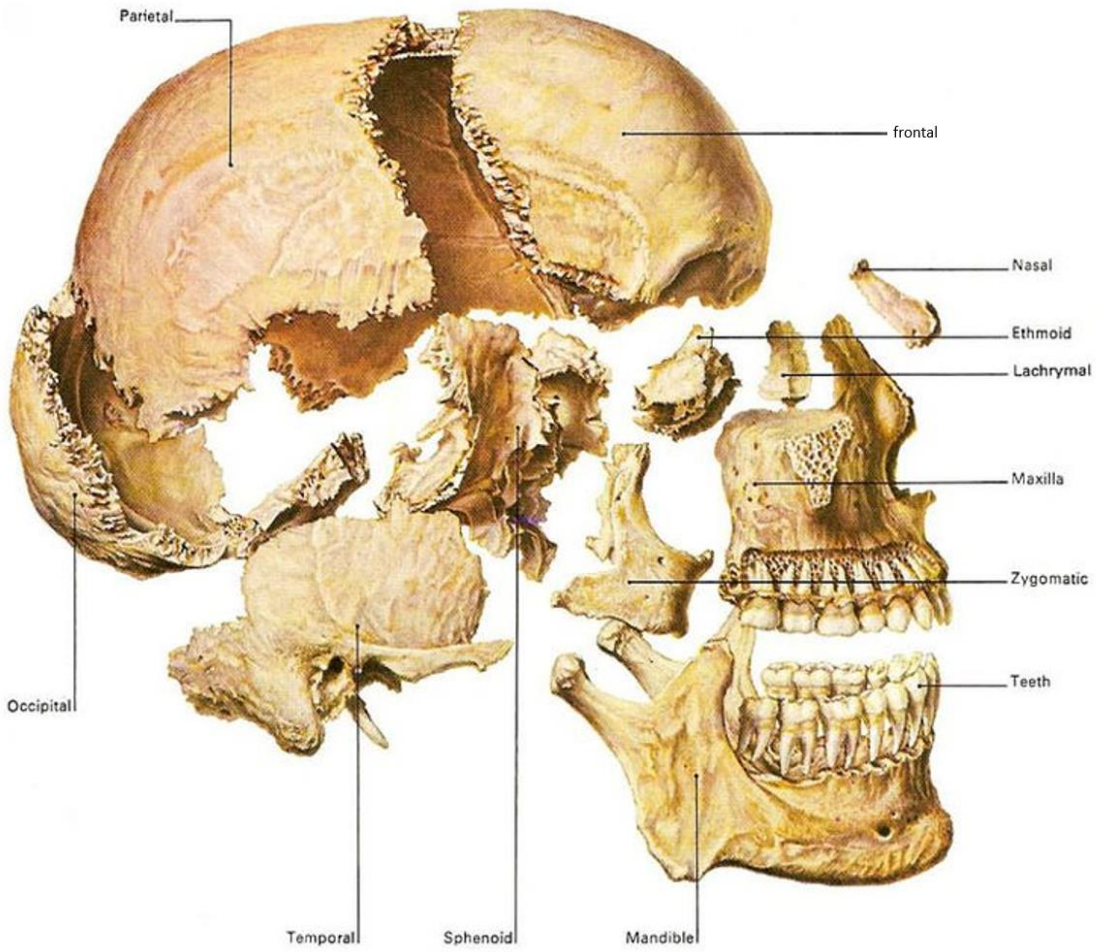

Figure 1.3. Disarticulated skull bones (medicienterprises.com).

1.1 Facial anatomy, ontogeny and evolution

The third cranial region of the skull is the viscerocranium, or facial complex. Embryonically, the facial skeleton is composed of dermal bone (arising from intramembranous ossification) and derives from ectodermal cells of the neural crest (responsible for the development of the neurocranium, teeth and a number of other skeletal components) (Wilson, 1979).

The viscerocranium consists of 16 individual bones that fuse together during development (Table 1.1 and Figure 1.4). Anatomically, the viscerocranium can be divided into the upper, middle and lower face, which correspond with the frontonasal, maxillary and mandibular primordia in the embryo. The upper face is the region comprising the orbital torus and the eye sockets. While the orbits have an initial rapid postnatal growth and development during early childhood and reach most of their final form around 6-7 years of age (Scott, 1954), the brow ridge is almost absent at birth and develops over a longer period of time, reaching its final form during adolescence and early adult life (Behrents, 1975). The lower face comprises the mandible and teeth. The middle face, or midface, denotes the portion of the face comprising the nasal, lacrimal, maxillary, zygomatic bones and upper dentition (Brooker, 2009). The maxilla is the largest element of the midface and comprises two maxillary bones, which join at the intermaxillary suture, forming the anterior nasal spine (Rice, 2008). The surface of the maxillary bones forms most of the nasal aperture, the top of the oral cavity (hard palate), the orbital floors, and the inferior orbital rims. Each maxilla possesses two processes or extensions—the frontal process is connected to the frontal bone and the zygomatic process articulates with the zygomatic bone. The maxillae also host, internally, the bony cavities called maxillary sinuses (Burns, 2013). The maxillary sinuses are hollows lined with mucoperiosteum, connected to the nasal cavity through the presence of a passage called ostium. Their biological and functional significance is hotly debated (Rae and Koppe, 2004). Their anatomy is described in Section 1.1.6 of this chapter. The zygomatic bones are paired and constitute the lateral portions of the orbits and the cheekbones. The maxillary, frontal, and temporal processes branch out from each zygomatic bone. This bone develops from a single centre of ossification and acquires a recognisable morphology by 4 to 5 foetal months (Kelley et al., 2007). The nasal bones are two small elongated bones located

between the orbits and articulated with the maxillae. They form, at their junction, "the bridge" of the nose and the superior rim of the piriform aperture. Each nasal bone grows from a single membranous ossification centre and is present and recognizable by the time of birth (Thiagarajan and Ulaganathan, 2013). Studies focussing on the study of the morphology of nasal bones in foetuses have analysed variation in the foetal nasal bones in different populations and found that differences are already present prenatally (Collado et al., 2004; Zelop et al., 2005). The lacrimal bones are the smallest of the facial bones. Their shape is rectangular and characterized by the nasolacrimal canal. The lacrimal bones are connected to two cranial bones: the frontal (superiorly) and ethmoid (posteriorly), and two elements of the facial complex, the maxilla (anteriorly and inferiorly) and the inferior nasal concha (inferiorly). The lacrimal ossifies from a single membranous ossification centre, which appears about the twelfth week in the membrane covering the cartilaginous nasal capsule. They acquire a recognisable morphology by 2 to 3 years of age (Berger and Kahn, 2012).

Bone	Paired/unpaired	Region
Conchae	Paired	Facial
Lacrimal	Paired	Facial (midface)
Mandible	Unpaired	Facial
Maxillary	Paired	Facial (midface)
Nasal	Paired	Facial (midface)
Palatine	Paired	Facial
Vomer	Unpaired	Facial
Zygomatic	Paired	Facial (midface)
Frontal	Unpaired	Facial
Sphenoid	Unpaired	Facial

Table 1.1. List of the facial bones, (modified from Gray, 2001).

The facial skeleton articulates with the basicranium through the sphenoid and is in contact with the calvarium through the frontal process of the maxilla and the temporal and frontal processes of the zygomatic. Because of these connections, the ontogenetic and evolutionary development of the face is integrated with the development of the cranial vault and basicranium (Anton, 1989; Cheverud et al., 1992; Kohn et al., 1993; Lieberman, 2000; Kuroe et al., 2004; Hallgrimsson et al., 2007; Ferros et al., 2015). The developmental interactions among these three regions are of interest in understanding how the cranium evolved. Recent ontogenetic studies suggest that the face is the last of the three to reach maturity in size and shape (Bastir et al., 2006). As such, its development is thought to be strongly subjected to the mechanical constraints imposed by the earlier maturing cranial vault and base (Cheverud et al., 1992; Hallgrimsson et al., 2007; Mitteroecker and Bookstein, 2008; Martínez-Abadías et al., 2009). A recent approach suggests that as encephalisation developed during hominin evolution, changes in the cranial base and neurocranium (Bruner, 2007; Bastir et al., 2008) have driven a general reduction in the viscerocranial complex (Holton et al., 2011; Freidline et al., 2012; Lacruz et al., 2019). However, Neanderthals and *H. sapiens*, which are the most encephalised among hominins, apparently evolved in two opposite directions, the former possessing a prognathic midface and the latter a short and flat one.

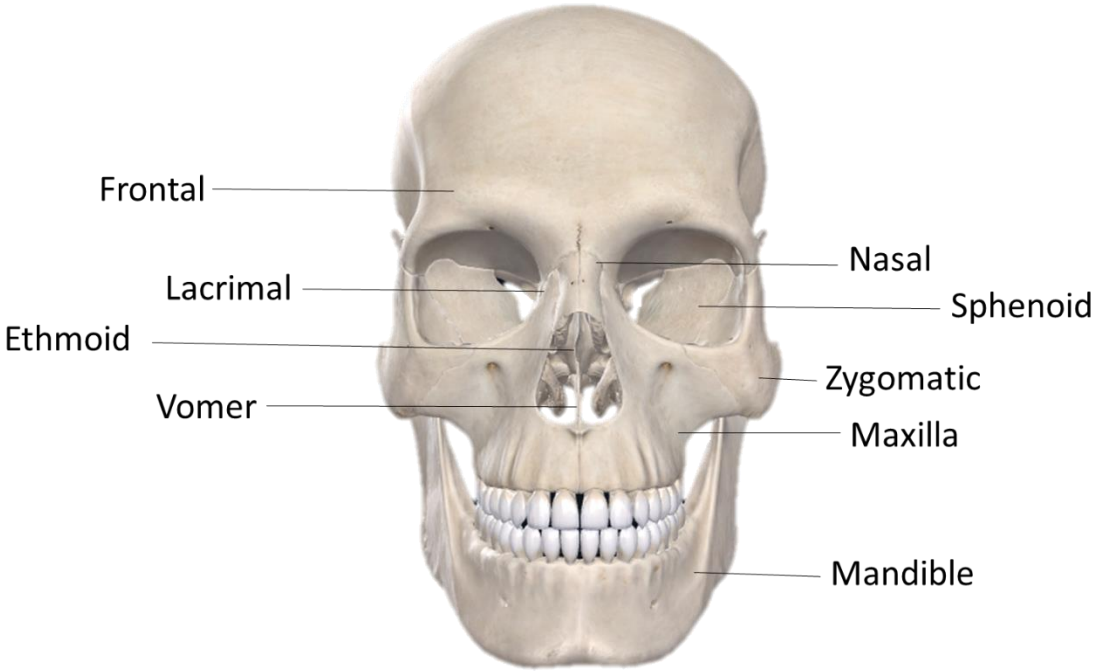

Figure 1.4. Bones of the facial complex (Image created by the author using Complete Anatomy.com (palatine bones not visible).

This is probably due to differences in the development and organisation of the brain (and thus differences in the nature and sequence of shape modifications in the neurocranial and basicranial regions during development) together with morphological changes in facial elements, which are due to functional adaptations as well as structural reorganisation (Lieberman, 2008). Indeed, the evolutionary hypotheses proposed in relation to the development of the facial complex in the genus *Homo* are heterogeneous, encompassing cranial architectural constraints, feeding mechanics, environmental change and genetic drift (Weaver et al., 2007). These hypotheses, together with an overview of the major morphological differences among *Homo sapiens* and *Homo neanderthalensis* will be examined in Sections 1.1.2 and 1.1.7 of this chapter.

1.1.1 Prenatal and postnatal development of the facial complex

The prenatal growth and development of the human body can be divided into three phases: the preimplantation phase (the first 7 days), the embryonic phase (the next 7 weeks), and the foetal phase (the next 7 calendar months).

In the embryonic phase, the basic tissue types have developed during the first 21 days post-conception (pre-somitic period). This is followed by the somitic period (21 to 31 days), characterized by differentiation of the basic tissues that convert the flat embryonic disk into a tubular body. This phase is characterized by the appearance of metameric segments (called somites) which form the basic patterning of the main body systems and organs. At the end of the somitic period, the embryo shows a prominent brain forming a predominant portion of the early head, whose "face" and "neck," are formed by pharyngeal arches. The eyes, nose, and ears are demarcated by placodes (Musumeci et al., 2015). The somitic period is followed by the postsomitic period, characterized by the formation of the body's external features. The head undergoes significant development and facial morphology becomes identifiable. During the last 7 months of foetal life (foetal phase- from the 60th day) the main changes concern growth and reproportioning of body elements. Ossification centres make their appearance in most bones during this period (Figure 1.7, Harding and Bocking, 2001).

At 5 months *in utero*, the face assumes a recognisably human appearance as the eyes move anteriorly and the ears rise to eye level (Radlanski and Renz, 2006) but the key stages in the embryonic formation of the human facial region can be already recognised between four and eight weeks post-conception. At five weeks, beneath a prominent forebrain, the oral pit, or stomodeum, becomes evident and this will form the mouth. Around it, are five prominences, or facial primordia, derived from the migration of neural crest cells: the central frontonasal, and the left and right maxillary and mandibular prominences, the latter two derived from the first pair of six pharyngeal arches (Sperber et al., 2010).

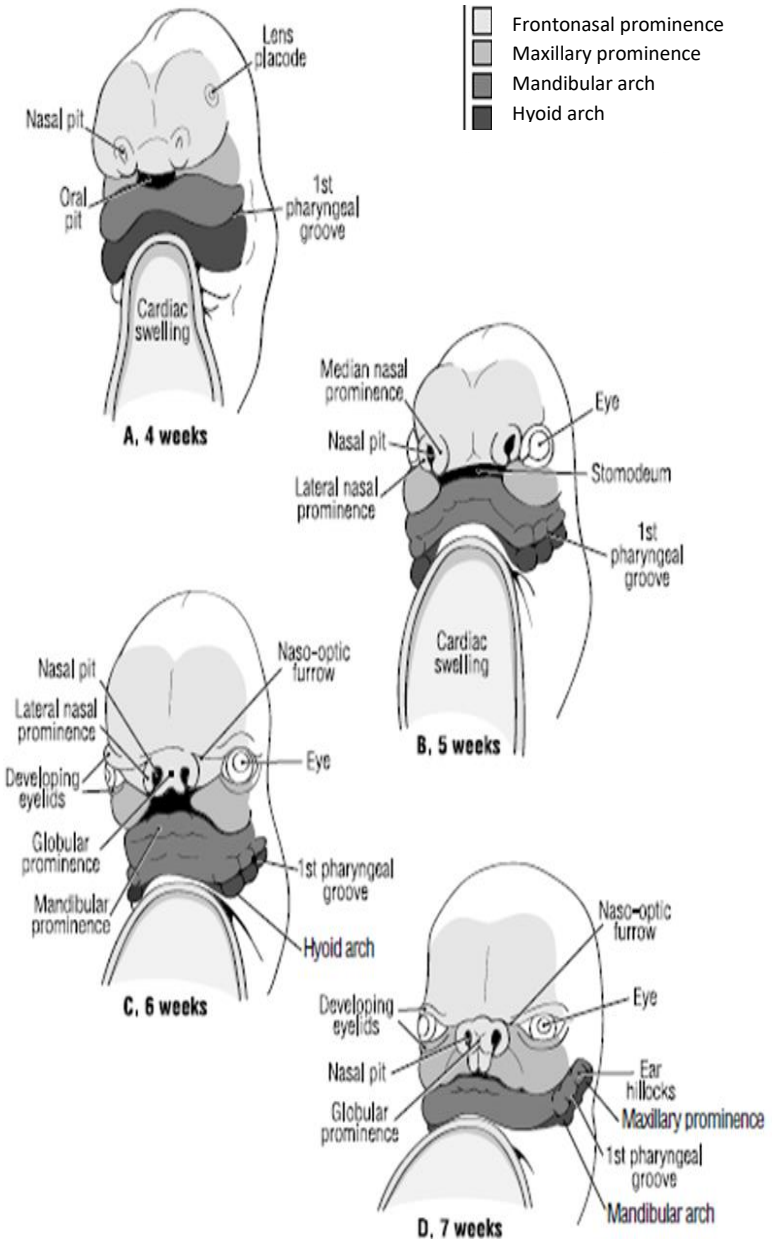

Figure 1.5. Schematic representation of facial formation at 4, 5, 6, and 7 weeks post-conception (Sperber et al., 2010).

Lateral to the forebrain are the optic diverticula, which, as already mentioned, will complete their anterior migration between the 5th and 9th prenatal week. Inferolaterally, each nasal pit is surrounded by medial and lateral nasal prominences and is initially connected to the stomodeum (Figure 1.5 and 1.6).

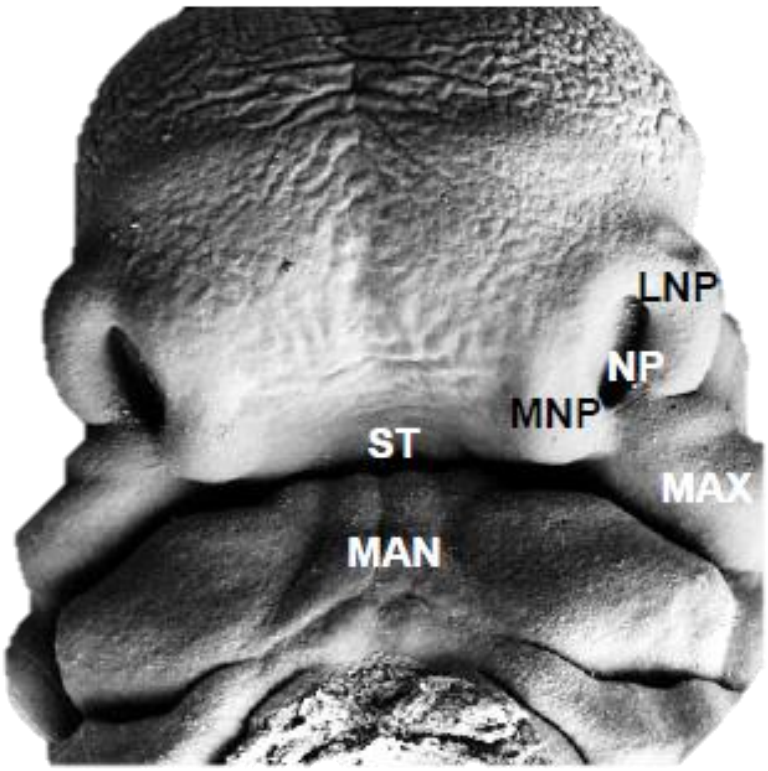

Figure 1.6. Face of a 37-day-old human embryo: nasal pits (NP); medial (MNP) and lateral (LNP) nasal prominences; the maxillary (MAX) prominences; stomodeum (ST); mandibular prominence (MAN) (Sperber et al., 2010).

Union of the facial prominences occurs by fusion of the frontonasal, maxillary, and mandibular prominences and by merging, i.e the elimination of the contacting tissue between the central maxillonasal components (called the nasal fin) (Wilderman et al., 2018). The merging creates the upper jaw and forms the palate, which separates the nasal pits from the future mouth. Each merging and fusion site is also the site of a potential facial or palatal cleft (Smith et al., 2004).

Meanwhile, the formation of the nose is finalised with a complex process involving contributions from the frontal prominence, the merged medial nasal prominences, the lateral nasal prominences (the alae), and the cartilage nasal capsule (Sperber et al., 2010). The cartilaginous nasal capsule will form the nasal septum and nasal conchae. It grows between the cranial base above and the “premaxilla,” vomer, and palatal processes of

the maxilla below. An incorrect or partial fusion of the nasal capsule during this period produces a deviation in the development of the nose and upper lip (Hall et al., 2013). In addition, incorrect growth and development of the nasal septum during this period has been recently claimed to impact on cranial base and maxillary normal growth and development (Howe et al., 2004).

During the postnatal period, the upper face is mostly influenced by the rapid growth of the eyes in the first 18 months of postnatal life (Krimmel et al., 2015), which contribute to the vertical expansion of the face and the separation of the neural and viscerocranial regions. The nasal cartilages, especially the septum, are at the centre of a debate about the forces acting to shape facial morphology during the postnatal period (Moss, 1968; Scott, 1953; Kim et al., 2011; Al Dayeh et al., 2013; Hall and Precious, 2013). Their role as a pacemaker of facial development will be debated in Section 1.1.5 of this chapter.

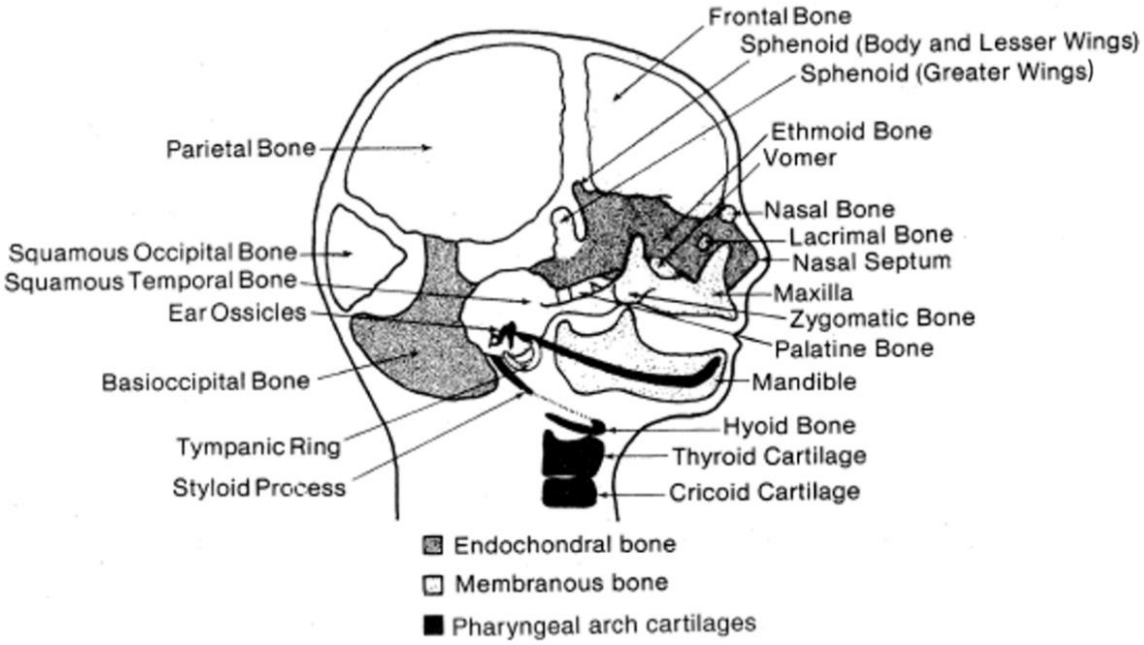

Figure 1.7. Skull bone ossification centres (Sperber et al., 2010).

When looking at the postnatal development of the lower face, the teeth have a significant impact on its morphology, the development of their alveolar processes contributing to the vertical growth of the face and the deepening of the palate (Garib et al., 2010). Indeed, the deposition of bone along the alveolar margins of the maxillae forms the emerging alveolar processes through which dental germs (tooth buds) grow; these processes fail to happen when dental germs are congenitally absent (Sperber et al., 2010; Alfaqeeh et al., 2013).

Facial postnatal growth and development are also influenced by suture growth. As for the neurocranium, facial sutures are no longer believed to possess intrinsic growth potential. Rather, they produce new bone at the sutural edges of the bone fronts in response to external inputs, possibly as a combination of biochemical and biomechanical signals (Opperman, 2000). While the fusion of cranial vault sutures happens in the third decade of life, the growth of the facial complex is generally complete by the second decade of life, with the facial sutures functioning as sites of fibrous union of the skull bones until the seventh or eighth decade of life, allowing for adjustments through remodelling (Opperman et al., 2005).

1.1.2 Hypotheses concerning the ontogeny of the face in *H. sapiens* and *H. neanderthalensis*

It is known that facial form is, to some degree, determined genetically. Nonetheless, it has been observed that dynamic interactions between cranial components during ontogeny play an important role in further modifying the morphology of the face (Lieberman et al., 2004). Since variations in the mechanisms that regulate and are involved in growth and development underlie variation in adult form, the comparison of ontogenies among species is informative in understanding how distinctive adult anatomies arose (Tillier, 1995). Differences in ontogeny between species can be identified in early patterning (the relative shapes and sizes and spatial organisation of cranial parts from early prenatal development to birth); in the length and orientation of the trajectory of postnatal ontogenetic changes in size and shape (the magnitude or

degree of changes in size and shape) and in the rate of these changes (Cobb and O'Higgins, 2004). Ontogenetic studies in living taxa have shown that divergence of the vectors of postnatal growth and development contribute to significant morphological differences between closely related species, for example among great apes and between these and *H. sapiens* (Bastir and Rosas, 2004; Cobb and O'Higgins, 2004; Mitteroecker et al., 2004; Viðarsdóttir and Cobb, 2004). In addition, recent studies show that ontogenetic shape trajectories differ even between modern human populations, contributing to the variation of our species (Viðarsdóttir et al., 2002). These findings suggest caution when making inferences about the taxonomic significance of differences in ontogenetic trajectories among fossil hominins, due to the high degree of plasticity found in modern human populations.

With regard to the comparison of ontogenies between *H. sapiens* and fossil hominins, it has been shown that modern humans and australopithecines have significantly divergent facial trajectories when comparing the first components (PC1s) of the Principal Component Analysis (PCA), (Cobb and O'Higgins, 2004). However, debate surrounds the extent of differences in facial ontogenetic trajectories among late Pleistocene hominins. Some authors have claimed that modern humans and Neanderthals share parallel trajectories, growing and developing in the same way (Ponce de Leon and Zollikofer, 2001; Ackermann and Krovitz, 2002). However, the similarity of trajectories was not tested, leading to conflicting claims in other analyses.

In this regard, two recent comparative studies of mandibular and neurocranial shape differences have suggested that modern humans seem to retain neotenous traits compared to Neanderthals, with the latter showing a more extended ontogenetic trajectory, leading to a larger, 'more developed' skull (Bastir et al., 2007; Zollikofer and Ponce de Leon, 2010). Nevertheless, the two studies disagree on whether or not these species share a common postnatal ontogenetic shape trajectory, with Bastir and colleagues strongly supporting the interpretation of divergent growth and development, implying differences in mechanisms of regulation.

Specifically, with regard to the comparison of facial trajectories, most work has focussed on the external facial skeleton (Ponce de Leon and Zollikofer, 2001; Ackermann and Krovitz, 2002; Viðarsdóttir et al., 2002; Rozzi and De Castro, 2004; Bastir et al., 2007), so far with little exploration of the internal anatomy of the face. New studies are needed to

shed light on Neanderthal and *H. sapiens* postnatal cranial differences, not only exploring the magnitude of these differences but also the morphological details of their ontogenetic changes in size and shape. Further analyses should clarify details of changes in the timing and patterns of growth and development of different facial regions, including the varying patterns of covariation, modularity and integration during ontogeny. Knowledge of these patterns might potentially contribute to a better understanding of the structural mechanisms and ontogenetic constraints that affect the growth and development of the skull.

Unfortunately, our ability to carry out ontogenetic comparisons with fossil species is affected by small sample sizes and uncertainty about the age at death of specimens (Cobb and O'Higgins 2004, Zollikofer and Ponce de Leon, 2010). This must be taken into account when comparing extant and extinct taxa.

1.1.3 Modularity and integration of the facial complex

In anatomical structures, constituent elements can interact ontogenetically through shared genetic, developmental, functional and spatial signals (Klingenberg and Zaklan, 2000).

Morphological integration during development refers to the extent to which changes over developmental time in anatomical elements are associated with modifications in other anatomical regions (Zelditch, 1987; Chernoff and Magwene, 1999; Olson and Miller, 1999; Bookstein et al., 2003; Porto et al., 2013). Adjacent craniofacial regions are always integrated to some degree, sometimes because they share the same embryonic development or simply because they are physically connected (Klingenberg, 2013).

However, the presence of integration between anatomical elements does not imply absence of a degree of independence of the same structures. A relatively developmentally independent unit, called a module, is characterized by its own ontogenetic trajectory (vector) of changes in size and/or shape (Bastir et al., 2006). Therefore, a module can be defined as a "[…] semi-autonomous complex of highly

intercorrelated traits" (Porto et al., 2013) that still possesses a degree of covariation and integration with the adjacent elements (Klingenberg, 2013). This autonomy allows for modifications in one region not to necessarily influence the development of adjacent regions (Raff, 2012). In fact, if the cranium could change only as an integrated whole, then the morphological evolution of individual cranial components would not be possible (Bastir, 2008).

Thus, modularity and integration are complementary concepts and the temporal and spatial patterns of modularity and integration among anatomical components are central in allowing or constraining mosaic evolutionary changes (Lieberman, 2011).

Because the human cranium comprises a set of integrated, but to some degree independent, modules, many have debated the extent to which its evolution occurred through a series of modular changes or, alternatively, was driven by one or a few modifications that affected a set of integrated cranial elements (Martinez-Abadias et al., 2011).

Recently, geometric morphometric analyses have been applied to study the degree of modularity and integration among cranial regions. These studies have shown that the skull is integrated to some degree with respect to the rest of the organism and that the cranium itself is made up of more or less integrated craniofacial modules (Bastir, 2008; Singh et al., 2012; Bookstein et al., 2003). In trying to identify the cascade of mechanisms shaping the human skull, some authors have suggested that skeletal modifications of the neurocranium and the cranial base during human evolution, such as those leading to a rounded globular braincase and a more flexed cranial base in modern humans relative to their ancestors, may have acted as structural constraints on the face (Enlow, 1990; Liebermann et al., 2000; Bastir et al., 2007; Bastir et al., 2008; Lieberman et al., 2008) (see Figure 1.8 describing the main hypothesised relationships among cranial regions).

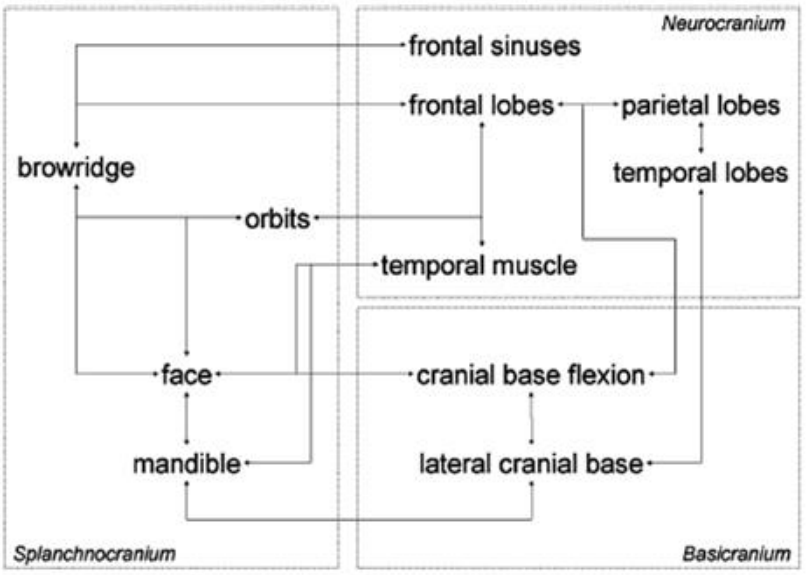

Figure 1.8. A scheme showing hypothesised relationships between craniofacial regions. The evolution of the whole system is constrained and characterised by adaptive pressures as well as structural and stochastic changes (Bruner, 2007).

That the developing cranial vault and basicranium influence the developing facial complex is supported by the timing of growth and development of these elements. Indeed, geometric morphometric studies have found that the human cranial base and vault reach their adult form earlier than the face, leaving the latter to adjust its further growth to the spatial limitations imposed by the formers (Bastir et al., 2006).

However, the picture seems to be more complicated, since it has been shown that only loose integrative relationships exist between midline and lateral components of the basicranium, thus implying the presence of two independent modules in the same cranial region (Bastir and Rosas, 2004; Bastir et al., 2006). Furthermore, if brain size alone constrains and drives facial evolution by acting on the neurocranial complex, it is surprising that the two most encephalised groups, namely *H. sapiens* and *H. neanderthalensis*, evolved such different facial morphologies (Bruner, 2007).

In considering growth and developmental morphological integration of mandibular and basicranial morphology with the face in great apes and *Homo*, some studies have rejected the hypothesis that these are fully developmentally integrated (Bastir and Rosas, 2004; Profico et al., 2017). However, some of these conclusions are based on the study of

midline landmark configurations and on the visual observation that changes in facial height were not followed by analogous vertical changes in cranial base and vault along the first and second principal components, without testing for modularity/integration between these anatomical regions.

On the contrary, Singh et al. (2012), when applying partial least squares to adults of *Hominoidea*, found that "[…] overall shape changes between the cranial regions show a uniform pattern of integration, particularly between the face and basicranium and the face and cranial vault." According to their results, a narrow and forward projecting face is associated with a narrow basicranium and cranial vault; a short and broad face is associated with a similarly shaped basicranium and vault. Lieberman et al. (2000) also found that the widths of the three regions are always highly correlated, and the orientation of the posterior face is always nearly perpendicular to the anterior cranial fossa. However, the significance of the associations among modules in the PLS analyses of Singh et al. (2012) is not presented in their results. These findings are supported by Bookstein et al. (2003), who also found the cranium to be highly integrated, but with vault and face shape more strongly associated than either of the two is with the cranial base. Other studies have found that the development of the sphenoid may be associated with the development of the midface, particularly with the form of the nasal septum and the extent of facial prognathism (Lieberman, 1998; Goergen et al., 2017).

To further complicate the picture, Hallgrımsson et al., (2007), using a set of linear measurements, volumes and angles, found that covariation between cranial widths, but not cranial length, of adjacent skeletal elements largely influence craniofacial variation in mice and that neurocranial and basicranial measurements (highly related to brain growth) correlate more between each other than with the facial complex. The pattern of influence of basicranial width on cranial development is confirmed in modern humans (Lieberman et al., 2000; Martinez-Abadiaz et al., 2009), with basicranial breadth affecting craniofacial morphology in terms of breadth, height and length.

Analyses of integration and modularity are often based on *a priori* definition of modules, derived from developmental and functional differences. A recent study (Makedonska, 2014) challenged this interpretation, testing if the integration between the face and cranial base in adult anthropoid primates was lower than that found within pairs of cranial and facial blocks, so to justify the use of the cranial base and facial complex as separate

modules. RV coefficient results found that not to be the case, the integration between the face and the cranial base not being significantly lower than the integration characterizing elements within the cranial and facial blocks. Thus, the paper concludes that the face and the cranial base cannot be considered separate modules (Makedonska, 2014).

All the findings here described (Lieberman et al., 2000; Bastir and Rosas, 2004; Martinez-Abadiaz et al., 2009) seem to show a more articulated picture than the one described by Enlow and Hans (1996), who sustained that modern human shape variation follows the two extreme trends of dolichocephaly and brachycephaly. While most studies confirm Enlow's general idea that overall the skull is an integrated module, they show that the relation between craniofacial elements is more complex and that the results or morphological analyses change also in relation to how we choose to measure sample's morphological variables and how we choose to test integration. Indeed, one of the methods largely used to study integration, the RV coefficient with relative permutation test, has been proved to be extremely biased by sample size, challenging some of the results based on this test (Adams, 2016).

When looking at covariation and integration, very few studies approached the matter from an ontogenetic perspective. However, what is the contribution brought by ontogenetic analyses when looking at covariation and integration? Looking at the study of modularity and integration from an ontogenetic perspective is fundamental for the understanding of the degree and nature of developmental and evolutionary interactions among skeletal elements and how these change over time (whether this is ontogenetic or evolutionary time).

According to Lieberman et al., (2002; 2004), adult differences between chimpanzee and human crania may well rest on relatively few changes in early ontogeny, such as growth of a bigger brain, which would lead to a shorter and wider cranial base and a less prognathic face. Bookstein et al., (2003) compare evolutionary and ontogenetic integration between cranial vault, base and face using a 2D landmark configuration in a sample of modern and fossil *Homo*. They find that evolutionary and developmental integration of vault and face are broadly equivalent among hominins.

Recently, a combined genetic and morphometric approach has been used to study integration in the skull. Results show that genetic factors can typically account for up to 50 per cent of the variation in most skeletal traits, with environmental stimuli having the same proportion of influence on growth and development of the phenotype (Martinez-Abadias et al., 2009; Smith, 2009; Von Cramon-Taubadel and Smith, 2012).

This combined approach provides evidence of morphological integration of the major cranial regions in modern humans (Martínez-Abadías et al., 2012) because simulation of selection of specific derived features produces a global, integrated response. This implies that, during evolution, selection acting on a morphological trait may have led to diverse secondary changes that can be misinterpreted as the target of selection. Therefore, attention must be paid towards evolutionary analyses of morphological adaptation and the selection of characters used to infer phylogenetic relationships between fossils.

However, a recent study (Spassov et al., 2017) challenged the view of the skull as a highly integrated structure. The study compared wild and congenitally muscular dystrophic mice, each divided into two groups and fed on a hard or soft diet. The modularity test showed that the "control group" (non-dystrophic and hard diet) possesses the highest values of modularity, while the group in which the genetics and diet were altered shows the highest level of integration. This result suggests that atypical changes in one cranial region lead to a process of integration of the other regions to accommodate the changes.

Allometry might be another fundamental factor to consider when approaching the investigation of the integration within the human skull during ontogeny. In most studies of primates, pronounced allometry has been found during ontogeny, and allometry may, therefore, be an important integrating factor in the primate head (Klingenberg and Marugán-Lobón, 2013). Some studies have thus applied size correction to 'remove' these effects, by using residuals from the multivariate regression of shape on size before performing further analyses of integration (Klingenberg, 2013).

Although numerous studies of integration and modularity have been published, it is surprisingly difficult to use this information to make comparisons or develop generalisations, because of conflicting results and the lack of organic continuity in methodological approaches and in the choice of the anatomical regions analysed (Klingenberg, 2013).

Concerning modularity and integration of the face, most of the studies focused on adult samples and considered the face as a single unit. Only a few attempts have been made to study the integration of the face by focusing on specific sub-regions during ontogeny. Studies on the pre-maxilla found that this region varies independently of the palate and the rest of the face in hominins (Villmoare et al., 2014). This result highlights the importance of decomposing the face into sub-regions, since they may provide deeper insights into the factors that underlie modern human facial variation. Understanding the cranial constraints on the face may clarify the role that non-adaptive factors played in the evolution of the modern human skull. Furthermore, an ontogenetic approach is necessary to link cranial covariation patterns to the mechanisms that generate them, and to understand their significance in the context of skull evolution (Hallgrımsson et al., 2009).

A suitable basis to divide the face into sub-regions is required in order to study interactions between them. In relation to evolution and development, a developmental subdivision is appropriate, since evolution itself proceeds by modification of ontogenies. For this reason, and because this thesis focuses on the face, the development of the face with a focus on the nasal septum is reviewed.

1.1.4 Embryological development of the nasal septum

Understanding the anatomy and development of cranial regions is fundamental to studying the mechanisms that underpin phenotypic variation (Hendrikse et al., 2007). What follows is a thorough description of the nasal complex and current hypotheses concerning its evolution, development and interaction with other craniofacial regions.

The midline roof of the nasal complex is made up of the nasal septum. This consists of three parts: the columellar septum (the fleshy external tip), the membranous septum (a double layer of skin between the columella and the septal cartilage) and the septum proper (consisting of the ethmoid, vomer, and septal cartilage). The lateral walls of the nasal complex are made up of the inferior, middle and superior turbinates or nasal conchae, which are responsible for filtration, heating, and humidification of inhaled air

(Churchill et al., 2004). The septum proper and conchae are cartilaginous, forming a capsule that surrounds the nasal cavity.

The cartilages of the nasal conchae and the nasal septum develop from the chondrified nasal capsule. The nasal capsule chondrifies in the 2nd prenatal month, forming a roof and lateral walls (also called ectethmoids, the precursors of nasal conchae) united to a vertical cartilaginous plate called the mesethmoid, a component of the early basicranium, part of which will constitute the perpendicular plate of the ethmoid bone of the nasal septum (Scott, 1953). Prenatally, in the lateral walls of the nasal cavity, two ossification centres will form the paired lateral masses of the ethmoid bone, while medially, two intramembranous ossification centres will form the initially paired vomer, which will fuse at birth.

In the newborn's face, the vomerine groove works as a hosting site for the nasal cartilage, which remains mainly cartilaginous, except in the area in which it articulates with the vomer. The ethmoid bone and the upper area of the posterior nasal cartilage join in the so-called "keystone area", creating a thick articulation (Sandikcioglu et al., 1994). This area is located where the caudal area of ethmoid bone overlaps with the upper lateral cartilage (Sperber et al., 2010). The nasal septum cartilage is also firmly united by fibrous tissue to the premaxillary region of the maxilla in front of the vomer (Figure 1.9, Al Dayeh et al., 2013).

Prenatally, the growth of the nasal septum is greatest from 6 to 9 weeks of development (Hall et a., 2013). Scott (1953) claims that the principal postnatal period of growth of the nasal cartilage is until 7 years of age. However, its growth period is highly debated, with other studies sustaining that nasal growth occurs until adulthood (Hall and Precious, 2013).

Another element of discussion when it comes to human nasal morphology concerns the role of the nasal septum in shaping the face during postnatal development. Some authors claim that modifications of the nasal septum cartilage affect subsequent facial development, while others sustain it possesses a secondary role in the architecture of the facial complex (Van et al., 1996; Hall and Precious, 2013).

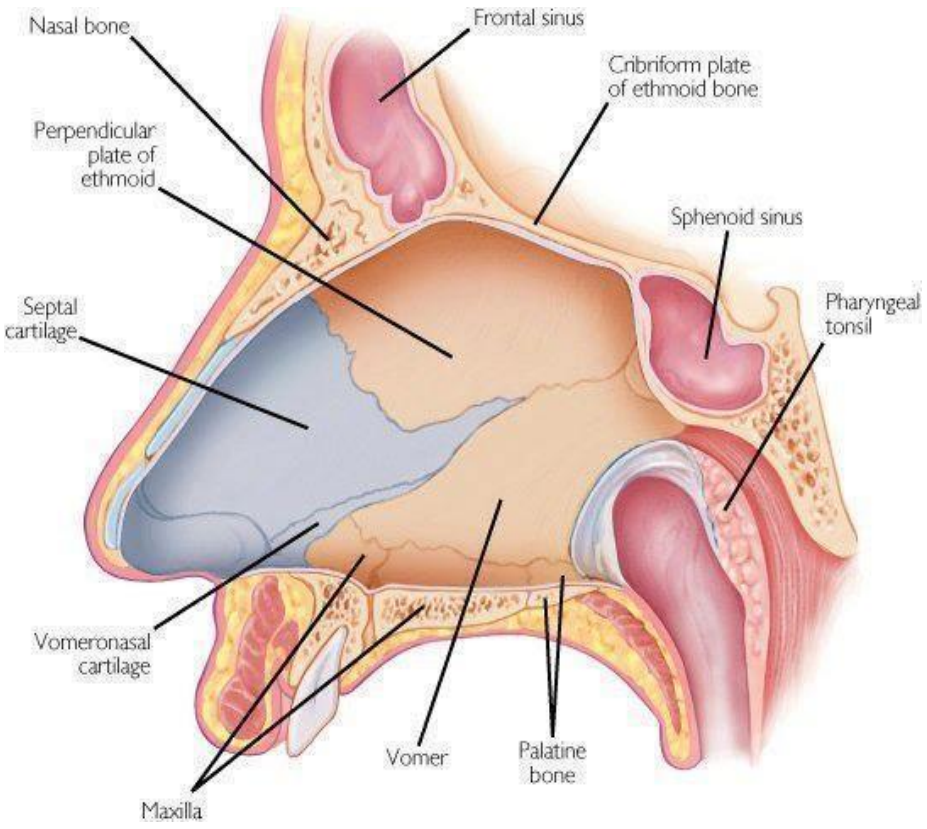

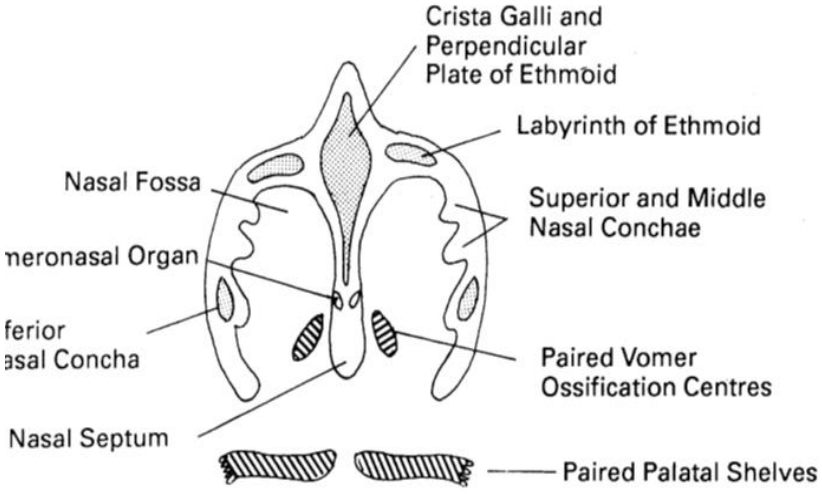

Figure 1.9 below. Top: bones of the nasal septum; bottom: ossification centres in the nasal region (Sperber et al., 2010).

1.1.5 Postnatal growth, development and integration of the nasal septum

Ontogenetic studies of integration seek to understand the extent to which morphological units interact and the strength of such interactions. However, often they do not focus on the mechanisms by which these patterns occur (Lieberman, 2011).

To explain the mechanisms of facial development, a series of hypotheses have been formulated in the last century, dealing with the relative importance of the main driving forces acting in the face during postnatal growth and development: the Functional Matrix and the Nasal Septum theories (Scott, 1954; Moss, 1968).

The Functional Matrix theory, elaborated by the anatomist Melvin Moss (Moss, 1968) suggests that the skeletal elements act purely as a supporting framework around the functional units of the organs (eyes, mouth, brain, teeth, muscles, etc.). Each functional matrix, defined as [...] "non-skeletal cells, tissues, organs, and operational volumes" in the body (Moss, 1997), has an associated skeletal capsule (bone or cartilage) that is subordinate to and supportive of the matrix it encloses. Thus, bone formation would be genetically controlled only to a minor degree and largely subordinated to the corresponding developing functional matrix (see Diagram 1.1).

According to the Functional Matrix theory "[…] the nasal septal cartilage grows as a secondary, compensatory response to the primary growth of the related oro-facial matrices" (Moss and Bromberg, 1968). This theory has been further elaborated and tested by many authors over the past 50 years, with a focus on the hypothesis that the nasal septum passively adapts to support the growth and development of the oro-facial matrices (or capsules) and adjacent midfacial skeletal structures (Latham and Burston, 1964; Babula et al., 1970; Goergen et al., 2017).

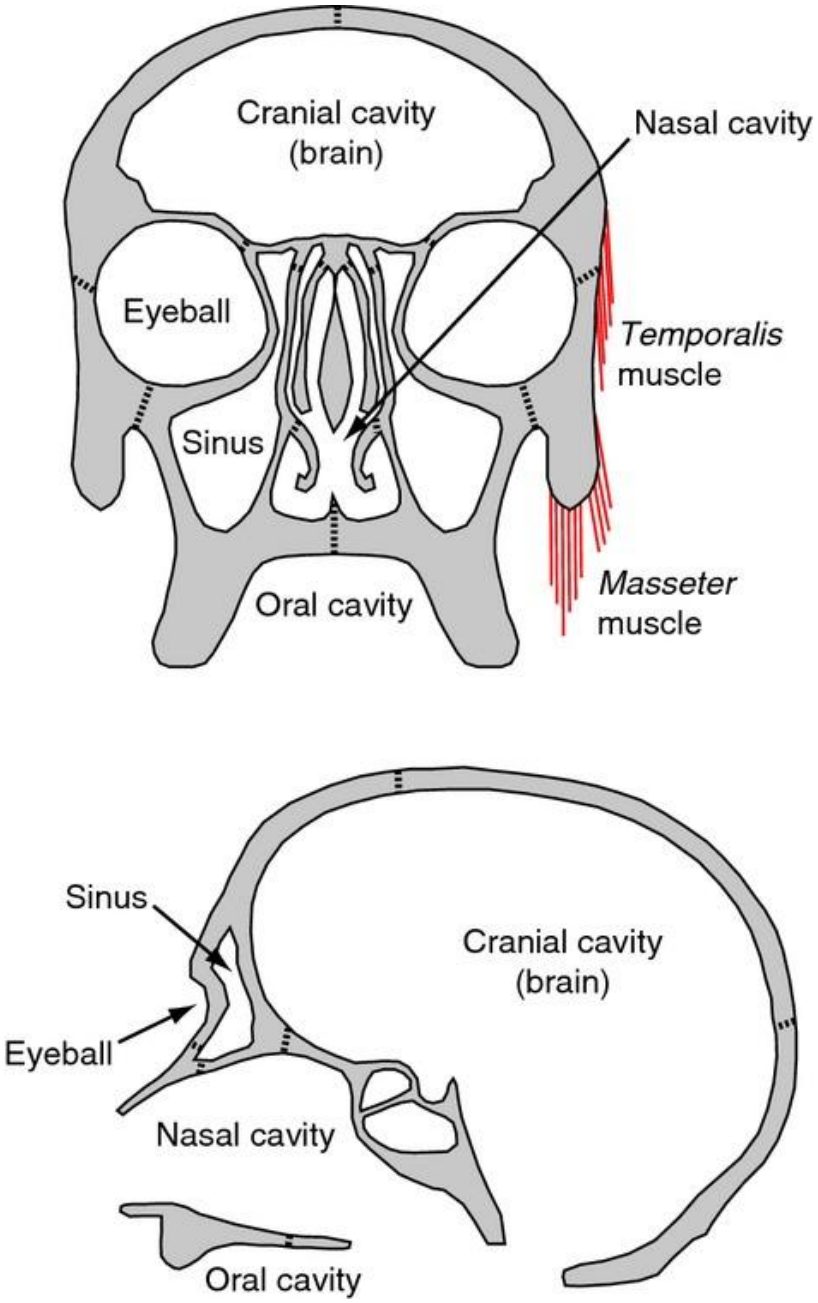

Diagram 1.1 Schematic representation of functional matrices proposed for the human skull. Examples of functional matrices are the brain, the nasal cavity, the eyeballs, the maxillary sinuses, the oral cavity and head muscles, such as temporalis and masseter; these cavities and soft tissues have been suggested to mediate bone growth (Esteve-Altava & Rasskin-Gutman, 2014).

In support of this interpretation, experiments comparing normal mice with mice displaying naso-palatal anomalies or undergoing nasal septum removal (Babula et al., 1970) did not show any growth deficiencies in the face (however, mouse skeletal connections are different from humans, thus mechanisms of growth and development may not be fully shared). Furthermore, evidence shows that septal dislocation does not affect the normal growth of the face in young rabbits (Wexler and Sarnat, 1965). Moss himself did not find any midfacial irregular development after removal of the septal structures in humans and believed that the only consequence could be the collapse of the roof of the nose, considering the nasal septum to function only as a structural pillar for the nasal cavity (Moss and Bromberg, 1968).

After examining a case of foetal arhinencephaly, the congenital absence of olfactory organs, Latham and Burston (1964) concluded that the nasal septum had a role in determining the anteroposterior growth of the upper face but that it did not account for the proper growth of vertical facial height. The same authors (Latham and Burston, 1966) reported a case with deviated nasal septum in a child as a consequence of cleft palate. In this situation, no anomalies in the activities of deposition and resorption of the palate nor in the development of the overall height of the face were observed, but the sagittal growth of the non-cleft maxillary side, toward which the septum was deviated, and its activity of deposition were more rapid and accentuated.

A more recent study has demonstrated that nasal septal deviation is associated with reduced height of the upper facial skeleton (Mays, 2012). This suggests that, in short faces, the nasal septum keeps growing, thus resulting in its deviation because of the limited height available. If this interpretation is correct, then nasal septum growth would be independent of and dissociated from facial growth. This explanation revisits Moss' original hypothesis of the nasal septum lacking growth power and being subordinate to midfacial changes, by hypothesising a lack of influence of the nasal septum on the overall midfacial architecture (as Moss suggested) but considering this structure to have its own growth potential.

However, this re-interpretation is challenged by Holton et al. (2011) who found that artificially induced restriction of facial growth in *Sus scrofa* produced nasal septum growth and subsequent compensatory premaxillary growth, fundamental to maintain the cranial architecture. The same authors also describe how, in humans, changes in nasal

septal volumes are associated to changes in facial morphology, which they interpret as a response to accommodate changes in nasal septum size (Holton et al., 2012).

However, although the nasal septum might have a certain degree of independence, a recent study showed that in humans, the shortening of midline elements of the cranium, particularly the sphenoid bone, is associated with nasal septum deviation (Goergen et al., 2017), possibly because of its anatomical connection with the ethmoid bone at the sphenoethmoidal synchondrosis. This shows that, even though the nasal septum might exert a certain degree of influence on facial modifications, it is also potentially subject to cranial changes.

Contemporary to the elaboration of the Functional Matrix theory, another theory was articulated by the anatomist James H. Scott, who proposed a unifying interpretation of craniofacial growth: the Nasal Septum theory. This theory is in contraposition to Moss' theory as it posits that the expansion and development of the cranium are driven by actively expanding cartilages, one of them identified as the nasal cartilage. According to Scott, growth takes place at the cranial sutures as these are separated, driven apart by the growth of the cartilage of the nasal septum and other cartilaginous centres of expansion in the cranium (Scott, 1954; 1956; 1962).

Many authors have supported this theory through experimental data (Young, 1960; Vetter et al., 1984; Pirinen, 1995; Wong et al., 2010; Al Dayeh et al., 2013; Hall and Precious, 2013). Diewert (1985), studying the timing of the development of human embryonic craniofacial morphology, observed that "[…] rapid directional growth of the nasal cartilage is important to the development of normal human facial morphology and interference with normal growth changes during this early critical period may produce irreversible effects on the face."

Indeed, the desire to understand the causes and consequences of facial growth and to plan surgical intervention in septal deviation has led to numerous clinical studies of nasal septum and facial development. The influence of nasal septum growth and deviation on facial anatomy has been examined using longitudinal cephalometric measurements of twins, with the finding that the nasal cartilage has an impact on the normal growth and development of the nose and maxilla, especially in the first decade of life (Grymer et al., 1991; Grymer and Bosch, 1997). Indeed, the twins with deviated nasal septum showed a

retrusive maxilla (vertically and horizontally shorter and anteriorly rotated) and a nose with columellar retraction. However, interestingly, total facial height did not differ among twins.

By measuring nasal septal versus nasofrontal suture growth rates in pigs to test whether the first precedes and impacts on the second, a recent study found a significantly higher rate of growth of the nasal septum, thus suggesting that the growth of the septal cartilage might drive the growth of the nasofrontal suture and the anteroposterior development of the midface (Al Dayeh et al., 2013). Indeed, septal cartilage growth potential has been considered similar to that of the epiphyseal growth cartilage of long bones (Scott 1954; Baume, 1961; Vetter et al., 1985).

Scott's Nasal Septum theory has also been supported by physiological evidence. Studies showed that increased activity of growth hormone during postnatal development leads to greater human facial dimensions, attributed in part to the stimulation of septal growth (Pirinen et al., 1994).

In addition, midfacial retrognathia associated with some anomalies such as achondroplasia and arhinencephaly has been attributed, in part, to defects in the nasal septal cartilage (Delaire and Precious, 1987). Support for the role of the septal cartilage as a pacemaker for midfacial growth also comes from *in vivo* extirpation experiments; partial or total extirpation of the cartilage resulted in diminished facial growth in rabbits and in rats (Kvinnsland, 1974). Anomalies in midfacial development have also been observed in humans when the nasal septum is deviated or develops abnormally during childhood (Grymer et al., 1989). Indeed, clinical conditions such as cleft palate, in which the nasal septum grows deviated and bent, cause the face to grow asymmetrically (Hall and Precious, 2013). Verwoerd and Verwoerd-Verhoef (2007) provide a literature review of clinical studies, indicating that loss of septal cartilage at different ages leads to abnormal development of the nose, maxilla and orbits.

However, as already discussed, this could suggest that, in situations in which the face is somehow constricted or altered during growth and development, the nasal septum would grow in a deviated way because of the limited space available. Indeed, all the findings in support of the Nasal Septum theory have been challenged by Moss and other authors, who attributed the altered midface development to the structural collapse of

the nasal roof after deviation of the nasal septum. Furthermore, some of the experiments of extirpation of nasal cartilage in animals have not led to any midfacial alteration (Wexler and Sarnat, 1965; Babula et al, 1970), leaving doubts about the mechanisms of growth and development of the face.

Mooney et al., (1989) applied path analysis, a method to analyse hierarchies of interactions, to the testing of the two major opposing visions: the Functional Matrix and Nasal Septum theories. In this paper, two different possible paths describing patterns of interaction and covariation between anatomical elements were compared in a small sample of prenatal individuals. The path in which nasal cartilage was hypothesised to act over time on surrounding anatomical elements, such as premaxilla length and nasal airway length, was better supported than the path representing an aspect of the functional matrix theory in which the orbicularis muscle is hypothesised to act on the surrounding structures. However, the authors did not analyse a full ontogenetic series but focused on a short period of foetal growth.

The Nasal Septum and Functional Matrix theories are still very much debated. Many authors believe that the growth of the nasal septal cartilage influences displacement and growth at facial suture sites. Others believe that facial growth is adaptive and occurs in response to functional demands, developing increased nasal airway volume and expansion of the nasal capsule, driven by the action of functional matrices. Attempts to test these two theories have led to contradictory findings. While prenatally it is evident that the growth of elements such as the brain and the eyeball covaries and influences the growth of the brain and the eye socket (Sperber et al., 2010), it is much less clear which forces are driving changes in the skull during the postnatal period.

Differences in the results of the research here described are likely caused by the choice of species (and so differences in the sutures and articulation of the bones) and by the way the experiments were performed, by, for example, focusing on different areas at different times of development. Indeed, it has been observed that nasal septum growth is not homogeneously distributed throughout the septum and is not constant in time (Al Dayeh et al., 2013). Further studies are needed to clarify the forces driving the growth of the face by looking at ontogeny specifically in humans and in relation to differences in facial morphology.

1.1.6 Maxillary sinuses in facial ontogeny

In palaeoanthropology, most studies concerning the evolution and variation of the face focus on the external morphology of the skull. However, it is important to recall that the face hosts several organs and internal structures that can potentially influence the adult morphological variability and its ontogeny (Lorkiewicz-Muszyńska et al., 2015). A very poorly understood element among these structures is that of the maxillary sinus. This anatomical feature is of interest to clinicians and evolutionary biologists, being investigated in the framework of craniofacial evolution and development and midfacial pathologies (Rae and Koppe, 2000; Sharan and Madjar, 2008; Maddux and Butaric, 2017). Nonetheless, no consensus exists on the function and the causes of variation of this cavity. The debates are summarised in the following sections.

1.1.6.1 Form and function of paranasal sinuses

Paranasal sinuses (which comprise maxillary, frontal, sphenoidal and ethmoidal sinuses) are cavities that are variable in presence and size within the mammalian cranium. Their function and aetiology have been the subject of a long debate, as evident from Blanton and Biggs's article "Eighteen hundred years of controversy" (1969). These anatomical structures triggered the curiosity of Leonardo Da Vinci, who described their morphology in modern humans in the 16th century (Marquez, 2008). Numerous clinical studies have since addressed the physiology and anatomy of human sinuses. A British surgeon, Nathaniel Highmore (1613-1685), is believed to be the first to furnish a highly detailed clinical description of the maxillary sinus, which then came to be referred to as "the antrum of Highmore"(Highmore, 1961; Mavrodi, and Paraskevas, 2013). Further precise descriptions and illustrations were then provided by 19th century Austrian anatomist Emil Zuckerkandl, considered by many the "father" of modern sinus anatomy (Zuckerkandl et al., 1895).

The high degree of variation and the presence of frequent anomalies in paranasal sinuses have led to a persistent clinical interest about these features, particularly in the 20th

century, when doctors started focusing on the treatment of acute and chronic sinusitis, cleft palate, non-odontogenic tooth pain and tooth-related sinus infections (Robinson et al., 1982; Shapiro et al., 1986; Fehrenbach and Herring, 1997).

Despite the attention they draw, paranasal sinuses are somehow still not completely described, because of their great morphological variation, the different terminology used to define them and the discrepancies resulting from it (Marquez et al., 2008). Differences in shape, size, symmetry and degree of pneumatisation of these structures are very frequent and these differences are sometimes reflected in the alteration of the nervous and blood pathways of contiguous structures (Lawson et al., 2008). This high degree of variation makes it difficult to produce a single concise description; it also suggests that sinus development might be a secondary phenomenon, possibly defined by the space available in the enclosing bones (O'Higgins et al., 2006). Therefore, morphologists and clinicians are still investigating the development, morphology, and functional significance of these internal structures. Many hypotheses have been formulated concerning their function within the naso-facial complex (Rae and Koppe, 2004). However, the high degree of plasticity and developmental variability of maxillary sinuses has recently led scholars to question if paranasal sinuses have any specific and necessary function, suggesting an alternative framework in which these elements develop passively in the space available in the enclosing bones, rather than having a dynamic and functional role in shaping the midface (O'Higgins et al., 2006, Rae and Koppe, 2004; Butaric and Maddux, 2016).

1.1.6.2 Prenatal and postnatal development of maxillary sinuses

The maxillary sinuses are the largest of the paranasal sinuses (Figure 1.10). They are generally described as air-filled cavities enclosed within the maxilla, although in some cases they can extend into the zygomatic (Rae and Koppe, 2000). Their surface is covered with mucoperiosteum and they are connected to the nasal cavity (more precisely to the semilunar hiatus of the middle meatus) through the ostium. This anatomical feature is one of the few anatomical regions of sinuses that can be clearly identified as developmentally homologous among individuals. Its location is relevant in comparative

studies of sinus pneumatisation (O'Higgins et al., 2006) and true landmarks can be reliably placed at this site.

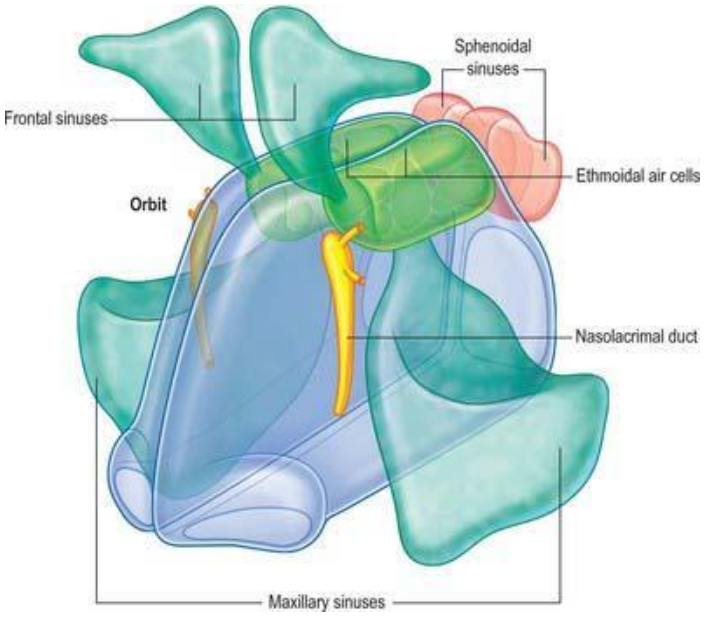

Figure 1.10. Anatomy of paranasal sinuses (medicina247.altervista.org).

Embryonically, maxillary sinuses develop as early as the 10th week of the prenatal period (primary pneumatisation). During this week, the tissue located next to the ethmoid infundibulum develops some invaginations. At the 11th week, the fusion of these folds creates a single hole, the maxillary sinus primordium (Figure 1.11, Nuñez-Castruita et al., 2012). From the 12th week, it is possible to observe a more complex structure with a lateral wall, bounded by the maxillary bone; a medial wall, limited by the inferior turbinate; and a roof, where the ostium lies. Subsequently, a second process of enlargement (secondary pneumatisation) takes place from the 5th prenatal month onwards, causing the maxillary sinuses to be radiographically recognisable at birth.

During secondary pneumatisation, maxillary sinus expansion depends on the resorption of the medial and lateral walls of the maxilla (Sperber et al., 2010).

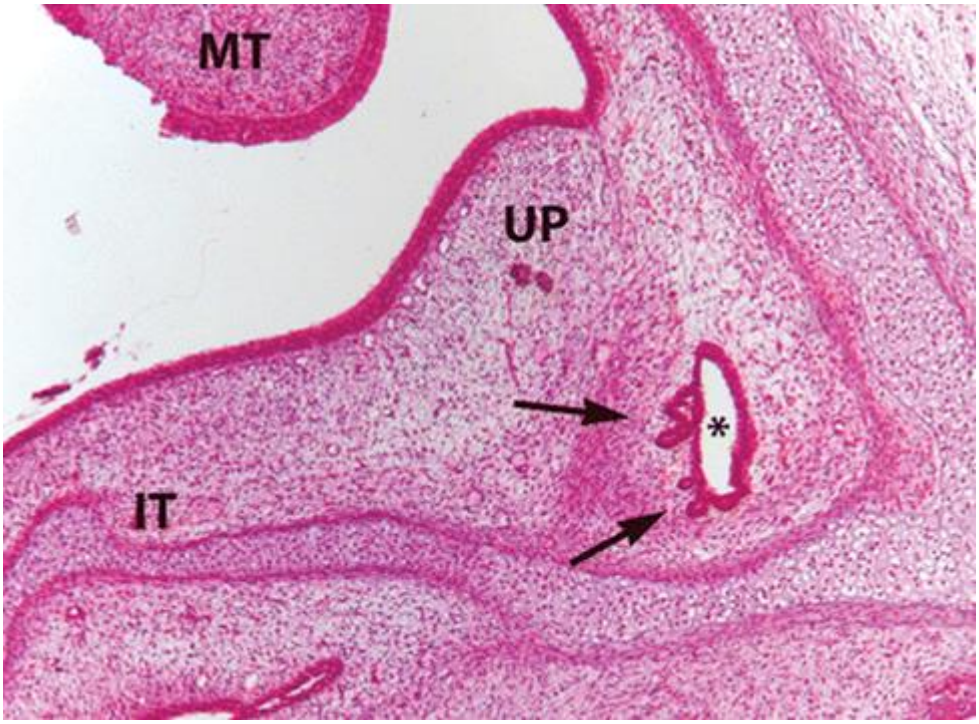

Figure 1.11. Frontal section of the head in a 10-week fetus. Ethmoid infundibulum (asterisk), invaginations of mucosa (arrows), middle turbinate (MT), uncinate process (UP), inferior turbinate (IT) (Adapted from Nuñez-Castruita et al., 2012).

However, it is after birth that the majority of maxillary sinus growth occurs (Sperber et al., 2010; Lorkiewicz-Muszyńska et al., 2015). After birth, maxillary sinuses expand laterally along the inferior rim of the orbit; inferiorly, they reach the alveolar ridge of the permanent dentition, invading the vacant crypts left behind after tooth eruption. The anterior limit is located in the first premolar area and the posterior limit is generally identified as the area of the third molar and maxillary tuberosity (Scuderi et al., 1993).

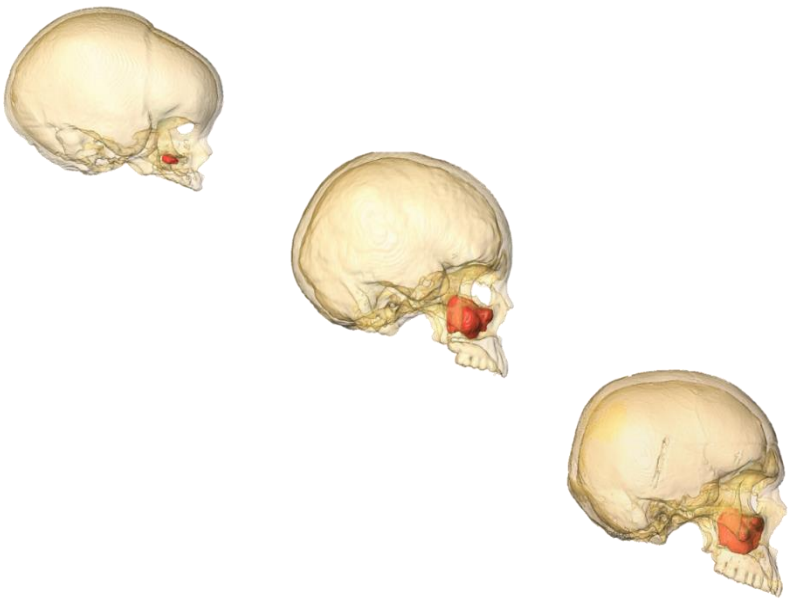

Figure 1.12. Lateral view of a maxillary sinus (red) in an infant (0.5 years old), juvenile (15 years old) and adult (>18 years old) of *H. sapiens* (Frankfort plane orientation). Image created in Avizo 9.0 by the author. All ages are estimated based on the dental development status according to AlQahtani et al. (2010). Image realised using Avizo 9.0 (courtesy of Anna Lucas).

Figures 1.12 and 1.13 illustrate the postnatal growth and development of the maxillary sinuses in ontogeny at different age stages, in coronal and lateral view. As noted by Adibelli et al., (2011), it is evident that the sinus grows predominantly along the antero-posterior axis until the first year, followed by a lateral and downward enlargement, which seems to be secondary to the lengthening of the face (Maddux and Butaric, 2017).

The rate of postnatal growth and the age by which the sinuses are said to reach their maximum volume varies considerably between studies, ranging between 12 and 30 years (Lorkiewicz-Muszyn´ska et al., 2015). This calls for clarification through further work. Moreover, some studies have observed further enlargement of maxillary sinuses in adults after posterior tooth extraction (Sharan and Madjar, 2008), suggesting that plasticity persists into adulthood, as also confirmed by studies who found incredibly high variation in modern human adult populations (Nikitiuk, 1983; Rosano et al., 2010).

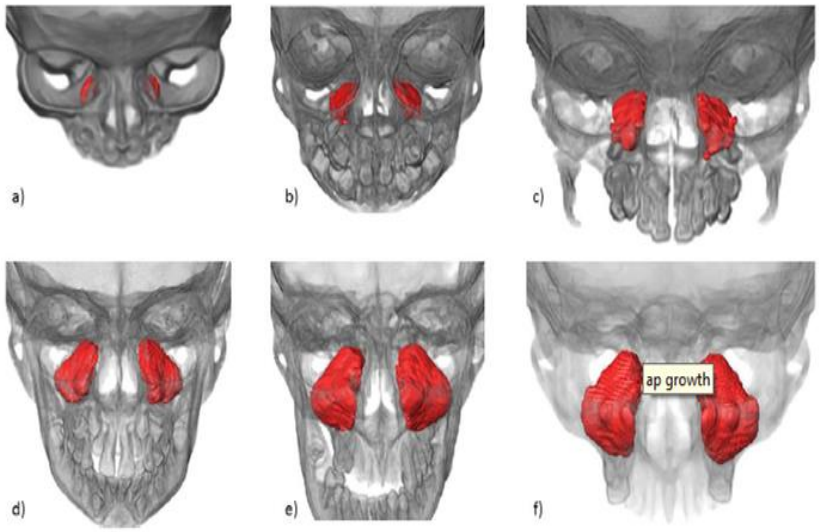

Figure 1.13. Frontal view of six different specimens of *H. sapiens*, showing the postnatal growth and development of maxillary sinuses (red). a) <1 year old, b) 1 year, c) 4.5 years, d) 7.5 years, e) 12 years, and f) 18+ years. All ages are estimated based on the dental development status according to AlQahtani et al. (2010). Image realised using Avizo 9.0 (courtesy of Anna Lucas).

Kim et al., (2002) have made an attempt at classifying the adult morphology of maxillary sinuses based on their morphology and the location of their walls in relation to the facial bones, with the aim of better identifying clinical anomalies. Grahe (1931) observed that when maxillary sinuses are not fully developed (specifically due to alteration of molar growth in his experiment) their soft tissue properties in terms of activity are not affected, thus suggesting that pneumatisation is not driven by soft tissue development.

The great degree of variation of maxillary sinuses between and within individuals (*e.g.* lack of symmetry, difference in sizes and volumes or even absence on one side, Radulesco et al., 2018; Gorza and Thevissen, 2019) supports the emerging hypotheses that paranasal sinuses play a subordinate role in the context of the prenatal and postnatal development of the cranium, responding to, rather than driving, maxillary growth and development. Their prenatal development has been shown to occur under a high degree of genetic control through a precise interaction of multistep cascade process (Gupta et

al., 2020), but, as is evident, the postnatal relationships between craniofacial components deeply influence maxillary sinus expansion (O'Higgins et al., 2006; Chaiyasate et al., 2007). The causal relationships and the magnitude of interaction between these elements are of interest to modern biologists and clinicians and should be further investigated.

1.1.6.3 Maxillary sinuses: evolutionary history and variation

Maxillary sinuses are found in most groups of mammals and are believed to be present in the last common ancestor of eutherians. In the primate order, maxillary sinuses are present in many new world monkeys and in all anthropoids as well as their ancestors, the Oligocene anthropoids *Aegyptopithecus* and *Apidium* (Rae and Koppe, 2004). Interestingly, the whole group of cercopithecoids shows a lack of these features, with the only exception being the genus *Macaca* (which possesses no other paranasal sinuses). This observation led, at first, to the suggestion that this whole group of primates may have undergone an early loss, a possibility supported by the absence of paranasal sinuses in *Victoriapithecus* (along with the similar extinct genus *Prohylobates*), a stem cercopithecoid from the Miocene (Rae and Koppe, 2004), and in other cercopithecoid fossils (*Mesopithecus,* Late Miocene, *Rhinocolobus,* middle Pliocene, and *Theropithecus oswaldi,* Plio-Pleistocene). These observations led to the conclusion that the presence of maxillary sinuses in the genus *Macaca* could be explained as reacquisition (Kuykendall and Rae, 2008). This view is supported by the presence of maxillary sinuses in the late Pliocene cercopithecine fossils *Paradolichopithecus* and *Macaca majori*.

However, recent evidence challenges this interpretation because of the presence of maxillary sinuses in three taxa of extinct cercopithecoids: the late Miocene *Cercopithecoides williamsi*, a colobine from South Africa (Kuykendall and Rae, 2008); the Asian cercopithecine *Paradolichopithecus sushkini* and *Libypithecus markgrafi*, a late Miocene colobine from North Africa (Rae, 2008).

The presence of maxillary sinuses only in the genus *Macaca* among extant cercopithecines has led researchers to focus on this genus. When maxillary sinus volume

is measured in different *Macaca fuscata* populations, the results show that, in cold regions, the volume is smaller (Rae et al., 2003). Likewise, a gradient toward smaller maxillary sinuses and larger nasal turbinates are observed in different Inuit populations with the increase of latitude (Shea, 1977). This suggests enlargement of the nasal cavity to function as a more effective air conditioning organ, causing a consequent reduction of the space available for maxillary sinuses to grow.

Reflecting this variation among anthropoids, modern human maxillary sinuses are highly variable, sometimes asymmetric, congenitally absent or, particularly pneumatised and the adult form can vary extremely, especially when considering populations from different habitats (O'Higgins et al., 2006; Shea, 1977; Butaric, 2015; Kim et al., 2002).

Maxillary sinus evolution has been investigated also in fossil hominins, with a focus on *H. neanderthalensis*. In particular, there is an ongoing debate as to whether this species possesses more pneumatised sinuses compared to modern human warm climate populations as an adaptation to cold climates, functioning for heating and humidifying inhaled air (Holton et al., 2011; Rae et al., 2011a, 2011b). Thus, a recent study from Marquez et al. (2014) analysed maxillary sinus volume in modern populations at different latitudes. It showed that relative maxillary sinus volumes (scaled by cranial length and endocranial volume) tend to be higher among the warm climate groups. Interestingly, the two Neanderthal specimens analysed in the study exceeded the values of all the human samples but were closest to the values of the tropical and South African human groups. Rae et al. (2011a) confirm that maxillary sinus pneumatisation in Neanderthals is not cold-adapted, being comparable in scale with that seen in *H. sapiens* from European temperate climates. These results suggest that the distinctive Neanderthal midface should not be interpreted as a direct result of increased pneumatisation, nor is it likely to be an adaptation to resist cold stress.

When analysing sinuses in modern humans, Butaric (2015) looked at modern human variation in the relationship between nasal cavity and maxillary sinuses. The author found that individuals from cold–dry climates have larger maxillary sinus volumes and narrower nasal cavities, while smaller volumes are associated with wider nasal cavities in hot–humid climates. These findings are in direct contrast with those outlined earlier (Marquez et al., 2014), who found individuals from warm climates to have bigger sinus volumes. According to Holton et al. (2013), there is a positive relationship between nasal cavity and

maxillary sinus volumes, indicating that maxillary sinuses do not accommodate variation in nasal cavity volume. However, in their study, maxillary sinus volume is inversely correlated with relative internal nasal breadth. Thus, the authors suggest that maxillary sinus volume appears to be important for accommodating nasal cavity shape rather than size. This interpretation is supported by Butaric (2015), who suggests that the maxillary sinus acts as a zone of accommodation allowing the nasal shape to maintain a certain degree of independence and allowing it to vary and adapt to different environmental pressures.

Recent works (Butaric and Maddux, 2016; Maddux and Butaric, 2017) found complex but consistent covariation between midfacial and maxillary sinus morphology in two modern human populations from the Sahara and Alaska. The authors conclude that previous results of Butaric (2015) indicating larger maxillary sinuses among cold-adapted populations are not exclusively related to relatively narrow nasal cavities, but primarily to greater maxillary and zygomatic heights. In conclusion, they suggest that sinuses may serve as sites of accommodation for multiple facial elements, potentially behaving like a buffer, by reducing the effect of morphological alterations in one facial component on another.

As is evident, maxillary sinus evolutionary history is all but simple, and the pattern of presence/absence in modern and fossil taxa needs to be further examined in a developmental and ecological framework. Future analyses should focus not only on sinus volume but also on its morphology and that of the surrounding anatomical structures such as nasal cavity, orbits, palate, and the zygomatico-maxillary complex.

1.1.7 Evolutionary hypotheses on facial differences between *H. sapiens* and *H. Neanderthalensis*

The European fossils attributed to late *H. neanderthalensis* (about 230-40.000 years ago, Sistiaga et al., 2014) show a number of distinctive cranial features when compared to modern humans (Weaver, 2009).

The Neanderthal brow ridge is thicker and double-arched and the eye sockets are larger and more rounded. The cranial capacity is bigger, with the occipital being projected more backwards, and the enlargement of the anterior cranial fossa creates a more expanded frontal. Neanderthal midface is also more prognathic, due to an everted and broad nasal cavity and to obliquely oriented and swollen cheekbones (Harvati, 2010; Harvati-Papatheodorou, 2013).

The appearance of 'anatomically modern humans' (Stringer et al., 1984) in Europe is currently linked to the passage from the Middle to the Upper Palaeolithic (Higham et al., 2011) and represents a considerable change in craniofacial architecture, marked by the presence of a series of autapomorphies. As a general description, these include the presence of a chin, the absence of a strong supraorbital torus, a short (anteroposteriorly and superoinferiorly) orthognathic face retracted underneath the anterior cranial fossa, a more flexed basicranium, a frontal bone vertically developed and a tall, wide, short and globular neurocranium (Lieberman et al., 2002).

Nonetheless, some of the early specimens of *H. sapiens* (Quazfeh IX, Zhokoudian, Skhul V, Jebel Irhoud) still retain some primitive characteristics such as the absence of the chin, a thick supraorbital torus, a large and rounded orbital margin, and a quite prognathic face (with a particularly tall midface), thus showing that modern human "gracile" characteristics are quite recent and have been gradually developing throughout the evolution of *H. sapiens* (Lieberman, 2011).

Many papers have looked into an evolutionary explanation for the morphological differences that clearly separate these two species. When focusing on the nasal aperture, despite their apparently peculiar midface, recent studies (Villmoare et al., 2014; Rae et al., 2011a) have observed that Neanderthal nasal cavity and maxillary sinus volumes fall within the range of modern African variation, thus challenging two major concepts: the

first related to their particularly large nasal dimension, the second related to this dimension as an adaptation to cold climates.

Indeed, the midfacial morphology of Neanderthals is sometimes seen as an environmental adaptation (Yokley, 2006; Holton and Franciscus, 2008), a view supported by recent papers on the nasal shape of modern human populations adapted to cold climates (Noback et al., 2011; Evteev et al., 2014). This perspective emphasizes the evolutionary role played by natural selection as the major force shaping Neanderthal and *H. sapiens* skull morphology. Nonetheless, Neanderthals differ from modern humans in a wide range of craniofacial features that provide a different basis upon which cold adaptation may have acted, therefore any comparison with modern human facial anatomy and adaptations must take this into consideration (Villmoare et al., 2014).

A recent study of nasal airflow using fluid dynamics also supports the climatic theory. The authors found that fluid residence time was similar for the reconstructed nasal cavity of Neanderthal and that of modern human arctic populations and concluded that the nasal performance in terms of airflow in Neanderthals and modern human arctic populations can be seen as a case of convergent adaptation for cold and dry environments (De Azevedo et al., 2017).

Another interpretation of Neanderthal facial features considers them a biomechanical adaptation to their postulated paramasticatory behaviour, as suggested by the heavy wear of their front teeth (Rak, 1986; Trinkaus, 1987; Demes, 1987). However, Wallace et al., (1975), comparing Neanderthal specimens with modern human populations and primates, suggest that incisor rounding is more likely the result of contact with abrasive food. Furthermore, other authors (O'Connor et al., 2005; Clement et al., 2012) observed that all Late Pleistocene hominins show heavy anterior tooth wearing and that Neanderthals are not different in this respect.

Another biomechanical hypothesis interprets the general reduction in size and thus robusticity of the modern human face as a result of reduced mechanical loading during mastication (Wang et al., 2010). However, a recent paper (O'Connor et al., 2005) measured bite force production and efficiency in modern humans and Neanderthals, concluding that differences in size, rather than in the morphology of the maxilla, reflect differences in the masticatory performance, thus suggesting that alternative explanations

for their facial architecture are more likely (*e.g*. physiologic, developmental, and/or stochastic mechanisms).

A further interpretation considers Neanderthal facial morphology as primarily the result of genetic drift (Ackermann and Cheverud, 2004). According to Weaver et al. (2007), cranial morphological differences between Neanderthals and *H. sapiens* can be explained by neutral diversification (drift) better than adaptive explanations.

As evident from most of the studies cited here, the debate about the origin of Neanderthal's autapomorphies is still very much open and further studies are needed to shed light on the processes leading to the peculiar morphology of this species.

Discussion about "why" they arose are elaborated in this section, while Section 1.1.2 analyses theories about "when" they arise during ontogeny and "how" they are carried into adulthood. Indeed, the evolutionary and ontogenetic mechanisms leading to these morphologically distinct species are still to be unravelled.

1.1.8 Objectives and hypotheses

The foregoing review has highlighted a number of areas where the current understanding of facial growth and how it may differ between modern humans and Neanderthals is limited. This thesis aims to address key aspects of these topics, pertinent to understanding how evolution has shaped the crania and particularly the faces of these two closely related hominins. This study quantifies and describes the patterns of cranial and facial growth, development and integration in modern humans and how they differ among different age classes, analysing the internal and external morphology.

While studies of craniofacial modularity and integrations in adult modern humans are numerous (Lieberman et al., 2002; Bookstein et al., 2003; Bruner, 2007; Bastir, 2008), little is known about the relationships among cranial regions when considering shape and size, or form and age, during ontogeny. Most studies of ontogeny have focused on the use of angles, linear measurements and cephalometric landmarks (Lieberman et al., 2000; Bastir and Rosas, 2005; Bastir et al., 2006), because of the ready availability of 2D data. The first part of this study fits into the context of the increasing number of studies that have examined the ontogeny of modern human crania using 3D measurements (Singh et al., 2012; Bastir and Rosas, 2016; Profico et al., 2017) but aims to a more complete analysis of the phenomena of growth, development and integration among cranial regions than has thus far been carried out.

In addition, recent research is progressively more interested in the relationships between internal and external elements of the cranium (Noback et al., 2011; Butaric and Maddux, 2016), therefore this study fits into the body of research focussing on investigating covariation among superficial and internal structures (both soft and skeletal tissues) of the head, with the purpose of increasing understanding of how the infant form develops into an adult and laying the foundation for the building of normative growth and developmental references in modern humans.

This project extends those studies to the ontogenetic growth and development of *H. sapiens* and Neanderthals by comparing their facial ontogenetic trajectories and covariation among facial sub-regions. As extensively addressed in this chapter, facial ontogenetic trajectories have been investigated in *H. sapiens* and *H. neanderthalensis* (Ackermann and Krovitz, 2002; Ponce de Leon and Zollikofer, 2001). However, there has

not been a focus on proper testing of divergence, with the exception of Bastir et al. (2007), who found a significant divergence in the mandible of these two species. This study is the first to test divergence in the upper and midfacial morphology of Neanderthals and modern humans, using a 3D landmark configuration that explores internal and external morphology of these two species. Building on top of the literature elaborated in previous sections, the thesis addresses four general hypotheses that will be broken into working hypotheses in Chapter 3:

1. Allometry, ontogenetic trajectories as well as patterns of integration of the cranial vault, cranial base and face do not differ between different age classes.

Integration between cranial base and face, and cranial base and neurocranium in modern humans has been investigated with contrasting results (Bookstein et al., 2003; Bastir and Rosas, 2004; Lieberman et al., 2008; Mitteroecker and Bookstein, 2008; Singh et al., 2012; Profico et al., 2017), which depend on the choice of the regions of interest and so, the landmark configuration. In this thesis, a comprehensive landmark and semilandmark configuration covering the entire cranial surface of an ontogenetic series is used to characterise and compare growth and developmental changes in allometry and integration.

2. Allometry, ontogenetic trajectories as well as patterns of integration of the zygomatico-maxilla, palate, sinus, nasal cavity and orbits do not differ between different age classes.

This general hypothesis builds on the literature cited in this chapter concerning growth and development of facial elements using linear measurements and cephalometric studies (Bastir and Rosas, 2004; Bastir et al., 2006; Bookstein, 2008; Evteev et al., 2018, Holton et al., 2018). It will be tested by assessing differences in the durations, rates and modes of growth and development and by comparing degrees of integration throughout ontogeny.

3. That the nasal septum and the soft tissues do not have marked growth interactions with each other or to other cranial regions that could drive overall facial growth and development

This hypothesis is derived from the controversy explored in Section 1.1.5 regarding the Functional Matrix and Nasal Septum theories (Scott, 1954, 1956; Moss and Young, 1960; Moss, 1968; Moss et al., 1968). It will be tested by quantifying the covariation among the skeletal bony and cartilaginous elements and the soft-tissue matrices of the face and their relative contributions to overall facial growth and development.

4. Facial ontogenetic trajectories do not diverge significantly among Neanderthals and modern humans. Patterns of integration among facial sub-regions are similar in these two species.

Contrasting results have been reported concerning postnatal facial ontogenetic trajectories in those two species (Ponce de Leon and Zollikofer, 2001; Ackermann and Krovitz, 2002; Bastir et al., 2007), and while it is evident that infant and adult morphologies differ significantly among modern humans and Neanderthals it is unclear how these differences are carried from infancy into adulthood and if similar morphological changes occur in the two species. This hypothesis will be tested by comparing and visualising differences in ontogenetic trajectories and by comparing patterns of facial integration between the two species.

To test these hypotheses, detailed craniofacial ontogenetic 3D models of modern humans and Neanderthals are compared using an approach based on landmarks and semilandmarks using geometric morphometrics and multivariate analysis.

2.0 Materials and methods

2.1 The modern human sample

The modern human sample consists of 68 three-dimensional segmented crania belonging to individuals aged from newborns to adults (see Table S1 of Supplementary Material for list of all specimens).

Segmentation and 3D surface extraction were also performed for the maxillary sinuses (the sinus segmentation was carried out by Anna Lucas for her MSc project and revised by the author). The segmentation procedure is described in Section 2.0.3 of this chapter). For all the specimens of unknown age, this was estimated based on molar eruption (Carr, 1962) up to a maximum of 23.5 years, when full dental maturity is reached (AlQahtani et al., 2010). Age class was defined for all the specimens as follows: younger subadults from 0 to 5.5 years (M1 in crypt), older subadults from 6 to 18 years (M1 erupted to M3 in crypt), adults from 18 years onward (M3 erupting). 19 specimens belonged to the younger subadult group, 21 specimens belonged to the older subadult group and 28 specimens belonged to the adult group.The specimens were obtained by segmenting CT-scans from several collections: the online database Nespos (www.nespos.org), courtesy of the University of Leeds (UK) and the University College London (UK); the Scheuer collection, courtesy of the University of Dundee (UK) and Dr Craig Cunningham.

For path analysis (see Section 2.0.6 of this chapter), linear measurements, volumes and surfaces were extracted from a collection of 227 medical CT-scans of specimens from 0 to 6 years old (age known) courtesy of Dr Evteev and the National Scientific and Practical Centre of Children's Health (SCCH), Moscow (Russia). The use of this dataset was approved by the Independent Ethics committee at the SCCH, Moscow (Russia), and by the Hull York Medical School Ethics Committee, York (UK).

2.2 The Neanderthal sample

The Neanderthal sample consists of: four CT-scans and Micro-CT scans of the younger subadults Mezmaiskaya 1, Le Moustier 2, Pech de l'Aze, Roc de Marsal; one photogrammetry model obtained using the protocol described by Evin et al. (2016) of a cast surface of the older subadult specimen of LaQuina18; the CT-scans of the following adults: La Ferrassie 1, Gibraltar1, Guattari, La Chapelle, Saccopastore 1, Saccopastore 2; one surface scan of the cast of the specimen Amud1. The approximate ages for the Neanderthal immature sample were derived from the literature (Ponce de Leon and Zollikofer, 2001; Martín-González et al., 2012, see Table S2 of Supplementary Material for the list of Neanderthal specimens).

The surface reconstructions and CT-scans of the younger subadults Mezmaiskaya 1 and Le Moustier 2 were kindly provided by Dr Gunz, Prof. Hublin, Prof. Maureille (Gunz et al., 2012). The micro-CT of the Pech de l'Aze specimen was kindly provided by Prof. Balzeau, Prof. Bahuchet, Prof. Grimaud-Hervé at the Musee de l'Homme, Paris (France). The micro-CT of the Roc de Marsal specimen was available on the Nespos Archive, courtesy of Prof. Macchiarelli, Dr Mazurier, and Dr Volpato at the University of Poitiers (France). The CT-scan of the Neanderthal specimens Gibraltar 1 was kindly provided by Dr Kruszynski and the Natural History Museum, London (UK). The Neanderthal cast of La Quina 18 belongs to the cast collection of the Laboratory of Palaeoanthropology and Bioarchaeology of the Sapienza University of Rome (Italy). The CT-scans of the Saccopastore 1 and Saccopastore 2 were kindly shared by Prof. Giorgio Manzi, Sapienza University of Rome (Italy). The CT-scans of La Chapelle and La Ferassie 1 specimens were provided by the Natural History Museum in Paris (France). The CT-scan of Guattari was provided by Dr Bondioli, Pigorini Museum, Rome (Italy). The Amud 1 surface scan was available on the Morphosource database.

2.3 Semi-automatic and automatic segmentation of 3D surfaces

The first step in making a 3D reconstruction from a stack of 2D images is segmentation, in which the structures of interest are labelled as particular materials by either automatically or manually delineating their physical boundaries in contiguous slices (Mansoor et al., 2015).

For this thesis, the CT-scans of the modern human sample were segmented semi-automatically using the software tool Avizo 9.0 (FEI Visualization). Because these scans are of dry bones, contrast is good between the cranium and air, therefore, the initial segmentation could be performed using a single global threshold that maximised the inclusion of bone material in the resulting virtual reconstruction of the crania.

For the global threshold applied to the crania, a histogram-based procedure was chosen. The grey level histogram being bimodal, the value of the threshold was placed in the valley between the two peaks, representing the cranium and the background (Pun, 1980). A second global threshold was applied to segment the maxillary sinus bone material (Figure 2.1). This semi-automatic segmentation often resulted in errors in the reconstruction of the orbital and nasal walls of the sinuses. This is because when CT-scanning, the acquired signal is sampled and not continuous and the effect of partial volume averaging becomes apparent after thresholding (Spoor et al., 1993). Therefore, thresholding of both cranium and sinuses was then reviewed, slice by slice, so that the presence of unwanted elements (such as the scanning bed) and errors in segmentation (small holes in thin-bone structures such as the eye sockets and sinus medial walls) were manually removed using the brush-tool available in Avizo 9.0. In addition, potential small holes in the surfaces were corrected using the Mesh Doctor tool, an automatic polygon mesh improvement tool (Carlson et al., 2016) of the software Geomagic Studio.

This semi-automatic segmentation process was repeated three times on separate days for 9 specimens of *H. sapiens* and error in volume reconstruction was estimated by comparing volumes of the extracted sinuses (see Table S3 of Supplementary Material for details). The mean percentage error was 3.3%. Further, to assess the impact of segmentation approach on estimates of maxillary sinus volume, the volume of the right maxillary sinus of the modern human adult specimens (N=20) obtained by applying an automatic, mesh-based segmentation procedure developed in the R environment, was

compared with that obtained using the traditional semi-automatic approach in the Avizo 9.0 imaging software. The mesh-based segmentation tool is embedded in the R package “Arothron”. The tool, called "ast-3d" (Profico et al., 2018), uses the "Hidden Point Removal" (HPR) operator developed by Katz et al. (2007). In brief, the HPR operator detects the visible points from a single point of view (POV). In the “Arothron” R package the HPR operator is implemented and specifically designed to "prune" skeletal cavities. The method requires the definition of a POV placed inside the cavity to be segmented. The POV was defined by placing a central landmark in the sinus cavity of each cranial mesh using Avizo 9.0. Using the R studio software (R Core Team, 2019), the POV was used as a viewpoint to extract the right sinus mesh. The small holes in the thin orbital and nasal sinus walls of the resultant mesh surfaces were repaired in Geomagic Studio using the Mesh Doctor tool.

The volumes of the sinuses obtained by semi-automatic segmentation in Avizo 9.0 and by automatic surface extraction in R studio were compared using a paired t-test. After the data were tested for their normal distribution (Shapiro-Wilks for manual= 0.9538, and automated= 0.9324), a paired t-test was carried out to test for significant difference in the measured volumes using the two methods. The results (t= 0.6244, p-value= 0.54063), show no significant difference in the estimation of sinus volume between the automatic and manual method (results carried out by Anna Lucas during herMSc).

Furthermore, two adult sinus meshes, one obtained by semi-automatic segmentation in Avizo 9.0 and the other by automatic surface extraction in R studio, were extracted and compared using the mesh distance tool in Avizo 9.0. The resulting colour map underlines that the largest differences in terms of mesh distances are recorded in areas in which, after segmentation, holes were present and fixed automatically using the Mesh Doctor tool in Geomagic Studio (see Figure S1 of Supplementary Material for colour map results).

When the automatic method “ast-3d” was applied to extract the sinus surface of the younger subadult specimens (age 1 to 5.5), this resulted in meshes that presented several large and irregular holes. This is likely because, in infants, sinus walls are thinner than in more mature individuals and were not detected by the automatic tool, which uses a single threshold value. In this case, the application of the Mesh Doctor tool (Geomagic) was not sufficient to fill all the holes appropriately; therefore, the comparison of the semi-automatic and the automatic methods was not possible for the younger subadult

category. Since R studio was unable to perform the sinus segmentation for the younger subadult group, the semi-automatic segmentation in Avizo 9.0 was chosen as the standard procedure for all the specimens.

For the segmentation of the fossil crania, global thresholding and surface rendering were performed on all the specimens for which Micro-CT scans or CT-scans were available.

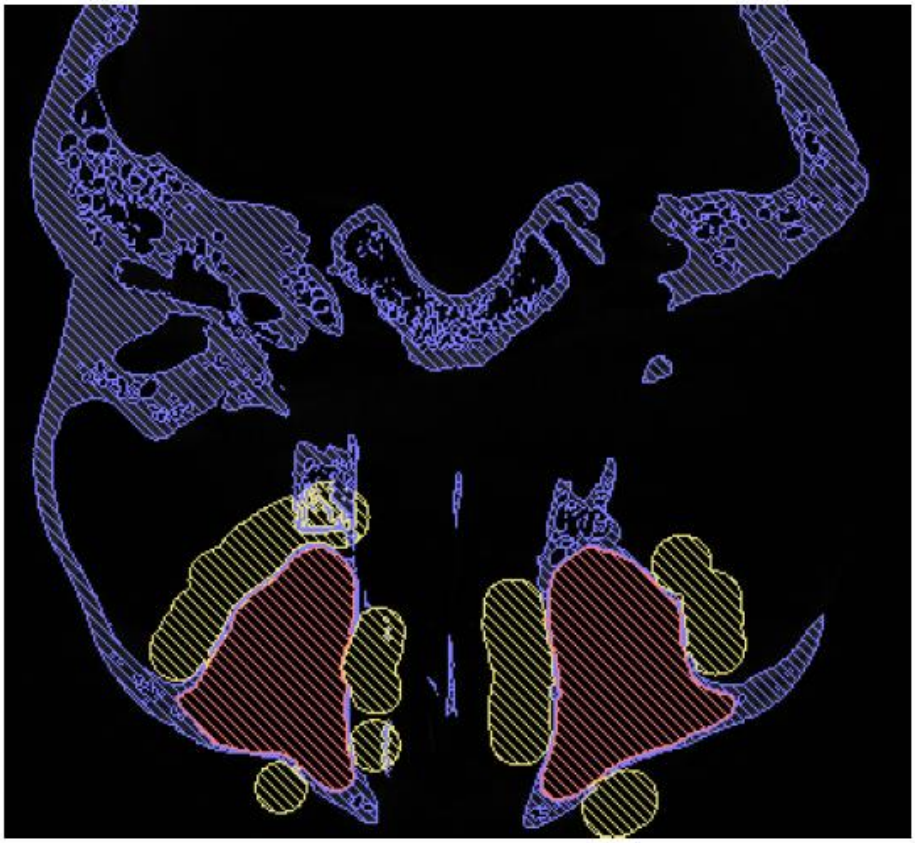

Figure 2.1. The sinus segmentation process performed in Avizo 9.0 showing three materials (transverse plane): blue – threshold defined cortical bone, yellow – temporary added material to close off the medial opening to the nasal cavity and reinforce thin bone walls, and red – the selected sinus cavities *(*segmentation carried out by Anna Lucas during her MSc project and supervised by the author).

2.4 Geometric Morphometrics

2.4.1 Quantification of morphology and analyses of variation

Comparative morphological analysis has always played a central role in biological studies (Adams et al., 2004). Qualitative descriptions of morphology have utility and a long-established history of application but are inherently subjective and lack repeatability. With the advent of multivariate statistical-quantitative approaches in the mid-twentieth century, linear measurements, indices and angles were used to explore shape variations and evaluate morphological differences between taxa (Sokal, 1958; Blackithand Reyment, 1971; Bookstein, 1998).

More recently, Geometric Morphometrics (GM) has provided a powerful tool for the investigation of shape variation and covariation that has been widely applied to the study of organismal growth, development and evolution (Bookstein, 1991; Drydenand Mardia, 1998; Slice et al., 2007; Zelditch, 2012). Increasing numbers of clinical and surgical studies have applied GM to study morphological changes in development, growth or pathology, to identify associations among skeletal units and between them and related soft tissues, to recognise proper and abnormal growth and development and document variation in anatomical structures (Singh et al., 2004; Hajeer et al., 2004). Before going on to consider GM in more detail it is worth reflecting on how it differs from standard morphometric approaches using linear measurements and angles.

Linear measurements between landmarks individually describe the distance between two points, while more than two measurements begin to describe the form, size and shape of an object. Multiple measurements taken on a sample can be submitted to multivariate analysis to assess and describe form variation. The use of linear measurements is well established and, with angular measurements formed the basis of what became known as multivariate morphometrics (Blackith and Reyment, 1971; Mardia et al., 1979). If we are interested in shape, scalings can be applied to the variables before further analysis. Visualisation of the results of multivariate morphometric analyses of form or shape based on linear measurements is possible if the measurements are designed in such a way that the original geometry of the object can be reconstructed (*e.g.*

in Euclidean Distance Matrix Analysis, EDMA; Lele and Richtsmeier, 1991; Richtsmeier et al., 1993 a,b; Adams et al., 2004; and truss measures, Strauss and Bookstein, 1982)

However, the use of linear measurements or angles to describe shape is problematic. The key issue is that the shape spaces resulting from scaling of inter-landmark distances and from angles have undesirable distributions in the resulting shape spaces and so are a poor choice for statistical analysis (O'Higgins, 2000; Rohlf, 2000).

These issues were the subject of intense debate and discoveries in the 1980s and 1990s (Bookstein, 1982; O'Higgins and Dryden, 1992; Richtsmeier et al., 1992; O'Higgins and Dryden, 1993; Bookstein, 1996; Marcus and Corti, 1996; Dryden and Mardia, 1998; Rohlf, 1999) and led to the advent of GM, an approach that caused a shift in the way in which biological structures were measured and investigated in many disciplines (Rohlf and Marcus, 1993).

In GM the geometry of an object, its form, is described using the landmark coordinates themselves, rather than measurements taken between them (Zelditch et al., 2012). To be comparable, these coordinates have to be equivalent in some sense, which means that they must correspond to points that are believed to have 'the same' developmental, evolutionary or functional significance in different organisms (O'Higgins, 1997; Bookstein, 1997).

Landmarks can be placed on 2D (X-rays, pictures) and 3D surfaces (mesh renderings from CT-scan, laser scan or photogrammetry) and should be chosen to provide an adequate representation of the object under study depending on the underpinning biological question (whether it is developmental, evolutionary, functional, etc) (O'Higgins, 1997; Lele and Richtsmeier, 2001). When equivalent points between specimens are scarce, semilandmarks (defined as those on curves or surfaces with location ill-defined; Bookstein, 1997; Mitteroecker and Gunz, 2009; Gunz and Mitteroecker, 2013) can be applied to improve visualisation and multivariate analyses, as long as a sufficient number of equivalent landmarks can be used as a fixed reference to control subsequent sliding to minimise location error between specimens (see Section 2.0.4.5 of this chapter on sliding semilandmarks).

2.4.2 Generalised Procrustes Analysis

The configurations of landmarks differ among objects in form (size and shape) and in location and orientation. Geometric morphometric analyses aim to investigate the shape of objects, regardless of 'size' (specifically, centroid size, see below), location and orientation in space. As such, GM relies on the computation of shape differences among objects, expressed as Procrustes distances. These distances are estimated through Generalised Procrustes Analysis (GPA; Gower, 1975; Kendall, 1984; Rohlf and Slice, 1990; Goodall, 1991). This proceeds by standardising size, position and orientation of the landmark configurations through registration. Squared distances between equivalent landmarks taken on all specimens are minimised by scaling, translating and rotating (aligning) the individual's landmark configurations using their centroid (the arithmetic mean of all landmark coordinates, Mitteroecker et al., 2013). Scaling is carried out such that the centroid size (CS or Csize - the square root of the sum of squared distances of a set of landmarks from their centroid, Mitteroecker and Gunz, 2009) of each configuration is scaled to 1 by dividing the raw landmarks by their centroid size. Configurations are then superimposed at their centroids and iteratively rotated with respect to each other to minimize the sum of squared distances of the specimens from the mean shape. In the first iteration, the specimens are aligned to an arbitrarily chosen one and once all configurations are fitted to this, the rotation minimises distances between equivalent landmarks. Once all specimens are fitted, the sample mean of each coordinate is computed. In subsequent iterations, the configurations are fitted to the mean, which is recomputed and used in the next iteration. The algorithm stops when the sum of residuals from the mean reaches a minimum, usually after 3-5 iterations. The resulting registered landmark coordinates are known as 'shape coordinates' and can be submitted to statistical analysis. In the present study, GPA was carried out using the function "ProcSym" of the package "Morpho" in R studio (Schlager, 2017).

After GPA, specimens come to lie on the manifold of a hypersphere known as Kendall's shape space (Kendall, 1984; Goodall, 1991; Dryden and Mardia, 1993). As long as variations are small, the scatter of points over this manifold will be concentrated and, for practical purposes, the region of shape space which they occupy can be considered approximately planar and so suitable for multivariate analyses using linear models

(Dryden and Mardia, 1993). However, it is common to linearize formally the region of Kendall's shape space occupied by the specimens under study by carrying out a tangent projection (Dryden and Mardia, 1993; Kent and Mardia, 2001).

The tangent projected shape variables are then submitted to statistical analyses pertinent to the question at hand. Centroid size differences are also of interest and these can be used to examine how shape covaries with centroid size in studies of allometry or combined with shape data, as an extra column in the shape coordinate data matrix (Mitteroecker et a., 2004; Mitteroecker et al., 2013), allowing analyses of size and shape differences or covariance with other factors using standard multivariate methods (Chatzigianni and Halazonetis, 2009; Pujol et al., 2016).

In GM the results of multivariate statistical analyses can readily be visualised as warpings of points. By interpolating the differences in the shape of the landmark configuration to the space between landmarks, using Thin Plate Splines (TPS), visualisations can incorporate surfaces and volumes. Such visualisations allow us to intuitively appreciate shape variations.

In this thesis, geometric morphometric methods were used to investigate growth trajectories, covariation and modularity between cranial regions in modern humans and the extent to which the same patterns can be observed in the ontogeny of Neanderthals.

2.4.3 Landmark and semilandmark configuration used in the study

For the modern human sample, 89 landmarks were recorded on the 3D surface mesh of each cranium, covering the external and internal surfaces of the face, base and cranial vault (Figure 2.2 and 2.3). A list of definitions of the landmarks used in this thesis is provided in Table S4 of Supplementary Material.

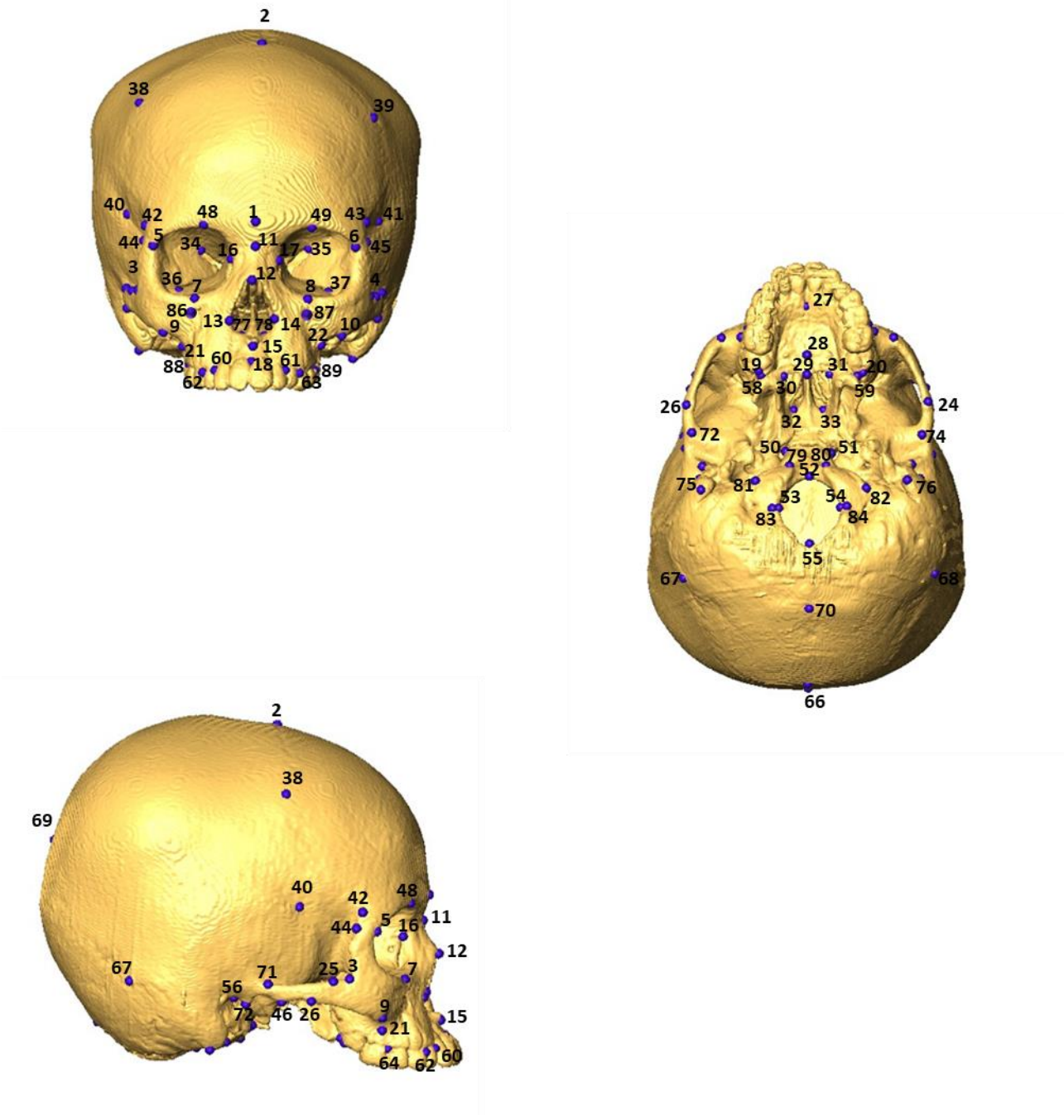

Figure 2.2. Landmark configuration (89 landmarks) shown on a juvenile specimen of modern human. Image created by the author using Avizo 9.0.

Another set of landmarks was designed for the maxillary sinuses (Figure 2.3). Six landmarks were located on the surface of each sinus, five of these were defined as geometrical landmarks: the most extreme surface points on the antero-posterior and dorso-ventral axes, and the most lateral points on the left-right axis, with crania oriented along the Frankfort Plane (Maddux and Butaric, 2017). One homologous landmark (type I) was collected on the internal surface of the maxillary sinuses, defined as the ostium, which connects the maxillary sinuses to the middle turbinate.

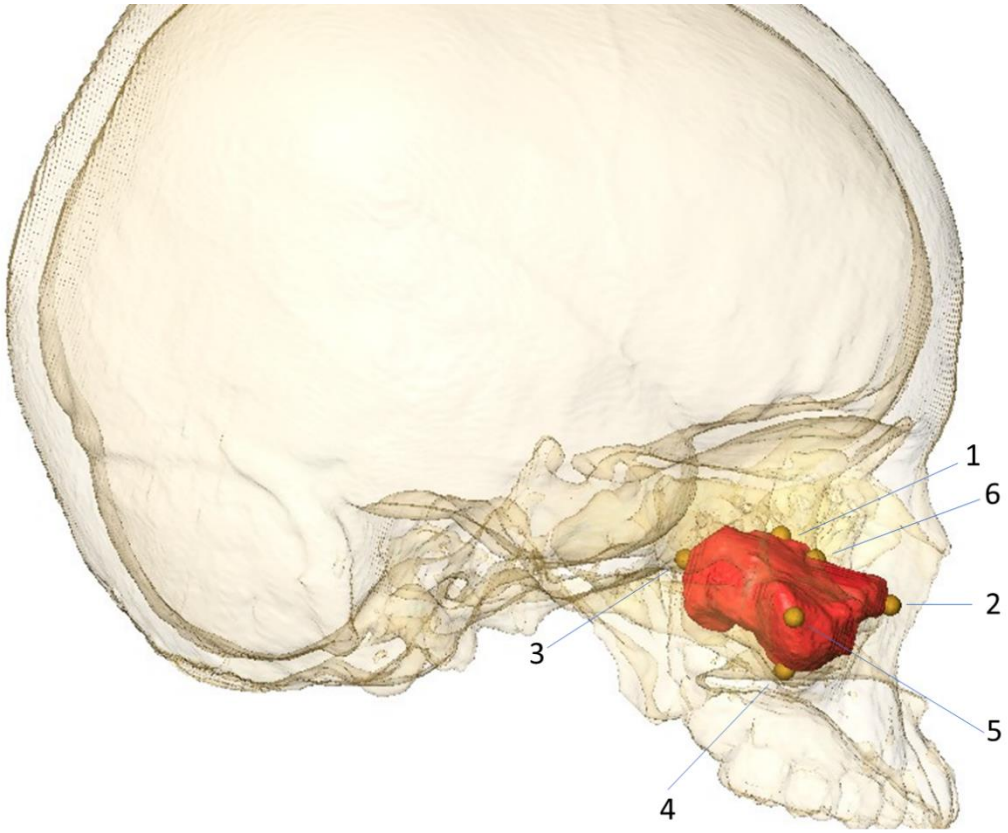

Figure 2.3. Maxillary sinus landmark configuration shown on a right sinus (6 Landmarks) with the cranium oriented on the Frankfort Plane: L1 most superior point on the maxillary sinus; L2 most anterior point on the maxillary sinus; L3 most posterior point on maxillary sinus; L4 most inferior point on the dorso- ventral axis of maxillary sinus; L5 most lateral point on the maxillary sinus; L6 point on the maxillary sinus ostium on the internal surface of maxillary sinus. Image created by the author using Avizo 9.0.

For the study of the cranial regions of the vault, base and face (Chapter 3 Section 3.1) the cranial landmark configuration (89 landmarks) was used as a reference for building a template of 155 3D surface semilandmarks covering the entire cranium (Figure 2.4). Semilandmarks (Gunz and Mitteroecker, 2013) are useful to capture shape variations on anatomical regions devoid of clearly delineated landmarks (*e.g.* cranial vault). The template of semilandmarks was built using the specimen that was closest (Procrustes distance) to the mean shape of the modern human sample, as assessed by Procrustes distance.

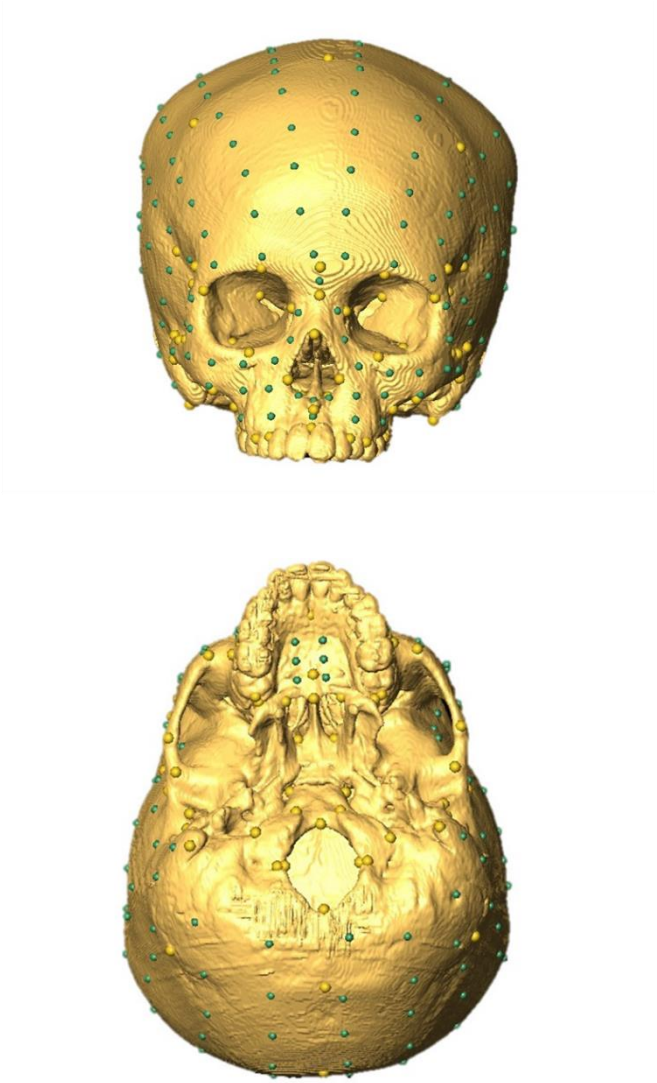

Figure 2.4. Landmark (yellow) and semilandmark (green) configurations used for the study of cranial ontogeny in modern humans shown on a juvenile specimen. Image created by the author using Avizo 9.0.

Additional semilandmarks were collected on curves to describe the complex morphology of the nasal rim, orbital margins and nasal choanae (Katina et al., 2007). A total of 44 curve semilandmarks was recorded for each specimen (Figure 2.5). The sliding of semilandmarks (see Section 2.1.6 of this chapter for details of the procedure) was performed considering fixed, surface and curved semilandmarks simultaneously.

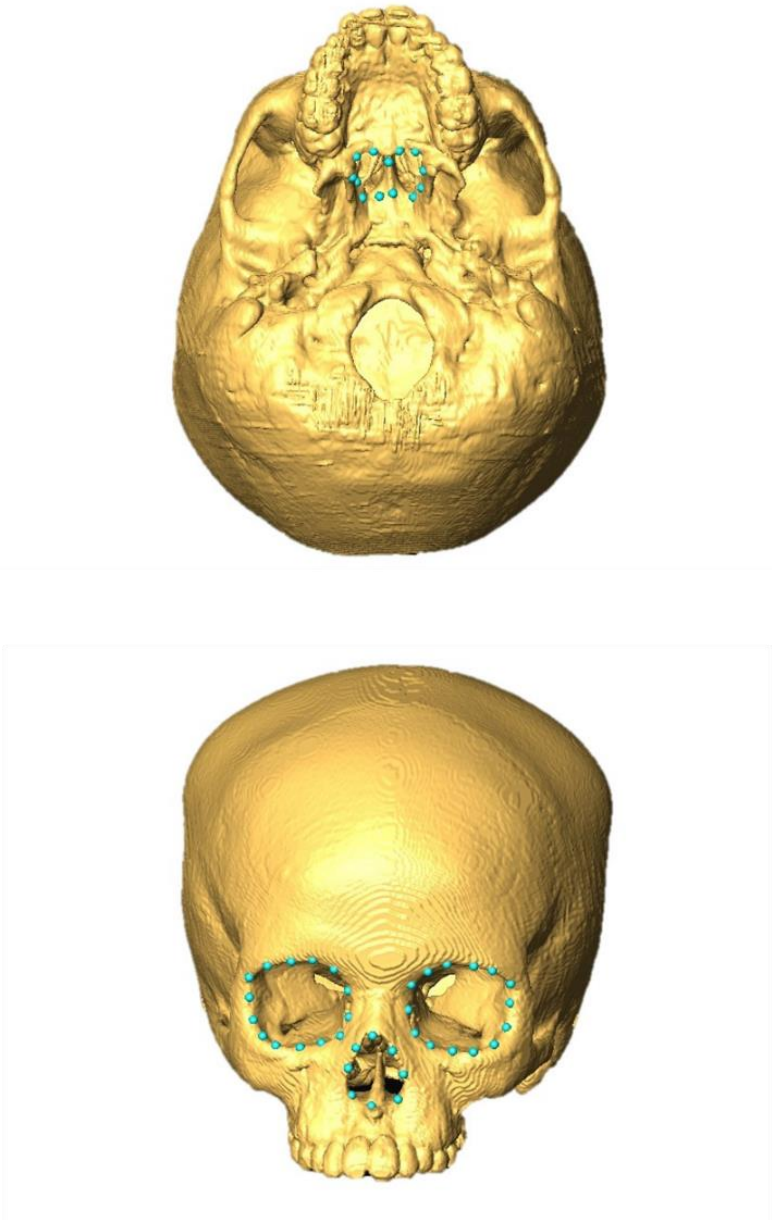

Figure 2.5. Curve semilandmark configuration used for the study of cranial ontogeny in modern humans shown on a juvenile specimen: orbital rims, piriform aperture, choanal rim. Image created by the author using Avizo 9.0.

A subset of the cranial landmark configuration covering only the face (43 landmarks) was used for the ontogenetic study of the facial morphology (Chapter 3 Section 3.2) and used as a reference to build another set of 36 surface semilandmarks and 22 curve semilandmarks (Figure 2.6). A separate process of sliding was performed for this dataset.

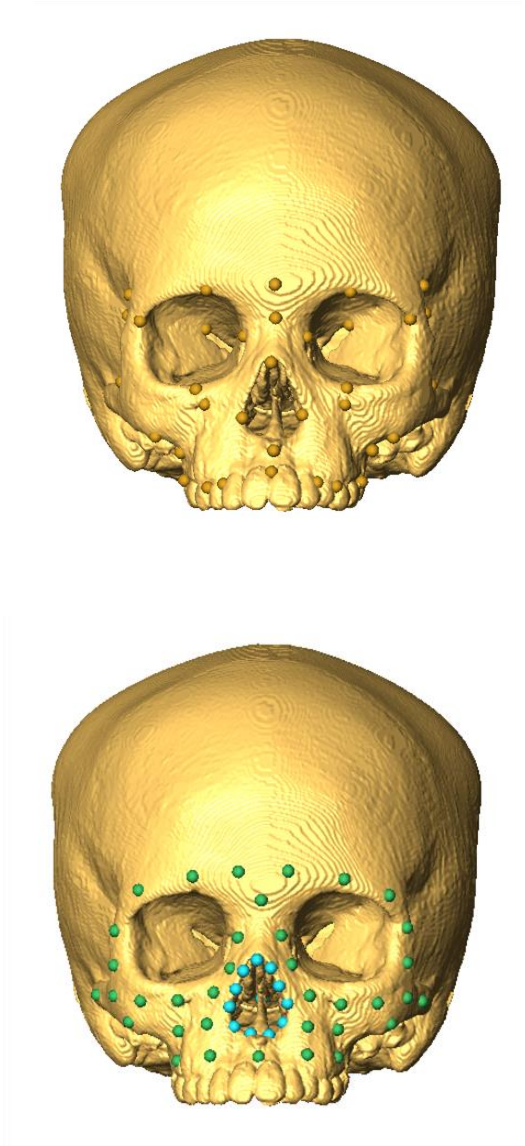

Figure 2.6. Landmarks and semilandmarks for the study of facial ontogeny in modern humans shown on a juvenile specimen: choanal rim semilandmarks not visible. Image created by the author using Avizo 9.0.

For the analyses that include the Neanderthal fossil sample, the same configuration of 43 facial landmarks was used (Figure 2.7). In order to obtain a landmark configuration that describes the internal and external anatomy of the midfacial region, missing landmarks

were estimated in each fossil specimen using TPS (Mitteroecker and Gunz, 2009, see Section 2.0.4.4 for further details).

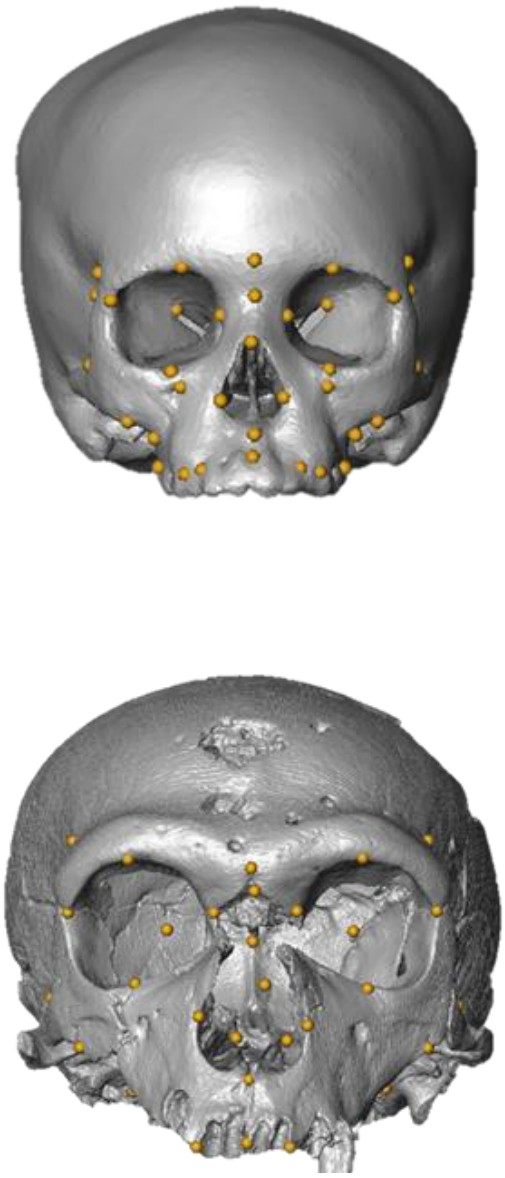

Figure 2.7. Set of 43 landmarks used to analyse the relations between *H. sapiens* and *H. neanderthalensis*. Top: juvenile of *H. sapiens*, bottom: adult of *H. neanderthalensis*.

2.4.4 Intraobserver error and missing data

To assess the intra-observer error in landmarking and to ensure the reproducibility of results, two adult and two juvenile modern humans were landmarked on five separate occasions (days) over one month. After performing a GPA, a PCA was carried out and the distribution of data was observed empirically to ensure that the variance due to repetition in landmarking the same specimen was smaller than the variance among specimen repeat means (Von Cramon-Taubadel et al., 2007; see Figure S2 of Supplementary Material for details).

Missing landmarks were estimated for the dataset of *H. neanderthalensis*. Although incomplete, specimens with missing landmarks can provide useful information and Arbour and Brown (2014) have argued that they should not be removed from the sample, except for those cases in which it is not possible to collect most of the landmarks of the total configuration. By comparing the variance structure within each data set, the authors were able to examine the point at which the inclusion of reconstructed specimens more closely matched the variation present within the original data set, than by analysing complete specimens alone. The results lead to the conclusion that removing incomplete specimens can affect landmark-based shape analyses more than estimating missing data.

Geometric mean, regression and TPS methods have been applied in the literature to estimate missing landmarks. The geometric morphometric mean method (Adams et al., 2004; Neeser et al., 2009; Brown et al., 2012; Arbour and Brown, 2014) estimates the mean shape (average Procrustes shape) of a dataset. After Procrustes registration of the specimen with missing landmarks to the mean, based on available landmarks, the shape coordinates of the mean are substituted for missing shape coordinates in the incomplete specimen. An alternative, the regression method, estimates missing data via least-squares regression (Adams et al., 2004; Couette and White, 2010; Brown et al., 2012; Arbour and Brown, 2014), predicting missing coordinates from the regression coefficients derived from complete landmark configurations. Missing landmarks can also be estimated using a TPS interpolation procedure (Gunz et al., 2009). Thin plate splines are used to interpolate differences in relative landmark locations between two specimens to the space between the landmarks. Interpolation using TPS has proven reliable for missing landmark estimation in skeletal material (Gunz et al., 2009; Arbour and Brown, 2014). TPS

estimates the missing landmarks by warping the mean shape of a complete configuration (reference) onto the incomplete configuration (target), based on the subset of common landmarks between the reference and the target. This interpolation function works by minimizing the bending energy (analogised as the energy required to deform a thin, uniform metal sheet between landmark configurations) of the warping. This leads to a smooth interpolation of the space between landmarks (Gunz et al., 2005; Mitteroecker and Gunz, 2009). To carry out TPS estimation of missing landmarks, a reference specimen is required as well as one or more target specimens, whose landmarks are missing. The reference can be a particularly well-preserved and complete specimen or a mean shape (Mitteroecker and Gunz, 2009).

A recent study has compared the performance of geometric mean substitution, regression and TPS in terms of accuracy of estimation of landmarks in incomplete specimens (Arbour and Brown, 2014). In 3 out of the 5 samples (each one consisting of one or more closely related species), for frequencies of incomplete specimens lower than 20% of the total sample, TPS, geometric mean substitution and regression performed equally in the estimation of missing values. In all cases, using any of the estimation methods was always better than excluding the incomplete specimens from the sample (results also confirmed by Couette and White, 2010). The authors conclude that TPS estimation generally performs less well than the other two methods, but that results depend on frequencies of missing data, type of dataset and number of landmarks. In fact, when using another dataset, Neeser et al. (2009) found that TPS is a better estimator than the geometric mean substitution method. Therefore, the efficacy of TPS is at least approximately equivalent to the other methods for low frequencies of incomplete specimens and landmarks (<20%) and in the absence of large morphological differences between the taxa used for the estimation (i.e closely related species, Arbour and Brown, 2014).

The missing data in the sample used for this study consist of 12 specimens (all belonging to *H. neanderthalensis*) over 81 total specimens (*H. neanderthalensis* and modern humans), thus the frequency of individuals with missing data is 15%. The number of missing landmarks for each of the 12 specimens varies between 4 and 9 (average of 7 missing landmarks). 43 landmarks are used in the present study, thus the missing landmarks represent about 15-20% of the total.

To assess the performance of TPS, geometric mean substitution and regression, an accuracy analysis was carried out in which known landmarks were treated as missing and estimated using each of these approaches. The resulting Euclidean and Procrustes distances (see Figure S3 of Supplementary Material) show that TPS was the most accurate method for estimating missing landmarks and therefore this method was applied to estimate missing landmarks in the present dataset. No good same-species fossil reference specimen was available for the estimation of the missing landmarks. Therefore, this was based on the sample of modern humans as Neeser et al., (2009) showed that using a closely related modern sample resulted in better estimation than using a phylogenetically closer single individual.

After superimposition of the modern human and Neanderthal dataset, the 10 closest complete specimens to each damaged individual (in terms of Procrustes distance) were chosen to estimate a mean individual and perform the warping using TPS. Mirroring was not performed at this stage as it reduces the asymmetric variation between sides and therefore potential information about developmental instability (Couette and White, 2010) and other-sided landmarks were often not available.

2.4.5 Sliding semilandmarks

Earlier in this thesis, semilandmarks were described as being those on curves or surfaces with ill-defined exact location over the surface or curve. This lack of adequate localisation of matched surface or curve points renders them 'noisy', *i.e.* they add error variance to the data. In order to resolve this, the idea of sliding semilandmarks was first raised by Bookstein (1996b) as a way of minimising error in location of semilandmarks among a sample of specimens. The basic idea is that a few true landmarks are located on surfaces and curves and then a fixed number of semilandmarks are placed with approximately even spacing over the surface or curve. The exact number of semilandmarks to be sited on any one surface or curve is determined by the practicalities of the study and the complexity of topography to be described by them. In a second step an algorithm is used

to slide the semilandmarks over the surface such that the differences (either measured by bending energy or Procrustes distance) among specimens are minimised.

The sliding procedure iteratively adjusts the positions of the semilandmarks until either the Procrustes distance or bending energy between the template and the target form is minimal. The choice of Procrustes distance or bending energy leads to different eventual semilandmark positions and there is no clear basis for choosing one over the other. However, minimisation of Procrustes distances takes the locations of all fixed landmarks equally into account to guide the sliding, whereas the minimisation of bending energy gives greater weight to landmarks near the surface or curve. For this reason, minimisation of bending energy is often preferred (Gunz et al., 2005). The sliding algorithm is iterative, first sliding all specimens to an arbitrarily chosen 'reference specimen' and then, in a second step, computing the mean of all slid specimens estimated after GPA and re-sliding against that. After sliding, landmarks and semilandmarks each have the same weight in subsequent statistical analyses (Gunz and Mitteroecker, 2013).

In the present study, sliding was performed in R studio and the Evan Toolbox. Different results were found on occasion because the EVAN toolbox was prone to projecting landmarks onto nearby surfaces (*i.e.* to the inner surface of the vault from the outer). The R studio package "Morpho" (Schlager 2017, functions "CreateAtlas", "PlacePatch" and "Slider3D") proved to be the most reliable for performing the sliding when the surface mesh has a double layer (*e.g.* cranial vault ecto and endocranial surfaces). This result is probably due to the inflation parameter implemented in the "Morpho" package that minimises the risk of semilandmarks being projected onto the wrong surface. The software R studio was also used to slide semilandmarks along the curves. Using the function "surface path" in Avizo 9.0, four curved lines (orbits, nasal rim, choanal rim) were acquired on each specimen. Subsequently, for each curve, a predefined number of equidistantly located semilandmarks was placed automatically (function "bezierCurveFit" of the R package "bezier"; Olsen, 2014). As already mentioned, after Procrustes superimposition of the landmark and semilandmark datasets, the mean shape was used to slide the semilandmarks along the curves and surface in a single iterative operation to minimise the bending energy between each specimen and the mean shape.

2.4.6 Thin plate splines, transformation grids and warping

Once landmarks have been collected, the form of specimens can be compared pairwise, visually, in terms of warpings between them, or patterns of variation within the entire sample can be assessed using Procrustes-based statistical analyses.

Warping of meshes representing surfaces or of volumes of specimens involves interpolation of differences in landmark configurations to the space in the vicinity of the landmarks, occupied by virtual objects representing surfaces or volumes (Whiteback and Guo, 2006). Thus, differences between two landmark configurations are used to smoothly warp surface meshes or volumes representing the anatomical structure on which the landmark configurations were taken (Bookstein, 1991). The two configurations are termed the reference configuration (the original object surface or volume) and the target configuration (into which the object will be warped). They could be two specimens or represent objects at opposite poles of a vector of interest arising from statistical analyses, as described below.

In GM, warping is most commonly achieved using two (for 2D) or three (for 3D) Thin Plate Splines (TPS) as interpolating functions. The thin plate spline comprises a uniform (uniform stretching and shears) and a non-uniform component. It interpolates differences in relative landmark locations to the space between them, minimising a quantity from the non-uniform component known as the bending energy, analogised as the energy required to deform a thin, uniform metal sheet. The 'metal sheet' is constrained at landmark coordinates but otherwise free to adopt the form that requires the minimum bending energy. This leads to a smooth interpolation of the space between landmarks (Mitteroecker and Gunz, 2009). As noted above, bending energy is commonly minimised by the algorithm used to slide semilandmarks. This is because bending energy is larger for localised deformations than global ones of the same magnitude. Thus, sliding of semilandmarks based on minimisation of bending energy gives greater weight to minimisation of localised 'errors' in their initial locations.

Transformation grids (Thompson, 1917) are often used to visualise local variations in shape differences between two landmark configurations as a deformation (Figure 2.8). They are calculated using one thin plate spline per dimension (2, for 2D or 3 for 3D data). The grids can be interpreted as indicating how the space in the region of a reference shape might be deformed into that in the region of the target such that landmarks of the reference map exactly onto those of the target. The graphical representation of shape differences resulting from these approaches is readily interpretable in 2D but less so in 3D, where warping of a surface or volume as a movie or a series of 'stills' may lead to a better understanding of the nature and degree of form differences between configurations. Care should be taken in balancing the visual appeal of transformation grids against the underlying assumptions (*e.g.* smooth interpolation) in their construction. From a biological perspective, it is important to bear in mind that this mapping is purely mathematical, and it is based only on the locations of the original landmarks (O'Higgins, 2000).

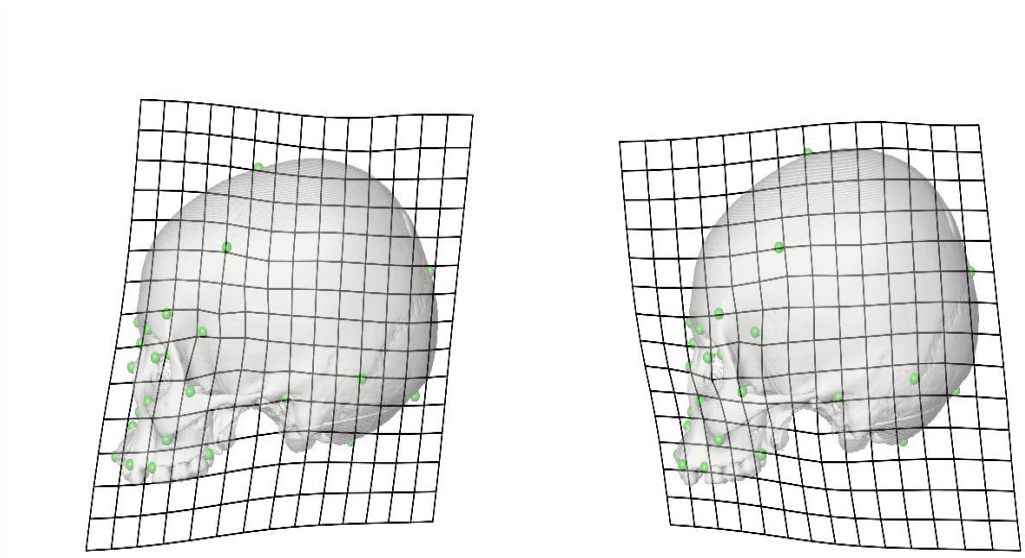

Figure 2.8. Transformation grids showing shape differences between two human crania. The grids are sited in the sagittal plane and the crania are rendered semi-transparent so the grids can be viewed. A regular square grid was drawn over the mean (reference) of the two crania and then it was deformed into each of them (targets). Thus, it shows equal and opposite deformations in each that indicate the local and global differences in shape between the two landmark configurations. Image created by the author using Avizo 9.0.

Visualisation of warped surfaces can be improved by colour mapping the surface mesh to represent regions of varying expansion or contraction (Profico et al., 2015; Piras et al., 2020). The result is registration-independent colour maps showing variations in rates of local expansion or contraction of the surface mesh. When preparing the mesh, its triangulation is adjusted (Delaunay triangulation; Joe, 1991) to ensure triangles are close to equilateral, which facilitate the plotting of a smooth colour map of changes in area over the surface. The rates of expansion of triangles in the warped surfaces (a reference and a target) are then colour coded and plotted on the target mesh, to represent differences in area between the warped reference and target crania (Figure 2.9).

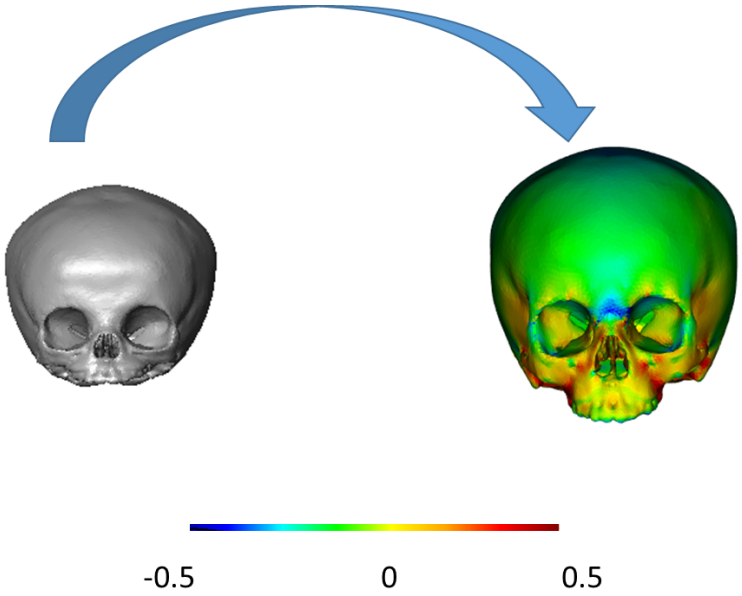

Figure 2.9. Example of a colour map resulting from calculation of differences in the surface areas of two warped meshes (actual size proportions). Left: reference, right: target.

2.5 Multivariate statistical methods

As already described earlier, with the advent of multivariate morphometrics (Blackith and Reyment, 1971; Mardia et al., 1979), which replaced qualitative descriptions, linear measurements, angles and indices were applied to explore biological forms (Sneath and Sokal, 1962; Blackith and Reyment, 1971; Bookstein, 1998).

However, the use of linear measurements or angles to describe shape causes some issues. The key issue is that after scaling of inter-landmark distances or using angles, the resulting shape spaces have undesirable statistical properties (independent isotropic error at landmarks does not result in isotropic distributions in the resulting shape spaces) and show some problematics when it comes to statistical analysis (Rohlf, 2000).

With the introduction of geometric morphometrics, a powerful set of tools for the investigation of shape variation and covariation was developed and applied to the study of organismal growth, development and evolution (Roth and Mercer 2000; Cobb and O'Higgins, 2004; Mitteroecker et al., 2004; Goergen et al., 2017).

2.5.1 Principal Component Analysis

Ordination methods are used to visualise the scatter of points representing specimens within the shape space. They allow groupings and modes of variation among specimens to be visualised. The most commonly applied ordination method in GM studies is principal component analysis (PCA). In this, new orthogonal (therefore independent and uncorrelated) variables, the principal components (PCs), are extracted from the matrix of shape variables previously computed using GPA (see Section 2.0.5.1). These are linear combinations, rotations, of the original variables, sorted by decreasing variance (Dryden and Mardia, 1992; Slice et al., 2007; Zelditch et al., 2012) and retain the relationships (distances) among points. They allow the scatter of points in the high dimensional space defined by the original correlated variables to be appreciated in fewer dimensions

defined by the uncorrelated PCs, retaining as much as possible of the variance of the original dataset (Jolliffe, 1986).

2.5.2 Multivariate regression

Multivariate regression considers shape as dependent on another variable of interest (such as size, time, diet, etc.), resulting in a vector of regression coefficients that indicates the change of shape per unit of change in the independent variable (Drake and Klingenberg, 2008; Klingenberg, 2013). Multivariate regression allows predicting specimen shape for a given value of the independent variable and allows the computation of the proportion of total shape variance explained by the independent variable (R^2) and the relative significance (estimated using p-values). By predicting shapes at extremes of the regression vector and computing transformation grids using warped surfaces or object volumes as described above, the shape changes along a regression vector can be visualised.

2.5.3 Partial Least Squares analysis

Partial Least Squares analysis (PLS) allows the covariation between two or more 'blocks' of variables to be quantified and visualised. PLS, when performed within a morphometric context is also called Singular Warp (SW) Analysis (Bookstein et al., 2003). It computes the linear combination of two sets or "blocks" of shape variables (two landmark sets) that maximise the explained covariance between blocks. It results in pairs of singular axes (also known as singular warps, singular vectors or PLS axes) which, when plotted against each other, display the association between blocks. This can be quantified for each pair of axes by computing Pearson's correlation coefficient between the scores of each block (Hollander et al., 2013). To calculate the significance of this, the estimated value is

compared to the distribution of values obtained by randomly permuting (1000 times) the individuals in one block. When the estimated covariation is larger than *e.g.* 5% of the permuted ones, the association is significant at the 5% level, p-value < 0.05 (Bookstein et al., 2003).

In the application of PLS to landmark data for studies of modularity and integration, GPA is first carried out in each block and then PLS is performed between these blocks of data. For each species, the two blocks of landmarks are aligned by Procrustes superimposition. GPA is performed separately for each block, because performing the registration of the entire dataset before running the PLS analysis leads to overestimation of the percentage of covariance between blocks (Klingenberg, 2009; 2013). This is because a common superimposition introduces an element of covariance between all specimens and across all landmarks, especially the more contiguous ones. PLS analysis results in a series of plots of pairs of singular axes. The proportion of total covariance explained by each pair of axes is also calculated. Beyond this, PLS also allows calculating the proportion of total variance in each block explained by each singular axis for that block (Cardini, 2019). It is important to consider the strength and significance of correlations, the proportion of the total covariance explained by pairs of singular axes as well as the proportion of total variance in each block explained by each singular axis in reporting the results of PLS analyses. This is because a strong association between blocks does not necessarily indicate that a large proportion of the variance of each block is explained by the analysis. Thus, blocks can be strongly associated, but this association may account for a large or a small proportion of variance in each block. A strong and highly significant association that accounts for a very small proportion of the total variance in one or other block, while being statistically significant, might have little real morphological or biological meaning. For the visualisation of the patterns of association resulting from PLS, the mean of each block is warped along each singular axis and the two warpings are presented.

2.6 Path analysis

The statistical method of path analysis is a multiple regression method elaborated by the statistician Wright (1921), commonly used to investigate the proportion of contribution of a series of variables to social outcomes (Pajares and Miller, 1994; Rudasill ad Kaufman, 2009). More recently, path analysis has been applied to the assessment of *a priori* causal hypotheses relating to developmental and evolutionary hierarchical interactions (Mooney et al., 1989; Holton and Franciscus, 2008; Caparros et al., 2012). To apply path analysis, it is necessary to formulate two or more path models (or one path model with two or more sub-paths, each led by an exogenous independent variable) that reflect the principal alternative hypotheses (Figure 2.10).

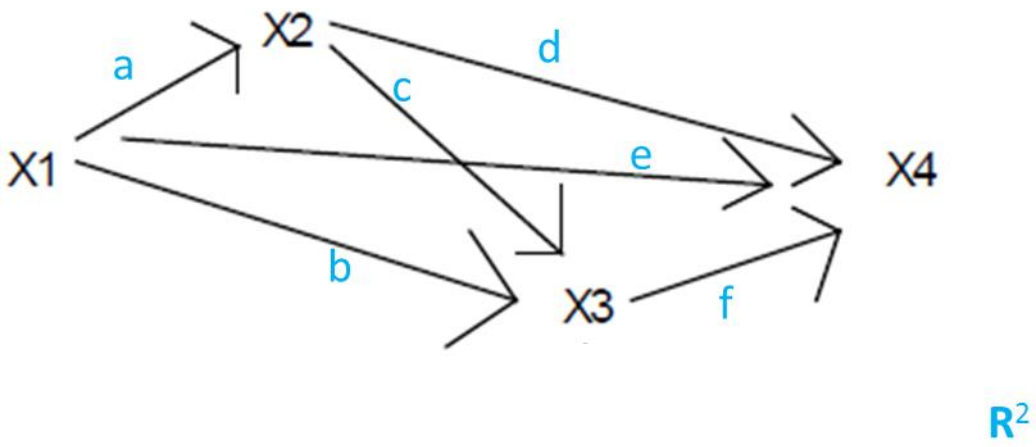

Figure 2.10. Modified from Williams (2015). A typical example of path analysis applied to a path model: X1 represents the exogenous, independent variable, affecting X4 directly, and indirectly through its influence on the intermediate variables X2 and X3. The multiple linear regressions (function "lm" in R studio) are estimated as follows: X1 (independent variable) is hypothesised to affect (arrow a) the variable X2 (dependent variable) so that their relation is lm(X2~ X1) with ~ indicating dependence of X2 on X1; X3 is affected by X1 (arrow b) and X2 (arrow c) so that their relation is lm(X3 ~ X2 + X1), with X2 and X1 acting simultaneously on X3; X4 (the endogenous variable) is affected by all the variables: X1 (via the path e), X2

(arrow d) and X3 (arrow f) so that their relation is lm(X4 ~ X2 + X1 + X3). Each multiple regression is characterised by a series of beta coefficients, each describing the relationship between the independent variable(s) and the dependent one. The R^2 statistic is used to describe the goodness of fit of each regression model. The overall R^2 of the entire path model is defined as the variance of the dependent endogenous variable X4 explained by its relation with all the variables in the model that have arrows pointing at it.

Each path comprises a series of interacting variables, with one or more exogenous (independent) variables that are not influenced by any of the others, some intermediate, endogenous variables that affect and are at the same time influenced by other variables, and one or more endogenous variables that do not influence but are fully dependent on other intermediate variables.

The patterns of interactions that are to be tested are derived from previous theoretical and experimental evidence. They are indicated by arrows pointing from the independent variables toward the ones they are hypothesised to affect. Thus in the hypothetical example (Figure 2.9, above) the variable X1 is anatomically connected to X2, X3, and X4 and it forms early in development, so it might be hypothesised that it directly influences the growth and development of each. Additionally, X2 is hypothesised, based on prior evidence, to impact the growth and development of X3 and X4, while X3 affects only X4. The hypothesis is that X1 is driving all the major changes in X2, X3 and X4, but the relative influence of each variable on the others is unknown and needs path analysis to be explored. In this model, X1 influences X4 through a direct path, and indirectly through its influence on X2.

This first model can then be compared with an alternative model, in which, for example, a new variable, X5, also anatomically connected to X2 and X3, replaces X1 and is hypothesised to influence the ontogeny of these anatomical regions.

Alternatively, two exogenous variables can be introduced in the same path, and their effect on the intermediate and final variables compared.

After building one or more path diagrams, the impact of the independent variables on the dependent ones is estimated using a series of multiple regressions, which provide a series of standardised beta coefficients (β or path coefficients or standardised regression coefficients or standardised partial regression coefficients if the model has two or more independent variables) and R^2 (% of variance of dependent variable explained by the

regression). The coefficients and R^2 are analysed within a path (or between different path diagrams if more than one path are designed), to identify the most likely causal/temporal sequencing of variables based on the strength of the associations.

If more than one model is compared, the best model (highest R^2 and beta coefficients) is considered most complete in terms of explanation of the interactions among parts. Holton et al., (2008) used such an approach to investigate growth and developmental interactions in the face of *H. sapiens*, focussing on how soft and hard tissues interact in infants from 0 to 6 years old. In this study, the multiple regressions were performed in R studio using the function “lm” of the package “stats”.

3.0 Research and results

3.1 Covariation and correlation in the human cranium: a 3D morphometric study of the interactions between cranial base, cranial vault and facial complex during ontogeny

3.1.1 The importance of cranial element interactions

The study of the dynamics of cranial ontogeny, *i.e.* the developmental interactions and integration of cranial components, the postnatal morphological changes in cranial regions and the rate and mode of these changes is of interest to workers in several fields (Ackermann and Krovitz, 2002). Thus, morphologists and clinicians aim to understand normal and abnormal patterns of growth and development to improve craniofacial surgical practice (Honn and Goz, 2007; Jiang et al., 2015; Gkantidis and Halazonetis, 2011; Escaravage and Dutton, 2013; Likus et al., 2014; Evteev et al., 2018), while physical anthropologists and archaeologists investigate modern and past anatomical trends (Viðarsdóttir et al., 2002; Rozzi and De Castro, 2004; Bastir et al., 2007; Cobb and O'Higgins, 2007; Zollikofer and Ponce de Leon, 2010; Lacruz et al., 2015). In this context, two central questions concerning the growth and development of the cranium are: i) how do the many components of the head manage to function and accommodate one another as they change in size and shape during ontogeny? And ii) are the patterns of interaction among parts of the cranium constant during ontogeny and between closely related species?

3.1.2 Modules and regions of the cranium

Increasing attention has been directed towards postnatal developmental interactions among cranial components, assessing the degree of independence and interaction among them. This is because such interactions are important in guiding development and allowing evolutionary adaptation of parts as well as of the whole. Differences in patterns

of interaction and relative autonomy among parts are therefore of interest in understanding how morphological differences have evolved. In this context, the term 'module' is used to indicate a unit that is internally integrated and coherent due to tight interactions among its elements, but that is relatively autonomous from other units with which it has weaker or less constrained interactions (Klingenberg, 2009). In development, hypothesised modules may comprise sets of genes, cells or tissues. In studies of the postnatal cranium, they are commonly identified based on morphology informed by knowledge of developmental origins or because they serve a single functional role (Marquez, 2008; Hallgrimsson et al., 2009).

To test whether hypothesised modules behave as cohesive units that are more or less independent of each other, a series of statistical tests can be performed, which measure the covariation among the subsets of landmarks that define hypothesised modules and contrast these with the covariation among randomised subsets of landmarks (Bastir, 2008; Klingenberg, 2008; 2009; 2013; Mitteroecker and Bookstein, 2008; Campbell and Willmore, 2009; Martínez-Abadías et al., 2012; Rolian, 2014). This allows the assessment of the significanceof apparent patterns of developmental integration and modularity within and among the hypothesised modules.

Independence among modules allows evolution to select for morphological change in a particular module that might subserve specific and distinct functions, while not affecting other modules; association among traits allows integrated development and functions of the cranium as a whole (Cheverud, 1996; Lieberman et al., 2000; Hallgrımsson et al., 2004; Sardi et al., 2007; Wagner et al., 2007; Hallgrımsson et al., 2007; Porto et al., 2013).

The description of the morphological growth and development of a specific cranial region in a species and of differences in the same region between closely related species has been the focus of several studies (Ross and Henneberg, 1995; Lieberman, 1998; González-José et al., 2004; Bulygina et al., 2006; Sardi and Rozzi, 2012). Other studies have looked at patterns of modularity and integration *among adjacent modules within a species,* by studying how specific changes in one cranial unit affect the others (Lieberman et al., 2000; González-José et al., 2004; Hallgrimsson et al., 2007, 2009; Martínez-Abadías et al., 2009; Klingenberg, 2013; Barbeito-Andrés et al., 2015). Using covariation analyses, regression analyses and analyses of modularity and integration between anatomical components (Mitteroecker and Bookstein, 2008; Klingenberg, 2013), it is possible to

investigate the extent to which cranial elements (hypothesised modules) develop independently of, or are integrated with other elements (Hallgrimsson et al., 2007; Cardini and Elton, 2008; Hallgrimsson et al., 2009; Klingenberg 2008, 2009, 2013; Porto et al., 2009, 2013). Furthermore, patterns of integration *among modules* can then be compared *between species,* to gain insights into the evolutionary mechanisms acting over time (Ackermann, 2005; Bastir et al., 2005; Bastir, 2008; Singh et al., 2012; Vilmoare et al., 2014; Profico et al., 2017).

3.1.3 Hypotheses on craniofacial growth and development

Differences in the tempo and mode of maturation of cranial regions are frequently addressed in medical, biological and evolutionary studies (Enlow and Hans, 1996; Bastir et al., 2006; O'Higgins et al., 2006; Porto et al., 2013). While understanding ontogenetic development can help to establish less invasive and more precise and effective surgical or medical interventions (Zarrinkelk et al., 1995; Nahhas et al., 2014), the spatio-temporal ordering of ontogenetic transformations is of interest in biological anthropology to explain differences in growth, development and adult form among species (Viðarsdóttir et al., 2002).

The cranium is commonly considered to comprise three major modules: cranial vault, base and the face (Bastir and Rosas, 2004; Richtsmeier and Ponce de Leon, 2009). These elements have a distinct embryological origin and serve separate functions (Gkantidis and Halazonetis, 2011). However, the face, vault and base are morphologically articulated, which means that during growth and development they are to some extent physically constrained by and interact with the other elements (Profico et al., 2017). Several studies using linear measurements, angles and cephalometric data (Lieberman et al., 2000; Bookstein et al., 2003; Bastir and Rosas, 2004; Bastir et al., 2006), and more recently using 3D landmarks (Singh et al., 2012; Bastir and Rosas, 2016; Barbeito-Andrés et al., 2015), have focussed on the extent to which these regions are independent during their growth and development, and the extent to which each of these regions is constrained and limited in its morphology by the others (Zollikofer et al., 2017).

In modern humans, the face typically grows in an analogous way to the skeleton, following a similar pattern of temporal variation in the rate of development as found in the postcranium, with rapid growth through infancy, followed by a slower growth during childhood, resuming a rapid growth during puberty until the eruption of the third molar (Hutton et al., 2003), with contrasting results on the age of the actual cessation of bone growth (Levine et al., 2003). The trajectories of the cranial vault and cranial base are different and more closely follow a neural pattern of growth, with the most rapid changes in size occurring in the first postnatal years; neurocranial growth then significantly decreases, as does brain growth, which is mostly complete in terms of total dimensions by the time of eruption of the first molar (Lieberman, 2011). When looking at cephalograms using midline landmarks, Bastir et al., (2006) found that the cranial base is the first to achieve shape maturation, while the cranial vault region is the first to reach adult size, followed by the cranial base and last, the midface and lower face. Since different modules reach maturity at different times, patterns of interaction among them change. For instance, if the growth and development of a module directly affect that of another module this can occur only until the first one reaches maturity. After this, changes in the, as yet immature, second module are no longer directly influenced by changes in the first module but are, to some degree, constrained by it (Ross et al., 2004).

As discussed above, the growth and development of these three regions and the time at which each of them reaches maturity in terms of size and shape and their interactions have been largely investigated using 2D measurements and cephalograms (Lieberman et al., 2000; Bookstein et al., 2003; Bastir and Rosas, 2004; Bastir et al., 2006). Three-dimensional landmarks have been used to describe the ontogeny in modern humans mostly by exploring the data using Principal Component Analysis (Gunz et al., 2010; Freidline, 2012). Nevertheless, only recently attention has been pointed toward the identification of the exact relations between size and shape (allometry), the rate of shape and size changes and the degree of covariance during growth and development within and across human cranial regions using three-dimensional data (Singh et al., 2012; Bastir and Rosas, 2016; Barbeito-Andrés et al., 2015; Zollikofer et al., 2017).

Because studies of cephalograms show that the basicranium matures in size and shape before the facial complex, it has been suggested that its growth, development and flexion might have a significant influence on the way in which the face subsequently develops,

especially on its orientation and prognathism (Buschang et al., 1983; Lieberman, 1998; Bastir et al., 2006; Bruner and Jeffrey, 2007; Bruner and Ripani, 2008; Gkantidis and Halazonetis, 2011). Indeed, in modern humans, a reduced cranial base angle (when compared to other hominins) has been linked to the phenomenon of brain globularisation (spatial packing hypothesis, Ravosa, 1988; Enlow, 1990; Ross et al., 2004). In addition, changes in locomotion in *H. sapiens* have also been associated to a reduced cranial base angle, which, in turn, have been associated to a less prognathic, more retracted face relative to the anterior cranial fossa (Lieberman et al., 2000).

In addition, brain changes in size and proportions (especially in the upper area of the brain) also affect the cranial vault morphology. Indeed, if the brain does not develop during prenatal ontogeny, the skullcap does not form (Evans et al., 2009). Changes in the cranial vault also appear to be linked to the temporal pattern of morphological maturation of the cranial base (Lieberman, 1998; Lieberman et al., 2002; Bastir and Rosas, 2006; Gkantidis and Halazonetis, 2011). However, as described by Zollikofer et al. (2017) in a paper that summarises current hypotheses of craniofacial integration, other authors postulate that is the facial orientation that impacts cranial base and vault morphology (Bolk, 1909; Schultz, 1942; Ross and Ravosa, 1993; Bienvenu et al., 2011), therefore implying that endocranial morphology is not entirely driven by brain evolution and development. In this scenario, the cranial base could be influenced by the facial complex and have an impact on brain morphology and development (Bruner, 2015).

The midface (specifically the ethmo-maxillary complex) is in connection with the middle cranial base fossa (McCarthy, 2001), and the facial orbital roof is linked to the anterior cranial fossa and the frontal lobes it hosts (Hallgrimsson et al., 2007; Bruner, 2015). As noted above, previous workers have postulated that the shape, relative position and orientation of the cranial base change to accommodate the spatial requirements of the face (Lieberman et al. 2002, 2008; Bastir and Rosas, 2004, 2009; Bastir et al., 2006, 2010; Hallgrimsson et al., 2007), through mutual interactions with the developing brain. Furthermore, it has been suggested that the cranial base may be influenced by factors involved in mastication because of the position of the middle cranial fossa relative to the mandibular articulation (Bastir and Rosas, 2005).

Studies of modularity and integration also show that the cranial base, vault and face, while traditionally seen as modules, actually show a high degree of integration (Martínez-

Abadías et al., 2012). These findings support Enlow's vision of the skull as a highly integrated unit (Enlow, 1968; 1990; McCarthy, 2004). However, it has been shown that the face has a certain degree of independence from the neurocranial complex during growth and development (Bastir et al., 2006; Bastir and Rosas, 2006; Esteve-Altava et al., 2015; Neaux et al., 2015; Profico et al., 2017). Furthermore, during growth, regions of the cranium increase in size. The extent to which they do this in a temporally and spatially coordinated way accounts for many aspects of integration among cranial elements during ontogeny (Porto et al., 2013). When size is taken into account, non-allometric patterns of variation suggest some autonomy in the development of the different cranial regions (Bastir and Rosas, 2004).

The extent to which developmental interactions between the brain, cranial vault, cranial base, and the face influence the evolution, development and variation of the cranium is still unclear (Bastir, 2008). While much research has been devoted to identifying craniofacial modules and understanding how and when they appear, become integrated and change during ontogeny, the interactions are still uncertain even in humans, which have been very intensively studied (Sardi and Rozzi, 2005). This is because of uncertainty in identifying modules (*i.e.* is the face a module, or does it comprise modules such as the alveolo-dental complex, nose, zygomatics, etc?) and the lack of 3D ontogenetic data, which could allow identification of modules and how the pattern and strength of their interactions change over time.

Further studies are needed to better identify developmental modules and understand the ways in which postnatal ontogenetic modularity and integration contribute to the adult morphology. In this section, modularity and integration among the three putative modules identified in previous work, the face, base and vault, are studied in 3D on a cross-sectional ontogenetic series of human crania using landmarks and semilandmarks. The aim is to address some unresolved questions: does the neurocranium act as a constraint on the growth and development of the facial complex? What are the strength and mode of intereaction between the cranial base, vault and faceduring ontogeny? How do the patterns of modularity and integration that we observe change through postnatal development?

3.1.4 The hypotheses

This section examines the ontogeny of the cranial base, vault and face in terms of size and shape changes and the patterns of covariation within and among them. An ontogenetic sample of 68 specimens of modern humans from newborn to adult stages is used to test the following null hypotheses:

Hypothesis 1a. *The mode of shape and form change is consistent throughout postnatal ontogeny for the whole cranium and for the cranial base, vault and face.*

This hypothesis can be rejected if the vector of ontogenetic shape and form change from birth to adulthood is not linear. Hypothesis 1a is likely to be falsified, since similar studies have reached this conclusion. However, the analyses characterise the mode and tempo of ontogenetic shape and form changes in the sample to guide interpretation of results from hypothesis 1b.

Hypothesis 1b. T*he cranium as a whole and the cranial base, vault and face each scale in a consistent way throughout ontogeny.*

This null hypothesis can be rejected if size-related shape changes in the cranium or in any of the three regions change significantly during ontogeny. While Hypotheses 1a is tested by comparing shape and form changes in the cranium and cranial regions over time, Hypothesis 1b is tested by comparing allometric scaling of the shape of the whole cranium, face, vault and base among age classes.

Hypothesis 1c. *The pattern and degree of shape covariation among the cranial base, vault and face do not change throughout development.*

This null hypothesis can be rejected if, when comparing different age classes, significant changes are observed in the absolute and relative magnitudes of covariation among these cranial regions. Hypothesis 1c is based on prior work which has shown that patterns of morphological integration and modularity undergo subtle changes during ontogeny, but very little is known about the extent of these changes (Martínez-Abadías et al., 2009,

2011). In the present study, patterns of covariation are compared among age classes, as well as among regions at the same ontogenetic stages. Shape variations represented by PLS axes are visualised using TPS warpings.

3.1.5 Material and methods

3.1.5.1 The sample

An ontogenetic sample of 68 modern human crania was used in the present study. The specimens consist of 3D meshes representing bone and teeth, segmented from CT-scans. For those specimens of unknown age, the patterns of dental eruption were used to estimate age class based on modern human standards (Carr, 1962; AlQahtani et al., 2010; see Table S1 of Supplementary Material for further information). Age class was based on dental eruption patterns and defined as follows: younger subadults from 0 to 5.5 years, older subadults from 6 to 18 years, adults from 18 years onward.

Sex was unknown for some of the specimens therefore this variable was not considered in the study.

3.1.5.2 The dataset

A combination of landmarks and sliding semilandmarks was employed to represent cranial size and shape. The landmarks comprise 89 points recorded on 3D surface meshes, covering the face, base and cranial vault (see Figure 2.2, Chapter 2). Additionally, 155 surface semilandmarks and 44 curve semilandmarks were acquired on a juvenile cranium used as the template specimen. Semilandmarks were used to characterise the form of regions where Type I or Type II landmarks are not plentiful, such as the neurocranium (Bookstein, 1991). As it has been shown in previous work (Bookstein, 1991,

1997; Mitteroecker et al., 2004; Gunz et al., 2005), semilandmarks also provide for more detailed visualisation of shape variations resulting from geometric morphometric analyses.

After the first step of sliding of the specimens against the template, the mean configuration (consensus) was created and sliding was performed again, using the mean as the new template. The cranial configuration (89 landmarks + 199 surface and curve semilandmarks) was then divided into 3 anatomical subsets: the cranial vault, cranial base and face. A third step of sliding against the consensus was then performed separately for each subset.

3.1.5.3 Statistical analyses

The hypotheses were tested using a set of multivariate statistical analyses.

Hypothesis 1a: *consistency in postnatal ontogeny.*

This hypothesis was explored using Principal Component Analyses (PCA) in order to identify any non-linearity in the mode of ontogenetic form and shape changes. Ontogenetic changes in shape and form of the entire cranium during ontogeny were explored by submitting landmark coordinates after Generalised Procrustes Analysis (GPA) to PCA. GPA/PCA was also used to explore ontogenetic changes in shape and form of the vault, base and face. Because changes in size and shape during ontogeny occur simultaneously, looking at form offers a more comprehensive approach to investigate ontogenetic changes (Mitteroecker et al., 2013). When considering form (size and shape) changes during ontogeny, a separate GPA was performed instead of the usual matrix of Procrustes shape coordinates being used in subsequent analyses (*e.g.* PCA). These coordinates were augmented by an additional column (dimension) of the natural logarithms (ln) of the centroid sizes of each specimen (Mitteroecker et al., 2004), thus creating a size-shape space in which form changes are visualised. The GPA was performed using the argument "sizeshape= TRUE" in the "ProcSym" function of the R package "Morpho" (Schlager, 2017). The logarithmic transformation of the centroid size guarantees that variance in centroid size does not dominate and for isotropic landmark

variation, the distribution in size-shape space is isotropic (Mitteroecker et al., 2013). The resulting distribution is (hyper)spherical and thus this space supports the interpretation of PCs (Mitteroecker et al., 2004; Klingenberg, 2016) in that, if a dominant vector of variation is found it is not simply because size variation is much greater than shape variation. Logarithmic correction is also common as a way to linearize relationships between traits and to account for different size units (Cardini and Polly, 2013; Mitteroecker et al., 2013).

To visualise differences between crania representing ontogenetic stages, warpings along PC axes or due to allometric scaling, a surface mesh of a juvenile specimen was warped using TPS (Bookstein, 1989). Surface mesh warpings were visualised as registration independent colour maps showing variations in rates of local expansion or contraction of the surface mesh. To prepare the mesh, its triangulation was adjusted (Delaunay triangulation; Joe, 1991) to ensure that as far as possible triangles were close to equilateral, to facilitate the plotting of a smooth colour map of changes in area over the surface as described below. The rates of expansion of triangles in the warped surfaces were colour coded to represent differences in area between the warped reference and target crania. The warpings were performed using Evan Toolbox 1.72 (O'Higgins et al., 2012) and the colour maps were calculated using the function "localmeshdiff" of the R package "Arothron" (Profico et al., 2015).

Hypothesis 1b: *allometric variation of the cranium during ontogeny*.

To test if ontogenetic allometric trends differ between age classes, multivariate regression was carried out for different age classes and regions. The multivariate regression analysis was performed in the Evan Toolbox 1.72. Testing of divergence in ontogenetic trajectories between younger subadults (younger than 5.5 years old) and older subadults (between 6 and 18 years old) and between the latter and adults (18+ years old) was performed using the regression vectors resulting from the multivariate regression for each of the two age classes and the angle between them computed (angle test). Its significance was assessed using permutation test, in which the age class membership was randomly permuted and the angle recalculated. One thousand permutations were carried out and the estimated angle between the species was compared with the distribution of permuted angles to assess its significance.

Hypothesis 1c, integration and modularity among the cranial base, vault and face.

To assess the degree of independence of each region from the others (face, cranial base and vault) or their mutual interactions during ontogeny, pairwise partial least squares (PLS) analysis was performed, comparing two anatomical regions at a time. The analysis was first performed on the entire sample, then on the three age categories separately: younger subadults, older subadults and adults. PLS quantifies the degree of covariance between two anatomical blocks by finding a new set of variables (known as singular warps or PLS axes) that account for the highest possible covariation between the two original anatomical sets (Bastir et al., 2005). Correlation coefficients between the scores on these singular warps for each of the two blocks give information about the strength of the association between blocks, while statistical significance is assessed by permutation tests.

In this study, PLS was used to investigate the magnitude and nature of covariance (*i.e.* modes of deformation that covary between blocks) among the three main regions of the cranium at different age classes. A full Procrustes superimposition was performed separately each time for the two blocks, because a common superimposition (as is commonly carried out; Bookstein et al., 2003; Klinbengerg, 2009; Baab, 2013) overestimates the degree of covariation between two blocks and might find significant correlations in random data (Cardini, 2019). To assess how much of the total shape variance of a single block is "explained" by its association with the other block in the PLS, the percentage of total shape variance accounted for by specific PLS axes (the ratio between the variance of PLS scores and the sum of the variances of the shape coordinates) was calculated for each block. This measure is important because two blocks may show a very strong association between PLS scores even though the proportion of variance of each of the blocks explained by the PLS axes is very small (Cardini, 2019). The PLS was performed using the function "Pls2B" from the R package "Morpho" (Schlager, 2017).

3.1.6 Results

Hypothesis 1 a. *The mode of shape and form change is consistent throughout postnatal ontogeny for the whole cranium and for the cranial base, vault and face.*

The PC plots of Figure 3.1.1 and Figure 3.1.2 show the distribution of the ontogenetic sample along the first two principal components of cranial shape (full GPA performed) and form (shape + ln centroid size). To visualise the regions of the cranium undergoing greatest changes in absolute and relative size during postnatal ontogeny, warpings of the mean along the principal components of the shape and form space (respectively Figure 3.1.1 and 3.1.2) were computed. Subsequently, differences in the areas of surface mesh triangles between the warped crania were calculated and represented using a colour map. The colour map indicates the changes in the areas of the mesh triangles from the reference to the target surface. Variations are plotted on the target mesh and are shown using a blue to red colour scale, indicating minimum (blue) or maximum (red) changes in area. While the colour of each triangle represents change in area alone, the resulting distribution of colours indicates changes in proportion, with red regions becoming relatively large, blue changing little and green representing intermediate relative size increases. To make the colour maps comparable among different PCAs, these were calculated using a common range of values determined by using the overall minimum and maximum range values obtained when first performing separate colour maps for the whole cranium, vault, face and base. Two different ranges were estimated when calculating the colour maps in the shape and form space.

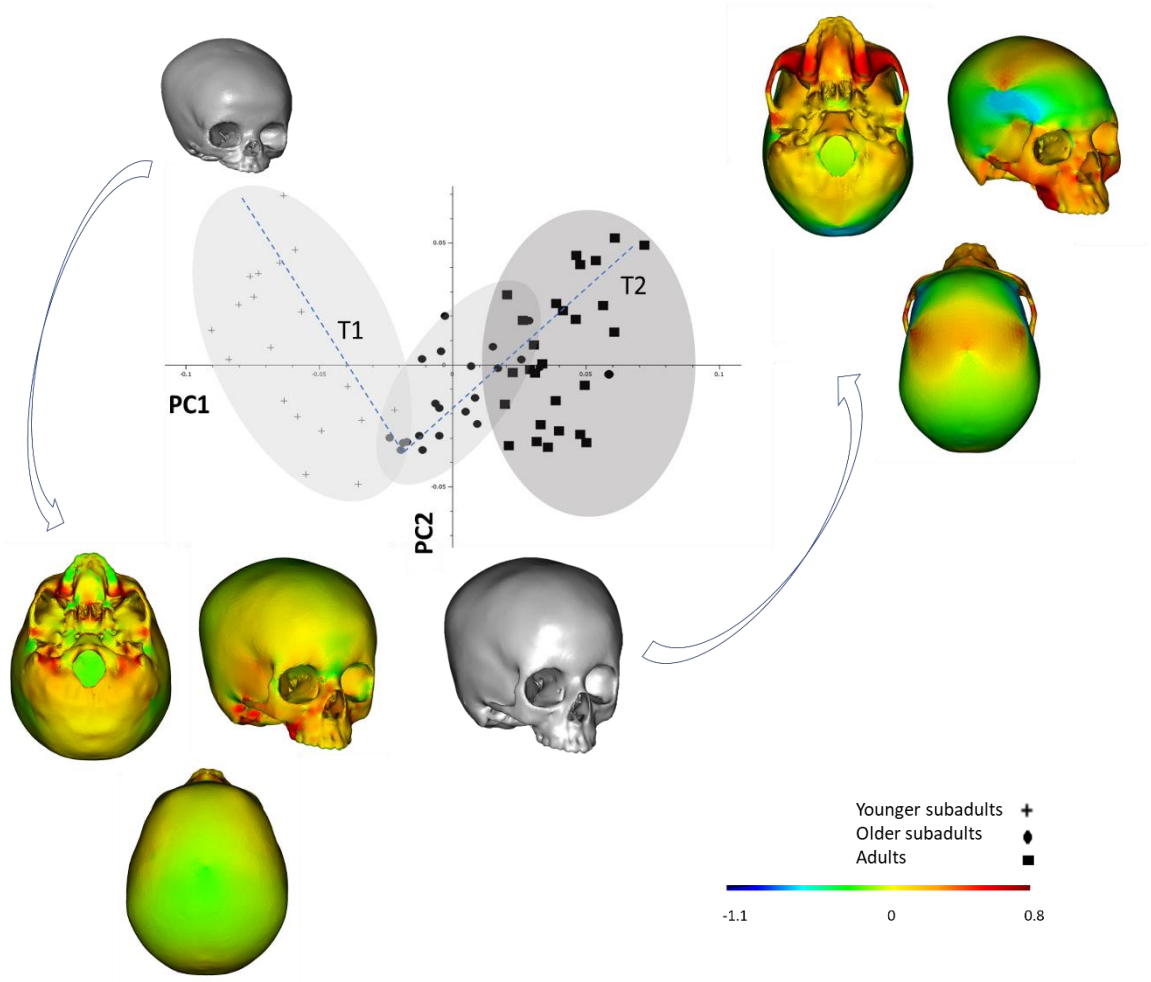

Figure 3.1.1. PCA of cranial shape for the modern human ontogenetic sample using landmarks and semilandmarks. The variance accounted for by the first three components is: PC1 35%; PC2 14%; PC3 7%). The grey ellipses encompass each of the 3 age classes: younger subadults, older subadults and adults. T1 and T2 lines were drawn manually to join younger to older subadults and those to the adult group, thus facilitating thereading of the plot: T1 spans along the younger subadult ellipse, T2 spans along the older subadult and adult ellipses and differs in direction from T1. The two lines have no statistical meaning. Warpings of the younger to older subadult and older subadult to adult trajectories are visualised using colour maps. Variations are shown using a blue to red colour scale, indicating minimum (blue) or maximum (red) changes in area. Arrows indicate the reference and target warpings used to calculate the colour maps.

In the shape PCA of Figure 3.1.1, the first principal component accounts for 35% and the second for 14% of the overall variation. The PCA shows a non-linear ontogenetic trend of development from newborns to adults as indicated by the lines.

Since PC1 shows the largest and most significant correlation with centroid size in the sample (PC1 R^2= 0.84, p-value < 0.001; PC2 R^2= 0.07, p-value < 0.05, PC3 not significant), variation described by this PC represents general aspects of allometry during ontogeny and accounts for about 35% of the total variance. It would be incorrect to conclude however that a single linear trajectory between birth and adulthood adequately explains ontogeny. Rather, there appears to be a distinct change between the younger and older subadult samples. As a result, the inset visualisations of the warped mean in Figure 3.1.1 show the variations in the cranial shape represented by the two ontogenetic trajectories : from younger subadults to first appearance of older subadults and fromolder subadults to adults. Along the first trajectory, the cranial vault expands in the frontal region (yellow area) but relatively less along the parietals (green colour), while the cranial base flexes and expands relatively (yellow to red areas), resulting in the globularisation of the neurocranium along this trajectory. Accompanying this, the facial complex undergoes the greater relative expansion (yellow to red areas), particularly in the region of the midface (maxilla and nasal regions) as warpings show an increasing relative forward projection of the nasal bridge and downward development of the maxillary complex. The orbits decrease in relative size and change in shape toward a more squared morphology.

A change from the first trajectory in the direction of development can be observed in the trajectory from older subadults to adults, indicating that shape changes differ from the first trajectory (younger subadults to first appeareance of older subadults). The midfacial complex undergoes even more relative expansion as the red areas on the colour map increase on the midfacial surface (on the anterior maxilla but even more on the maxillary arch and posterior palate) and the warpings show the maxilla continuing to develop inferiorly, particularly in the posterior region. There is an accompanying increase in the relative size of the nasal cavity and the alveolar region becomes more elongated and slightly more pronounced.

Along the second trajectory , changes in the cranial vault appear to be more marked in the bregmatic region (yellow to red area on the vault warping on the top right of the graph) and less pronounced on the squamous part of the occipital (blue region) as well

as in the lateral contact region between the parietal and the temporal bone (pterion-cyan and blue area). However, this region was prone to error in landmarking as the sutures were difficult to locate, therefore this result could be influenced by this observation. The frontal region undergoes relative contraction from the older subadult to the adult morphology (green area). Patterns of colour in the cranial base remain similar to what observed for the first trajectory, although less pronounced.

After performing a GPA, a PCA in the size-shape space (or form space) was produced, in which the natural logarithm of centroid size was included as an additional column to the shape data matrix.

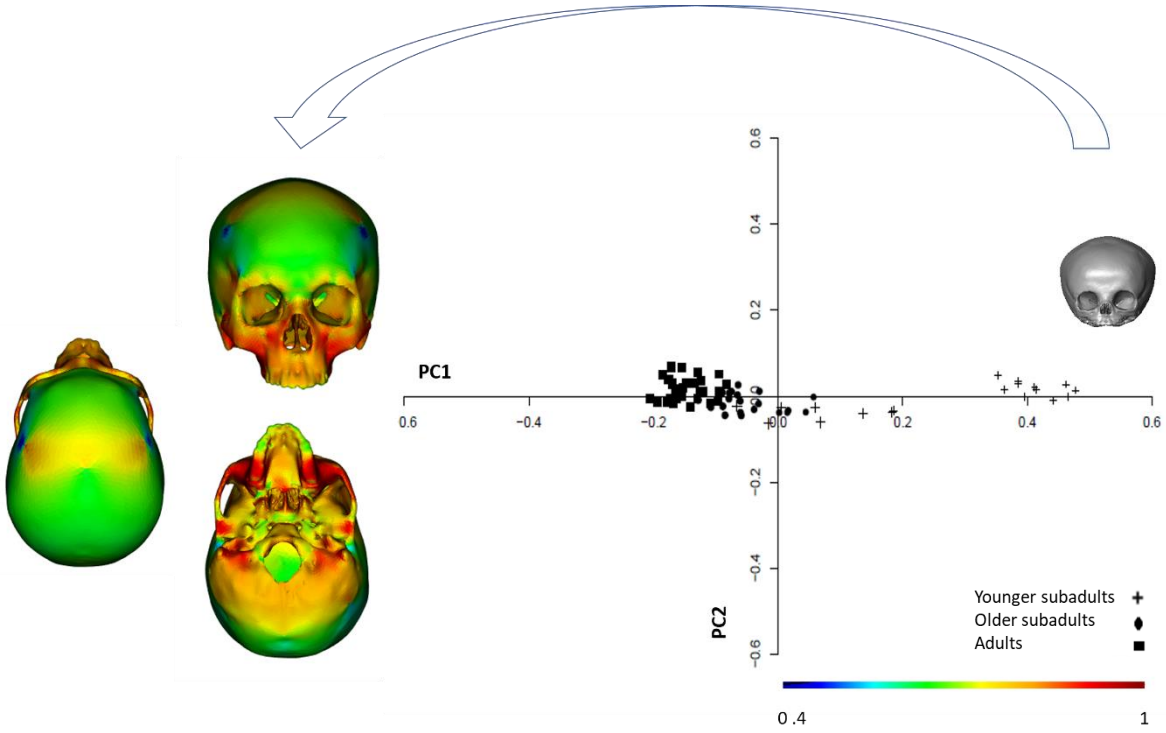

Figure 3.1.2. PCA of cranial form (ln centroid size + shape) of the modern human ontogenetic sample. The variance accounted by the first three components is: PC1 91%; PC2 2%; PC3 1%). Warpings between the extremes of PC1 are visualised using colour maps with a blue to red scale, indicating minimum (blue) or maximum (red) absolute changes in area. Arrows indicate the reference and target warpings used to calculate the colour maps.

The use of form for analysing variation is biologically interesting because, in nature, changes in size and shape occur concurrently (Mitteroecker et al., 2013) and form analyses allow assessing size, shape and allometric relative contributions. Figure 3.1.2 shows the first two PCs of the form PCA and a visualisation of changes in the cranial form along the first principal component (PC1 of total variance). The first PC accounts for a considerably greater proportion of total variance (91%) than the second (2%). This is because it is dominated by size variation and accompanying allometric shape variation. Size is clearly the major way in which crania change during ontogeny. Warpings between the limits of the distribution on PC1 (PC1= -0.25 and 0.5) were used to create colour maps as in Figure 3.1.1.

The colour map shows absolute (rather than relative as in Figure 3.1.1) changes in local area over the cranium. From the younger subadults to the adults there is an increase in overall size, with the facial region and posterior cranial base undergoing the largest changes in form (yellow-red areas).

In the cranial vault, the pterionic region, as seen in the PCA of shape variation (Figure 3.1.1), undergoes least form change. The occipital region does not expand significantly during ontogeny (cyan colour) and the area around the bregma shows a greater absolute degree of expansion and modification, although less marked (yellow) than in the analysis of shape alone (Figure 3.1.1).

To more deeply dissect ontogenetic shape and size changes in the cranium, separate PCAs of the cranial base, vault and face were performed.

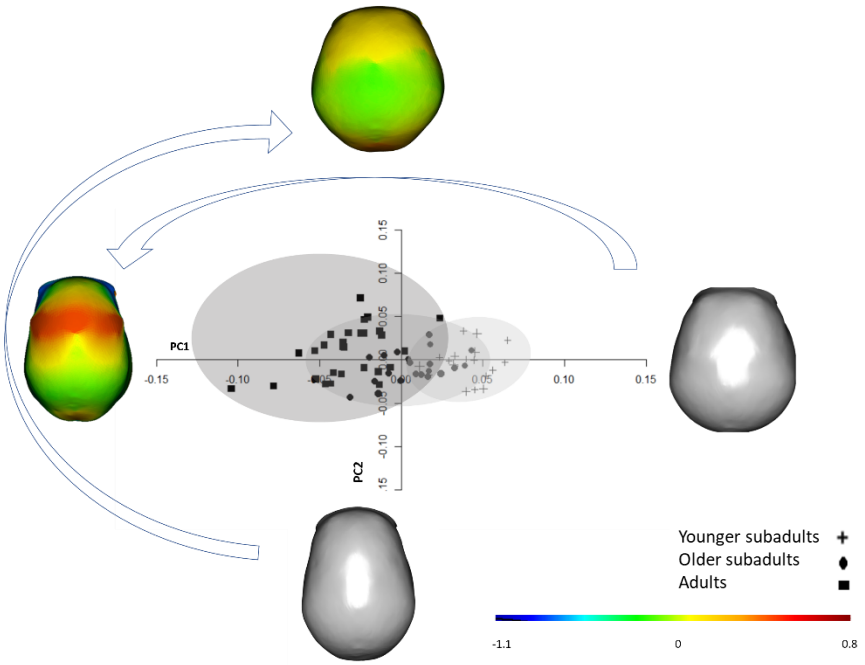

Figure 3.1.3. PCA of cranial vault shape of the modern human ontogenetic sample (11 landmarks and 89 semilandmarks). The variance accounted for by the first three components is: PC1 33%; PC2 14%; PC3 9%. Warpings along the extreme PC score values of PC1 and PC2 are visualised using colour maps. Variations are shown using a blue to red colour scale, indicating minimum (blue) or maximum (red) changes in area. Arrows indicate the reference and target warpings used to calculate the colour maps.

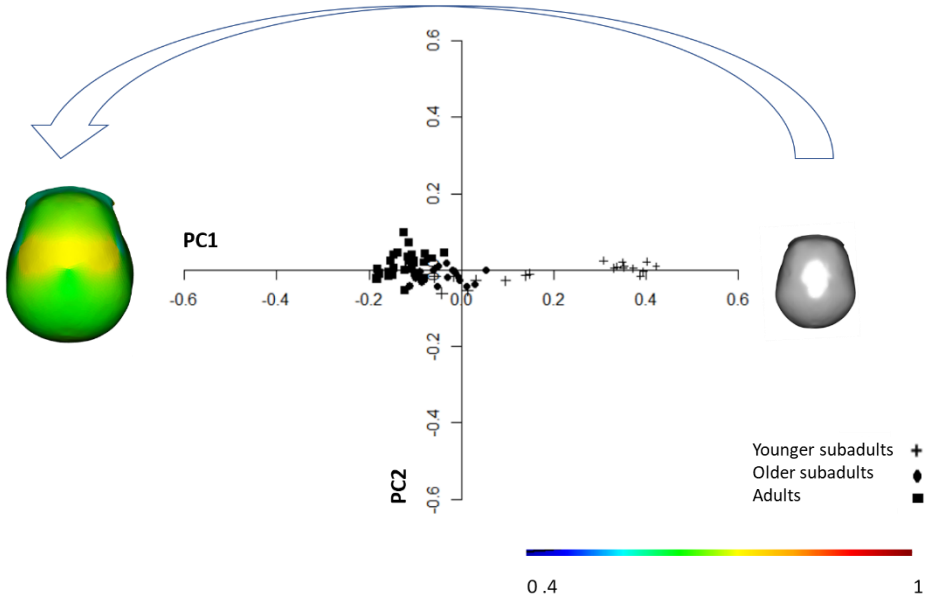

Figure 3.1.4. PCA of cranial vault form of the modern human ontogenetic sample (11 landmarks and 89 semilandmarks). The variance accounted for by the first three components is: PC1 90%; PC2 2.40%; PC3 1.70%. Warpings between the extreme PC score values of PC1 are visualised using colourmaps. Variations are shown using a blue to red colour scale, indicating minimum (blue) or maximum (red) changes in area. Arrows indicate the reference and target warpings used to calculate the colour maps.

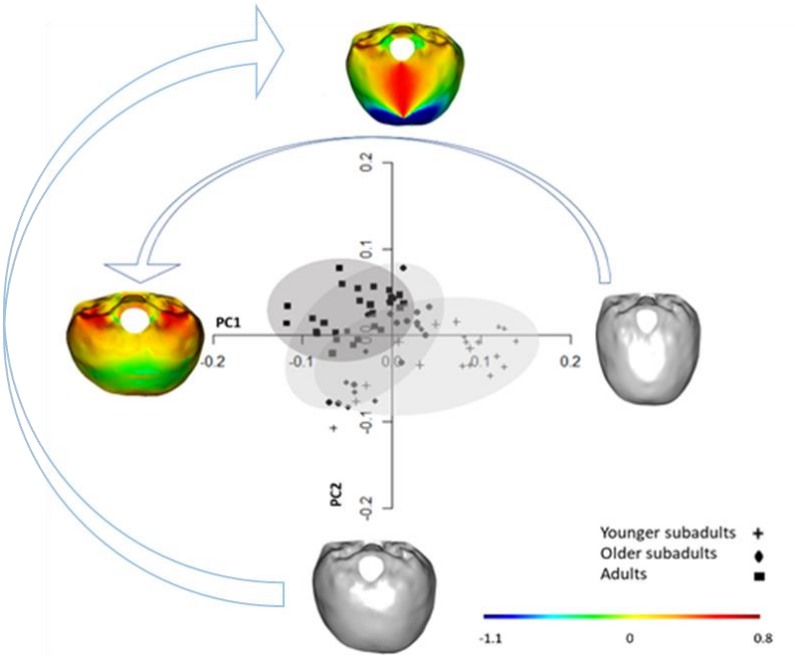

Figure 3.1.5. PCA of cranial base shape in the modern human ontogenetic sample (18 landmarks and 24 semilandmarks). The proportion of total variance accounted for by the first three components is: PC1 37%; PC2 16%; PC3 8%. Warpings between the extreme PC score values of PC1 and PC2 are visualised using colourmaps. Variations are shown using a blue to red colour scale, indicating minimum (blue) or maximum (red) changes in area. Arrows indicate the reference and target warpings used to calculate the colour maps.

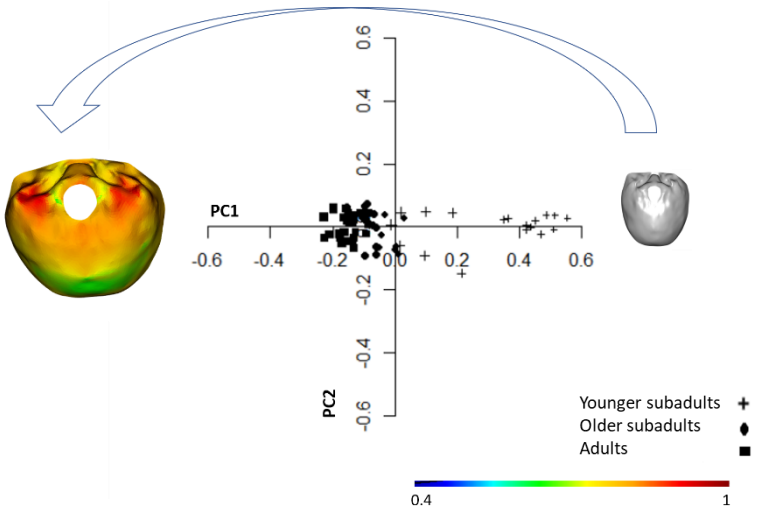

Figure 3.1.6. PCA of cranial base form of the modern human ontogenetic sample (18 landmarks and 24 semilandmarks). The variance accounted for by the first three components is: PC1 86%; PC2 4%; PC3 2%. Warpings between the extreme PC score values of PC1 are visualised using colourmaps. Variations are shown using a blue to red colour scale, indicating minimum (blue) or maximum (red) changes in area. Arrows indicate the reference and target warpings used to calculate the colour maps.

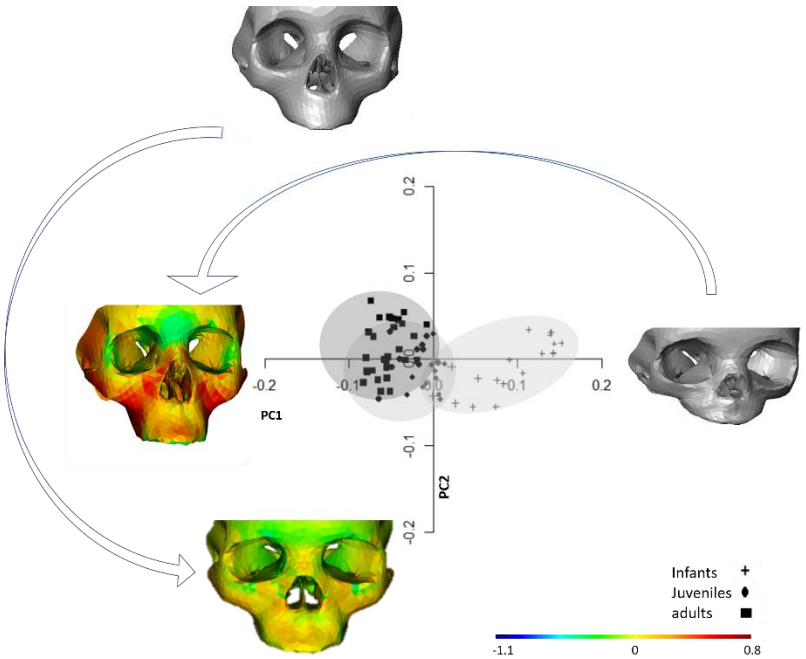

Figure 3.1.7. PCA of facial shape of the modern human ontogenetic sample (60 landmarks and 85 semilandmarks). The proportion of total variance accounted for by the first three components is: PC1 43%; PC2 8%; PC3 5%. Warpings between the extreme PC score values of PC1 and PC2 are visualised using colourmaps. Variations are shown using a blue to red colour scale, indicating minimum (blue) or maximum (red) changes in area. Arrows indicate the reference and target warpings used to calculate the colour maps.

d

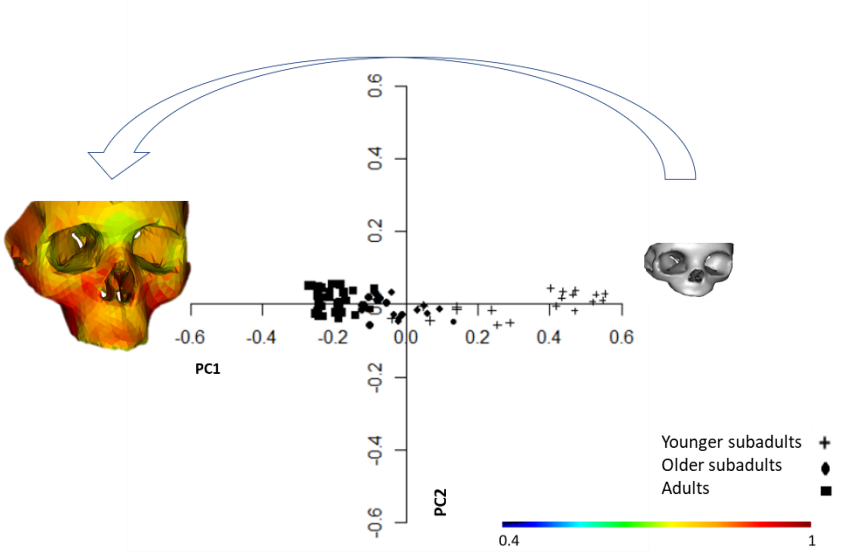

Figure 3.1.8. PCA of facial form of the modern human ontogenetic sample (60 landmarks and 85 semilandmarks). The variance accounted for by the first three components is: PC1 90%; PC2 1.40%; PC3 0.80%. Warpings between the extreme PC score values of PC1 are visualised using colourmaps. Variations are shown using a blue to red colour scale, indicating minimum (blue) or maximum (red) changes in area. Arrows indicate the reference and target warpings used to calculate the colour maps.

Figures 3.1.3 and 3.1.4 show the first two components of the PCAs of cranial vault shape and form.

Along PC1 of Figure 3.1.3 (shape), the vast majority of developmental morphological changes of the cranial vault can be observed as this region changes from a wide cranial vault in younger subadults (expanded mostly at the level of the posterior parietals) to a narrow one in adults. Interestingly, as already observed in Figure 3.1.1 and 3.1.2, but more clearly evident in Figure 3.1.3 and 3.1.4, the bregmatic region undergoes the greatest changes (red). PC2 represents a mode of variation reminiscent of the classical descriptions of dolichocephaly and brachycephaly, with the colour map showing the frontal (yellow) and posterior parietal (red) as the regions undergoing major changes. There are no differences between age classes on the second or higher PCs. The warping along PC1 of Figure 3.1.4 confirms the trend observed in the PCA of shape variations towards expansion around bregma. No warping along PC2 is shown in Figure 3.1.4, because almost identical to that of Figure 3.1.3.

Figures 3.1.5 and 3.1.6 show the first two components of the PCAs of cranial base shape and form. In the PCA of Figure 3.1.5 (shape), during ontogeny (mostly represented by PC1), the region around the foramen magnum undergoes the most marked changes (yellow-red area), while the squamous region of the occipital bone is the least variable area (green area). The young subadults possess a more elongated cranial base, while adults exhibit a wider and more flexed (not shown) basicranium. In both analyses of form and shape, expansion of the base is locally greatest between the foramen magnum and the mastoid processes. The mode of cranial base shape change (Figure 3.1.5) seems to shift after infanthood (younger subadults), with increasing scores on PC2 of older individuals. This represents the accentuation of antero-posterior elongation, especially by relative expansion of the non-squamous occipital (red area in warping along PC2, Figure 3.1.5). PC2 of the form analysis is not shown because similar to that of the shape analysis.

The PCA in Figure 3.1.7 shows the first and second principal components of face shape. The visualisations show that, along PC1, the face principally elongates, expanding vertically, leading to relatively increased midfacial and nasal heights from younger subadults to adults. The midfacial region shows relative expansion of the posterior region (posterior palatal-molar area in red) as well as around the zygomatico-maxillary suture

(orange-red). Since these data are scaled, there is an apparent relative medio-lateral narrowing of the face, bringing the orbits relatively closer, while their size decreases relative to the other facial elements (green area around the orbits in the left warping of Figure 3.1.7). All these changes are confirmed when looking at the expansion of the face in absolute terms in Figure 3.1.8 (PCA of form).

From negative to positive values along PC2 of Figure 3.1.7, the nasal cavity, the orbits and the maxillary complex show a relative medio-lateral narrowing and the orbits change from a rectangular to a more squared morphology with the relative distance between them reduced. The distribution of the data in the PCA in Figure 3.1.7 shows a clear flexion in the plot, indicating a shift in the mode of ontogenetic shape change with juveniles (older subadults) and adults having higher PC2 scores than younger subadults and so developing relatively longer and narrower faces and more square orbits.

Interestingly, when comparing the magnitude of changes both in the shape and form space of the whole cranium, base, face and vault using the colour maps, the regions that undergo the greater absolute and relative changes are the midface, the posterior cranial base and the bregmatic area, where the frontal and parietals meet.

Hypothesis 1b. T*he cranium as a whole and the cranial base, vault and face each scale in a consistent way throughout ontogeny*

Allometry was investigated by multivariate regression, assessing the influence of size on shape and that of age on shape and form of the whole cranium throughout postnatal ontogeny in the entire sample and in each of the three age classes, thus allowing comparison of the two developmental trajectories (younger subadults) and (older subadults to adults) identified in the PCA of the cranium (Figure 3.1.1). Additionally, identical multivariate regressions were carried out for each of the three cranial regions in the entire sample and in each of the three age classes. After multivariate regression, the regression vectors for different age classes were compared, testing for divergence between them in the cranium and in the three regions (Table 3.1.1).

a.

Skull: multivariate regressions		
	Shape vs size	
	R^2	P-value
all	30 %	0.001
0-5.5	25 %	0.001
6-18	8 %	0.02
18+	3 %	**n.s**
	Shape vs age	
	R^2	P-value
all	30 %	0.001
0-5.5	22 %	0.001
6-18	11 %	0.002
18+	4 %	**n.s**
	Form vs age	
	R^2	P-value
all	62 %	0.001
0-5.5	75 %	0.001
6-18	34 %	0.001
18+	3 %	**n.s**

b.

Cr. Base: multivariate regressions		
	Shape vs size	
	R^2	P-value
all	25 %	0.001
0-5.5	20 %	0.002
6-18	8 %	**n.s**
18+	2 %	**n.s**
	Shape vs age	
	R^2	P-value
all	24 %	0.001
0-5.5	19 %	0.002
6-18	8 %	**n.s**
18+	7 %	**n.s**
	Form vs age	
	R^2	P-value
all	54 %	0.001
0-5.5	6 %	0.001
6-18	18 %	0.001
18+	5 %	**n.s**

c.

Cr. Vault: multivariate regressions		
	Shape vs size	
	R^2	P-value
all	19 %	0.001
0-5.5	13 %	0.001
6-18	8 %	**n.s**
18+	6 %	**n.s**
	Shape vs age	
	R^2	P-value
all	26 %	0.001
0-5.5	12 %	0.001
6-18	10 %	0.02
18+	4 %	**n.s**
	Form vs age	
	R^2	P-value
all	58 %	0.001
0-5.5	75 %	0.001
6-18	24 %	0.003
18+	3 %	**n.s**

d.

Face: multivariate regressions		
	Shape vs size	
	R^2	P-value
all	38.38 %	0.001
0-5.5	31.97 %	0.001
6-18	10.52 %	0.001
18+	3.30 %	**n.s**
	Shape vs age	
	R^2	P-value
all	32.13 %	0.001
0-5.5	26.19 %	0.001
6-18	8.93 %	0.004
18+	3.19 %	**n.s**
	Form vs age	
	R^2	P-value
all	70.14 %	0.001
0-5.5	72.06 %	0.001
6-18	35.94 %	0.001
18+	3.78 %	**n.s**

e.

Skull: angle tests		
	Shape vs size vectors	P-value
0-5.5 VS 6-18	82°	0.001
6-18 VS 18+	n.a	
	Shape vs age vectors	P-value
0-5.5 VS 6-18	88°	0.001
6-18 VS 18+	n.a	
	Form vs age vectors	P-value
0-5.5 VS 6-18	27°	0.001
6-18 VS 18+	n.a	

f.

Cr. Base: angle tests		
	Shape vs size vectors	P-value
0-5.5 VS 6-18	n.a	
6-18 VS 18+	n.a	
	Shape vs age vectors	P-value
0-5.5 VS 6-18	n.a	
6-18 VS 18+	n.a	
	Form vs age vectors	P-value
0-5.5 VS 6-18	39°	0.001
6-18 VS 18+	n.a	

g.

Cr. Vault: angle tests		
	Shape vs size vectors	P-value
0-5.5 VS 6-18	n.a	
6-18 VS 18+	n.a	
	Shape vs age vectors	P-value
0-5.5 VS 6-18	85°	0.001
6-18 VS 18+	n.a	
	Form vs age vectors	P-value
0-5.5 VS 6-18	29°	0.001
6-18 VS 18+	n.a	

h.

Face: angle tests		
	Shape vs size vectors	P-value
0-5.5 VS 6-18	79°	0.001
6-18 VS 18+	n.a	
	Shape vs age vectors	P-value
0-5.5 VS 6-18	69°	0.001
6-18 VS 18+	n.a	
	Form vs age vectors	P-value
0-5.5 VS 6-18	21°	0.001
6-18 VS 18+	n.a	

Table 3.1.1. Multivariate regressions of shape on centroid size and shape/form on age of the whole ontogenetic sample (all) and of the three age classes, from 0 to 5.5 years old (younger subadults), from 6 to 18 years old (older subadults) and from 18 onward (adults) for the whole cranium (a), cranial base (b), cranial vault (c) and facial (d) regions. After multivariate regression, the regression vectors for each region were compared among different age classes, testing for significance of the angle of divergence using permutation test: e: comparison of regression vectors of different age classes for the cranium, e; for the cranial base, f; for the cranial vault, g; for the face, h. In the tables, the R^2 values (coefficient of determination) represent the percentage of total variance explained by the regression. N.a (not applicable) was used when no comparison was possible, n.s= non-significant regressions.

The results of the multivariate regressions in Table 3.1.1 (a) show that 30% of cranial variance is explained by the influence of size on shape, and the same is the case for regression of age on shape. In younger subadults, the influence of size and age on shape is most marked and significant, with 25% of shape variance explained by the regression with centroid size, and 22% explained by that with age. These percentages drop

respectively to 8% and 11% in older subadults, while adults show no significant relationships. The highest R^2 coefficients are found in the regressions of form on age, with 75% of total variance explained in younger subadults (0-5.5) and 34% in 6-18 year olds. This relationship is not significant in adults. The permutation test on the angle between the vectors from the regressions of shape on size in younger and older subadults (Table 3.1.1: e) indicates that they diverge significantly, with an angle of 82°. Similarly, the regression vectors of shape on age diverge significantly between these age groups, with an angle of 88°, and those of form on age diverge significantly, at 27° (Table 3.1.1, e). No regressions diverge significantly between older subadults and adults, consistent with their distributions in the PC plot of Figure 3.1.1.

For the cranial base (Table 3.1.1, b) and cranial vault (Table 3.1.1, c) the regressions of shape on centroid size are only significant in the 0-5.5 group. The shape shows a significant regression on age in the younger subadult group in both these regions and in older subadults the regression of vault shape on age is weak (variance explained is 10%) but significant and diverges (85°, Table 3.1.1, g) significantly from the regression of vault shape on age in younger subadults. The regressions of form on age for both the cranial base and vault are significant in the younger and older subadult groups. These diverge significantly between these age groups in both regions (Table 3.1.1, f and g).

Unlike the cranial vault and cranial base, in the face the regressions of shape on centroid size, shape on age and of form on age are all significant in younger and older subadult groups, but not in adults. In the younger subadults (0-5.5), 38% of facial shape variance is explained by the regression on centroid size. In the older subadult group (6-18) the influence of centroid size on facial shape decreases but is still significant, with 11% of the facial shape variance being related to size.

Consistent with the trajectories observed in the PC plot of Figure 3.1.7, vector comparison of facial allometric trajectories between younger and older subadults shows that these diverge significantly, with an angle of 79° (Table 3.1.1, h). Younger and older subadult face shape vs age (developmental) trajectories also diverge significantly with an angle of 69° as do the vectors of the regression of face form on age, with an angle of divergence of 21°.

Hypothesis 1c. *The pattern and degree of covariation among the cranial base, vault and face do not change throughout development.*

To test how patterns of covariation among cranial components change during growth and development in each cranial region, two-block PLS analyses were performed between the cranial base, vault and face shape variables by dividing the sample into age classes. PLS analysis of form was not performed because the size component dominates the analyses, growth (size increase over time) being a common factor affecting all regions simultaneously. The focus is instead on how shape variations in one region relate to those in others. Table 3.1.2 presents the results of 2-block-PLS analyses between the cranial base, vault and face in younger subadults, older subadults and adults. PLS1 from these analyses was the only significant axis as assessed by permutation test. The correlation

PLS shape analyses between cranial modules in age classes					
Younger subadults					
Block 1 vs Block 2	TOT.COVAR	CORR.COEFF	P-VALUE	EXPLAINED VARIANCE BLOCK 1	EXPLAINED VARIANCE BLOCK 2
Cr.vault- Face	59.45 %	0.95	0.001	15.08 %	38.08 %
Cr.vault- Cr.base	50.71 %	0.92	0.01	12.96 %	37.24 %
Face- Cr.base	74.50 %	0.78	0.001	34.92 %	34.91 %
Older subadults					
Block 1 vs Block 2	TOT.COVAR	CORR.COEFF	P-VALUE	EXPLAINED VARIANCE BLOCK 1	EXPLAINED VARIANCE BLOCK 2
Cr.vault- Face	35.87 %	0.90	0.05	21.08 %	12.93 %
Cr.vault- Cr.base	56.06 %	0.72	0.03	24.35 %	36.28 %
Face- Cr.base	42.42%	0.87	**ns**	**n.a**	**n.a**
Adults					
Block 1 vs Block 2	TOT.COVAR	CORR.COEFF	P-VALUE	VARIANCE BLOCK 1	VARIANCE BLOCK 2
Cr.vault- Face	62.63 %	0.85	0.001	33.52 %	17.14 %
Cr.vault- Cr.base	69.33 %	0.86	0.001	30.82 %	23.26 %
Face- Cr.base	55.33 %	0.82	0.001	17.61 %	22.53 %

Table 3.1.2. PLS results of covariation among the three cranial regions of the cranial vault, base, and face: TOT.COVAR= percentage of total covariance explained by the first pair of singular warps, CORR.COEFF= correlation coefficients between blocks for PLS1 scores with p-value assessed by permutation test between pairs of blocks. For each block, the proportion of its variance explained by its covariance with the other block was estimated (n.s= not significant, n.a= not applicable).

coefficients among PLS1 scores are large and all but one are significant, indicating that the cranium is an integrated structure.

However, in younger subadults, only a small amount of variance of the cranial vault is explained by its covariance with the other two blocks (15% of the total variance of the cranial vault is explained by its covariation with the face, and 13% by its covariation with the cranial base). The proportion of total cranial vault variance explained by its covariation with the other regions becomes greater in older subadults and adults. In younger subadults, total facial variation is, in good part, explained by its covariation with the cranial base (35%) and vault (38%). However, it seems that the facial complex becomes progressively more independent during development, because a smaller percentage of its total variance is explained by its covariation with the other two regions in older subadults and adults.

About 37% of the total variance of the cranial base is explained by covariance with the vault in younger and older subadults and this falls to 23% in adults. In contrast, 35% of the total variance of the cranial base is explained by its covariation with the face in younger subadults, and 23% in adults, while in older subadults the cranial base and face appear to develop relatively independently (non-significant association).

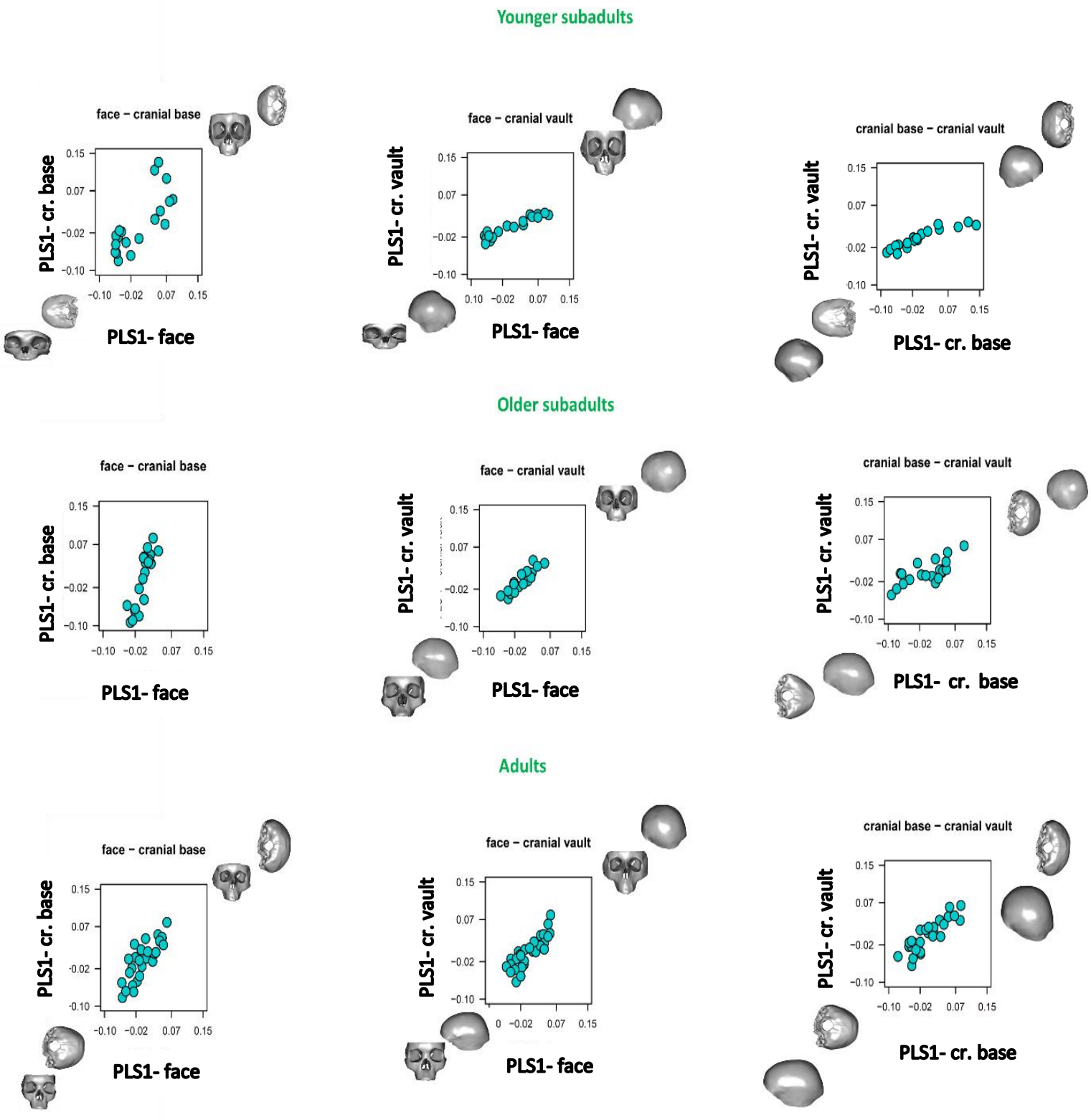

Figure 3.1.9. PLS1 shape covariation graphs and warpings of the cranial vault, base and face when analysed in pairs.

Figure 3.1.9 shows the PLS1 graphs and warpings for all combinations of blocks analysed in Table 3.1.1. In the top row, the covariation among the face and base, face and vault and base and vault is analysed in younger subadults. In this group, warpings show that the face covaries with the cranial base such that a wider, shorter and flatter face is associated with a narrow and elongated base and vice versa. The face and cranial vault covary such that a wider, shorter and flatter face is associated with a less rounded vault and a more prominent temporal region. Cranial base and vault covary such that an antero-posteriorly elongated vault is associated with a similarly elongated base and vice versa. In younger subadults (middle row), the covariation between the cranial base and face is not significant, therefore shape variations are not shown. The face covaries with the cranial vault such that taller and narrower faces, suggesting a more mature and adult morphology, are associated with a more elongated vault and vice versa while a narrow and long cranial base is associated with an elongated and low cranial vault and vice versa. In the adults (bottom row) a wider, shorter and flatter face is associated with a narrow and elongated base and a less rounded vault while an antero-posteriorly elongated vault is associated with an elongated base.

3.1.7 Discussion

3.1.7.1 Summary of the key findings

Prior work has shown that several mechanical factors can affect the growth and development of the bones of the cranium: *e.g.* the timing of the closure of sutures (Herring, 2008; Heuzé et al., 2012), the loading of the masticatory apparatus (Kiliaridis et al., 1993), the differential expansion of organs and the constraints imposed by connective tissues (*e.g.* the falx; Bruner, 2007). Because of these and other factors, patterns of morphological integration and modularity undergo subtle changes during ontogeny, but very little is known about the extent of these changes (Martínez-Abadías et al., 2009, 2011). Frequently, angles, linear measurements and 2D geometric morphometrics have been applied to compare general ontogenetic trends in the cranial base and face or in the cranial base and neurocranium in modern humans (Buschang et al., 1983; Ross and

Henneberg, 1995; Lieberman, 2000; Bastir et al., 2006). While previous studies have laid the ground by exploring the ontogenetic shape variations of these cranial regions in Hominoidea (Gunz et al., 2010, Singh et al., 2012, Profico et al., 2017; Zollikofer et al., 2018), in the present study, patterns of growth and development of each of these regions are described and compared in modern humans as are patterns of integration and modularity among them at different ontogenetic stages. The analyses of this section tested three hypotheses concerning the growth and development of the cranium and the ontogenetic interactions between the cranial base, cranial vault and face of modern humans.

Hypothesis 1a stated that *the mode of shape change is consistent throughout postnatal ontogeny for the whole cranium and for the cranial base, vault and face.*
This hypothesis can be rejected if the vector of ontogenetic shape change from birth to adulthood is not linear. Hypothesis 1a was tested through PCA of the shape of the whole cranium and of each cranial region, examining the scatters of individuals in the resulting PC plots for deviations from linearity. Hypothesis 1a was falsified since the ontogenetic shape vectors of the whole cranium, face and base showed non-linear trends (alterations in mode of shape change).

Hypothesis 1b stated that *the cranium as a whole and the cranial base, vault and face each scale in a consistent way throughout ontogeny*. This null hypothesis can be rejected if allometric scaling of any of the three regions changes during ontogeny.

This hypothesis was tested by applying a series of linear regressions of shape on centroid size, shape on age and form on age in younger subadults, older subadults and adults for the whole cranium and each of the three cranial regions of vault, base and face. After performing the regressions, the results for each age class were compared for the cranium as a whole and across the three morphological regions. Hypothesis 1b was falsified, showing that while allometry is evident in each of the three regions in younger subadults, its influence drops significantly in older subadults and is absent in adults, except for the facial complex, which experiences significant allometric development also in adolescents (older subadults). Interestingly, the facial allometric growth vectors are significantly different between younger and older subadults. Therefore, Hypothesis 1b can be rejected

because the allometric patterns differ significantly between age classes among the three cranial regions.

Hypothesis 1c stated that *the pattern and degree of integration among the cranial base, vault and face do not change throughout development*. This null hypothesis can be rejected if, when comparing different age classes, significant changes are observed in the absolute and relative magnitudes of covariation among these cranial regions. Hypothesis 1c was tested applying 2-block partial least squares analyses to assess covariation between the morphology of the cranial base, vault and face in the three age classes: younger subadults, older subadults and adults. Hypothesis 1c was falsified since associations among regions change significantly from infancy, through adolescence and adulthood in terms of covariation.

3.1.7.2 The cranium and its regions: the cranial vault, base and face

3.1.7.2.1 Cranial ontogeny and allometric trends

The results of this section build upon an extensive literature on human craniofacial growth, development and integration (Ponce de Leon and Zollikofer, 2001; Viðarsdóttir et al., 2002; Zollikofer and Ponce de Leon, 2002; Bastir and Rosas, 2004; Cobb and O'Higgins, 2004; Gunz et al., 2010; Zollikofer and Ponce de Leon, 2010). Previous studies have noted that modes of development and rates of growth of crania and their elements follow non-linear trajectories (Viðarsdòttir et al., 2002; Bastir et al., 2007; Gunz et al., 2010). Likewise, the analyses presented here (Figure 3.1.1) show that ontogenetic shape changes are not linear. Indeed, there appear to be two phases: younger to older subadults and older subadults to adults. This indicates that the cranium changes in different ways at different times. The analyses of cranial regions indicate that this non-linearity reflects changes in the ontogeny of the facial complex as well as the cranial base. The findings in the face reflect Lieberman's, (2011) description of the face as growing

along a “skeletal growth trajectory”, showing rapid neonatal growth, followed by a deceleration during late childhood, ending with rapid growth during adolescence until adulthood (eruption of third molar). The same author identifies a “neural growth trajectory” for both the cranial vault and cranial base indicating the most rapid growth in the first 5 years, while the current study highlights the presence of a flexion in the trajectory of the latter.

Globularisation of the cranial vault is described by the younger to older subadult trajectory in Figure 3.1.1, as well as the flexion of the cranial base, with the facial complex undergoing vertical lengthening and medio-lateral compression. The orbits decrease relatively in size while the nasal cavity and its apertures (nasal rim and choanae) show relative increase. The colour map indicates that the facial complex, specifically the midfacial region, undergoes the most marked changes during this first ontogenetic phase, together with the basi-occiput, while the squamous and sphenoid regions of the cranial base show smaller relative expansion (yellow) or, in some areas, relative contraction (green). In addition, the lateral side of the frontal and parietal bones undergo less marked expansion while the rest of the neurocranium shows change. The observed expansion of the frontal lobe during early years reflects previous findings (Bruner, 2007; 2010) that enlargement of the brain is associated with a relative widening of the frontal lobes, (Bruner, 2010, states that this allows the development of Broca’s area), and a relative reduction in parietal areas. In addition, isometric enlargement of the whole parietal surface has been described as characteristic of *Homo sapiens*. This parietal expansion is associated with the early postnatal period (Neubauer et al., 2009) and is absent in chimps and in Neanderthals (Neubauer et al. 2009; Gunz et al., 2010). Furthermore, the dissociation observed in the colour map in terms of growth and development for different areas of the cranial base supports previous studies which show different patterns of integration among midsagittal and lateral components of the cranial base (Bastir et al., 2006) and among the three cranial fossae (Bastir and Rosas, 2005).

The second trajectory (Figure 3.1.1, older subadults to adults), continues the relative vertical development of the anterior and posterior facial complex, including the zygomatic and orbital regions (red), while modifications of the braincase are relatively less marked. Different from the first trajectory, along this second trajectory, the

bregmatic region is the part of the cranial vault that undergoes the most marked expansion.

These results are confirmed and extended by the PCA of form (Figure 3.1.2). From this, it is evident that changes in size and the consequent allometric changes in shape dominate variations. Warping along PC1, the colour map visualisations show variations in the degree to which surface regions expand. The posterior face and the maxilla and alveolar regions undergo the greatest expansion (yellow to red), with the cranial vault experiencing relatively less (green to blue). These variations confirm previous observations that used 2D morphological data to describe the main developmental changes occurring during ontogeny in skull regions (Bastir et al., 2006; Evteev et al., 2018). In addition, the significant growth and development of the facial region indicated by the colour map is in accordance with studies showing that the facial complex is the last region of the cranium to end growth and development (Bastir et al., 2006), with a significant proportion occurring during adolescence (Evteev et al., 2018).

The comparison of cranial ontogenetic vectors of younger and older subadults in Table 3.1.1 (e) confirms that their trajectories significantly diverge. This is in contrast with the findings from Zollikofer and Ponce de Leon (2002), who found that cranio-mandibular ontogeny in modern humans follows a fairly linear shape trajectory (along PC1), implying that the spatial patterns of shape change remain constant between the age of 3 years and adulthood. However, their study does not take into consideration the entire shape space and does not test the observed linearity in a multivariate fashion.

3.1.7.2.2. Cranial vault, base and face ontogeny and allometric trends

The PCAs of the face, base and vault show that while the vault shows a linear scatter on PC1 and PC2, the facial complex and cranial base show a flexion in their ontogenetic trajectories, with the younger subadults following a different mode of shape change to that of juveniles and adults. These differences in the trajectories are well known (*e.g.* Lieberman, 2011), and the face is said to follow a "skeletal" growth pattern as opposed

to the "neural" growth pattern of the base and vault. However, the current study highlights the presence of a flexion in the trajectory of the cranial base, considered further below. Overall, the three regions undergo different postnatal changes from younger subadults to adults, and these are considered below.

Cranial vault PC1 (Figure 3.1.3) describes allometric changes, with the vault expanded at the level of the posterior parietals in infants and becoming more globular in adults. The colour map illustrating shape changes represented by the first PC (Figure 3.1.3) shows that during ontogeny, the region of the fronto-parietal suture (bregmatic region) undergoes the greatest change, as observed in the PCA of the entire cranium (Figure 3.1.1). This may well reflect growth at the suture. Interestingly, the underlying brain region is proposed by Bruner (2015) to be particularly relevant in relation to the evolution of specific visual-spatial skills in *Homo sapiens*, as well as being prone to evolutionary modification (Jung and Haier, 2007). The regressions in Table 3.1.1 (c) show that while cranial vault shape scales in younger subadults, this relationship is not significant in the other two age classes, reflecting the fact that the brain reaches 95% of its final mass and volume by the time of M1 eruption (Lieberman, 2011). Interestingly, age affects shape in both older subadults and adults, showing that while size changes in the cranial vault are mostly greater in younger subadults from 0 to 6 years old, shape changes continue during later stages, so that younger and older subadults possess different cranial vault morphologies, with trajectories that significantly diverge (Table 3.1.1, g). This result reflects the dissociation between size and shape of the cranial vault found in modern humans during ontogeny (Bastir et al., 2006).

In the PCA of shape of the cranial base (Figure 3.1.5) there appear to be differences in modes of development between age classes. In the younger subadults, changes are most marked along PC2, which reflects variations (relative expansion) of the occipital region, and in the older subadults along PC1, which displays relative lengthening and narrowing of the whole cranial base. Cranial base regressions indicate that the regression of shape on size and that of shape on age is significant only in the younger subadult group, in agreement with Bastir et al. (2006). In their study, this region was the first to reach maturity.

The PC plot in Figure 3.1.7 shows a similar distribution of age classes for the face as was observed for the base (Figure 3.1.5). Unlike the neurocranium, in the face, the regressions of shape on size, shape on age and of form on age are significant in both younger and older subadults (Table 2, d). This is in line with other findings which suggest that facial growth and development continues long after the cranial base and vault are ontogenetically mature (Lieberman, 2011; Bastir et al., 2006). The tests of regression trajectory divergence between the two subadult groups (Table 3.1.2, h) indicate that they significantly differ in terms of allometry (shape on size) and development (shape on age) and in the regression of form on age. The warping and colour map displaying the shape variations of the first PC of face shape (Figure 3.1.7) show that during ontogeny the reduction of the relative size of the orbits and the relative medio-lateral narrowing of the face occurs, together with great expansion of the midfacial complex and the posterior facial region, which elongates both anteriorly and vertically. The region of the zygomatico-maxillary suture shows great expansion in Figure 3.1.1, and so it accounts for a significant portion of increase in facial height. This may well reflect rapid growth of the nasal septum (Al Dayeh et al., 2013).

It is evident from the foregoing analyses that facial growth and development proceeds in a complex manner. Allometry differs in importance between cranial regions. Further, divergence of trajectories between younger and older subadults indicate changes with time. These findings are in line with other studies that have reported intraspecific postnatal divergence in different human populations (Viðarsdóttir et al., 2002) and underline that these differences arise very early during ontogeny.

3.1.7.2.3 Partial least squares analysis: the cranial vault, base and facial blocks

Partial least squares analyses were performed to assess the patterns of interaction among cranial regions at different stages of ontogeny. The results indicate that the strength of interaction (covariance between blocks) and the variance accounted for by the covariation varies by region and age class. More specifically, the cranial base, which

shows very early infant maturation (Bastir and Rosas, 2016) shows significant covariance with both the face and the cranial vault in all age classes, with the exception of the relationship between face and base in older subadults, which is not significant.

The cranial vault in younger subadults seems to undergo a first phase in which most of its morphological variance is not explained by covariation with any of the other regions. This could be due to rapid growth of the neurocranium during infancy (Anzelmo et al., 2015), mostly determined by brain growth. In older subadults and adults, the proportion of cranial vault variance explained by its covariation with the face and base increases, indicating that after the initial period of rapid development and modular behaviour, this region becomes more integrated.

The findings of the PLS analyses suggest that the early developed cranial base subsequently becomes integrated with both the cranial vault and the face which continue to develop. Further, in younger subadults, the face is highly associated with the cranial base and vault, but becomes more independent in older subadults, and more integrated again in adults.

These results indicate that the cranium shows varying levels of integration throughout ontogeny. These findings accord with previous studies that have investigated the timing of development of the regions of the skull (Bastir et al., 2006), in that regions undergoing rapid periods of development show low levels of covariation with other elements of the skull. This suggests that during phases of rapid development, local influences render a region more modular and as local development slows, the underlying large scale influences that affect several regions together, such as allometry and masticatory loads, become more significant, and act as integrators, so that functions are preserved (Porto et al., 2013).

3.1.8 Conclusions

This section focussed on the development of the cranium, providing detailed insights into the growth of cranial regions and the spatio-temporal interactions among them. This study explored trends of growth and development in the cranium and the three cranial regions, identifying and visualising significantly divergent trajectories among younger and older subadults for most cranial regions. In addition, this study built on prior work on covariation among cranial base, face, and vault (Cheverud et al., 1992; Lieberman et al., 2000; Bookstein et al., 2003; Gkantidis and Halazonetis, 2011), by focusing on the description and comparison of covariation at different age stages. The results show significant ontogenetic variation in degrees of interaction among cranial regions and that phases of developmental flexibility coincide with more modular behaviour. Ideally, a larger sample size, longitudinal 3D data and information about the sex of the individuals could give even more comprehensive insights into the patterns of growth and development of the cranium and its regions.

3.2 Growth, development and covariation of the facial elements in modern humans

3.2.1 Ontogenetic interactions between facial elements

In Section 3.1 the growth and development of the cranium were explored and described. Growth (centroid size vs age), allometry (shape vs centroid size) and development (shape vs age) were described for the cranium and the ontogenetic interactions among face, cranial base and vault were quantified at different postnatal stages.

In the present section, a detailed study of growth, allometry and development is performed on individual facial regions to characterise their postnatal ontogenies, and to better understand the pace and timing of their development. This is followed by a detailed analysis of ontogenetic interactions among the facial regions. These are performed in a pairwise fashion comparing facial regions (blocks) through two block Partial Least Squares analyses (PLS), which allows the magnitude and nature of the interactions between regions to be quantified and compared among developmental stages.

The findings of these studies are relevant to subsequent analyses presented in this thesis in that interactions between regions are later extended to path models that test hypotheses related to cascades of interaction and hierarchies among several facial regions (Section 3.3). Furthermore, the results of all of these studies of human cranial ontogeny provide the baseline against which to compare the facial development and developmental dynamics of Neanderthals with modern humans (Section 3.4).

This section begins with a brief review of the relevant background (also see Chapter 1) to these studies before presenting the analyses described above.

3.2.2 The hypotheses

There is a long history of comparative studies of changes in facial morphology and covariation during ontogeny in modern humans (Cheverud et al., 1992; McCollum, 1999; Rosas and Bastir, 2002; Bastir and Rosas, 2004; Gonzalez-Jose et al., 2004; Ackermann, 2005; Bastir et al., 2005). However, facial growth and development in modern humans is still poorly understood. The technologies available for imaging and the statistical basis for the analysis of these images have been limited until relatively recently. Thus, while underpinning many clinical studies, cephalometric analyses offer limited data on 3D anatomy (Brodie, 1941; Riolo, 1974; Broadbent et al., 1975; Buschang et al., 1983; Hunter et al., 1993; Cross and McDonald, 2000) and may distort midfacial structures (Evteev et al., 2018). Advances in 3D CT imaging and landmark-based analysis of 3D meshes allow for a more complete understanding of the dynamics of growth and developmental interactions within the cranium.

The first step when analysing patterns of covariation within the face is to delineate putative modules (parts that are hypothesised to behave autonomously during development). These potential modules are often recognised based on differences in prenatal formation and postnatal growth and development (Bastir, 2008; Klingenberg, 2013). This chapter considers the relationships among the orbits, zygomatic and maxilla (zyogomatico-maxillary module), maxillary sinuses, palate and nasal cavity. Many previous studies have explored facial modularity, integration and covariation, seeking to identify likely modules. Evteev et al. (2018) provides a quantitative description of human midfacial ontogeny by dividing the cranium into putative developmental modules: the nose, the zygomatico-maxillary complex and the orbits. These were chosen based on prior literature about functional and developmental modularity of the cranium (Cheverud, 1982; Gonzalez-Jose et al., 2004). Their work shows that these regions manifest diversity in timings of growth and developmental events. Another study (Ryan et al., 2019) investigating modularity and integration in the human cranium found that the orbit and the palate covary, both lengthening as the face lengthens along the anteroposterior axis. A further study (Villmoare et al., 2014) tested the independence of the palate from the rest of the cranium with the conclusion that it shows a significant degree of autonomy, potentially due to “its clear morphological and functional distinctiveness”. However, the palate forms the floor of the nasal cavity and is known to

interact with the maxillary sinuses, which can invade the space previously occupied by erupting teeth (Baykul et al., 2006; Erdur et al., 2015).

Previous studies have investigated maxillary sinus variations in different populations in relation to changes in latitude (Marquez et al., 2014; Butaric and Maddux, 2016; Maddux and Butaric, 2017) while ontogenetic studies have focussed on size and volume changes during growth (Holton et al., 2013; Butaric, 2015; Lorkiewicz-Muszyńska et al., 2015). However, there are few studies on maxillary sinus form during ontogeny. One attempted to classify its highly variable morphology into shape categories based on the location of their inferior wall (Kim et al., 2002), while others focused on shape covariation between the maxillary sinuses and the surrounding facial skeleton in adults, using 3D landmarks but more often linear measurements (Marquez, 2008; Lorkiewicz-Muszyńska et al., 2015; Butaric and Maddux, 2016; Maddux and Butaric, 2017; Evteev and Grosheva, 2019). The findings of these studies suggest that among different modern human populations, sinus size has an inverse relation with nasal cavity breadth, so that narrow nasal cavities host wide sinuses because these are able to expand laterally in the zygomatico-maxillary complex. Therefore, the sinuses have different degrees of covariation with different structures. Indeed, the fact that these structures have a low but significant covariation with many different elements in the face has led authors to propose that sinuses grow passively, acting as a zone of accommodation between facial elements (Butaric and Maddux, 2016).

Regarding the orbits, during prenatal development, the bones that make up the orbit grow and develop in coordination with the globe of the eye, which manifests its own independent developmental trajectory and shifts in position relative to the other soft tissues during prenatal development (Sperber et al., 2010). During postnatal development, the orbits show the most rapid growth among facial skeletal elements, contributing greatly to overall facial proportions (Krimmel et al., 2015; Evteev et al., 2018), as is also observed in Section 3.3 of this thesis. Because the orbits undergo the most rapid growth among facial components in early infancy (Barbeito-Andrés et al., 2016), they potentially set spatial constraints upon, and so interact with, the growing sinuses, whose roof is in contact with their floor.

Prenatally, expansile growth of the septal cartilage within the nasal cavity has been shown to cause vertical expansion of the midface between the 10th and 40th weeks post-

conception. The growth of the nasal cavity then continues (but at a slower rate) throughout childhood, contributing to further increase in facial height via downward displacement of the nasal floor relative to the orbits (Sperber et al., 2010). Several competing hypotheses attempt to explain the growth and development of the nasal cavity. Some authors claim that septal growth and development is a phenomenon confined to childhood and early adolescence and that it is constrained and influenced by the surrounding structures (Goergen et al., 2017). Other authors claim that this region has a major role in shaping the surrounding facial elements and that this role continues throughout adulthood (Holton et al., 2011; Al Dayeh et al, 2013; Hall et al., 2013). Some experiments have tested the main growth theories (Cupero et al., 2001; Hartman et al., 2016).

Studies supporting a passive role for the nasal septum noticed that animals with naso-palatal anomalies or in which the septum was removed or dislocated showed no sign of growth anomalies in the face (Wexler and Sarnat, 1965; Babula et al., 1970). In addition, analysis of twins with normal and abnormal septal growth shows no increased asymmetry or anomaly in maxillary growth in the affected individual, according to Moss et al. (1968). In addition, after examining a case of congenital absence of olfactory organs, Latham and Burston (1964) concluded that the nasal septum has a role in determining the anteroposterior growth of the upper face but that it does not account for vertical facial height. The same authors (1966) when analysing a case of deviated nasal septum in a child report no anomalies in overall facial growth but notice an increase in bony deposition on the side toward which the septum was deviated. A more recent study has demonstrated that nasal septal deviation is associated with a reduced height of the upper facial skeleton (Mays, 2012). This suggests that, in short faces, the nasal septum keeps growing, resulting in its deviation because of the limited height available. If this interpretation is correct, then nasal septum growth would be independent of, and dissociated from, facial growth.

Other authors believe that the growth of the nasal septal cartilage influences displacement and growth at facial suture sites (Scott, 1954; 1956; 1962). Holton et al., (2011, 2012) found that artificially induced restriction of facial growth in *Sus scrofa* produced changes in premaxillary displacement, caused by nasal septum growth. The influence of nasal septum growth and deviation on facial anatomy has been examined

using longitudinal cephalometric measurements of twins, with the finding (*contra* Moss et al., 1968) that the nasal cartilage has an impact on the normal growth and development of the nose and maxilla, especially in the first decade of life (Grymer et al., 1991; Grymer and Bosch, 1997). Indeed, the twins with deviated nasal septum showed a retrusive maxilla (vertically and horizontally shorter and anteriorly rotated) and nose with columellar retraction. However, interestingly, total facial height did not differ among twins. The principal role of the nasal septum as pacemaker has also been supported by physiological evidence. Studies showed that increased activity of growth hormone during postnatal development leads to greater human facial dimensions, attributed in part to the stimulation of septal growth (Pirinen et al., 1994). Anomalies in midfacial development have also been observed in humans when the nasal septum is deviated or develops abnormally during childhood (Grymer et al., 1989). Clinical conditions such as cleft palate, in which the nasal septum grows deviated and bent, cause the face to grow asymmetrically (Hall and Precious, 2013). However, as already discussed, this could suggest that, in situations in which the face is somehow constricted or altered during growth and development, the nasal septum would grow in a deviated way because of the limited space available. As evident, due to differences in the selection of the species and methods adopted, results are still inconclusive.

This chapter explores the issues raised above. It begins by characterising the growth, development and allometry of individual facial components and then compares them. To do this, the following hypothesis is tested:

Hypothesis 1. T*he skeletal components of the modern human face do not differ in their growth, development or allometry among different age classes.*

To test the interactions among pairs of facial components a second hypothesis was formulated and tested, to characterise the degree of independence or integration of these components, how changes in one are associated with changes in the other.

Hypothesis 2. T*he nature (modes of) and magnitude of covariation among facial components is constant throughout ontogeny.*

All the skeletal components of the human face: the sinuses, palate, orbits, nose and the zygomatico-maxillary complex, have been analysed as separate modules in previous studies, not only because they have different embryological origins and serve different

functions but also because studies of the skeletal and soft tissues show that these regions possess different rates of growth and development (Kimmel et al., 2015; Evteev, 2018). However, their differential growth, development and allometry as well as the magnitudes and modes of covariation among them during postnatal ontogeny are not known in detail.

The two hypotheses here formulated helps clarify the details of the mechanisms of growth, development and integration among facial structures during ontogeny.

3.2.3 Materials and methods

3.2.3.1 The sample

An ontogenetic sample of 68 modern human crania was used in the present study. The specimens consist of 3D meshes segmented from CT-scans. For those specimens of unknown age, the patterns of dental eruption were used to estimate age class based on modern human standards (Carr, 1962; AlQahtani et al., 2010; see Table S1 of Supplementary Material for further information). Age class was based on dental eruption patterns and defined as follows: younger subadults from 0 to 5.5 years, older subadults from 6 to 18 years, adults from + 18 years onward. Sex was unknown for a part of the sample, therefore this variable was not considered in the study.

3.2.3.2 The dataset

A total of 43 landmarks were employed to represent facial size and shape on the 3D surface mesh of each cranium. The maxillary sinuses were manually segmented using the software Avizo 9.0. Six landmarks were located on the surface of each sinus; five of these are defined as geometrical landmarks: the most extreme surface points on the antero-posterior and dorso-ventral axes, and the most lateral point on the left-right axis, with crania oriented along the Frankfort Plane (Maddux and Butaric, 2017). One homologous landmark (type I) was collected on the internal surface of the maxillary sinuses, defined as the ostium, which connects the maxillary sinuses to the middle turbinate (see Section 2.0.3 of Chapter 2 for further information).

Additionally, 58 surface and curve semilandmarks were acquired on a juvenile cranium used as the template specimen. Surface and curve semilandmarks were used to characterise the form of regions where Type I or Type II landmarks are not plentiful, such as the nasal and choanal rim and the maxilla and alveolar regions (Bookstein, 1991). As has been shown in previous work (Bookstein, 1991, 1997; Bookstein et al., 2003; Mitteroecker et al., 2004; Gunz et al., 2005), semilandmarks also provide for more detailed visualisation of shape variations resulting from geometric morphometric analyses. After the first step of sliding of the specimens against the template, the mean configuration (consensus) was created and sliding was performed again, using the mean as the new template. The landmarks and semilandmarks were split into anatomical components as shown in Figure 3.2.1.

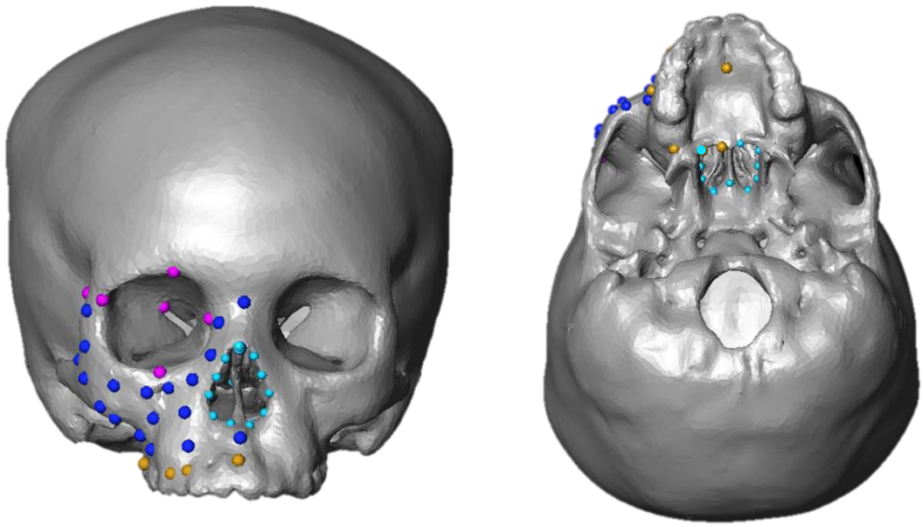

Figure 3.2.1. Configuration of landmarks and semilandmarks split into facial components for the present study. Purple= orbit; yellow= palate; cyan= nose; blue= zygomatico-maxillary. The maxillary sinus is not visible in the picture but is clearly represented in Figure 2.3 of this thesis.

3.2.3.3 Statistical analyses

This chapter explores the issues raised above. It begins by characterising the growth, development and allometry of individual facial components and then compares them. To this end, Hypothesis 1 states that:**Hypothesis 1**. T*he skeletal components of the modern human face do not differ in their growth, development or allometry among different age classes.*

It is expected that this hypothesis will be falsified given that many prior studies have shown differential timings and rates of morphological change for different components of the face during ontogeny. However, the testing of this hypothesis will lead to detailed data on the nature of these differences. In order to test this hypothesis for each facial component, how centroid size changes over time (growth), how shape changes over time (development) and how shape scales (allometry) are characterised statistically. The results are then compared between age classes in order to assess differences in growth, development and allometry. To test **Hypothesis 1**, growth trends (a linear regression of centroid size vs age) are compared among different facial regions. To test the influence of size on shape (allometry), age on shape (development) and age on form (growth and development), a series of multivariate regressions are carried out for different age classes and regions. Then, the significance of divergences in ontogenetic trajectories between younger subadults and older subadults and older subadults and adults is assessed. As for the analyses in Chapter 3.1, testing of divergence in ontogenetic trajectories between younger subadults (younger than 5.5 years old) and older subadults (between 6 and 18 years old) and between the latter and adults (18+ years old) was performed using the regression vectors resulting from the multivariate regression for each of the two age classes and the angle between them computed (angle test). Its significance was assessed using permutation test, in which the age class membership was randomly permuted and the angle recalculated. One thousand permutations were carried out and the estimated angle between the species was compared with the distribution of permuted angles to assess its significance.

The second hypothesis states that:

Hypothesis 2. T*he nature (modes of) and magnitude of covariation among facial components is constant throughout ontogeny.*

This hypothesis will be falsified if, comparing different age classes, significant changes are observed in the modes or magnitudes of covariation among pairs of facial components. Hypothesis 2 is tested by estimating the magnitude and significance of size and shape covariation among pairs of facial components ('blocks') using Pearson correlations (size) and 2-block Partial Least Squares analysis (PLS) of shape variables. As for Section 3.1, to assess how much of the total shape variance of a single block is "explained" by its association with the other block in the PLS, the percentage of total shape variance accounted for by specific PLS axes (the ratio between the variance of PLS scores and the sum of the variances of the shape coordinates) is calculated for each block (Cardini, 2019).

3.2.4 Results

Hypothesis 1 states that *the skeletal components of the modern human face do not differ in their growth, development or allometry among different age classes.*

For each facial component, growth was assessed through plots of centroid size on age and by calculating the correlation between them. The plots and correlations indicate that all regions grow similarly with the greatest scatter (variance in Csize) in the maxillary sinus and palate (Figure 3.2.2).

The results of the regressions of shape on centroid size (allometry), shape on age (development) and form on age (growth and development) for each facial region in each of the 3 different age classes are presented in Table 3.2.1 (a to e). Vector comparisons between younger subadults and older subadults and older subadults and adults are also presented.

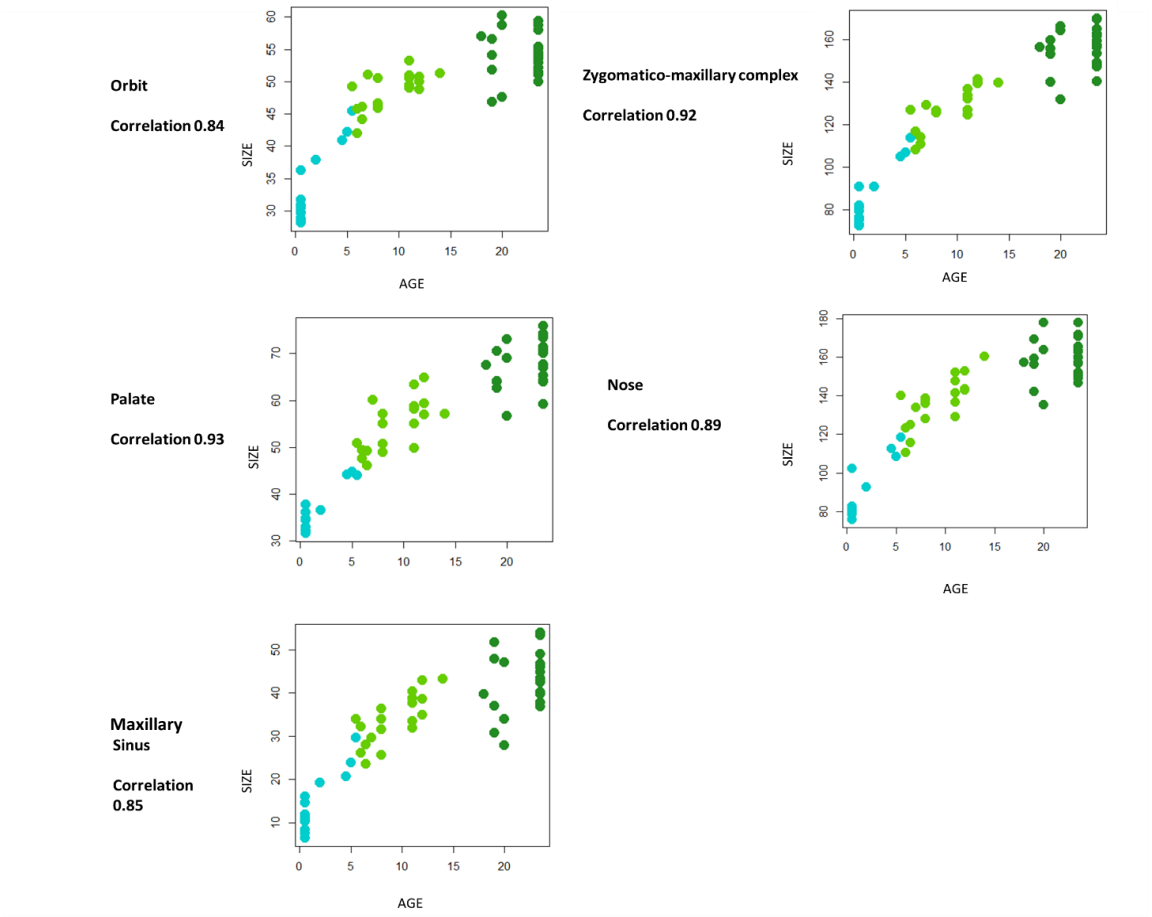

Figure 3.2.2. Changes in size with age for all the facial regions. All correlations (R^2) are significant (p-value < 0.001).

For the zygomatico-maxillary region (Table 3.2.1, a), allometry (shape on centroid size) accounts for a large proportion of the total variance. Indeed, in the 0-5.5 year group, 40% of the changes in shape are associated with growth (p-value < 0.001), while this value decreases to 11% (p-value < 0.008) in the older age group (6-18). In adults, the regression is not significant indicating that centroid size variance is very small and does not affect significantly the zygomatico-maxillary shape. Very similar results were obtained from the regressions of shape on age in the three age classes. The regressions of shape on age or centroid size after accounting for centroid size or age (residual variation) are not significant. The regressions of zygomaxillary form (centroid size and shape) on age, show that centroid size is an important aspect of subadult variation because they account for a very large proportion of total variance, 72% overall and 74% and 37% in the younger

and older age groups respectively, while the adults show no significant regression of form on age. The permutation tests that assess the significance of the divergence of these ontogenetic regression vectors between younger and older subadults (Table 3.2.1, f) are highly significant. This indicates that the ways in which infant and juvenile zygomatico-maxillary regions grow and develop differ significantly. Divergences between older subadults and adults were not tested because the regressions in adults are not significant.

Regarding the nasal complex (Table 3.2.1, b), only 19% of the total variance is explained by the regression of nasal cavity shape on centroid size. However, the regression of shape on centroid size is significant in all three age classes, with centroid size explaining 41% of nasal variance in younger subadults, 10% in older subadults and 9% in adults. The regression of shape on age shows that age accounts for similar proportions of total variance as did centroid size and that regression of form on age again accounts for a large proportion of total variance in each analysis. The regression of shape on centroid size after accounting for age (residual variation) is highly significant while the regressions of shape on age after accounting for centroid size is not. In all cases, the divergence of regression vectors is significant for the comparison between younger and older subadults. The divergence between older subadults and adults is either not significant or not tested because of insignificant regressions in the latter (Table 3.2.1, g).

In the palatal region (Table 3.2.1, c), 44% of the total shape variance is accounted for in the regression of shape on centroid size when considering the entire sample. In younger subadults, this is 24% while in older subadults the regression is not significant. Interestingly, in adults, the regression of palatal shape on centroid size becomes significant again (p-value 0.003), with 16% of the total variance of the palatal shape being explained. In contrast, the regressions of shape on age are significant for the whole sample and for both younger subadults and older subadults, but not for the adult age group. The regressions of palatal form on age are significant only in the younger subadult and adult groups. The regressions of shape on centroid size after accounting for age (residual variation) and of shape on age after accounting for centroid size are not significant. The analyses of divergences of regression vectors show that the regression vectors of shape on age (80°, $p < 0.001$) and form on age (31°, $p < 0.001$) diverge significantly between younger and older subadult groups (Table 3.2.1, h).

Allometry of the orbit (Table 3.2.1, d) is only significant for the whole sample and in the two subadult groups, with 13% and 19%, respectively of the total variance in orbital shape explained in younger subadults and older subadults. Similar results are obtained for the regressions of orbital shape on age, while all regressions of form on age are significant except in adults. The regressions of residual shape on centroid size and age, after regressing out age and centroid size respectively, are not significant. The analysis of divergence of the regression vectors show that there are no differences except between the vectors of the form on age regression for the younger and older subadult groups (27°, p-value= 0.002, Table 3.2.1, i).

Finally, when considered over all ages, maxillary sinus allometry is highly significant, explaining 17% of the total variance (Table 3.2.1, e p-value= 0.001). However, it is not significant within any single age class. The regression of shape on age is significant (p-value= 0.001) when computed over the whole sample, not significant within any of the two subadult groups and significant in the adult group (R^2= 13%, p-value= 0.004). All regressions of sinus form on age are significant. As with the orbit, regressions of residual shape on centroid size and age, after regressing out age and centroid size respectively, are not significant. Comparisons among age groups of regression vectors, only find significance for form vs age where all age classes differ significantly in this relationship (Table 3.2.1, l).

Table 3.2.1. Multivariate regression of shape on centroid size and age, and of form on age for the whole sample and for the three age classes for the right zygomatico-maxillary complex (a), nasal cavity (b) right palate (c), right orbit (d) and right sinus (e). After multivariate regression, the regression vectors of different age classes were compared for each region, testing for significance of the angle of divergence: right zygomatico-maxillary complex (f), nasal cavity (g), right palate (h), right orbit (i), right sinus (l). The R^2 values (coefficient of determination) represent the percentage of total variance explained by each multivariate regression. N.a (not applicable) was used when no comparison was possible due to non-significant results; n.s = non-significant.

a.

Right zygomatico-maxillary complex		
	Shape vs size	
	R^2	P-value
all	45%	0.01
all (age regr. out)	2%	**n.s**
0-5.5	40%	0.001
6-18	11%	0.008
18+	4%	**n.s**
	Shape vs age	
	R^2	P-value
all	38%	0.01
all (size regr. out)	0.5%	**n.s**
0-5.5	37%	0.001
6-18	9%	0.04
18+	4%	**n.s**
	Form vs age	
	R^2	P-value
all	72%	0.001
0-5.5	74%	0.001
6-18	37%	0.001
18+	4%	**n.s**

b.

Nasal cavity		
	Shape vs size	
	R^2	P-value
all	19%	0.001
all (age regr. out)	14%	0.001
0-5.5	41%	0.001
6-18	10%	0.04
18+	9%	0.01
	Shape vs age	
	R^2	P-value
all	14%	0.001
all (size regr. out)	0.9%	**n.s**
0-5.5	43%	0.001
6-18	11%	0.03
18+	3%	**n.s**
	Form vs age	
	R^2	P-value
all	66%	0.001
0-5.5	73%	0.001
6-18	40%	0.001
18+	2%	**n.s**

c.

Right palate		
	Shape vs size	
	R^2	P-value
all	44%	0.001
all (age regr. out)	2%	**n.s**
0-5.5	24%	0.001
6-18	8%	**n.s**
18+	16%	0.003
	Shape vs age	
	R^2	P-value
all	41%	0.001
all (size regr. out)	0.8%	**n.s**
0-5.5	23%	0.001
6-18	10%	0.04
18+	3%	**n.s**
	Form vs age	
	R^2	P-value
all	73%	0.001
0-5.5	67%	0.001
6-18	25%	0.002
18+	5%	**n.s**

d.

Right orbit		
	Shape vs size	
	R^2	P-value
all	13%	0.001
all (age regr. out)	2%	**n.s**
0-5.5	19%	0.007
6-18	8%	**n.s**
18+	8%	**n.s**
	Shape vs age	
	R^2	P-value
all	9%	0.001
all (size regr. out)	1%	**n.s**
0-5.5	18%	0.02
6-18	3%	**n.s**
18+	6%	**n.s**
	Form vs age	
	R^2	P-value
all	50%	0.001
0-5.5	71%	0.001
6-18	24%	0.003
18+	5%	**n.s**

e.

Right maxillary sinus		
	Shape vs size	
	R^2	P-value
all	17%	0.001
all (age regr. out)	1%	**n.s**
0-5.5	10%	**n.s**
6-18	10%	**n.s**
18+	8%	**n.s**
	Shape vs age	
	R^2	P-value
all	15%	0.001
all (size regr. out)	0.8%	**n.s**
0-5.5	9%	**n.s**
6-18	7%	**n.s**
18+	13%	0.004
	Form vs age	
	R^2	P-value
all	53%	0.001
0-5.5	57%	0.001
6-18	24%	0.001
18+	13%	0.01

f.

Right zygomatico-maxillary complex: angle tests		
	Shape vs size vectors	P-value
0-5.5 VS 6-18	83°	0.001
6-18 VS 18+	**n.a**	
	Shape vs age vectors	P-value
0-5.5 VS 6-18	85°	0.001
6-18 VS 18+	**n.a**	
	Form vs age vectors	P-value
0-5.5 VS 6-18	29°	0.001
6-18 VS 18+	**n.a**	

g.

Nasal cavity: angle tests		
	Shape vs size vectors	P-value
0-5.5 VS 6-18	88°	0.001
6-18 VS 18+	**ns**	
	Shape vs age vectors	P-value
0-5.5 VS 6-18	77°	0.001
6-18 VS 18+	**n.a**	
	Form vs age vectors	P-value
0-5.5 VS 6-18	24°	0.001
6-18 VS 18+	**n.a**	

h.

Right palate: angle tests		
	Shape vs size vectors	P-value
0-5.5 VS 6-18	**n.a**	
6-18 VS 18+	**n.a**	
	Shape vs age vectors	P-value
0-5.5 VS 6-18	80°	0.001
6-18 VS 18+	**n.a**	
	Form vs age vectors	P-value
0-5.5 VS 6-18	31°	0.001
6-18 VS 18+	**n.a**	

i.

Right orbit: angle tests		
	Shape vs size vectors	P-value
0-5.5 VS 6-18	**n.a**	
6-18 VS 18+	**n.a**	
	Shape vs age vectors	P-value
0-5.5 VS 6-18	**n.a**	
6-18 VS 18+	**n.a**	
	Form vs age vectors	P-value
0-5.5 VS 6-18	27°	0.002
6-18 VS 18+	**n.a**	

l.

Right maxillary sinus: angle tests		
	Shape vs size vectors	P-value
0-5.5 VS 6-18	**n.a**	
6-18 VS 18+	**n.a**	
	Shape vs age vectors	P-value
0-5.5 VS 6-18	**n.a**	
6-18 VS 18+	**n.a**	
	Form vs age vectors	P-value
0-5.5 VS 6-18	22°	0.002
6-18 VS 18+	58°	0.002

Hypothesis 2, that the nature (modes of) and magnitude of covariation among facial components is constant throughout ontogeny.

Table 3.2.2 shows the results of the two-block PLS shape analyses between pairs of facial regions (blocks) in younger subadults, older subadults and adults. In younger subadults, most analyses show significant association between regions, with high correlation coefficients among all pairs of blocks. However, the maxillary sinus covaries significantly only with the orbit and the zygomatico-maxillary region, having no significant association with the nasal cavity and palate. The proportion of the total covariance of the sinus and orbit explained by PLS1 is 62%, while that between the sinus and the zygomatico-maxilary complex is larger (72%), potentially because this complex encases most of the shape of the sinus. The zygomatico-maxillary region shows high and significant associations with all the other modules, while the nasal cavity, palate and orbit all show a lower but still significant degree of covariation. The palate and orbit do not covary. The percentage of total shape variance accounted for by PLS1 within each block is large for the nasal cavity and zygomatico-maxillary complex, where about 50% of their total shape variance is accounted for in their covariance with the other blocks.

In older subadults, the associations are reduced in magnitude (% of total covariance) and most are not significant. The zygomaxillary complex is the only module maintaining a significant relationship, which it does with all of the other regions of the face, except the maxillary sinus. In adults, the only significant associations are found between the shapes of the nasal cavity and those of the palate and maxilla. PLS plots and warpings are not presented because they are of limited interest with respect to the hypothesis.

PLS shape analyses between facial modules in age groups					
Younger subadults					
Block 1 vs Block 2	TOT. COVAR.	CORR. COEFF.	P-VALUE	EXPLAINED VARIANCE BLOCK 1	EXPLAINED VARIANCE BLOCK 2
N.cavity- R.palate	73.09 %	0.84	0.004	52.22 %	26.11 %
N.cavity- R.zygomatico-maxilla	92.23 %	0.93	0.001	53.15 %	49.23 %
N.cavity- R. Maxillary sinus	71.11 %	0.81	**ns**	**n.a**	**n.a**
R.zygomatico-maxilla- R. Maxillary sinus	72.06 %	0.84	0.04	48.27 %	25.14 %
R.Orbit- R.palate	54.35 %	0.85	**ns**	**n.a**	**n.a**
R.Orbit- R.zygomatico-maxilla	76.02 %	0.89	0.003	29.05 %	49.18 %
R.Orbit- N.cavity	79.03 %	0.84	0.01	27.23 %	52.16 %
R.Orbit- R. Maxillary sinus	62.01 %	0.85	0.01	29.44 %	32.04 %
R.Palate- R.zygomatico-maxilla	71.34 %	0.85	0.006	27.18 %	47.06 %
R.Palate- R. Maxillary sinus	32.13 %	0.76	**ns**	**n.a**	**n.a**

PLS shape analyses between facial modules in age groups					
Older subadults					
Block 1 vs Block 2	TOT. COVAR.	CORR. COEFF.	P-VALUE	EXPLAINED VARIANCE BLOCK 1	EXPLAINED VARIANCE BLOCK 2
N.cavity- R.palate	34.05 %	0.75	**ns**	**n.a**	**n.a**
N.cavity- R.zygomatico-maxilla	45.26 %	0.89	0.004	23.12 %	19.15 %
N.cavity- R. Maxillary sinus	48.18 %	0.75	**ns**	**n.a**	**n.a**
R.zygomatico-maxilla- R.sinus	46.32 %	0.85	**ns**	**n.a**	**n.a**
R.Orbit- R.palate	41.27 %	0.47	**ns**	**n.a**	**n.a**
R.Orbit- R.zygomatico-maxilla	66.09 %	0.83	0.005	43.28 %	18.12 %
R.Orbit- N.cavity	59.12 %	0.73	**ns**	**n.a**	**n.a**
R.Orbit- R. Maxillary sinus	40.26 %	0.37	**ns**	**n.a**	**n.a**
R.Palate- R.zygomatico-maxilla	42.03 %	0.91	0.02	24.17 %	16.21 %
R.Palate- R. Maxillary sinus	40.17 %	0.67	**ns**	**n.a**	**n.a**

PLS shape analyses between facial modules in age groups					
Adults					
Block 1 vs Block 2	TOT. COVAR.	CORR. COEFF.	P-VALUE	EXPLAINED VARIANCE BLOCK 1	EXPLAINED VARIANCE BLOCK 2
N.cavity- R.palate	66.10 %	0.88	0.001	19.22 %	37.11 %
N.cavity- R.zygomatico-maxilla	59.02 %	0.95	0.001	23.14 %	26.34 %
N.cavity- R. Maxillary sinus	44.05 %	0.72	**ns**	**n.a**	**n.a**
R.zygomatico-maxilla -R.sinus	46.23 %	0.71	**ns**	**n.a**	**n.a**
R.Orbit- R.palate	49.17 %	0.54	**ns**	**n.a**	**n.a**
R.Orbit- R.zygomatico-maxilla	40.20 %	0.73	**ns**	**n.a**	**n.a**
R.Orbit- N.cavity	34.18 %	0.56	**ns**	**n.a**	**n.a**
R.Orbit- R. Maxillary sinus	47.02 %	0.62	**ns**	**n.a**	**n.a**
R.Palate-R.zygomatico-maxilla	43.07 %	0.74	**ns**	**n.a**	**n.a**
R.Palate- R. Maxillary sinus	53.15 %	0.60	**ns**	**n.a**	**n.a**

Table 3.2.2. Associations among facial blocks as assessed by two-block PLS analysis in younger subadults (a), older subadults (b) and adults (c). TOT.COVAR= percentage of total covariance explained by the first pair of singular warps, CORR.COEFF= correlation coefficients between blocks for PLS1 scores with p-value assessed by permutation test. For each block, the proportion of its total shape variance explained by its covariance with the other block was estimated (ns=not significant, n.a= not applicable).

Younger subadults	R. Orbit	R. Zygomatico-maxilla	R. Palate	Nose	R. Maxillary sinus
R. Orbit	-	0.99***	0.96***	0.97***	0.97***
R. Zygomatico-maxilla	-	-	0.97***	0.98***	0.97***
R. Palate	-	-	-	0.97***	0.94***
Nose	-	-	-	-	0.94***
R. Maxillary sinus	-	-	-	-	-

Older subadults	R. Orbit	R. Zygomatico-maxilla	R. Palate	Nose	R. Maxillary sinus
R. Orbit	-	0.81***	0.62***	0.78***	0.66**
R. Zygomatico-maxilla	-	-	0.84***	0.89***	0.77***
R. Palate	-	-	-	0.67***	0.53**
Nose	-	-	-	-	0.73***
R. Maxillary sinus	-	-	-	-	-

Adults	R. Orbit	R. Zygomatico-maxilla	R. Palate	Nose	R. Maxillary sinus
R. Orbit	-	0.78***	0.67***	0.63***	0.27 **ns**
R. Zygomatico-maxilla	-	-	0.66***	0.74***	0.37 **ns**
R. Palate	-	-	-	0.45*	0.17 **ns**
Nose	-	-	-	-	0.47*
R. Maxillary sinus	-	-	-	-	-

Table 3.2.3. Pairwise Pearson's correlation among the Csize of the facial blocks in younger subadults (top), older subadults (middle) and adults (bottom). P-values are indicated with asterisks, *** = p.value < 0.001, ** = p.value < 0.01, *= p.value < 0.05.

Correlations among Csizes of the facial modules in Table 3.2.3 indicate that in younger subadults, for all facial blocks, changes in size in one module are significantly associated with changes in size in another module, with similar and high correlation coefficients for

all pairs. In the older subadult group, all correlations are smaller than in the younger subadults but moderately large and significant, except for the palatal module. The Csize of this region is strongly correlated only with that of the zygomatico-maxillary region (Pearson's coeff.= 0.84***) and less so with the sinus (Pearson's coeff.= 0.53**), nose (Pearson's coeff.= 0.67***), and orbit (Pearson's coeff.= 0.66**). This, combined with the PLS results for the subadults, which show palatal shape has no significant covariation with the other facial modules except for the zygomatico-maxillary region, suggests a degree of modularity of this region between 6 to 18 years. In the older subadult group, Csize of the zygomatico-maxillary region has the highest correlation with Csize of all the other variables. This, combined with the PLS results for the same age group, which show that this region has the highest and most significant covariation coefficients with the palate, orbit and nose, suggests that this region has a central role as an integrating element of the facial complex.

In adults, all correlations are lower compared to the two subadult groups, however, the zygomatico-maxillary complex maintains high correlations with the nasal cavity (Pearson's coeff.= 0.74***) and orbits (Pearson's coeff.= 0.78***). The maxillary sinus does not correlate with any other region in adults except the nasal cavity (Pearson's coeff.= 0.47*).

3.2.5 Discussion

Numerous studies have examined the growth and development of the facial skeleton and the covariation among facial elements in different populations (Butaric and Maddux, 2016; Paoloni et al., 2017). However, detail of how different regions grow, develop and scale and how they interact during postnatal ontogeny in modern humans are not yet fully understood. In part, this is because of methodological limitations. Beyond this, facial growth is a complex phenomenon that varies among populations (Viðarsdòttir et al., 2002) and it is hard to study because of variability and because of the limitations of sampling due to lack of quality and quantity of CT scans (as was also the case in this study). Additionally, because of the difficulty of obtaining large and complete ontogenetic series

from single individuals, most studies have to rely on cross-sectional data, which bring along many issues limiting what can be learnt (German, 2004). However, knowledge of facial ontogeny and ontogenetic interactions is fundamental to both the treatment of craniofacial dysmorphologies and in understanding the evolutionary mechanisms of morphological differentiation among modern humans and their closely related relatives (Ackermann and Krovitz, 2002; Krimmel et al., 2015; Evteev et al., 2018).

The aim of this chapter is to investigate how different facial modules grow and develop during ontogeny, how they covary, how their shape relates to centroid size and how shape and form relate to age.

Hypothesis 1 stated that *the skeletal components of the modern human face do not differ in their growth, development or allometry among different age classes.*

Figure 3.2.1 shows that size changes with age, unsurprisingly, are a common feature of all regions with the variance in centroid size observed in subadults being least in the orbits and zygomatico-maxila and greatest in the maxillary sinus and palate. Thus, size changes during ontogeny are highly integrated, with differences between regions becoming more evident with age. The maxillary sinus and palate are least integrated through allometry. It is clear from Table 3.2.1 that, for each region, the relationship between shape and centroid size, shape and age, centroid size and age and form and age is not consistent during ontogeny and that the ways in which these regions grow and develop is significantly different among age classes as well as among regions.

For the zygomatico-maxillary complex (Table 3.2.1, a), all the regressions are significant in younger subadults and older subadults but not in the adult group, although the proportion of total variance explained by the regressions drops in the older subadult sample. This indicates that changes in shape due to changes in size (allometry) or age (development) and changes in form over time persist until at least the age of 18. Furthermore, in the younger and older subadult groups, these changes occur along significantly divergent trajectories, as shown by the angle tests in Table 3.2.1 (a). This suggests that the vectors of shape change in these anatomical regions are profoundly different between the two age classes. These results show that divergent midfacial trajectories are not only present in different populations at birth and further accentuated

during growth (Viðarsdòttir et al., 2002; Viðarsdòttir and O'Higgins, 2003), but that, within the same trajectory, divergence exists between different age classes.

When looking at the nasal cavity (Table 3.2.1, b), interestingly, the relationship between shape and centroid size is significant in all three age classes, indicating that allometric development of this structure continues throughout adulthood. However, divergence of ontogenetic vectors is only found between the younger and older subadult groups, indicating that the older subadults and adults scale along the same trajectory. Previous research has focussed on the growth rate of the nasal septum, with results highlighting that growth is most significant from 10 to 30 years of age (Kim et al., 2008). Other studies have focussed on the nasal septum asymmetry and its influence on the maxillary complex (Kim et al., 2011). The analysis in Table 3.2.1b, examining the allometry of the entire nasal cavity, confirm the trends observed in other studies for the size of the nasal septum and builds on these results, indicating that the prolonged changes in size of the nasal cavity also have a prolonged impact on nasal shape, with effects that extend from infancy to adulthood. The regressions of both shape and form on age are significant in the younger and older subadult groups but not in adults; however, as previously discussed, limitations due to lack of age information for the adults might affect this result.

The regression of palatal shape on centroid size (Table 3.2.1, c) is significant for the younger and adult groups, but not for the older subadult group. The regressions of shape and form on age are significant for younger and older subadult groups, and the resulting ontogenetic trajectories differ significantly between the younger and older subadults, suggesting that the changes in shape with age differ between the two age classes, and that when size is included in the analysis of shape (form) the divergence still exists among different age classes.

For the orbit, the regression of shape on centroid size and on age (Table 3.2.1, d) shows that allometric development is significant only in the younger subadult group, up until the age of 5.5 years old. This is in agreement with what is observed in the literature (Evteev et al., 2018) and with Section 3.3, where the growth of the orbit, its impact on shape and its interaction with the other facial regions are significant in the first years of life and become less prominent as age increases.

Looking at the regressions for the maxillary sinus (Table 3.2.1, e) its shape is not significantly associated with its centroid size or age for any of the age classes. However,

the regressions of form (shape and size) on age are significant in all age groups, with significantly divergent trajectories between younger and older subadult groups and between older subadults and adults. These results suggest that the significance is driven by the introduction of the size information (form), suggesting that there is an association between size and age, rather than shape. The absence of significant regressions between centroid size and shape in all the age classes indicates that the maxillary sinus morphology is highly variable during ontogeny, reflecting the difficulties that previous workers encountered in classifying their shape (Kim et al., 2002). Therefore, Hypothesis 1 is falsified, since growth and allometric development differ significantly among different age classes and different regions, with divergent trajectories between age groups within single regions.

Hypothesis 2 stated that *the nature (modes of) and magnitudes of covariation among facial components is constant throughout ontogeny.*

PLS analyses indicate that the associations among the shapes of facial elements in the younger subadult group are all significant, except between the palate and orbit, with the highest total covariation found between the nasal cavity and the zygomatico-maxillary complex. This suggests that developmental changes are highly integrated (as defined by Klingenberg, 2009, Goswami and Polly, 2010) in terms of covariance among regions during childhood. As other authors have observed (Gkantidis and Halazonetis, 2011), allometry, which in the regressions of Table 3.2.1, explains a greater proportion of total variance in younger subadults, influences the strength of morphological covariation. Marked size increases result in stronger associations between facial modules in younger subadults. The only significant covariation identified from the PLS analyses of shape in the older subadult group is found between the zygomatico-maxillary region and the palate, orbit and nasal cavity. Thus, the zygomatico-maxillary region seems to play a central role in the integration of all of the elements of the face at these stages of growth. This result is supported by Bastir and Rosas (2013), who addressed the covariation among facial regions and found higher covariation between the midface and other regions. Thus, even though the zygomatico-maxillary complex, nasal cavity and other facial elements develop somewhat independently prenatally, during childhood and adolescence these regions come to show degrees of covariation, with the midface mediating the integration between facial elements. Only two pairs of modules covary significantly in the PLS

analyses of the adults: the nasal cavity with the palate and the nasal cavity with the zygomatico-maxillary complex. This last association is consistently significant throughout the entirety of ontogeny, and in younger subadults the nasal cavity shows significant covariation with all other regions except the sinuses.

These results, together with the regression results in Table 3.2.1, which indicate that the relationship between nasal shape and centroid size is significant in all three age classes, support prior studies that suggested a central role of the nasal cavity in shaping the facial complex (Pirsig, 1992; Holton et al., 2012; Al Dayeh et al., 2013, Hartman et al., 2016). Indeed, the nasal complex changes throughout life, with allometry affecting nasal proportions from infancy through adulthood. Despite these changes, this region maintains high covariation and integration with adjacent structures, particularly the zygomatico-maxillary complex and palate. This last association (nose-palate) has been observed in *in vivo* experiments on animals and has been linked to the potential for growth of the nasal septum to affect the growth and development of the alveolar region (Holton et al., 2011). While it is not possible to determine causality when looking at covariation, it is evident from these results and previous research that the nasal cavity plays a central role, which will be further investigated in Section 3.3 of this thesis.

The maxillary sinus is significantly associated only with the zygomatico-maxillary complex and the orbits and only in the younger group. This is likely because orbital growth and development are most pronounced during early childhood (Krimmel et al., 2015), therefore the PLS is reflecting the simultaneous development of the orbit and sinus in the first years of life, the floor of the former constituting the superior boundary of the latter. Surprisingly, while the maxillary sinus and the zygomatico-maxillary region show significant shape covariation in the younger subadult group, this is not observed in older subadults and adults, even though most of the maxillary sinus is encased in the zygomatico-maxillary complex. Thus, the PLS analyses indicate that sinus development is not associated with the development of adjacent facial regions. These results support studies indicating a minor role of this structure in shaping the human face (Butaric and Maddux, 2016, Evteev and Grosheva, 2018).

Complementing the studies of shape covariation among regions, analyses of the strength of association of ontogenetic size variation find strong, significant and widespread correlations among pairs of blocks in younger and older subadults, although correlations

are lower in the latter with the exception of the zygomatico-maxillary complex. This reflects the shape covariation observed in the PLS analyses, in which this region maintains significant and strong associations throughout postnatal ontogeny. These results further indicate that the zygomatico-maxillary complex acts to integrate elements of the face (Bastir and Rosas, 2013).

In contrast, palatal size shows relatively weak correlations with the size of other facial modules, reflecting the PLS analyses of palatal shape, which shows a degree of independence of this region especially in older subadults.

In adults, correlation coefficients remain large and significant among all pairs of variables except the maxillary sinus, which shows no significant correlation with any other facial structure except for the nasal cavity. This reflects the PLS analyses of shape associations which showed maxillary sinus shape is not significantly associated with the shapes of adjacent facial regions at all age stages (except for two significant covariations with the orbit and zygomatico-maxilla in older subadults). These findings reflect those of a previous study that attempted to classify sinus adult shape in terms of the location of the sinus walls with respect to parts of the face (Kim et al., 2002). The study found at least six different morphological types, indicating how highly variable this structure is in adult modern humans. Other studies, when looking at maxillary sinus form in adults of different populations, also found an exceptionally high level of within and between-group variance (Evteev and Grosheva, 2018), as well as a positive correlation between the size of the maxillary sinuses and that of the nasal cavity, so that larger faces have a larger nose and sinuses (Holton et al 2013; Evteev and Grosheva, 2018). In conclusion, these findings falsify Hypothesis 2 because the nature (modes of) and magnitudes of covariation among facial components vary markedly and significantly throughout ontogeny.

3.2.6 Conclusions

It is evident that during postnatal ontogeny, significant differences arise in allometry between different age classes within each facial region and in the covariation among regions. Most facial regions show divergence of ontogenetic (allometry and

development) trajectories between younger and older subadults (Table 3.2.1). Thus, the ways in which facial elements change in size, shape and in their interactions with other elements change over time. Similar shifts in modes of shape change during ontogeny are observed in the colour maps of Section 3.1., Figure 3.1.1 and 3.1.7, where differences in the development of the nose and maxilla are evident between younger and older subadults.

In addition, size and shape (allometry) of the nasal cavity are significantly associated from infancy to adulthood. Indeed, as emerging from the PLS analyses, the nasal cavity is the only region that possesses significant covariation in the adult group, its changes being significantly associated with the palate and zygomatico-maxillary complex, and the only region that shows significant covariation with the zygomatico-maxillary complex throughout the entire postnatal ontogeny. This suggests a major role of the nasal complex within the face, which is further explored in Section 3.3.

Some interesting insights from the results of this section also concern the palatal region, which shows reduced interactions with other parts of the face from 6 to 18 years (Table 3.2.2). In addition, shape changes appear not to be associated with size changes but to ageing (Table 3.2.1, c). This could provide useful insights into palatal clinical procedures, especially for the treatment of the cleft palate (Rohrich et al., 2000). Indeed, information about the palate being a relatively independent unit during the 6 to 18 year time range could help identify better procedures for palatal surgical intervention without affecting adjacent structures.

The results of this section also shed light on orbital development. The orbital region, as already observed (Evteev et al., 2018) appears to grow and develop rapidly during the period 0 to 6 years, during which it shows some significant interactions with other regions. In the older subadults and adults, its allometric development ceases and covariation with adjacent regions is less significant. This is also evident when looking at the colour maps of Section 3.1 Figure 3.1.1 and 3.1.7, which show this region undergoes little expansion throughout ontogeny.

These studies present some interesting insights into the maxillary sinuses and their interactions within the facial complex. The shapes of these sinuses covary very little with the shapes of adjacent structures, but size changes of the sinuses are associated with size

changes elsewhere in the face. Thus, while maxillary sinuses grow as the face grows, their shape, as seen in previous studies (Evteev and Grosheva, 2019) is highly variable and does not develop in an integrated way with adjacent regions. These results, as already mentioned in the discussion, support the conclusion that sinuses have a minor role in cranial architecture and probably develop somewhat arbitrarily within the available space. This is consistent with prior studies that have suggested these sinuses arise through mechanical cues that stimulate remodelling. Thus, their morphology is variable because their development depends on local strains developed within the maxilla from the interaction between available space, and the (variable) forces experienced by it during life. These findings are consistent with prior finite element analyses (O'Higgins et al., 2006; O'Higgins et al., 2012) that have shown that the maxillary sinuses occupy regions that, if filled with bone, would experience very low strains. These findings support the view that the sinuses develop opportunistically in response to mechanical signals, rather than under genetic control.

In conclusion, this study aims at starting the investigation of the relation among facial elements during ontogeny with the goal of shedding light on the patterns of variation and covariation during growth and development. Results show that allometric patterns vary significantly among different age classes and among different facial regions, with divergent trajectories between different age classes of a single region indicating that modes of development differ significantly among younger and older subadults. Shape and size covariation patterns also vary significantly between different age classes, with the younger subadults having the strongest interactions. Limitations of this study include the sample size and the lack of precise information about gender and age. Further studies including a larger sample and variables such as gender and exact age should aim at building a normative study of the human face during the entire life cycle from infancy to old age.

3.3 Path Analyses applied to growth models: contribution of skeletal and soft-tissue matrices to facial ontogeny

3.3.1 Background

This chapter aims to clarify the interactions among facial components in driving the growth and development of the human face in the first years of life. It will do this by applying the statistical method of path analysis to infer interactions among skeletal and soft tissue facial elements including derivatives of the nasal capsule, maxilla, orbit and alveolar region.

Human craniofacial ontogeny has been the subject of intensive study in several disciplines. This body of research spans studies of evolutionary patterns of variation in hominins (O'Higgins et al.,2000; Ponce de Leon and Zollikofer, 2001; Ackermann and Krovitz, 2002; Cobb and O'Higgins, 2004; Bastir et al., 2007), through anthropological analysis of current growth trends in different modern populations (Viðarsdóttir et al., 2002; Gonzalez et al., 2010), to the creation of normative reference data for surgical and clinical studies (Buschang et al., 1983; Landes et al., 2002; Jiang et al., 2015; Gkantidis and Halazonetis, 2011). The common aims are to understand the mechanisms that regulate craniofacial growth, the major driving forces and constraints acting on it over ontogenetic and evolutionary time and how the cranium grows and develops to reach its final size and shape. Particularly relevant to this chapter, many studies have addressed the interactions among the cranial base, neurocranium and mandible and their influence on human craniofacial development (Lieberman et al., 2002; Bastir and Rosas, 2006; Bastir et al., 2006). These suggest a hierarchy of ontogenetic interactions that impacts on the development of aspects of facial form such as its vertical development, its orientation and prognathism (*e.g.* Lieberman et al., 2002; Bastir and Rosas, 2006; Bastir et al., 2008; Neaux et al., 2015). Although patterns of craniofacial growth, development and interactions among regions are becoming better understood, there is a lack of understanding of the mechanisms underlying these interactions, especially when considering the face and its sub-regions (Bastir and Rosas, 2004, Butaric and Maddux, 2016; Maddux and Butaric, 2017). Several attempts to identify the drivers of change in the facial region during ontogeny have been made, with contrasting results supporting

either skeletal or soft tissue components as the principal pacemakers for facial growth and development (McLaughlin, 1949; Scott, 1956; Wexler and Sarnat, 1965; Burston and Latham, 1964; 1970; Moss, 1968; Babula et al., 1970; Diewert, 1985; Delaire and Precious, 1987; Grymer et al., 1989; Grymer et al., 1991; Pirinen, 1995; Verwoerd and Verwoerd-Verhoef, 2007; Wong et al., 2010; Holton et al., 2011; 2012; Al Dayeh et al., 2013; Hall and Precious, 2013; Goergen et al., 2017).

Differences in conclusions may be attributable to the choice of species (and so differences in the form of sutures and articulations of bones) and to the differences in approaches and sampling (i.e focusing on different areas at different times of development).

In this chapter, growth interactions among skeletal components of the face are assessed using path analysis. These relations are explored by building a path model in which a specific network of interactions was designed to test the relationships between facial bony elements. These results are then compared with those from a path that also includes measurements of capsular and periosteal matrices as defined by Moss (Moss and Young, 1960; Moss, 1968; Moss et al., 1968; Moss and Salentijn, 1969). The aim is to investigate likely interactions among soft and hard tissues during growth and so, test hypotheses concerning potential drivers of facial growth, first elaborated by Scott (1954; 1956; 1962) and Moss (Moss and Young, 1960; Moss, 1968; Moss et al., 1968, see Section 1.1.5 of Chapter 1 for further details).

3.3.2 Path analysis in literature

Path analysis is a statistical method used to test interactions in a network of dependent and independent variables linked by hierarchical relations. The design of the network represents hypothesised interactions derived from prior knowledge. Path analysis allows the relative contributions of different hypothesised interactions to be evaluated and compared.

Path analysis was first conceived by the geneticist Wright (1921, 1934) as a means of testing the interactions between multiple variables in a system to understand the functional relations among them. It was designed to test alternative hypotheses about cascades of interactions, to assess which are the most likely directions of action based on the strength and significance of these interactions. Its aim is to assess the potential connections between variables in a path model, analyse the relative contribution of each to the dynamics of the designed path (Stage et al., 2004), and allow alternative paths to be compared in these terms. The tests are performed using standardised multiple regression, which computes the strengths and significance of the interactions between the dependent and the independent variables. Conclusions can be drawn by comparing the results (i.e strengths and significances of interactions) between sub-paths of a path model or between two different path models. This approach is particularly useful in testing complex models with multiple dependent and independent variables (Streiner, 2005).

Path analysis has been applied in psychology and social sciences (Duncan, 1966; Pajares and Miller, 1994; Streiner, 2005; Rudasill and Rimm-Kaufman, 2009), ecology (Mitchell, 2001) and more rarely to analyse the interactions among morphological elements (Mooney et al., 1989; Bullmore et al., 2000; Holton, 2008; Zollikofer et al., 2017). It is important to note that each path model is designed using prior knowledge. Therefore, the hypothesised hierarchy of interactions between variables is embedded in the design of the model and needs to be based on a solid theoretical background. It is also important to clarify that Path Analysis cannot be applied to determine causality but it can assess the adequacy of the designed model in describing the relationships among variables and if these are consistent with the model. If the variables inadequately account for observed effects (the dependent variables) this is an indication that other factors not considered in the original model should be considered for inclusion.

3.3.3 The hypotheses

As applied in this study, path analysis aims to yield information about the proportional contribution of the skeletal and soft tissue variables to the growth and development of facial height in the early years. Two path models based on current hypotheses of interactions among facial components, derived from the literature were designed. The first (P1, Figure 3.3.1) is designed to test the relative contributions of different facial skeletal elements to the vertical growth of the face. This path tests the intrinsic growth model, hypothesised by Scott and other authors (Scott 1954, 1956, 1962; Young, 1960; Vetter et al., 1984; Pirinen, 1995; Wong et al., 2010; Al Dayeh et al., 2013; Hall and Precious, 2013), which states that primary cartilaginous growth centres (i.e nasal septum) drive facial growth. The second path model (P2, Figure 3.3.2) assesses the contributions of soft and skeletal tissues to facial ontogeny. This path aims to test aspects of the Functional Matrix hypothesis, first elaborated by Moss (Moss and Young, 1960; Moss, 1968; Moss et al., 1968), and supported by authors over the years (Latham and Burston, 1964; Babula et al., 1970; Goergen et al., 2017), which hypothesises that soft tissues interact with skeletal elements to drive facial growth (see Section 1.1.5 of Chapter 1 for further details).

The structure of a general path diagram and of the two paths designed for this study is explained in more detail below.

In a path diagram, the relationships and postulated interactions among variables are indicated by arrows. A variable with no arrows pointing to it indicates an independent variable, not affected by any of the others in the path diagram. A variable with one or more arrows pointing toward it is a dependent variable that has one or more independent variables acting on it. Bidirectional arrows indicate hypothesised two-way interactions between variables (covariation). If a variable within the path is never dependent, this is called an exogenous variable. Furthermore, a sub-path is a specific path in the diagram leading from one exogenous variable to the final variable of the path, which acts always and solely as a dependent variable. A variable that acts on, and is acted upon by, other variables is an intermediate variable.

After building a path diagram, the strengths of the hypothesised interactions between dependent and independent variables are tested using standardised multiple regressions. Standardised coefficients have a mean of 0 and a standard deviation of 1. The resulting standardised partial regression coefficients, termed β coefficients or path coefficients, indicate the change in the dependent expected when there is a one-unit change in that particular independent variable while holding all the other independent variables constant (Allen, 1997). Additionally, the proportion of the total variance of each dependent variable explained by the independent ones in the path leading to it is assessed by computing the R^2, or coefficient of determination.

The first path diagram (P1, Figure 3.3.1) constructed in this section was designed to test hypothesised interactions among the orbit, the derivatives of the nasal capsule, the maxilla and the peri-alveolar region. The variables used in the path diagram were selected by considering their function and development; each not only serves a different purpose within the facial complex but is also derived from a different growth centre. The orbital height and medial orbital height were used as proxies for orbital growth and development; the height of the nasal cavity was chosen as a proxy for the growth and development of nasal capsule derivatives, specifically the septum; the subnasal and maxillary heights were chosen as proxies of, respectively, peri-alveolar and midfacial growth and development.

In the path P1 (Figure 3.3.1), the role of nasal height (as a proxy for the growth of nasal septum) on facial elements is compared to that of orbital height (proxy for the growth of the orbital region). This first path diagram aims to test Scott's nasal septum hypothesis (1954). In his theory, Scott (1954) states "[…] The cartilage of the nasal septum is an important factor in separating the bony elements which have developed around it and may be regarded as a pacemaker for facial growth. This power of cartilage to separate growing bones at sutures resides in its method of interstitial growth, its turgidity and its ability to resist deforming forces" (Scott, 1954). This position has been supported by Hall and Precious (2013), who using evidence from *in vivo*, *in vitro* and surgical records, suggest that vertical nasal septum growth is the prevalent force acting on facial growth when compared to other skeletal and soft tissue facial elements. Furthermore, experimental studies in animals, in which vertical facial growth was constrained, show

evidence that this restriction causes changes in premaxillary growth and displacement due to continued nasal septal growth (Holton et al., 2011).

Therefore, in path P1, nasal height is chosen as an independent exogenous variable, hypothesised here to not be influenced by the other skeletal variables in the model but rather acting as a pacemaker for growth of the entire facial skeleton and all its variables. Another hypothesised independent variable in the first path P1 is orbital height. This is because some authors claim that, in the early years, the growth and development of the orbit are rapid compared to other facial regions. This is said to have a major impact on facial morphology in not only largely defining facial form during early stages but also driving the growth, development and proportions among other facial elements (Sarnat, 1982; Farkas et al., 1992; Furuta, 2001).

Therefore, in P1, to compare the influence of these two exogenous variables, arrows from nasal and orbital heights point at the intermediate variables of medial orbital height, maxillary and subnasal height and at the final variable of facial height.

Specifically, medial orbital height is potentially influenced by the growth of the maximum height of the orbit, but it could also reflect the development of the adjacent nasal bridge, whose growth is directly proportional and potentially linked to the growth of the nasal septum (Mondin et al., 2005). Therefore, in the path diagram P1 (Figure 3.3.1), arrows point at this variable from the nasal and orbital heights.

In addition, the vertical development of the maxilla has been suggested to be influenced by the rapid growth of the orbit during early childhood (Pool et al., 2020). Furthermore, several studies have proposed that the maxillary and subnasal region are each primarily influenced by the nasal septum, given its position within the central maxilla and its anatomical connections at its inferior border with the palate and the alveolar region (Holton et al., 2011). Therefore, in the first path diagram, P1, the maxilla is hypothesised first to act as a dependent variable, affected by nasal and orbital heights, while subnasal height is hypothesised as being influenced by nasal height.

In addition, subnasal height is hypothesised as dependent on maxillary height. Indeed, the vertical development of the maxilla has been hypothesised to impact on the development of the adjacent subnasal premaxillary region, in that patients with maxillo-palatal deformities show abnormal premaxillary growth and development (Liao et al.,

1998). Therefore, within the path P1, maxillary height is hypothesised to act on subnasal height, and through that on facial height.

To end the path, all the variables, exogenous and intermediates, act on overall facial growth (facial height).

The first path (P1) in Figure 3.3.1 was designed to test the following hypothesis:

Hypothesis 1. *The interactions within the sub-path leading from nasal height to facial height are stronger than those in the sub-path leading from orbital height to facial height in all age groups.*

Thus, the first path (P1, Figure 3.3.1), assesses the influence of nasal height on all the dependent variables in all age groups relative to that of orbital height, and so assesses Scott's hypothesis that the nasal septum acts as a pacemaker during growth and development (Scott, 1954; 1956; 1962) against the alternative, that the height of the orbit is more important. As described above, these hypotheses are based on prior experimental studies. The aim of this first path is to compare the relative strengths and potential directions of the hypothesised interactions.

P1.

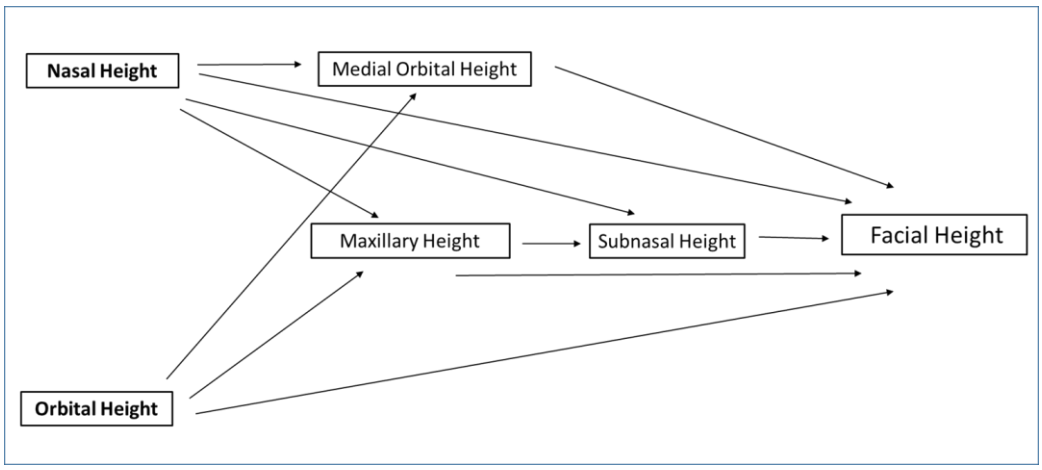

Figure 3.3.1. Path analysis diagram (P1) of the skeletal variables used to test Hypothesis 1. Image produced by the author.

The aim of the second path diagram (P2, Figure 3.3.2), is to compare the role of the skeletal and cartilaginous components of the face with that of some of the cranial functional matrices proposed by Moss (1960) in influencing facial height during growth. Therefore, a second hypothesis was built, which states that:

Hypothesis 2. *The interactions within the sub-paths leading from the soft tissue elements to facial height are greater than those in the sub-paths leading either from the skeletal elements to facial height.*

According to Moss (1960), a functional matrix is "a tissue or space necessary to carry out a given function" (Moss, 1968). In this context, the skeletal elements of the skull serve to protect and support their related functional matrices (Moss, 1968). Periosteal matrices are defined as muscles, blood vessels and nerves, and they act directly on the bone, modifying it. Capsular matrices are defined as a space or an organ and are hypothesised to act indirectly by modifying the capsular space they occupy, causing translation of other cranial components in space. Moss counters Scott's findings and those of other authors supporting the Nasal Septum theory (Scott, 1956; Hall and Precious, 2013), claiming that the nasal septal cartilage does not act through interstitial growth as a primary driver of facial height and antero-posterior lengthening (Moss, 1968). By reviewing studies investigating post-operative recovery after maxillo-facial surgery in children (Moss, 1968), Moss comes to the conclusion that the nasal septum is not a primary growth site, but that its only role is to act as a pillar by physically supporting the nasal cavity, and its growth is always secondary and compensatory to that of the facial soft tissue matrices. According to Moss, the growth of soft tissues such as the orbital globe, the intra-oral soft tissue and the facial muscles influences not only the growth of their supporting skeletal elements, the maxilla, the orbit and the alveolar region, but also overall facial growth, development and proportioning.

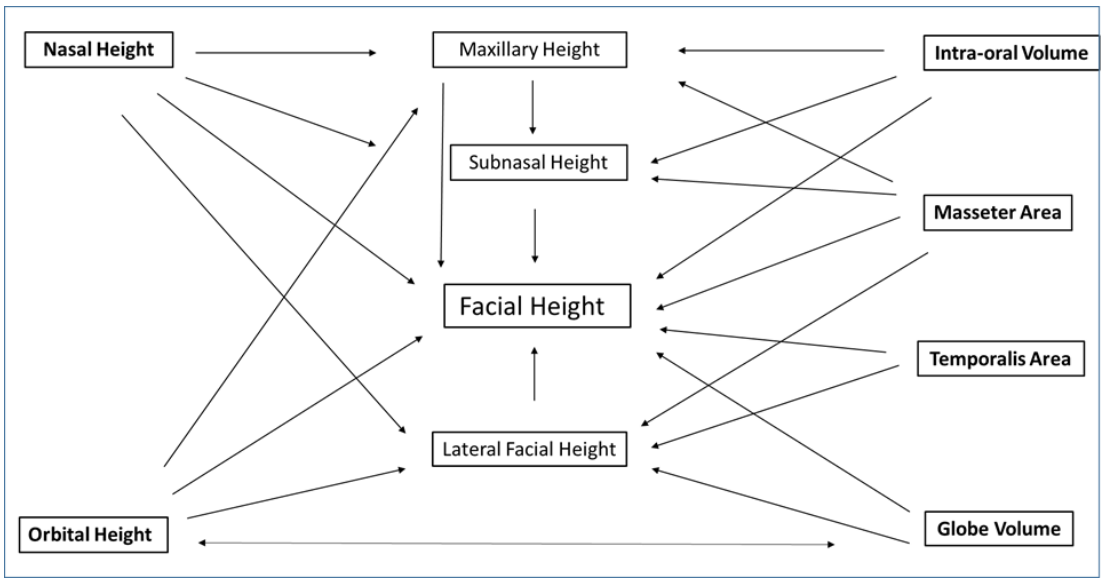

Figure 3.3.2. Path analysis diagram of the skeletal variables (P2) used to test Hypothesis 2. Image produced by the author.

Therefore, in the second path (Figure 3,.3.2, P2) built for this study, the masseter and temporal areas (as proxies for muscle forces) and the intra-oral soft tissue and orbital volumes (cube roots) are considered as exogenous variables acting on the maxilla, subnasal, medial orbital and facial skeletal measurements together with the skeletal exogenous variables of orbital and nasal heights. Finally, orbital volume and orbital height are likely to covary (double-ended arrow).

If the impact of capsular and periosteal matrices (the exogenous variables of the intra-oral soft tissue and globe volume and the masseter and temporal areas) on the intermediate variables representing their skeletal support is bigger than the influence exercised on the same intermediate variables by the independent exogenous variables of the septum and orbit, this would support Moss's functional matrix hypothesis. In fact, according to Moss, the skeletal elements grow passively, to accommodate the growth and development of the functional elements of the capsular and periosteal matrices (such as muscles, soft tissues filling cavities and organs) of the skull (Moss, 1968).

3.3.4 Material and methods

3.3.4.1 The explanation of the paths

This study examines the period from 0 to 6 years of age, in which the face experiences its most rapid changes (Bulygyna, 2006). This rapid growth is also confirmed by the PCAs and the results of the multivariate regressions between age and size and size and shape in Sections 3.1 and 3.2.

The first path (P1) in Figure 3.3.1 was designed to test Hypothesis 1 as explained in the introduction:

Hypothesis 1. *The interactions within the sub-path leading from nasal height to facial height are stronger than those in the sub-path leading from orbital height to facial height in all age groups.*

This hypothesis allows an assessment of the main factors that have been postulated to drive facial skeletal changes. It specifically aims to test the hypothesised major role of the septum (nasal height) in contributing largely to and acting as a driver of increases in facial height. The role of the nasal septum as a primary pacemaker is studied by testing the strength of association between the development of nasal height (exogenous variable) and that of the intermediate variables of medial orbital height, maxillary height, subnasal height and the final variable of the overall facial height. Simultaneously, the influence of orbital height, the other exogenous variable, on medial orbital height and maxillary height, and through these, on subnasal height and the final variable of overall facial height is assessed. Whenever two variables point at the same dependent variable, they are considered as acting simultaneously and the net effect of one is estimated by taking into account the effect of the other.

Testing of this hypothesis will lead to estimates of the relative contributions of each of the skeletal facial elements to overall growth in facial height in early postnatal ontogeny. The analyses will examine the impact of the nasal and orbital variables on the regions potentially affected by their growth and development, as well as the impact of all the variables of the path on overall facial height increase in the period 0-6 years.

If the null hypothesis is falsified, this would indicate that the orbits play a bigger role in shaping facial proportions than suggested by Scott and that the nasal septum does not act as a primary pacemaker during early years. Furthermore, it could indicate that other developmental mechanisms possibly involving other variables not accounted for in the path P1 (Scott's 1954 model) contribute to shaping facial growth and development.

To test Moss's functional matrix hypothesis the second path diagram, P2 (Figure 3.3.2), is designed to assess the hypothesised relationships between soft and skeletal tissues, or, as Moss termed them, between the facial functional matrices and their skeletal supports. As stated in the introduction, Hypothesis 2 As sustains that:

Hypothesis 2. *The interactions within the sub-paths leading from the soft tissue elements to facial height are greater than those in the sub-paths leading either from the skeletal elements to facial height.*

If the null hypothesis is falsified, i.e if the soft tissue functional matrices defined in the path P2 (the masseter and temporal areas and the cube roots of intra-oral soft tissue and orbit volumes) have a weaker relationship with the intermediate variables of the maxilla, the alveolar subnasal region, the medial orbit and overall facial height than these have with the exogenous variables of orbit and nasal height, this would falsify Moss's Functional Matrix hypothesis particularly with regard to the impact of capsular and periosteal matrices of the cranium in driving facial height.

3.3.4.2 The sample

For this study, linear measurements, areas and volumes were extracted from a collection of medical CT-scans of infants from 0 to 6 years of age from the National Scientific and Practical Centre of Children's Health (SCCH), Moscow (Russia), (Courtesy of Dr Evteev, Lomonosov Moscow State University). The use of this dataset was approved by the Independent Ethics committee at the SCCH, Moscow and by the Hull York Medical School Ethics Committee, York. The sample used for the skeletal measurements to test the first path (P1) comprises 227 specimens. Because of practical (all digitising to be done

remotely via Moscow due to ethical constraints) and time limitations, a subsample of 46 specimens was used to measure soft and skeletal tissues to test the second path (P2). The small sample was also due to the necessity to clearly recognise soft tissues, which led to the consequential exclusion of several specimens. This resulted in a small sample for such a complex path, and as such, the results from this second path should be viewed with caution.

For the analyses, the sample of 227 individuals used to test the first path (P1) was divided into age groups as follows: 0 to 1 year old (91 specimens), 1 to 2 year old (27 specimens), 2 to 3 year old (25 specimens), 3 to 4 year old (27 specimens), 4 to 5 year old (32 specimens), 5 to 6 year old (25 specimens). The sample of 46 specimens used to test the second path (P2) includes: 17 specimens of 0 to 1 years old, 8 specimens of 1 to 2 years old, 5 specimens of 2 to 3 years old, 7 specimens of 3 to 4 years old, 3 specimens of 4 to 5 years old and 6 specimens of 5 to 6 years old.

3.3.4.3 Skeletal measurements

The skeletal linear measurements were acquired by estimating the Euclidean distance between pairs of landmarks acquired on the 3D mesh of the skulls using Avizo 9.0.

The landmarks and the measurements acquired for the study are described in Table 3.3.1.

Linear measurements of skeletal tissues	Definition of the landmarks used for linear measurements (Frankfort orientation)
Nasal Height	Rhinion- Subspinale (lm 1-2)
Medial Orbital Height	Between the most superior and inferior points on the lacrimal bone (lm 3-4)
Maxillary Height	Between the most superior and inferior points on the Zygomatico-maxillary suture (lm 5-6)
Subnasal Height	Subspinale- Alveolar (lm 2-7)
Orbital Height	Most superior point on upper border of the orbit - Zygomatico-maxillary suture at the orbital margin (lm 8-5)
Facial Height	Nasion- Alveolar (lm 9-7)

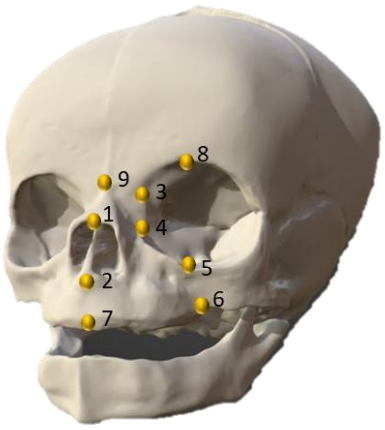

Table 3.3.1: Left: linear measurements and landmarks (lm) used to estimate them; right: picture of an infant skull with the landmarks used to estimate the linear measurements.

3.3.4.4 Soft tissue measurements

A series of soft tissue measurements was acquired on the CT-scans. The segmentation and measurements were undertaken using Avizo 9.0.

To measure the soft tissues, the skull was first reoriented to the Frankfort plane axially (Figure 3.3.3) and along a symmetric midline plane vertically (Figure 3.3.4).

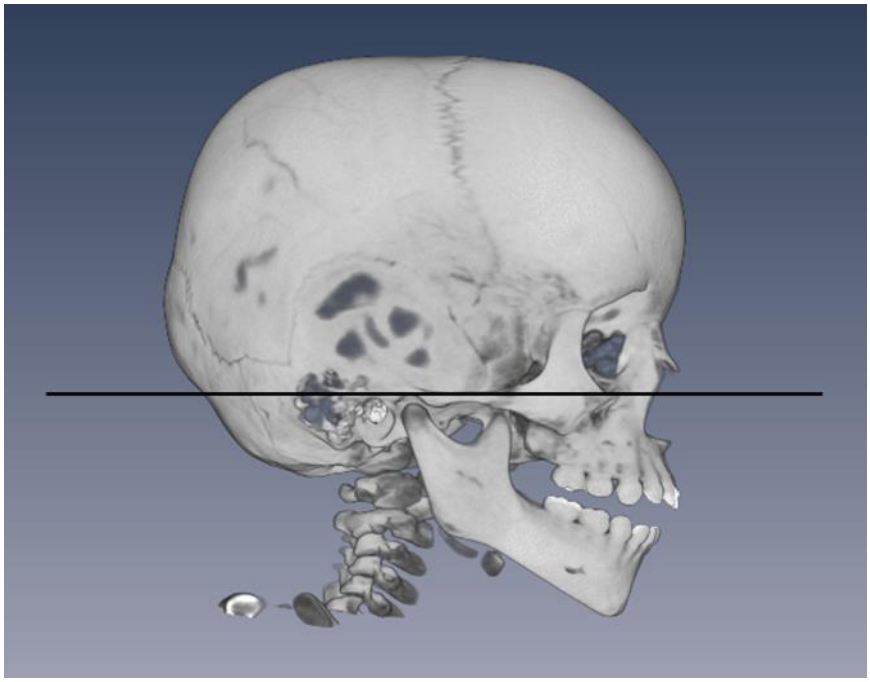

Figure 3.3.3. Image showing the 3D mesh rendering of a CT-scan of an infant (soft tissues temporarily removed) oriented along the Frankfort plane (black line). Image produced using Avizo 9.0. Courtesy of Dr Barraclough.

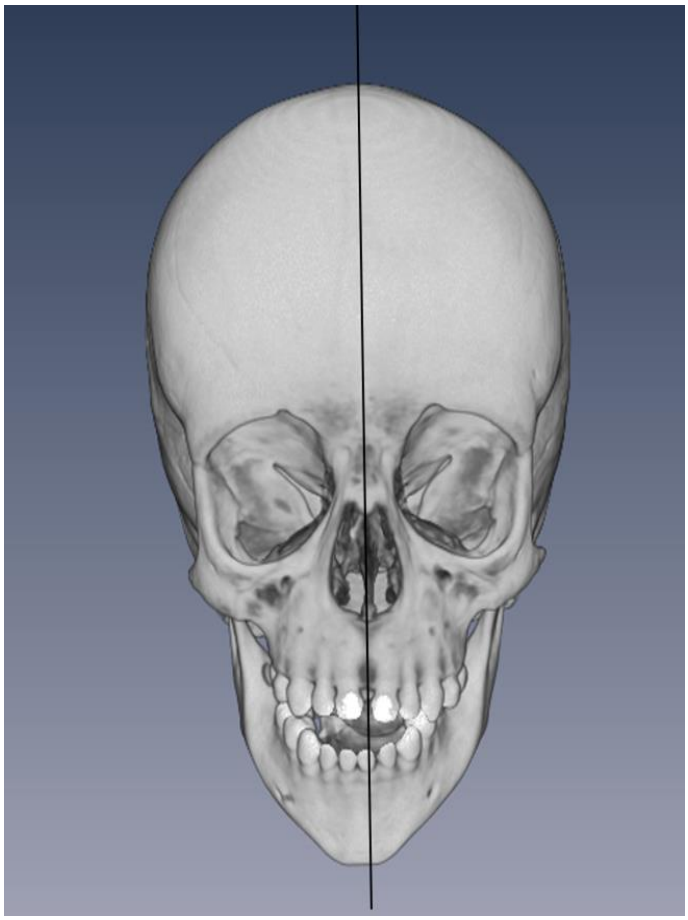

Figure 3.3.4. Image showing the 3D mesh rendering of a CT-scan of an infant (soft tissues temporarily removed) oriented along an imaginary midsagittal vertical plane. Image produced using Avizo 9.0. Courtesy of Dr Barraclough.

The cross-sectional area of the globe of the eye was chosen and measured after selecting the slice with the largest globe width and height in the axial plane (Figure 3.3.5). The volume of the globe was then estimated using the radius. For the linear regression analysis, the cube root of the orbital volume was used.

Figure 3.3.5. Axial view of the surface area measurement of the ocular globe. The measurement of the radius of the ocular globe (r) was taken at the point in which the surface area is largest (red circle). The white line of the sclera was included in the measurement. Image produced using Avizo 9.0. Courtesy of Dr Barraclough.

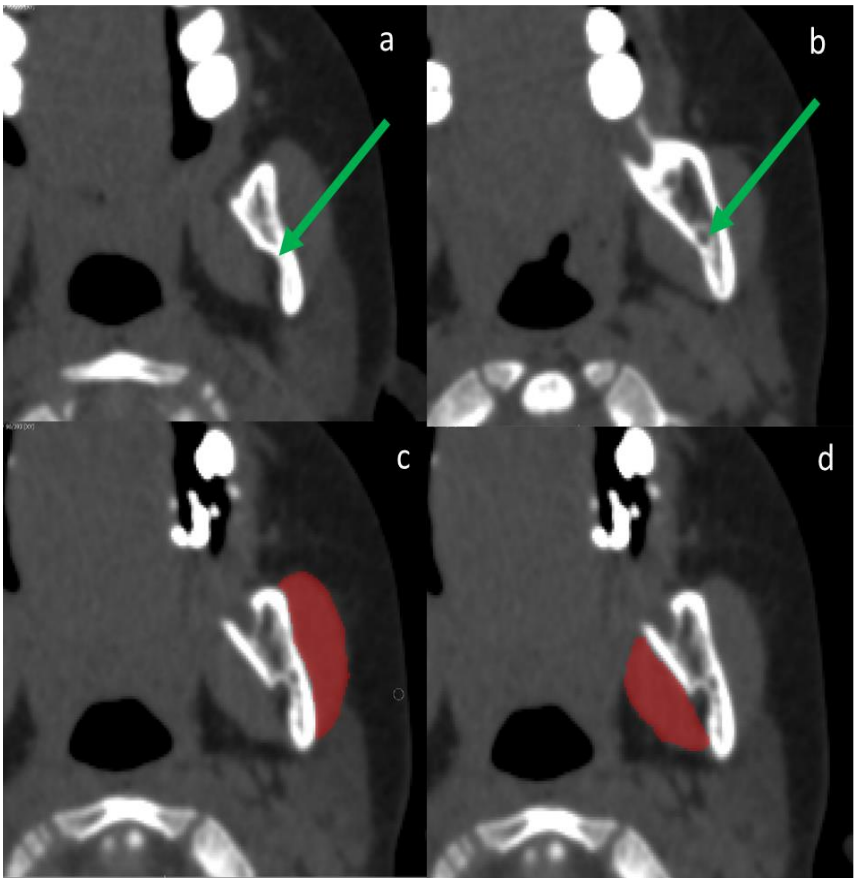

Figure 3.3.6. a. Axial view of skull showing the beginning of the formation of the mandibular lingula when scrolling the slices supero-inferiorly; b. Axial view of the skull showing the point at which the lingula is no more visible. c. Segmentation of the area of the masseter muscle (red area). d. Segmentation of the area of the pterygoid muscle (red area). Image produced using Avizo 9.0. Courtesy of Dr Barraclough.

The cross-sectional areas of the masseter and medial pterygoid were segmented and measured in the axial plane by choosing the slice at the midpoint between the opening and closing of the mandibular lingula (Figure 3.3.6). This region lies within the range of distances from the zygomatic bone over which the cross-sectional area of the two muscles is the largest and changes very little (Toro-Ibacache et al., 2016).

The cross-sectional area of the temporalis was segmented and measured along the axial plane. The area was segmented using the slice at which the full zygomatic arch was fully visible when scrolling the slices from the most superior to the most inferior slice in axial view (Figure 3.3.7).

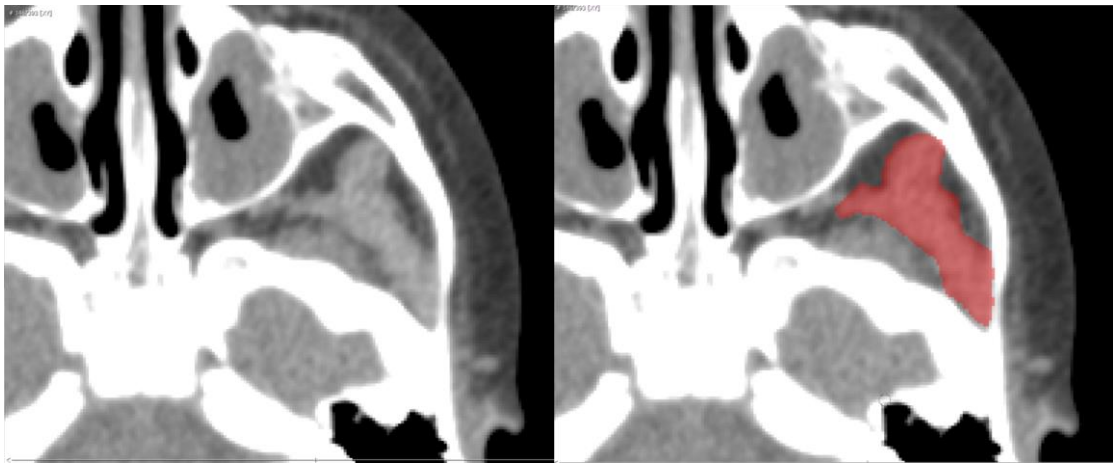

Figure 3.3.7. Axial view of the surface area measurement of the temporalis muscle. The segmentation and subsequent measurement of the area of the temporalis muscle (red area) was taken at the point in which the zygomatic arch was fully visible when scrolling the slices from the most superior to the most inferior slice in axial view. Image produced by the author using Avizo 9.0.

The area of the intra-oral soft tissue capsule including the tongue, sublingual musculature and the soft palate was segmented in sagittal view along the midsagittal line (Figure 3.3.8).

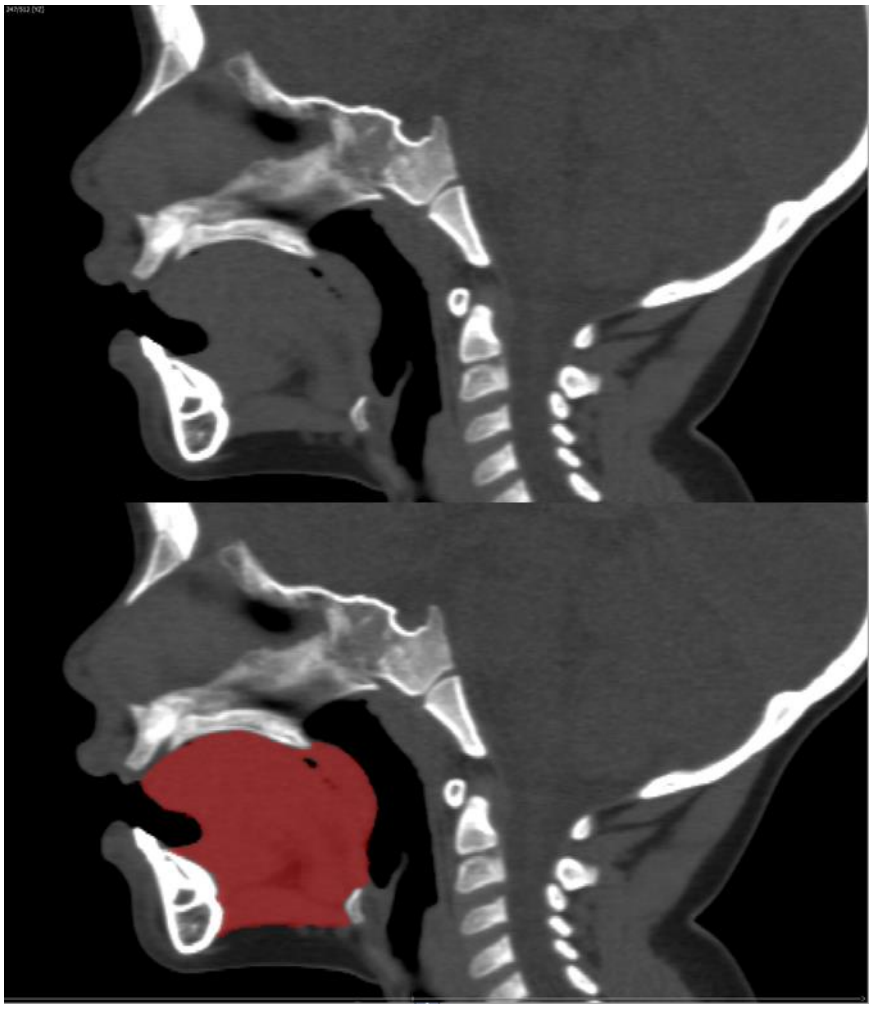

Figure 3.3.8. The area of the intra-oral soft tissue capsule including the tongue, sublingual musculature and the soft palate was segmented in sagittal view along the midsagittal line. Image produced using Avizo 9.0. Courtesy of Dr Barraclough.

The breadth of the tongue was then measured between the buccal fat pads in the coronal plane in the slice located at the angle between the mandibular body and the mandibular ramus (Figure 3.3.9). The intra-oral soft tissue volume was approximated by multiplying its sagittal area by the tongue breadth. For the linear regression analysis, the cube root of the intra-oral soft tissue volume was used.

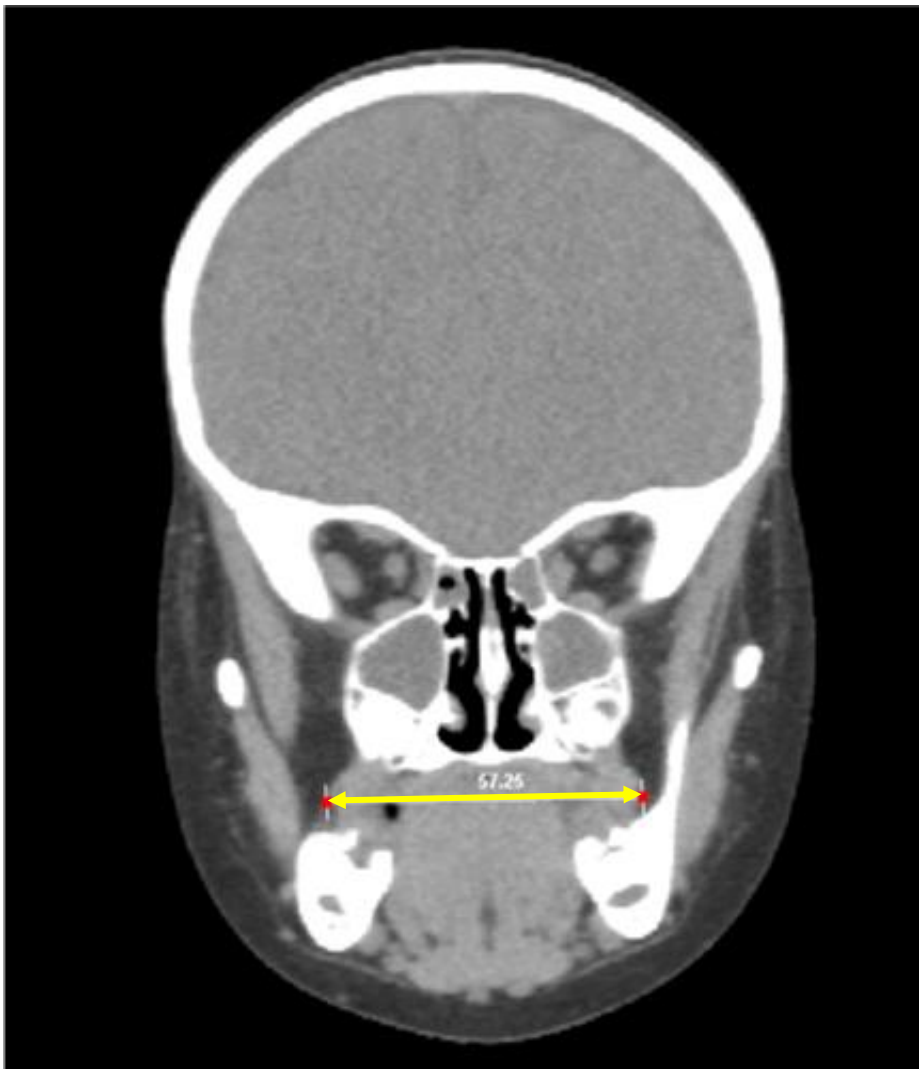

Figure 3.3.9. The breadth of the tongue (yellow arrow) was measured between the buccal fat pads when viewing the specimen from the coronal view, using the slice located at the angle between the mandibular body and the mandibular ramus. Image produced by the author using Avizo 9.0.

To verify the accuracy of the soft tissue measurements, three specimens were measured five times over five weeks. Analysis of variance (ANOVA) was performed to test if measurement replicates were reproducible, *i.e.* if each replica is more similar to its specimen mean than to the mean of other specimens. The ANOVA was therefore performed using the 5 replicates of the 3 individuals as dependent, and the "specimen" factor as independent. The ANOVA showed a significant difference across specimens (Df:

1, F: 55.134, p-value: 0.001**) but not among replicates, indicating that the measurement replicates are consistent with the specimen mean.

3.3.4.5 Statistical analyses

The extent to which the hypothesised paths are supported by data was assessed by standardised multiple regression analysis, testing the interactions indicated by the arrows in the model.

A series of standardised multiple regressions were performed, as structured in the path and sub-paths, each time considering the effect of one or multiple independent variables on a dependent one. Each standardised multiple regression returned a series of beta coefficients (β), indicating the strength of each regression once the other independent variables, affecting the same component, are taken into account. For each regression, R^2 indicates the proportion of the variance of the dependent variable accounted for by the regression.

As an example, in P1 (Figure 3.3.1), maxillary height is hypothesised to be a dependent variable, affected by the exogenous independent variables of the nasal and orbital heights (therefore this regression will have one dependent and two co-independent variables). Maxillary height is also hypothesised to be an independent variable, affecting the dependent variable of the subnasal height, together with nasal height (therefore this regression will also have one dependent and two co-independent variables).

When analysing the sub-path of P1 that leads from the nasal cavity to the facial height by passing through the medial orbital height, this sub-path hypothesises that medial orbital height acts, first, as a dependent variable, influenced by nasal and orbital height. Then, moving along the same sub-path, medial orbital height, together with other variables, is hypothesised as independent, acting on overall facial height (Figure 3.3.1).

Finally, note that if, in a path, all tested associations are significant, by looking at the beta coefficients, it is possible to determine the relative strengths of different sub-paths.

For the first path (P1), the results were obtained by re-running the same path analysis after dividing the sample into age groups: from 0 to 1, 1 to 2, 2 to 3, 3 to 4, 4 to 5, 5 to 6 and finally 0 to 6 (entire sample). In this way, it was possible to assess changes in the strengths and directions of the interactions among variables at different stages of development. For the second path (P2, Figure 3.3.2), due to sample size, a single analysis pooling all individuals from 0 to 6 years old was performed.

3.3.5 Results

3.3.5.1 Skeletal measurements

Figure 3.3.10 (A to G) represents the results for the first path (P1), which hypothesises a cascade of influence of different skeletal variables on overall vertical growth and development of the facial skeleton. The analysis was performed after dividing the sample into age categories: from 0 to 1, 1 to 2, 2 to 3, 3 to 4, 4 to 5 and 5 to 6 years old and finally on the entire sample 0 to 6. This, in order to discover and analyse in detail any changes in the proportional contribution of each variable to the path during ontogeny.

In discussing these results, recall that the beta coefficients indicate the expected change in the dependent variable when there is a one-unit change in that particular independent variable while holding all the other independent variables constant (Allen, 1997). Thus, in describing the results, when the *influence* or *contribution* of the independent with respect to the dependent variable is referred to, it is in the sense of the extent to which we expect the dependent to change in response to a one-unit change in the independent. Additionally, the proportion of the total variance of each dependent variable explained by the independent ones in the path leading to it is assessed by computing the R^2.

The results of the path diagram from 0 to 1 years old (Figure 3.3.10: A) show that, in the first year of life, all the variables make a significant contribution to facial height, with the exception of medial orbital height (non-significant relation). In turn, medial orbital height is influenced by orbital height (β= 0.59***) but not by nasal height (non-significant

relation). Nasal height and orbital height directly interact to similar degrees with facial height (β= 0.24*** and β= 0.21***, respectively). Maxillary height is more dependent on orbital (β = 0.48***) than nasal height (β= 0.29*), with half of its variance explained by these two variables (R^2= 0.53). Maxillary height then has a significant influence on subnasal height (β= 0.40**) but the proportion of the total variance of subnasal height explained by its interaction with maxillary height is low (R^2 = 0.22).

The direct contribution to facial height of orbital height (β= 0.21***) together with nasal height (β= 0.24***), maxillary height (β= 0.13**) and subnasal height, which makes a significant and strong contribution (β= 0.59***), explains 94% (R^2= 0.94) of the total variance in facial height.

The strongest and most significant influences are found in the sub-path that lead from orbital height to maxillary height, from that to subnasal heights, and from subnasal height to facial height. While both nasal and orbital heights directly and indirectly contribute to facial height, the indirect effect of orbital height is stronger in path A, while their direct effect is comparable.

Figure 3.3.10 (below). Results of the path analysis with the skeletal variables used to test Hypothesis 1. The numbers next to the arrows represent the beta coefficients (β), the stars indicate the significance of each standardised multiple regression: *< 0.05, **< 0.01, ***< 0.001, ns= non-significant regression. The R^2 values indicate the proportion of the total variance of the dependent variable that is explained by the independent variables of each multiple regression. Path analyses - A: infants from 0 to 1 years; B: infants from 1 to 2 years; C: infants from 2 to 3 years; D infants from 3 to 4 years; E infants from 4 to 5 years; F: infants from 5 to 6 years; G: all infants from 0 to 6 years.

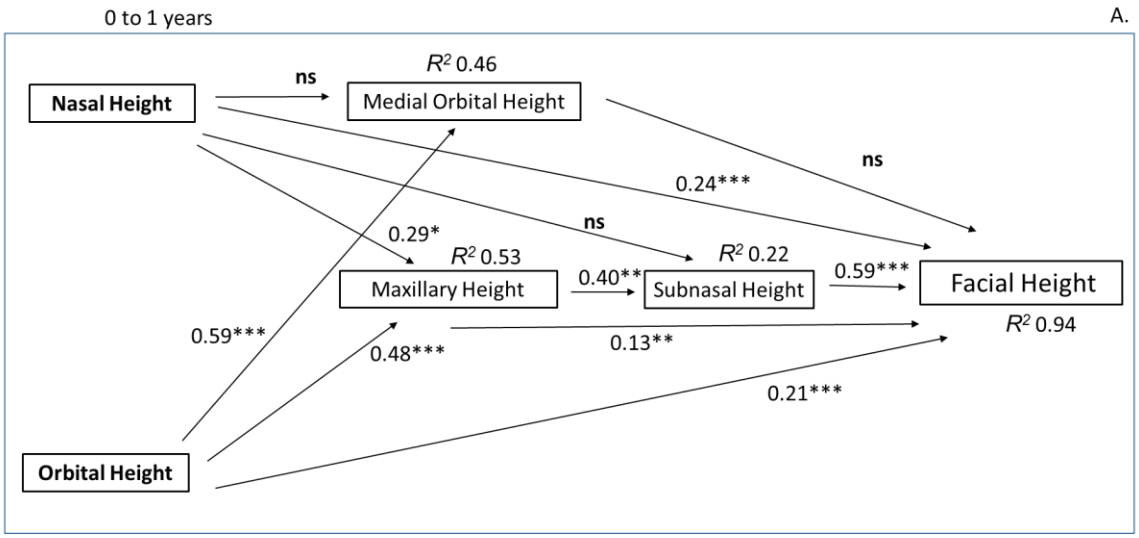

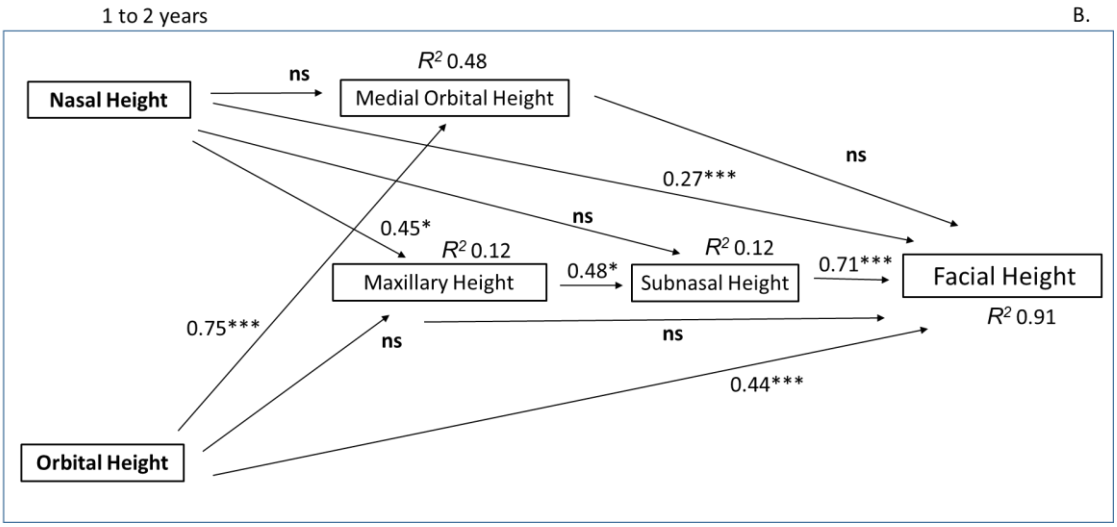

The second analysis (Figure 3.3.10: B), assesses the same hypothesised interactions among facial elements, but in infants from 1 to 2 years old. In this, nearly all of the significant beta coefficients in the previous model (Figure 10: A) become larger. However, maxillary height is now only influenced by nasal height (β= 0.45*) and not by orbital height (this has become non-significant). In addition, maxillary height no longer contributes directly to overall facial height (non-significant), but does so through its influence on subnasal height (β= 0.48*).

Thus, after the first year of life, as the growth and development of the orbital region slow, orbital height no longer contributes to maxillary height while nasal height continues to influence maxillary height. However, the R^2 of this regression, i.e the variance in maxillary height explained by nasal height, is low (R^2= 0.12). This is also true for the impact of maxillary height on subnasal height (R^2= 0.12). This suggests that other elements not present in the path likely impact subnasal height which, in this age range, has an even stronger standardised partial regression with facial height (β= 0.74***). Overall these paths continue to explain a very high proportion of the total variance in facial height (R^2= 0.91), albeit with a different balance of direct and indirect influences of independent variables.

The third analysis (Figure 3.3.10: C) assesses the same hypothesised interactions in the age range from 2 to 3 years old. Interestingly, none of the indirect beta coefficients is

significant, while the direct effects of the independent variables on facial height remain significant (except for maxillary height, which was already non-significant in path B), if slightly reduced in magnitude. It is as if, at this stage, there is a lack of integration among facial elements, which do not interact and do not influence the other variables in the path. Despite this apparent difference from earlier stages in development, the direct interactions still account for a large proportion of the total variance in facial height (R^2= 0.80).

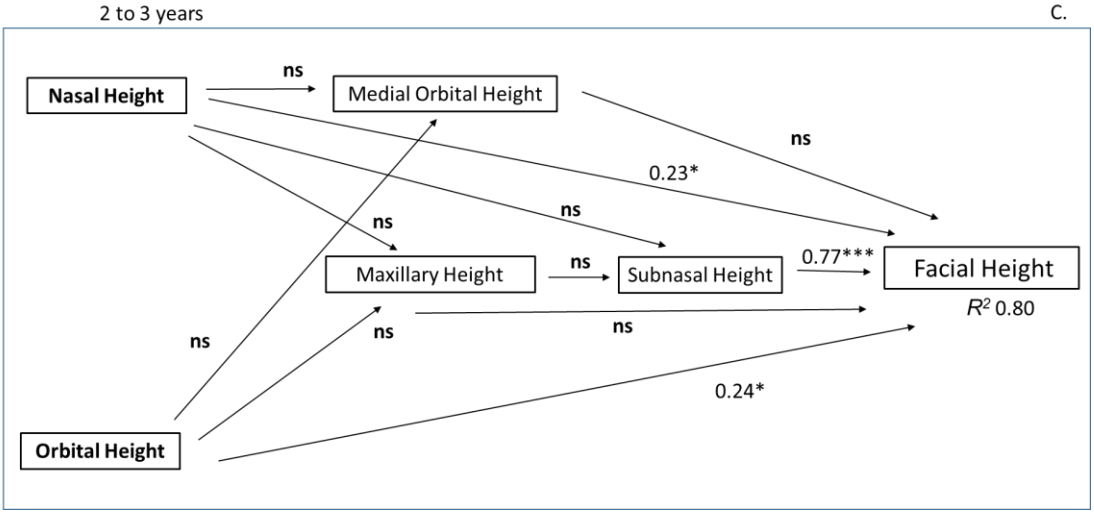

The fourth analysis (Figure 3.3.10: D) explores the interactions among facial elements from 3 to 4 years. Only subnasal height has a significant influence on facial height (β= 0.94***). The proportion of the total variance in facial height explained by this relationship is large (R^2= 0.82). Uniquely, in this age range, orbital height has a weak, negative relationship with maxillary height (β= -0.37*), explaining a small proportion of its total variance (R^2= 0.17).

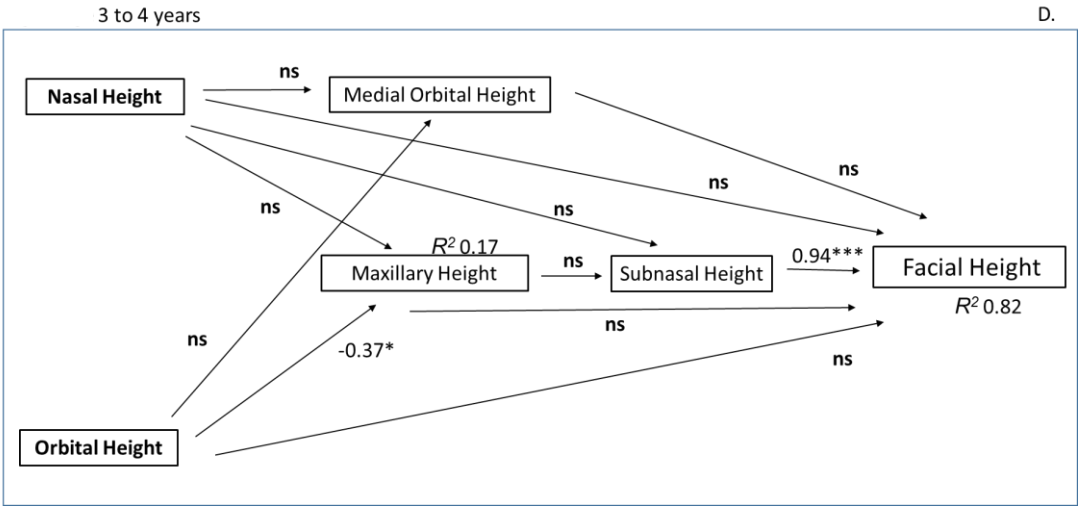

From 4 to 5 years (Figure 3.3.10: E), facial height is only affected directly by nasal and subnasal heights (β =0.28** and 0.77***, respectively), which explain a high proportion of its total variance (R^2= 0.85). Nasal height also affects maxillary height (β =0.53**), although it accounts for a small proportion of its total variance (R^2= 0.23). Likewise, orbital height has a significant influence on medial orbital height (β= 0.37*), but explains a small proportion of its total variance (R^2= 0.18). The other variables behave independently and do not interact with each other.

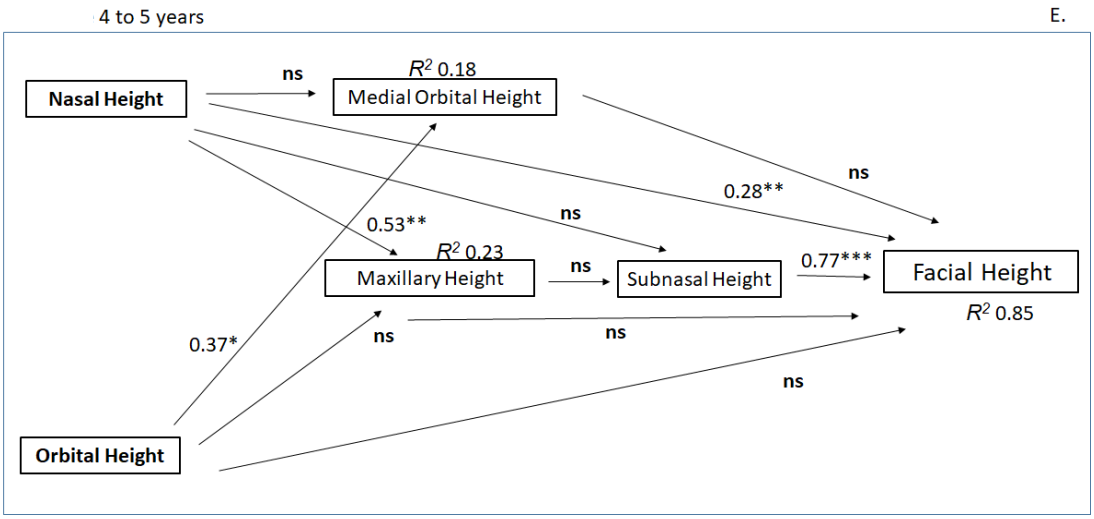

From 5-6 years (Figure 3.3.10: F) the influence of nasal height and subnasal height on facial height remains similar to the previous year group (β= 0.15* and 0.77***, respectively). However, now both orbital height and maxillary height contribute directly to influence facial height (β= 0.47*** and β= 0.21** respectively). Nasal height also manifests a new and negative relationship with medial orbital height. Overall the direct effects (in ascending order) of nasal, maxillary, orbital and subnasal heights account for a very high proportion of the total variance in facial height (R^2= 0.93) in this age group.

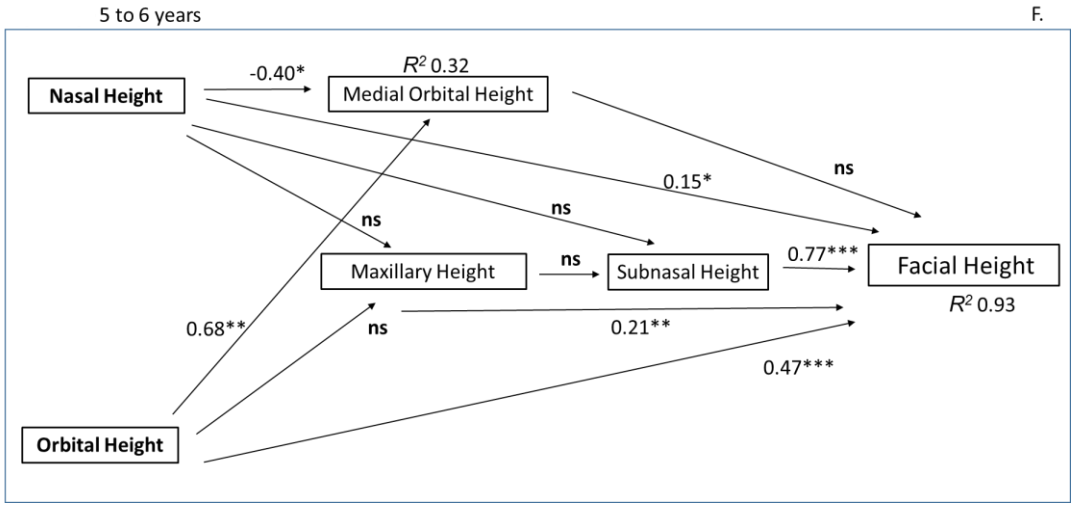

Finally, the path is evaluated for the whole sample, from 0 to 6 years old (Figure 10, G). Facial height is almost completely explained by the effects of all the variables (R^2= 0.96). Nasal height and subnasal height make the strongest and most significant direct contributions to facial height (β= 0.44*** and 0.46***, respectively) while orbital height makes minor direct and indirect contributions. A substantial proportion of the total variance in medial orbital height (R^2= 0.62) and maxillary height (R^2= 0.70) is explained by other variables in the path while only 30% of the variance in subnasal height is explained by its relation with the independent variables. This indicates that other variables not included in the path have an important role in the development of subnasal height and, through this, on facial height.

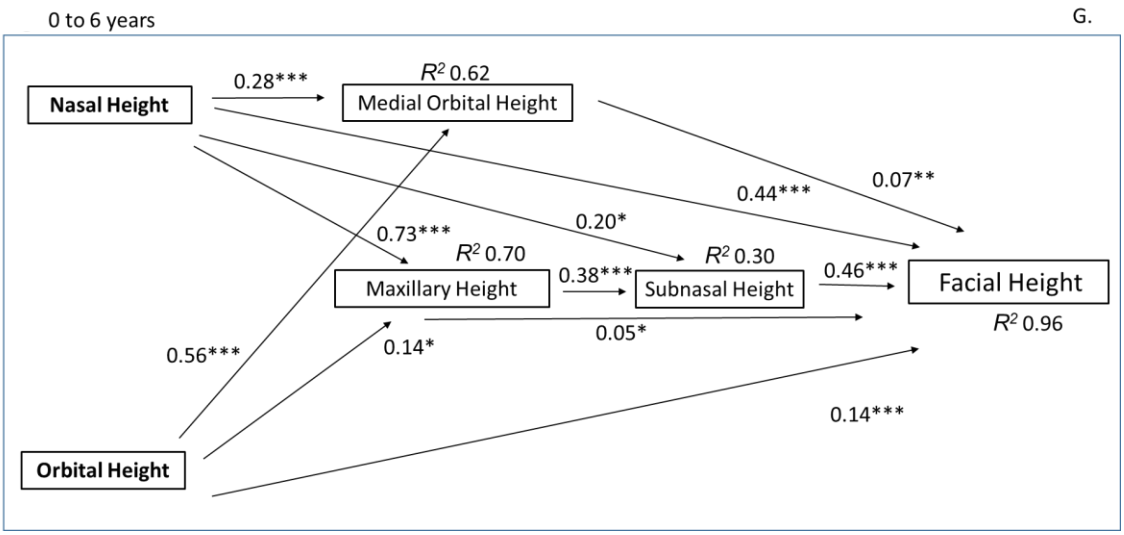

These results indicate that the relationships among facial elements are not constant during the first few years of postnatal life. Orbital height seems to have a significant role in affecting the growth and development of other facial elements and of overall facial height in the early stages, while nasal height and subnasal height progressively become more dominant in influencing facial height later on and are dominant when analysing the whole sample.

3.3.5.2 Soft and skeletal measurements

The results of the second path analysis (P2) are presented in Figure 3.3.11.

The full set of interactions assessed in this path (P2) are diagrammed in Figure 3.3.2 but in Figure 3.3.11, to avoid an overly complex diagram, the non-significant relations are represented by light-grey arrows.

In this path (P2, Figure 3.3.11), nasal height and subnasal height have the strongest and most significant influence on facial height (β= 0.32*** and 0.38*** respectively), while orbital height plays a smaller but significant role (β= 0.23***).

Nasal height does not affect any other variable in the path and so it does not impact on facial height indirectly. This is also the case for orbital height, while it has a significant and

strong impact on medial orbital height (β= 0.76***, R^2= 0.67), the latter, as already seen in most of the analyses of path P1, has no impact on overall facial growth and development.

Maxillary height plays a significant indirect role in influencing facial height variance via its relationship with subnasal height but it has no significant direct influence on facial height. This is similar to the result observed when analysing all the specimens together in Figure 3.3.10 path G, in which maxillary height has only a small direct influence on facial height (β= 0.05*) and mainly acts through subnasal height.

When analysing the soft tissue components, not surprisingly, orbital height covaries with the cube root of the volume of the globe (double arrow, indicating an association rather than dependency of one variable on another, Figure 3.3.11, β= 0.54***), however, unlike orbital height, the globe volume has no direct impact on facial height. The (cube root of the) volume of the intra-oral soft tissues influences maxillary height and subnasal height (β= 0.10**). The proportion of total variance in maxillary height explained by intraoral soft tissue volume is substantial (R^2= 0.71) despite the low β. The intraoral soft tissue volume together with the masseter area, a surrogate for maximum masseteric force, and maxillary height explain a substantial proportion of the total variance in subnasal height (R^2= 0.73).

Masseter area significantly affects subnasal height (β=0.30*) but not that of the maxilla (non-significant). The area of the temporalis muscle (a surrogate for its force) has no significant relationship with any of the variables in the path.

Figure 3.3.11. Result of the path analysis using skeletal and soft tissue variables (P2) to test Hypothesis 2 from 0 to 6 years old. The numbers next to the arrows represent the beta coefficients (β), the stars indicate the significance of each regression (p-value): *< 0.05, **< 0.01, ***< 0.001). The R^2 values indicate the proportion of the total variance of the dependent variable is explained by the independent variables of each multiple regression. The light-grey arrows represent non-significant relations.

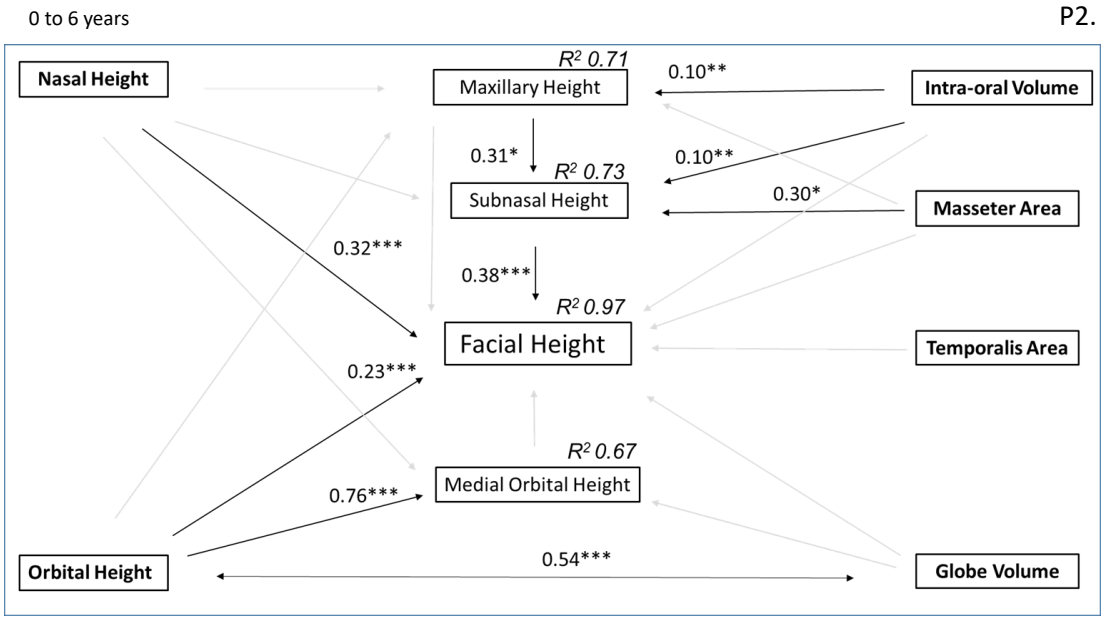

In summary, there is a significant impact of the development of the intra-oral soft tissues on the maxilla and subnasal region in the first 6 years, the latter being also affected by the development of the masseter area as well as the maxillary height. However, it is clear that the strongest and most significant relations lie among the skeletal elements and that facial height is influenced by nasal, subnasal and orbital heights. Interestingly, when the soft tissue elements are inserted in the diagram, nasal height no longer manifests a significant partial regression with the maxillary and subnasal heights and it comes to act only independently and directly in shaping the facial height. The temporalis muscle area does not affect any facial region. The cube root of the volume of the globe, as one might expect, covaries with the vertical height of the orbit but has no other significant relation with the variables in the path.

It has to be mentioned that, although not present in this thesis, an alternative version of Path 2, excluding orbit height, was originally modelled. The aim was to analyse a more direct comparison of the relative contribution of growth of the nasal septum and functional matrices to overall facial height. Results, however, were similar to those presented in Path 2, therefore are not included in this piece of work.

3.3.6 Discussion and Conclusions

This chapter examined the interactions among facial elements during growth and development in infants from 0 to 6 years. The aim of this study was to determine the relative contributions of skeletal and soft tissue variables to facial height growth and development during infancy. Thus, the study tests alternative hypotheses relating to the drivers of facial vertical growth (facial height) by comparing the effects of growth of the nasal septum (represented by nasal height) with those of soft tissue growth. First, a path diagram was designed to assess the interactions of skeletal variables with each other and their effects on facial height. In this path (P1), the nasal septum (nasal height) and orbital height were hypothesised to be exogenous variables, acting on the intermediate variables of maxillary height, subnasal height and medial orbital height. All the variables were then hypothesised to contribute to facial growth. The design of this path is based on the literature on facial growth and development that was reviewed in the introduction (Sections 3.3.1, 3.3.2). The path diagram P1 allowed assessment of the relative contributions of each of these skeletal facial components to facial height and of the relations among them.

Hypothesis 1 stated that *the interactions within the sub-path leading from nasal height to facial vertical height are stronger than those in the sub-path leading from orbital height to facial height in all age groups.*

The results show that the associations between facial components are not constant throughout ontogeny and that the most significant interactions vary over time. In the first

year of life (y0 to y1), both orbital and nasal heights contribute significantly to the overall facial height as well as to that of the adjacent maxilla. All the intermediate variables also make a significant contribution. However, the strongest sub-path is the one leading from the orbit, through the maxilla and subnasal region, to overall facial height suggesting the influence of the orbit is dominant in the first year of life.

These relationships rapidly change starting from the second path (path B: y1 to y2, Figure 3.3.10). In this, the orbit still significantly contributes to facial height but has no interaction with the midface (maxillary and subnasal heights).

From 0 to 1 and 1 to 2 years old, subnasal height is the variable with the most significant influence on facial height. In turn, subnasal height is not significantly influenced by nasal height but is influenced by maxillary height.

Path C (2-3 years, Figure 3.3.10) suggests a phase of decreased integration, or increased modularity, in which nasal, orbital and subnasal heights all contribute to facial height but do not interact with any other elements in the path. This modularity phase becomes extreme in path D (3-4 years, Figure 3.3.10), in which only subnasal height strongly influences facial height. Between 4 and 6 years, nasal height (path E, 4-5 years, Figure 3.3.10), and orbital height (path F, 5-6 years, Figure 3.3.10), contribute to facial height, together with subnasal height. Initially, in this age range, nasal height contributes significantly to maxillary height but later this interaction is lost. Finally, considering interactions over the entire sample (path G, 0-6 years, Figure 3.3.10), it is evident that nasal and subnasal heights make the largest and most significant contributions to facial height, with orbital height contributing less strongly. Indeed, subnasal height is a very important contributor to facial height in all the tested paths (Figure 3.3.10, paths A to F).

Overall, interactions among variables change over time with nasal and subnasal heights showing the greatest and most consistent interactions with facial height.

This finding supports prior studies that the nasal septum has a significant influence on prenatal and early postnatal human midfacial growth (Pirinen, 1995; Wong et al., 2010; Al Dayeh et al., 2013; Hall and Precious, 2013). Results of the path analyses in Figure 3.3.10 are consistent with the nasal septal traction model, which emphasises the morphogenetic capacity of the nasal septum and considers the midface, including the premaxilla, as responsive to developmentally induced forces placed on the facial skeleton

(*e.g.* along the premaxillary suture) by septal expansion (Latham, 1970; Siegel and Sadler, 1981; Holton et al., 2010). However, in this study, our results indicate that the height of the peri-alveolar region (subnasal height) is influenced intermittently by the nasal septum, as well as by the height of the maxilla. In addition, dominance of the subnasal height in influencing facial height during the 2nd to 4th years of life could reflect the development of the upper anterior dentition, which becomes fully functional around the 3rd year of life (Dean and Turner, 2016).

Orbital height also has significant, but progressively less strong interactions with facial height and the other variables. This finding is in line with prior literature on orbital growth that found in infants that the most rapid and significant growth in orbital height occurs in the first year of life (Evteev et al., 2018). Therefore, from the results in Figure 3.3.10, it is evident that the orbit does not make as important a contribution to facial height as nasal height and, despite the balance among these changing from the youngest to the oldest age groups, overall nasal height has a larger impact on facial height and the intermediate and final variables over time.

Therefore, while skeletal interactions change over time, the strong and significant relationship of nasal height with variables describing adjacent structures and with facial height does not falsify the null hypothesis. Our results evidence an important but variable contribution of the nasal septum to the determination of facial height, therefore Hypothesis 1 is not falsified.

Hypothesis 2 examined the influences of both soft and skeletal tissues during facial ontogeny. It states that *the interactions within the sub-paths leading from the soft tissue elements to facial height are greater than those in the sub-paths leading either from orbital or nasal height to facial height.*

For this hypothesis, a path was designed that included the significant parts of the skeletal paths tested in Hypothesis 1 and variables reflecting the functional matrices of the intra-oral soft tissue, globe, and facial muscles, as defined by Moss (Moss, 1968; Moss et al., 1968). In testing this hypothesis, the aim was to determine if the soft tissue matrices have a stronger influence on the surrounding skeletal elements and on facial height than the skeletal measurements. Since data acquisition was limited to a smaller sample of 46

specimens, the path was assessed for the entire sample, ranging from 0 to 6 years rather than age subsamples.

Results show that the interactions of skeletal elements with each other and facial height do not change particularly when the soft tissue variables are included (Figure 3.3.11). Indeed, among the skeletal components, as already noted in the path in Figure 3.3.10, nasal and subnasal height most affect facial height, with orbital height playing a smaller but significant role. Maxillary height influences subnasal height, and this is the only significant relationship among the skeletal measurements that do not directly involve the facial height. In fact, nasal and orbital heights only significantly influence facial height and have no impact on intermediate variables, indicating that the skeletal components act more independently when the soft tissue variables are included in the path (compare with Figure 3.3.10 G).

Furthermore, the results show that there is no significant direct interaction of the soft tissues with facial height, rather they act more locally, particularly on the maxillary and subnasal regions. This is an important result, indicating that the growth of the masseter and of intra-oral soft tissues, rather than the nasal septum (represented by nasal height) affects the growth and development of the subnasal region. Thus, the growth and development of intra-oral soft tissues seem to affect the development of the skeletal maxilla (height) and, together with the masseter, a muscle whose actions are strictly related to mastication, these interact with subnasal height and through that, impact facial height.

These results find support in a recent study that measured the correlation between the pharyngeal airway volume and the position and orientation of the lower jaw. Indeed, the authors found that changes in the pharyngeal volume did not have an impact on overall facial proportions and vertical height (Grauer et al., 2009), thus supporting the interpretation that soft tissues act more locally than globally in facial growth and development.

To summarise, while the current study recognises a bigger importance of the intra-oral and masseter capsules on subnasal growth than the role played by the nasal septum, it is clear from the results in Figure 3.3.10 and Figure 3.3.11 that the latter plays a central role in facial development. In addition, other skeletal elements such as the growth of the

maxilla (maxillary height) influence subnasal growth, underlying the importance of the skeletal component in acting locally in concomitance with soft tissues. These results are partially in line with the findings from Mooney et al., (1989), which compared the action of the skeletal elements and that of the capsular and periosteal matrices on facial growth in foetuses. Their findings support a larger contribution (stronger interactions) of the skeletal elements to the growth and development of the premaxilla and face when compared to the action of the orbicularis oris muscle and other facial functional matrices.

In conclusion, the null Hypothesis 2 of stronger influence of soft tissues (operating through capsular and periosteal matrices) than skeletal elements on facial height is falsified.

Path analysis is a method that has been used previously to explore the relationships among skull components (Mooney et al., 1989; Holton et al., 2008). In this study, it was adopted to investigate the relationships between skeletal and soft tissue components in infants ranging from 0 to 6 years old. The results indicate the presence of a hierarchy of interactions as well as differences in the strengths and directions of relationships among facial elements over time. The findings of this study are that overall facial height is strongly influenced by nasal height, a proxy for the nasal septum, but earlier in ontogeny, orbital height is more important. Subnasal height is also very important but is more dependent on tongue volume and masseteric force, both acting directly and through maxillary height. These findings lend support to Scott's Nasal Septum theory (Scott, 1954; 1962) but also find evidence that functional matrices involving soft tissues are important. There is evidence that both the nasal septum and the functional matrices operate to influence facial growth and that the balance of influences among factors impacting facial height varies throughout postnatal facial growth.

3.4 The facial ontogeny of *H. neanderthalensis* and *H. sapiens*

3.4.1 Ontogenetic trajectories in Neanderthals and modern humans

This chapter compares the trajectories of growth and development of the facial complex in *H. neanderthalensis* and *H. sapiens* and the patterns of covariation among facial elements during ontogeny in the two species.

The differences in growth and development between these two species have been investigated in several studies (Ponce de Leon and Zollikofer, 2001; Ponce de Leon et al., 2008; Gunz et al., 2010; Zollikofer and Ponce de Leon, 2010). Neanderthal adult autapomorphies are well-known and genetic and morphological data define this species as possessing a unique suite of characters with respect to *H. sapiens* (Franciscus, 1999; Trinkaus et al., 2006). However, how and when during ontogeny the morphological differences between *H. sapiens* and Neanderthals arise is still largely debated (Bastir et al., 2007). A common view is that some, if not most, aspects of their adult differences are established prenatally (Ponce de Leon and Zollikofer, 2001). Nonetheless, there is debate about whether or not these differences are simply carried into adulthood unchanged along parallel ontogenetic trajectories, with a shift in the timing of growth. This would result in an extension of allometry in Neanderthals relative to modern humans (Ponce de Leon and Zollikofer, 2001; Rozzi and De Castro 2004; Smith et al., 2007; Gunz et al., 2010; Tallman, 2016), meaning that *H. sapiens* and Neanderthals share the same spatio-temporal pattern of growth and development among cranial components, with the latter being simply "overgrown" (hypermorphic) with respect to modern humans. Thus, differences in these two species would be established in the prenatal and early postnatal period and postnatal growth (changes in size) would change the shape of these two species in the same way (similar allometric development). Ponce de Leon and Zollikofer (2001) interpreted their findings from a geometric morphometric principal component analysis as showing that Neanderthals and *H. sapiens* have parallel ontogenetic trajectories. Likewise, using Euclidean distance matrices, Ackermann and Krovitz (2002) found that cranial ontogenetic trajectories are not only common between Neanderthals and *H. sapiens* but are also shared with *Australopithecus africanus*.

However, other studies have found that differences between *H. neanderthalensis* and *H. sapiens* not only exist in early postnatal stages, but that these differences are accentuated during ontogeny through divergence in growth and developmental trajectories. Bastir et al. (2007), using geometric morphometric regression and principal component analyses, found significant divergence of 44 degrees in the trajectories of growth and development of the mandible of *H. sapiens* and Neanderthals. These results, although needing further confirmation, suggest that postnatal, as much as prenatal transformations, are responsible for differences between these two species. Another geometric morphometric study compared neurocranial ontogeny in the two species (Gunz et al., 2010) and observed that prenatal differences are accentuated after birth and that, in general, the cranium of Neanderthals appears hypermorphic compared to modern humans, although these differences are not tested in the paper. In addition, observed differences in the patterns of resorption and deposition of bone tissue on the face of Neanderthals and modern humans (Lacruz et al., 2015) suggest differences in their growth trajectories. Furthermore, preliminary histological analysis suggests that differences in bone remodelling exist between *H. sapiens* and *H. heidelbergensis*, currently considered as an ancestor of *H. neanderthalensis* (Rosas and Martinez-Maza, 2010). Other studies on tooth eruption patterns showed that Neanderthals do not simply have a more prolonged growth, but they might have a more rapid eruption pattern, potentially accompanied by more rapid size and shape changes in the cranium when compared to *H. sapiens* of similar age (Smith et al., 2007).

The different conclusions arising from these studies may be attributable in part to methodological differences and inadequacies but whatever the reason, the question of whether or not the mid and upper faces of Neanderthals and modern humans share a common postnatal pattern of ontogeny remains open. Similarities and differences in the ontogeny of the facial complex have not been assessed in detail. Despite the large body of literature describing morphological differences between adult individuals of the two species (Rak, 1986; Franciscus, 2002; Stringer, 2002; Weaver et al., 2007), we have incomplete knowledge of how they arise.

3.4.2 Covariation patterns in Neanderthal and modern humans

It is known that there are common aspects of covariation and integration of the skull among mammalian species during evolution (Mitteroecker and Bookstein, 2008). However, closely related species have been shown to differ significantly in aspects of cranial covariation and integration (de Oliveira et al., 2009), indicating that covariation patterns have diverged over time (Ackermann, 2009). Thus, differentiation of specific morphologies can arise through changes in trajectories of morphological variation over time, possibly underlying changes in patterns of interaction among developing facial components. Considering all the synapomorphies present in Neanderthals, and their differences in facial architecture when compared to modern humans, this adds to the question of whether these two species share similar trajectories of growth and development, or if they share covariation patterns among facial regions during postnatal ontogeny.

To address those questions, this chapter applies Partial Least Squares (PLS) analysis to compare patterns of covariation among skeletal elements of the facial complex of Neanderthals and modern humans. Such comparisons have previously been performed in adult hominoids (Bastir et al., 2005; Klingenberg, 2008; Mitteroecker and Bookstein, 2008; Ackermann, 2009; Singh et al., 2012; Profico et al., 2017). In general, findings indicate that patterns of covariation are similar among human and non-human primates. This suggests that, despite having different morphologies, the patterns of modularity and integration of the facial complex are conserved among hominoids. However, the lack of large ontogenetic (and non-ontogenetic) fossil hominin datasets makes it difficult to extend these studies to extinct hominin species. Only for Neanderthals such study is possible, but even then the subadult sample is limited in terms of the total number of finds and accessibility to researchers. Although the sample size of Neanderthals available for this study is small, it is sufficient to begin assessing differences and similarities in covariation patterns among facial regions during growth and development.

The hypothesised modules of this research chapter are based on prior studies and the analyses of Section 3.2, which examined covariation in the internal and external facial regions of younger and older subadults and adults of modern humans. The following facial sub-regions were identified in modern humans: the orbits, the maxillae, the palate

and the nasal cavity. These were chosen based on differences in development and function and because of prior testing of their modular nature (see Section 3.2, Villmoare et al., 2014). As evident from Section 3.3, it is not possible to readily infer cause and effect among covarying facial elements. However, it is possible to determine the extent to which each grows independently and, if there is integration, to assess the nature (anatomical variation) of this interaction.

Although the current section does not analyse age groups separately because of the paucity of sampling in Neanderthals, the aim of this section is to test hypothesised facial modularity in Neanderthals and compare the findings with modern humans. This will allow and assessment, albeit limited by available fossils and their quality of preservation, of the extent to which Neanderthals and modern humans share similar patterns of covariation among cranial regions (Ackermann, 2002). Indeed, even though the significance of the covariation is not directly comparable between the two species due to difference in sample sizes, it is possible to assess broadly the degree of difference in ontogenetic covariation, *i.e.* if the regions that show the strongest covariation in modern humans are the same in Neanderthals.

3.4.3 The hypotheses

The foregoing review has identified two areas where our knowledge about the differences in growth and development between Neanderthals and *Homo sapiens* is incomplete. The first concerns the extent to which differences in adult form arise prenatally and are carried into adulthood with relative extension (hypermorphosis in Neanderthals) or curtailing (hypomorphosis in modern humans) of a common ontogenetic trajectory of size and shape changes. The second relates to the extent to which ontogenetic interactions are shared betwewn the two species. These issues are addressed in this chapter by testing the following hypotheses.

Hypothesis 1. *Neanderthals and modern humans exhibit no significant difference in their facial ontogenetic trajectories.*

If this hypothesis is not falsified, this would indicate that postnatal changes in craniofacial form do not differ significantly in nature (mode of variation) between Neanderthals and modern humans; that postnatal ontogenetic modifications in shape and size are not different (parallel trajectories) between these two species. If it is falsified, this would indicate the opposite: that postnatal ontogenetic trajectories are divergent.

Hypothesis 2. *During postnatal ontogeny, Neanderthals and modern humans show no differences in the ways in which facial components covary.*

If this hypothesis cannot be falsified, it would imply that despite clear differences in their adult morphologies, the ways in which the orbits, palate, nasal cavity and maxilla interact during development do not differ in the two species.

3.4.4 Material and methods

3.4.4.1 The sample

The sample used for this study includes an ontogenetic series of CT-scans of modern humans (68 specimens) and an ontogenetic series of 3D meshes reconstructed from CT-scans or photogrammetry of Neanderthals (12 specimens of which 4 are younger subadults, 1 older subadult, and 7 adults). Table S2 of Supplementary material shows the list of the Neanderthal specimens used for the study.

3.4.4.2 The dataset

A configuration of 43 landmarks (a subset of the landmarks defined for the studies of 3.1 and 3.2 and listed in Table S4 of Supplementary Material) was defined as in Figure 3.4.1.

Missing landmarks were estimated by Thin Plate Splines (Bookstein, 1989) by warping the 10 closest individuals to the deficient configurations and then calculating a weighted average estimate based on the Procrustes distance. This approach was used because it

was shown to be the most reliable method in estimating missing landmarks in humans (see Chapter 2, Section 2.0.4.4). Data estimation has been performed in R studio by using the function “fixLMtps” in the R package “Morpho” (Schlager, 2017). The missing landmarks were estimated using only Neanderthal specimens as this thesis (see Chapter 2 Section 2.0.4.4) and prior studies have shown that using a conspecific sample gives a

more accurate estimation of missing landmarks than a mixed sample (Neeser et al., 2009).

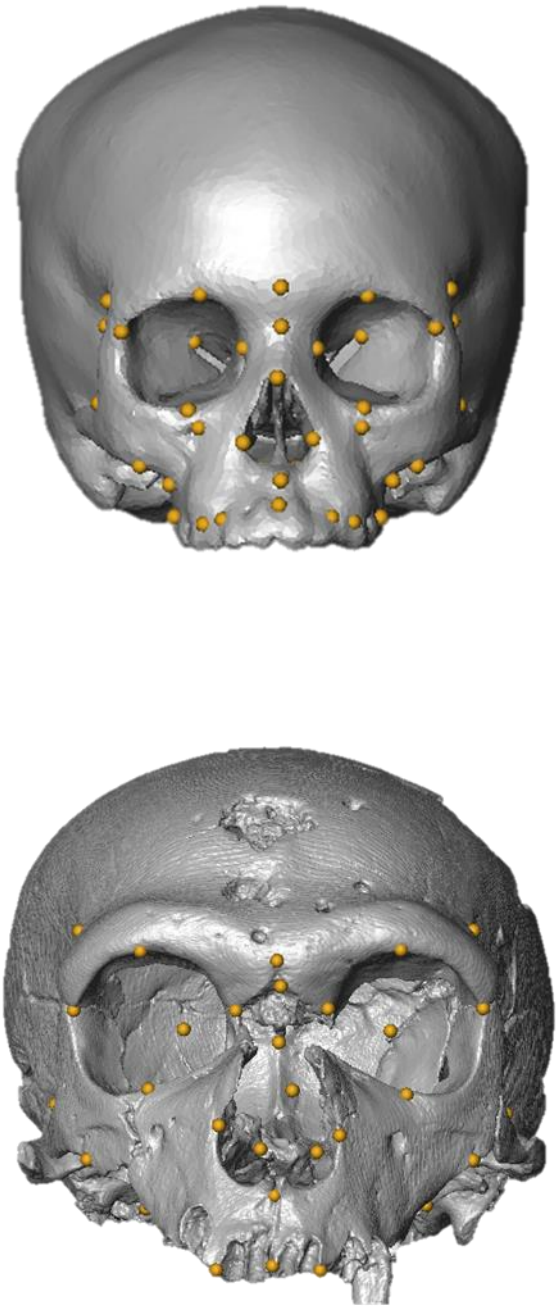

Figure 3.4.1. Set of 43 landmarks used in this study to compare *H. sapiens* and *H.neanderthalensis*. Top: juvenile *H. sapiens*, bottom: adult *H. neanderthalensis*.

3.4.4.3 Statistical analyses

A series of multivariate analyses were performed to test the two hypotheses.

Hypothesis 1. *Neanderthals and modern humans exhibit no significant difference in their facial ontogenetic trajectories.*

To test Hypothesis 1, a principal component analysis (PCA) was performed to explore morphological variation within and among the two species (after common GPA). The PCA was performed both in shape and form (shape +Ln CSize) spaces (Mitteroecker et al., 2004). Differences were visualised by warping the mean surface mesh along the first and second principal components for the shape PCA (form PCA warpings are not shown as very similar to shape PCA with only differences in absolute size). Subsequently, for each species, a multivariate regression of facial shape on size was performed. The regression vectors for the two species were extracted and the angle between them was computed. Its significance was assessed using permutation test, in which species membership was randomly permuted and the angle recalculated. One thousand permutations were carried out and the estimated angle between the species was compared with the distribution of permuted angles to assess its significance.

The divergence in ontogenetic trajectories calculated from multivariate regressions was visualised by first performing a GPA combining the predicted adult and infant mean shapes from both species, and then calculating the ontogenetic trajectories as the differences between mean adult and infant coordinates. To ease visualisation, these were then added to a common mean infant. This does not affect the distances among, or PCAs of, the means. A PCA was performed on the resulting shapes to directly compare ontogenetic trajectories and visualise the differences between them.

To visualise expansions and contractions of facial regions between regression estimates of a mean infant and a mean adult forms of the two species, two meshes (infant and adult) were generated by warping the mean mesh to the extremes of the sample distribution on the regression vector. As explained in Section 3.1, the changes in the warped meshes were colour coded to represent differences in the area of each triangle of the mesh between the warped adult and the warped infant crania, mapping regions of expansion and contraction. The warpings were performed using the EVAN Toolbox 1.72

and the colour maps were calculated using the function “localmeshdiff” of the R package “Arothron” (Profico et al., 2015).

Hypothesis 2. *During postnatal ontogeny, Neanderthals and modern humans show no differences in the ways in which facial components covary.*

To test this, two-block PLS analyses were performed, computing and extracting the eigenvectors of the covariance among pairs of anatomical regions (blocks; see Section 3.1.7.2.3 in Chapter 2 for a full explanation). To look into shape covariation, a full GPA was performed. Form covariation was not taken into account because, during ontogeny, size changes simply overwhelm other changes, obscuring subtle distinctions in covariation patterns due to shape interactions.

The GPA for the PLS analysis was performed separately for each block (region). Figure 3.4.2 shows the anatomical regions considered for the analysis and the landmarks that constitute each block. Only one side of the cranium was considered for this analysis to minimise use of estimated landmarks for the analyses involving Neanderthals.

For each PLS analysis, the percentage of total covariance among the blocks explained by the first pair of singular axes (also commonly termed ‘PLS axes’) was calculated in order to assess how well they explain the total covariance. The correlation coefficients between blocks were calculated for PLS1 scores and their p-values were estimated using permutation test between pairs of blocks. For each block, the proportion of its total variance explained by the first PLS axis was estimated (Cardini, 2019).

The analyses were first performed on the entire sample of modern humans, then on the full sample of Neanderthals, and the results were compared.

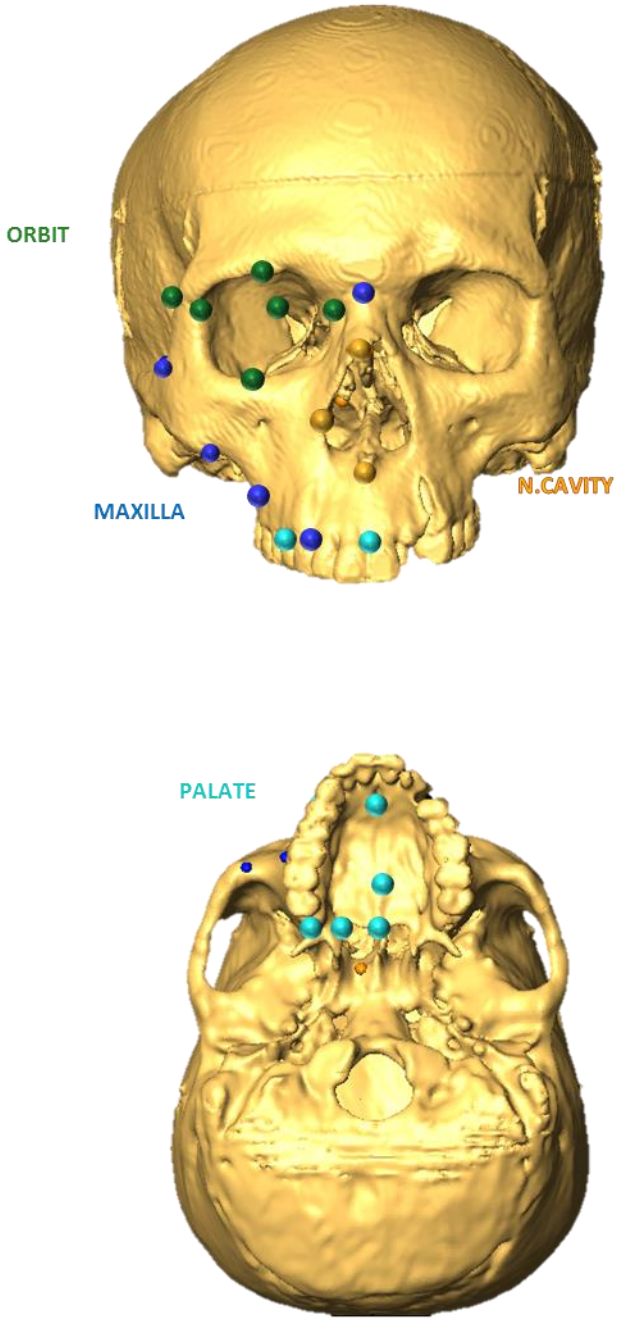

Figure 3.4.2. Different colours indicate the different landmarks used to build the facial modules for the PLS analysis (modern human juvenile cranium in picture).

3.4.5 Results

Hypothesis 1 states that *Neanderthals and modern humans exhibit no significant difference in their facial ontogenetic trajectories.*

To test this hypothesis PCAs of the ontogenetic series were performed in shape and form spaces, to observe general trends. The principal component analysis in Figure 3.4.3 shows the ontogenetic samples of modern humans and Neanderthals plotted on the first and second principal components of shape. From the earliest stages, Neanderthal and human faces differ on PC2. The faces drawn to the left of the PC plot show the differences in shape represented by PC2, produced by warping the mean shape landmark configuration to the extremes of PC2 scores (0.15 for the upper warping and -0.05 for the lower warping). A Neanderthal adult surface mesh is warped to fit the resulting landmark configurations, to ease visualisation. The major differences are found in the shapes of the orbits, with Neanderthals having a more horizontal upper orbital border, relatively bigger and wider nasal aperture and bridge, a more prominent midface showing a relatively wider, taller and more "inflated" zygomatico-maxillary complex. When looking at the directions of the ontogenetic trajectories of the PCA plot, it appears that these differences are present at all stages of postnatal ontogeny, and that the two species show approximately parallel ontogenetic trajectories. However, the PCA accounts for only 54% of the total variance.

The PCA performed in the form space (Figure 3.4.4), when compared to that performed in the shape space, shows a very similar distribution of the specimens along the first two principal components, with PC1 representing aspects of allometry. Warpings for this PCA reflect similar morphological differences to those found for the PCA of shape and, therefore, are not shown.

The PCAs of both shape and form (Figure 3.4.3 and 3.4.4) show that Neanderthal newborns (Meizmaskaya and Pech de l'Aze) are displaced along PC1 toward lower PC1 scores compared to newborn modern humans. This is also true for the Neanderthal adult specimens, which are displaced toward lower PC1 scores if compared to adult *H. sapiens*. Since PC1 represents aspects of allometry in both analyses, this indicates that Neanderthals, newborns and adults are hypermorphic in these respects, relative to modern humans, because they are scaled up allometrically relative to equivalently aged

modern humans. This finding is consistent with several previous studies (Krovitz, 2003; Ponce de Leon and Zollikofer, 2001; Smith et al., 2007; Ponce de Leon et al., 2008; Gunz et al., 2010; Zollikofer and Ponce de Leon, 2010).

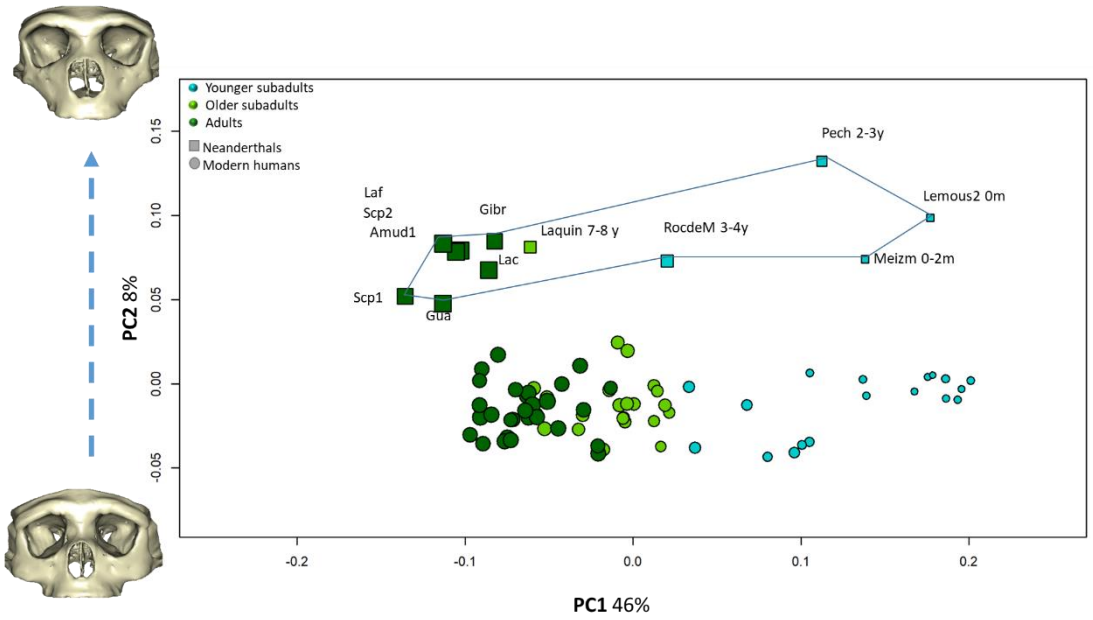

Figure 3.4.3. Principal component analysis of facial shape in the ontogenetic samples of *H. sapiens* and *H. neanderthalensis*. The Neanderthal sample is bounded by a light blue line. Laf= La Ferassie, Gibr= Gibraltar1, Pech= Pech De l'Aze, Lemous2= Le Moustier 2, Meizm= Meizmaskaya, Gua= Guattari1, Scp1= Saccopastore 1, Lac= La Chapelle, Amud1= Amud 1, Scp2= Saccopastore 2, La quin= La Quina, RocdeM= Roc de Marsal. The ages shown alongside each subadult Neanderthal are estimates from the literature, in years (y) and months (m).

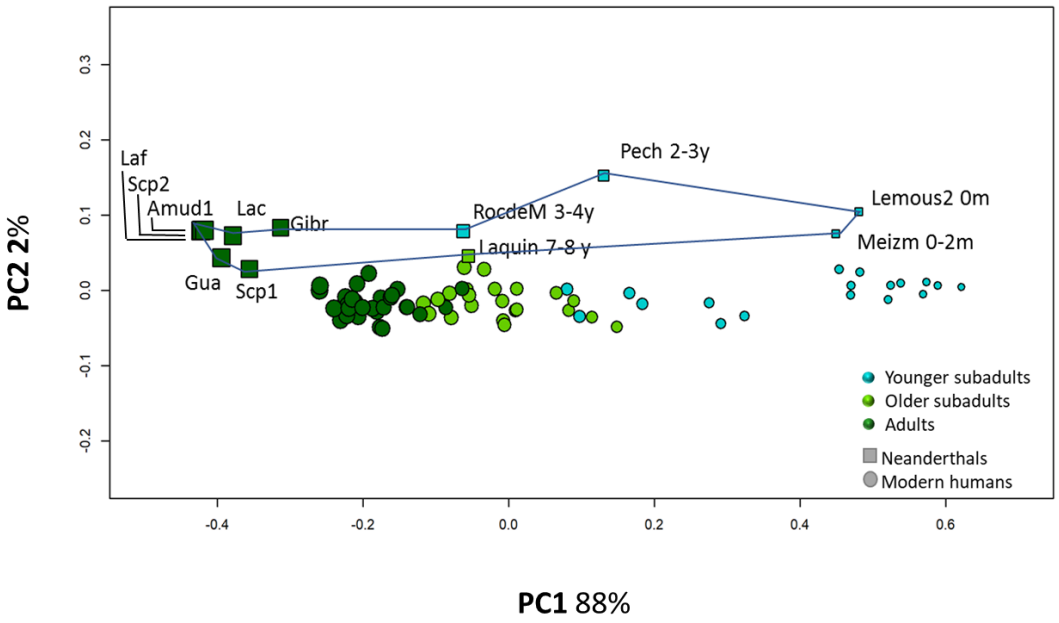

Figure 3.4.4. Principal component analysis of facial form in the ontogenetic samples of *H. sapiens* and *H. neanderthalensis*. The Neanderthal sample is bounded by a light blue line. Laf= La Ferassie, Gibr= Gibraltar1, Pech= Pech De l'Aze, Lemous2= Le Moustier 2, Meizm= Meizmaskaya, Gua= Guattari1, Scp1= Saccopastore 1, Lac= La Chapelle, Amud1= Amud 1, Scp2= Saccopastore 2, La quin= La Quina, RocdeM= Roc de Marsal. The ages shown alongside each subadult Neanderthal are estimates from the literature, in years (y) and months (m).

In the PCA of Figure 3.4.3, PC1 seem to represent allometry, but this view is likely incomplete because principal components are not specifically constructed to assess shape covariance with size and both species are included in the PCA. In order to fully account for allometry, multivariate regression of facial shape on size was performed in *H. sapiens and H. neanderthalensis.* In both cases, about 45 % of the total shape variance was explained by allometry (Neanderthals= 45.37%, p-value: < 0.001; modern humans 45.61, p-value: < 0.001). Allometry was visualised in each species by warping the mean shape and its mesh to the mean adult and mean infant centroid sizes in the regressions. The colour map shown in Figure 3.4.5a represents differences in the areas of the mesh triangles between the mean infant (reference) and mean adult (target) forms (size and shape) of both species predicted by two separate multivariate regressions (shape on size), rescaled to the mean size of modern human infants and modern human adults,

respectively. These differences are plotted using colours to represent the degree of local expansion or contraction of the adult surface in both species. This visualisation allows a comparison of ontogenetic transformations that is independent of registration.

The colour map shown in Figure 3.4.5b shows the difference between a mean infant *H. sapiens* (reference) and a mean infant *H. neanderthalensis* (target) plotted on the infant form of *H. neanderthalensis,* rescaled to the mean size of modern human infants. Likewise, the colour map shown in Figure 3.4.5c shows the difference between the mean adult *H. sapiens* (reference) and the mean adult *H. neanderthalensis* (target) forms, plotted on the adult form of *H. neanderthalensis,* rescaled to the mean size of modern human adults. Note that different ranges of values are used in each colour map to maximise the range of colours in each visualisation.

Figure 3.4.5 below. **a**: differences in form between a mean infant (reference) and a mean adult (target) *H. sapiens* (left) and an infant (reference) and an adult (target) *H. neanderthalensis* (right) using warpings extracted from the multivariate regression of size on shape and then rescaled to modern human infant and adult mean Csize. The colour maps show the degree of expansion of surface regions as a result of differences between infant and adult forms for each species plotted on the adults. The magnitude of local expansion is indicated by colours as shown in the key: small=blue, to large (red). **b**: differences in form between a mean infant (reference) *H. sapiens* and a mean infant (target) *H. neanderthalensis* (both rescaled to modern human mean infant Csize) using warpings extracted from the multivariate regression of size on shape. The differences are plotted on the infant Neanderthal. **c:** differences in form between a mean adult (reference) *H. sapiens* and a mean adult (target) *H. neanderthalensis* using warpings (both rescaled to modern human mean adult Csize) extracted from the multivariate regression of size on shape. The differences are plotted on the adult Neanderthal.

a.

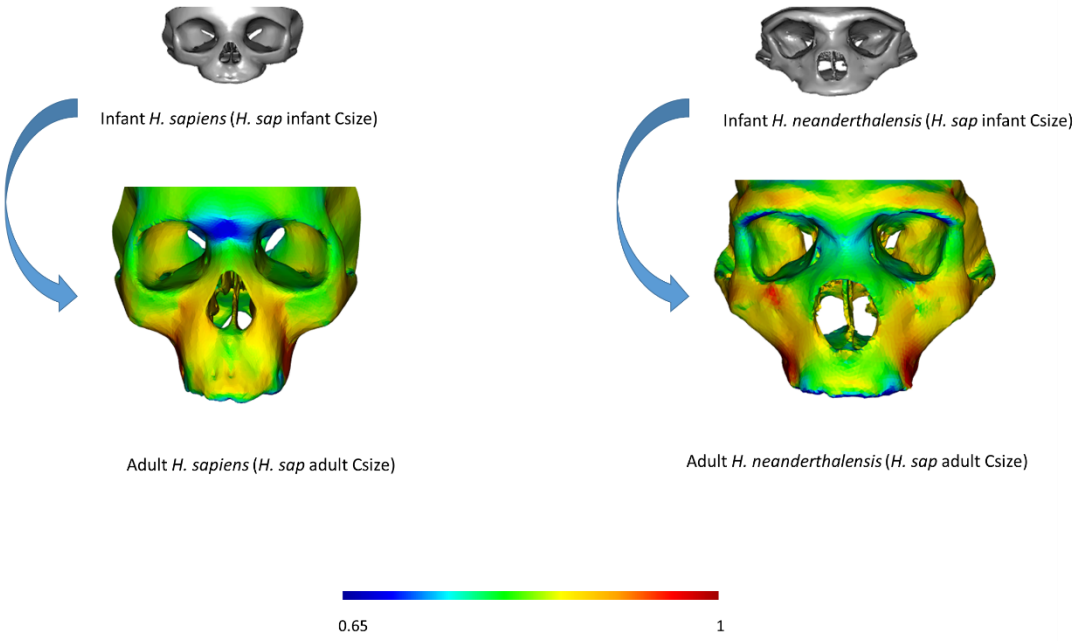

b.

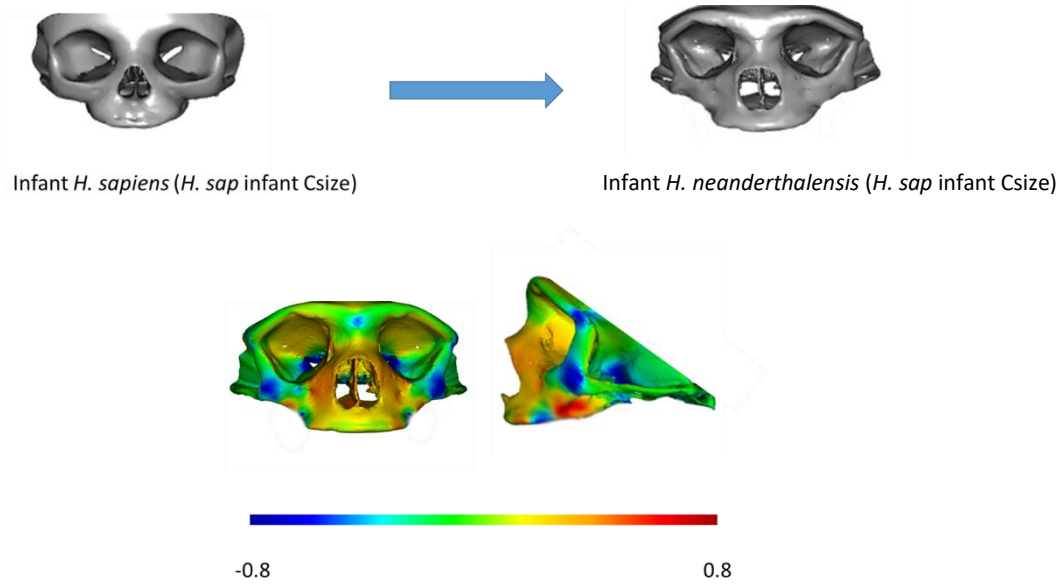
Infant *H. sapiens* (*H. sap* infant Csize)
Infant *H. neanderthalensis* (*H. sap* infant Csize)
-0.8
0.8

c.

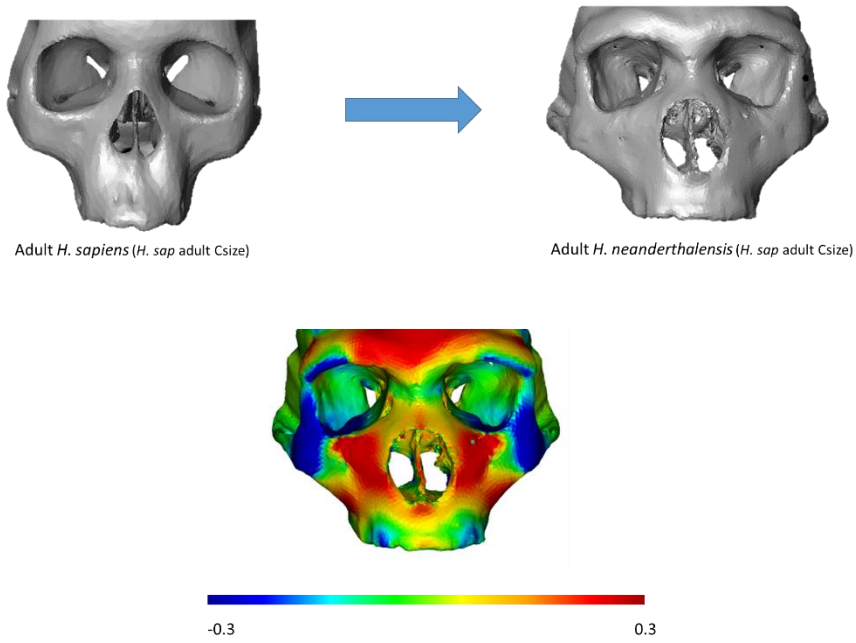
Adult *H. sapiens* (*H. sap* adult Csize)
Adult *H. neanderthalensis* (*H. sap* adult Csize)
-0.3
0.3

The colour map in Figure 3.4.5a (left) comparing infant and adult modern humans is similar to those visualised in the PCA analysis of the face in Section 3.1. The warped surface shows marked vertical elongation of the face and changes in proportion between the mid and upper face such that the nasal and subnasal alveolar regions become relatively larger and more prominent. During ontogeny, the greatest rate of expansion (orange-red) is located in the posterior maxilla, specifically over the molars and the inferior aspect of the zygomatic arch as it meets the maxilla. Further marked expansion occurs from the lateral aspect of the nose to the posterior maxilla. Less marked expansion is identified over the lower central nasal and alveolar regions (green to yellow), the anterior pillar of the face (Rak, 1986). The orbital and infraorbital regions with the supraorbital torus show relatively little change indicated in green.

When compared to modern humans, Neanderthals (Figure 3.4.5a, right) undergo a more uniform and widespread expansion of the entire midface which is a little more marked (more red/orange) than in humans (Figure 3.4.5a, left), suggesting that, during ontogeny, the development of the midface is greater in Neanderthals than modern humans, particularly in the region of the lateral maxilla and zygomatic bone (body and temporal process). The double-arched supraorbital torus is identified as another area of great expansion during ontogeny. This shows that the characteristic Neanderthal adult morphology is achieved through expansion and modification principally of the lateral midfacial and supraorbital elements during ontogeny. A common area of expansion among Neanderthals and modern humans is identified in the posterior maxilla, which is red in both species.

Also similar to modern humans, in Neanderthals, the superior orbital border of the orbit, and the region around the nasion face (light blue to blue areas in Figure 3.4.5, a and b), and the subnasal region (green area in Figure 3.4.5, a and b) expand least during ontogeny.

Considering differences between the two infants when plotted on the infant Neanderthal (Figure 3.4.5b), the colour map on latter shows that, compared to infant modern humans, infant Neanderthals have a more expanded (red) posterior face (molar region). Further, marked differences are focused around the midface and nose (yellow to orange in Figure 3.4.5b). Thus, early postnatal differences among the two species are characteristic of what are considered to be typical Neanderthal autapomorphies; a prominent and

"inflated" midfacial complex and more developed posterior face, which likely relates to the retromolar space in the mandible of Neanderthals.

Comparing the two adults (Figure 3.4.5c), the largest differences are located in the midface (perinasal maxilla) and the central part of the supraorbital torus (indicated by the colour map as areas of expansions in Neanderthals), while the lateral orbits and lateral zygomatics undergo less expansion and some regions are contracted in Neanderthals relative to modern humans (blue).

The angle between the ontogenetic allometric trajectories of the two species (resulting from two separate multivariate regressions of size on shape after a common GPA) is 29°, significantly different from zero (p-value < 0.001, 1000 random permutations). This is strong evidence of divergence of ontogenetic allometry, indicating that the two species have different modes of shape change with size during ontogeny. This result is a crucial contribution to the ongoing debate about postnatal trajectories in Neanderthals and modern humans and is of fundamental importance, as the divergence of facial ontogenetic trajectories between the two species was never tested in the literature.

In Figure 3.4.6, the differences from the common mean shape of Neanderthal and modern human infants to the mean adult shape of each species are visualised. These are calculated after translating the ontogenetic vectors of each species to a common origin, the mean infant shape of modern humans and Neanderthals. Because there are now only three data points, the common mean infant, the mean adult modern human and mean adult Neanderthal, the allometric vectors can be fully represented in two dimensions, visualised in a plot of the first two PCs of shape from a PCA of these three means. In the plot, the angle between the trajectories is 29 degrees (as it was in the angle test) and the trajectories represent the differences in postnatal ontogeny between the species. The differences among adults arise through these divergent trajectories and are in addition to those that are present at birth and that were noted in the earlier shape and form PCAs of Figure 3.4.3 and 3.4.4 and the regressions of Figure 3.4.5.

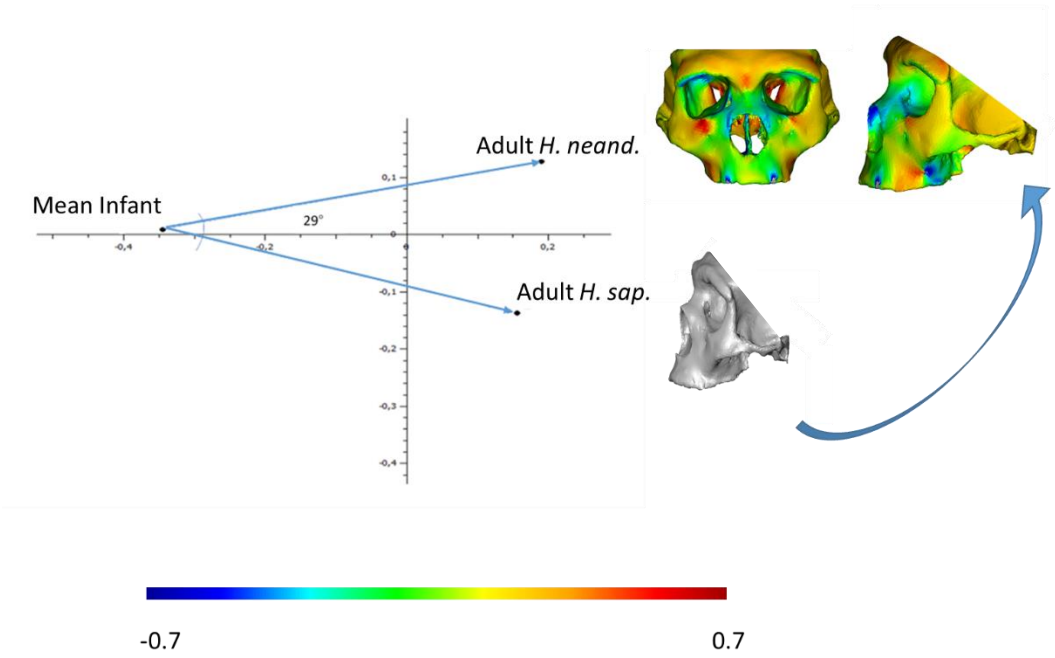

Figure 3.4.6. PCA of ontogeny of H. *sapiens* and *H. neanderthalensis* with visualisation of divergence angle. Colour map show differences between the adult *H. sapiens* (reference) and the adult *H. neanderthalensis* (target). Differences are plotted on the adult Neanderthal.

Figure 3.4.6 shows the warpings and colour map derived between the two 'adult' shapes (plotted on the adult Neanderthal). These represent the differences that arise purely due to divergence, ignoring differences already present at birth, and those that arise through extension of growth into larger sizes in Neanderthals (hypermoprhosis). The insets and colour map show that Neanderthal facial allometric development differs from modern humans particularly in the regions of the zygomatic, lateral maxilla and orbital torus, all of which become taller, more massive, "inflated" and heavily built in Neanderthals. The posterior face, particularly near the premolars, also shows marked differences (yellow-red) with a taller posterior face in Neanderthals compared to modern humans. Contrary to what one might expect, the anterior pillar, namely the nasal bridge and subnasal region, is relatively contracted in the adult Neanderthal compared to the adult modern human. In addition, the Procustes distance between the mean infant and mean adult modern human is 0.278 while that between the mean infant and the mean adult *H.*

neanderthalensis is 0.291 indicating that the Neanderthals undergo a marginally greater degree of allometric shape change during postnatal ontogeny.

Hypothesis 2 states that *during postnatal ontogeny, Neanderthals and modern humans show no differences in the ways in which facial components covary*.

This is tested to assess the extent to which different patterns of ontogenetic covariation among parts of the facial skeleton underlie the divergence in postnatal ontogenetic trajectories between the two species. Unlike the PLS analysis of Section 3.2, in which differences in covariation among regions were assessed between age groups, here covariances were compared between the entire ontogenetic samples of modern humans and Neanderthals because the Neanderthal sample is small, and cannot reasonably be divided into age groups.

Table 3.4.1 shows the results of the PLS analyses performed between the anatomical 'blocks' (regions) of the maxilla, palate, orbit and nasal cavity, first in modern humans then in Neanderthals. In modern humans, the total covariance is large between each pair of regions. The least total covariance is found between orbit and maxilla (69.3) and the greatest between the palate and other regions (95.16 -97.65). The highest correlation coefficients (between first singular warps) are found between the maxilla and the other regions: palate, orbit and nasal cavity. All correlation coefficients are significant and remain significant after Bonferroni correction, which requires a p-value of 0.05/6 = 0.0083. The percentage of variance within each region explained by its covariance with other regions is similar for each pair of comparisons (between 25% and 38%) except for those involving the palate, for which the proportion of its variance explained by its covariation with other regions is consistently about 65%.

PLS analyses of Neanderthals suffer from small sample size, therefore the analysis has less statistical support. Only two correlation coefficients are significant, those between the maxilla and the orbit and the maxilla and palatal region (and neither is after Bonferroni correction). The magnitude of the correlation coefficients is similar to those found in modern humans as the maxilla shows the highest correlation coefficients with other regions in both species. There are, however, some notable differences. The correlations between the first singular axes from the PLS between the nasal cavity and

palate and between the nasal cavity and maxilla are much reduced in Neanderthals (0.77 in modern humans vs 0.53 in Neanderthals in the former comparison and 0.83 vs 0.70 in the latter). In addition, in tests of association between the nasal cavity and other regions, total covariance is much reduced when compared to modern humans. These findings indicate that the nasal cavity of Neanderthals is less integrated with other parts of the face than in humans, being more independent of the palate and maxilla in its development. In contrast, in Neanderthals, the correlation coefficients (albeit mostly insignificant because of small sample size) are larger in between the orbit and the palate (0.85 vs 0.64) and between the orbit and the nasal cavity (0.75 vs 0.65). In Neanderthals, the proportion of variance within each block explained by its covariance with other blocks is not greatly different from modern humans. However, the percentage of explained variance is greater in *H. sapiens* for all pairs of regions except for those between the maxilla and the palate and orbits.

Thus, these analyses suggest some differences between Neanderthals and modern humans in the degree of association among facial regions during ontogeny, particularly with respect to the nasal cavity and its association with other regions. However, the small sample size of Neanderthals and consequent lack of significance of correlation coefficients urges caution in interpretation.

PLS shape analyses between facial modules in modern humans					
All sample					
Block 1 vs Block 2	TOT. COVAR.	CORR. COEFF.	P-VALUE	EXPLAINED VARIANCE BLOCK 1	EXPLAINED VARIANCE BLOCK 2
N.cavity- R Palate	97.65 %	0.77	0.001	35.22 %	65.51 %
N. Cavity- R Maxilla	88.77 %	0.83	0.001	37.10 %	37.10 %
R Orbit- R Palate	95.16 %	0.64	0.001	29.40 %	64.75 %
R Orbit- R Maxilla	69.63 %	0.86	0.001	32.91 %	32.45 %
R Orbit- N. Cavity	88.98 %	0.65	0.001	26.45 %	37.13 %
R Palate- R Maxilla	97.56 %	0.86	0.001	65.52 %	37.24 %
PLS shape analyses between facial modules in Neanderthals					
All sample					
Block 1 vs Block 2	TOT. COVAR.	CORR. COEFF.	P-VALUE	EXPLAINED VARIANCE BLOCK 1	EXPLAINED VARIANCE BLOCK 2
N. Cavity- R Palate	68.28 %	0.53	**ns**	21.57 %	56.76 %
N. Cavity- R Maxilla	53.02 %	0.70	**ns**	30.37 %	32.30 %
R Orbit- R Palate	81.86 %	0.85	**ns**	18.85 %	60.25 %
R Orbit- R Maxilla	61.39 %	0.83	0.04	25.27 %	38.11 %
R Orbit- N. Cavity	41.56 %	0.75	**ns**	19.80 %	28.17 %
R.Palate- R Maxilla	87.76 %	0.76	0.01	58.66 %	39.80 %

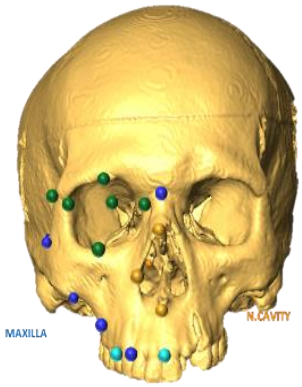

Table 3.4.1. PLS analysis of shape covariation between facial regions in modern humans (top) and Neanderthals (below). TOT.COVAR= percentage of total covariance explained by the first pair of singular warps, CORR.COEFF= correlation coefficients between blocks for PLS1 scores and the p-value assessed by permutation test between pairs of blocks (ns= not significant relations in bold). For each block, the variance explained by the correlation with the other blocks was estimated.

3.4.6 Discussion and conclusions

A key unresolved question regarding the differences between Neanderthals and modern humans is whether or not they differ in the way in which infants reach their final adult morphologies. While it is evident that cranial architecture is different among newborns and adults of the two species, it has been unclear if postnatal ontogeny further accentuates the differences between adults and, if so, to what degree and how.

Hypothesis 1 states that *Neanderthals and modern humans exhibit no significant difference in their facial ontogenetic trajectories.*

From the PCA in Figure 3.4.3 and 3.4.4 and the colour maps in Figure 3.4.5, it appears evident that both modern humans and Neanderthals undergo significant changes in facial morphology during ontogeny. While differences in adult facial morphology between the two species have been previously described (Rak, 1986; Ponce de Leon and Zollikofer, 2001; Bastir et al., 2007; Marquez et al., 2014) differences in postnatal trajectories between the two species, although compared using PCA, have never been formally tested using regression.

Previous studies (Ponce de Leon and Zollikofer, 2001, Ackermann et al., 2002), based on distributions along PC1 and PC2 in the form and shape space, suggested parallel ontogenetic trajectories between the two species. Observing the PCAs in Figure 3.4.3. and 3.4.4 one might agree. Neanderthals also appear to be displaced along PC1, which represents some aspects of allometry in both PCAs, such that they are more advanced, with adult Neanderthals achieving greater sizes and more “developed” shapes. This result confirms previous studies that noted that adult human crania are more similar in shape to those of adolescent Neanderthals, while adult Neanderthals have considerably larger faces and, accordingly, more cranial superstructures (brow ridges and bony crests) than adult humans. (Ponce de Leon and Zollikofer, 2001; Krovitz, 2003; Zollikofer and Ponce de Leon, 2010). However, PCAs offer an incomplete description of differences, therefore by calculating the colour maps derived from the regression warpings it is possible to fully describe ontogenetic trends and differences between the two species in terms of mode and magnitude of changes.

The results of Figure 3.4.5 (a) suggest that there are some similarities in the two species in the ways in which infants reach their adult form, with midfacial and posterior molar regions in both species being the areas of greatest expansion during ontogeny. However, in detail, the distribution of areas of expansion, particularly over the midface, differs. In modern humans, vertical growth and development of the inferior maxilla is the most dominant feature of postnatal ontogeny, with the colour map indicating areas of greatest expansion lateral to the nose extending to the alveolar region. The Neanderthal colour map and warpings show some similarities with that of modern humans, reflecting common aspects of postnatal ontogeny. However, there are differences. The lateral zygomatico-maxillary complex, becomes taller and more prominent (orange/red) than in modern humans (green/orange). In addition, the entire supraorbital torus undergoes greater expansion/modification. Thus, while the characteristic Neanderthal feature of a marked suprorbital torus develops during the postnatal period, the heavily-built midface does not seem to arise at the same time, although it is somewhat enhanced. Indeed, the expanded midface of Neanderthals relative to modern humans appears to already be present in infancy as indicated by the colour map of Figure 3.4.5 b. This difference is carried into adulthood (Figure 3.4.5 c) with only moderate additional development during the postnatal period (Figure 3.4.5 a). Instead, postnatal ontogeny most markedly differs between these species in the degree of expansion of the central supraorbital torus, which is marked in Neanderthals and nearly absent in modern humans.

Considering the colour maps of form and shape differences from Figure 3.4.5 and the Figure 3.4.6 respectively, the lateral midface (temporal and frontal processes of the zygomatic bone) and the orbital torus show the greatest differences in allometric scaling. The lateral midface becomes taller, wider and more anteriorly projecting in Neanderthals compared to modern humans, and the orbital torus does not develop to any marked degree in modern humans compared to Neanderthals who grow a massive double-arched structure. Although Neanderthals are commonly described as having taller and more forward projected midfaces (Zollikofer and Ponce de Leon, 2010), this analysis shows that the lateral region of the midface and the orbital arch are the areas that show the greatest differences in allometry between the two species. The differences in midfacial projection are already largely established in infants.

Consistent with the complex picture of similarities and differences in ontogeny presented by the colour maps, the multivariate allometric vectors of the two species significantly differ in direction, indicating different ontogenetic allometries. Therefore, Hypothesis 1 of parallel ontogenetic trajectories is rejected. This result contrasts with previous findings that suggested that the two species follow identical patterns of allometric development (Ponce de Leon and Zollikofer, 2001; Ackermann and Krovitz, 2002) but agrees with recent findings from comparative studies of mandibular and cranial vault ontogeny (Bastir et al., 2007, Gunz et al., 2010).

Hypothesis 2 states that *during postnatal ontogeny, Neanderthals and modern humans show no differences in the ways in which facial components covary.*

This was investigated using PLS analyses (Table 3.4.1). In modern humans, the shape of the maxilla shows the strongest association with that of other facial elements: the nose, orbit and palate. When significant, in Neanderthals the interactions among cranial components are generally similar to those observed in modern humans, showing that despite divergence in their ontogenetic trajectories, some regions of the face such as the maxilla covary with adjacent regions in a similar way in the two species, these appear to be conserved in these two hominins. However, the findings also highlight that there may be differences, particularly in the ways in which the nasal cavity interacts with the rest of the face during ontogeny. In this study, the most characteristic trait of the Neanderthal face, namely the nasal cavity shows patterns of cranial integration dissimilar to those observed in modern humans. This is important because it reflects the very major difference in nasal form between these species and suggests that the differences in nasal form alone do not explain all of the differences in adult facial morphology.

This result suggests a more complex picture of differences between Neanderthals and modern humans compared to what has been found in other studies of closely related taxa, where patterns of interaction appear to differ less (Cheverud, 1982; Ackermann, 2002; Hallgrimsson et al., 2009; Roseman et al., 2011; Singh et al., 2012). Since patterns of covariation do differ between the two species, Hypothesis 2 is rejected.

In conclusion, there are clear differences in morphology at all stages of ontogeny between modern humans and Neanderthals. This is evident from the study of the colour

maps derived from the multivariate regressions and the angle test, which show that the two species possess divergent trajectories, with Neanderthal possessing a more derived morphology. Patterns of covariation are similar only for certain facial regions, while others show clear indication that the cranial regions can be integrated at different levels in closely related species, thus resulting in different morphologies.

Further studies including a bigger fossil sample size and inclusion of other hominin species such as *H. heidelbergensis* should investigate in more detail when these differences arose at an evolutionary level and if some of these patterns are shared among recent and archaic fossil hominins.

4.0 General discussion and conclusions

This project aims to define the role of changes in postnatal growth and development in shaping the face throughout the evolution of late Pleistocene *Homo* and modern humans. An ontogenetic perspective is applied to clarify the ontogenetic trends in terms of the trajectories, integrations and dependencies among cranial and facial components during development. The ultimate goal of this project is to determine to what extent the face is integrated within the skull and constrained by its parts, and how different facial regions develop, covary and have evolved.

To that end, a virtual statistical approach, which includes geometric morphometrics and multivariate statistical analyses as well as new visualisation methodologies were applied to investigate the ontogeny of *H. sapiens* and *H. neanderthalensis* and provide new insights into this topic. The dissertation is divided into 4 main chapters. The first chapter (Chapter 1) provides a literature review of the core topics approached in the dissertation. The second chapter (Chapter 2) goes over the methodologies applied in the collection and estimation of data, testing their reliability, as well as the methodologies applied in the statistical tests of the hypotheses (principal component analysis, partial least squares analysis, path analysis, multivariate regression). The third chapter (Chapter 3) is divided into four sections, each focussing on a different research topic. Lastly, this conclusion summarises and synthesises the key findings.

4.1 Synthesis of key findings

Chapter 3, Section 3.1 addressed the strength and mode of interactions among the cranial base, vault and face during ontogeny.

While previous studies have laid the ground by starting to explore ontogenetic shape variations of these cranial regions in Hominoidea (Gunz et al., 2010, Singh et al., 2012, Profico et al., 2017; Zollikofer et al., 2018), lack of modern human ontogenetic data has often constrained the study of modern human ontogeny to the use of cephalometric

data. This of necessity focused research on specific aspects of development (basicranial flexion, midface orientation, etc.) and used bespoke measurements to approximate them. A better understanding of the development and inter-relationships between cranial regions can be obtained by using Geometric Morphometric Methods (GMM) based on 3D landmarks and semilandmarks.

In Section 3.1, patterns of growth, development and ontogenetic trajectories of the cranial vault, base and face are described and compared in modern humans as are patterns of integration and modularity among them at different ontogenetic stages using a 3D landmark and semilandmark based approach.

The results show non-linear trajectories of development for the entire cranium and face, and identify changes in trajectory between the younger and older subadult stages, with significant divergence of trajectories between the two phases. In addition, using a novel visualisation approach, the morphological changes in each region from younger subadults to adults are visualised using warpings, enhanced by colour mapping local relative and absolute expansions/contractions.

The study of covariation among the three regions during ontogeny suggests that phases of accelerated developmental change and flexibility coincide with a more modular behaviour of cranial regions. This suggests that local influences become more dominant in control of their development rather than the underlying large scale influences that affect several regions together, such as allometry and masticatory loads, that act as integrators, preserving function (Porto et al., 2013). This result might clarify why the literature shows such contradicting results considering covariation of these three regions. While most studies focus on the entirety of ontogeny (Bastir et al., 2006) or the resulting adult variation (Profico et al., 2017), the results of this section highlight that while a region might be ontogenetically integrated overall, depending on the age stages represented in the ontogenetic data, different degrees of integration will be found. Indeed, more detailed studies of integration at different ontogenetic stages are needed to characterise the developmental dynamics of modes of covariation within the skull.

Section 3.2 of this thesis explores ontogenetic trajectories, allometry and integration among facial components during ontogeny. The aim was to explore in detail how different regions grow, develop and scale and how they interact during postnatal ontogeny, and

to use this information as a starting point to build a statistical model of normal craniofacial growth and development to apply in evolutionary studies as well as in surgical planning and clinical investigation.

Results suggest that significant differences arise during ontogeny through changing allometry and covariation among regions and, within a region, between different age classes.

The findings indicate that the nasal region develops allometrically throughout the entirety of ontogeny and covaries significantly with adjacent structures in all age classes. These findings support the hypothesis that the cartilaginous elements comprising the septum and walls of the developing nasal cavity play a central role in shaping the facial complex of modern humans as postulated by Scott (1956; contra Moss, 1968), and sustained by many experimental studies (Verwoerd and Verwoerd-Verhoef, 2007; Wong et al., 2010; Holton et al., 2011; 2012; Al Dayeh et al., 2013; Hall and Precious, 2013; Goergen et al., 2017).

Interestingly, the palatal region goes through a phase of increased modularity during the older subadult phase. This result, if sustained by further data, could give useful insights into the optimal timing for cleft palate surgery. Indeed, while it has been found that early surgery can impact on normal speech, late operations (after 4-6 years of age) are hypothesised to impact on normal maxillofacial development (Rohrich et al., 2000). Therefore, the current findings could facilitate the planning of surgical interventions by taking into consideration the best age range and the lowest impact on adjacent structures.

Section 3.2 also highlights the central role of the maxilla as an integrating element throughout ontogeny. This finding is sustained by preliminary studies (Bastir and Rosas, 2013) which found integration between the nasopharynx and maxilla and between the latter and the piriform aperture in modern humans. The role of the maxilla during ontogeny is further explored in Section 3.4.

While Section 3.2 explored modes and magnitudes of integrations and allometric development, Section 3.3 aims to clarify the hierarchies of interactions among facial components in driving the growth and development of the human face in the first years of life. It does so using path analysis, a methodology that aims to define pathways of

interactions among variables in a model of hypothesised relationships by testing strengths of relations. In the first path model, growth of the nasal septum is opposed to that of the orbits as a pacemaker for the growth and development of the maxilla, alveolar region, medial orbit and overall vertical facial development. This path is built based on previous theories, which put in competition the role of nasal septal growth versus other skeletal elements as principal pacemakers for facial growth and development (Scott, 1956; Mooney et al., 1989, Holton, 2011, 2012; Moss, 1968; Babula et al., 1970; Goergen et al., 2017). Analyses are performed after dividing the sample into age classes by year from 0 to 6. Results show that interactions among variables change significantly over time, with nasal and subnasal heights showing the greatest and most consistent interactions with facial height. This finding supports the hypothesis that the nasal septum has a significant influence on prenatal and early postnatal human facial growth (Scott, 1956; Verwoerd and Verwoerd-Verhoef, 2007; Wong et al., 2010; Holton et al., 2011; 2012; Al Dayeh et al., 2013; Hall and Precious, 2013; Goergen et al., 2017). In the second path model, the growth of the soft tissue components of the face is compared to that of the skeletal elements with the aim of testing the major influences on the growing elements of the face and defining the relations among soft and skeletal tissues during ontogeny. Results show that the interactions among skeletal elements and overall facial growth do not change significantly when the soft tissue variables are included in the path model. However, skeletal components act more independently, most of the skeletal tissues having significant impact (significant path coefficients) only on overall facial development and not among them. In addition, soft tissues, particularly those related to mastication, such as the oral capsule and masseter muscle, tend to act only locally, affecting adjacent skeletal components linked to chewing actions (subnasal region). These results highlight that the morphology of the cranium is constantly undergoing modification throughout ontogeny and reflects a balance between developmental patterning, mechanical-load-induced remodelling and other factors. Further studies using Finite Element Analysis (FEA) should investigate the extent to which muscular loadings impact on local and global morphological changes during ontogeny (Conith et al., 2019).

Chapter 3 Section 3.4 compares the ontogenetic trajectories of *H. sapiens* and *H. neanderthalensis*, as well as their modes and magnitudes of ontogenetic change and the

integration among their facial components to answer the question: do these patterns differ significantly between the two species? And if yes, how? Results show that when comparing the ontogenetic trajectories as they are projected onto the first two principal components of joint analyses of the two species, they appear parallel. However, comparing trajectories in the entire shape space, the multivariate allometry of the two species, permutation test on the angle between them indicates that the two trajectories diverge significantly, this divergence indicating differences in the way the midface changes during ontogeny. This result support previous findings that found divergence in the mandibular trajectory of the two species (Bastir et al., 2007) and highlight the need to perform statistical testing in addition to data exploration using principal component analysis. Interestingly, the main ontogenetic morphological differences which cause divergence between the two species are not located in the region of the nasal cavity, which in Neanderthals appears to have its peculiar shape since infant stages and is probably established before birth. Rather, the differences accentuated postnatally are located mostly in the zygomatico-maxillary region, which, as observed in Section 3.2, is one of the principal elements of integration in the face. Thus, differences in the rest of the face between the two species arise mainly from differences in the interaction and integration between the zygomatico-maxillary complex and the other adjacent facial elements.

Furthermore, results show that difference in trajectories is reflected in different modes of integration among facial regions in the two species, particularly in the midfacial region and the nasal cavity.

As already observed for modern humans in Sections 3.1, 3.2 and 3.3 for modern human ontogeny, the orbits play a minor role in the development and so in driving differences among the two species.

In summary, regarding the biologically pertinent questions of this thesis, it is concluded that in both Neanderthals and modern humans, interactions among cranial and facial components change significantly during postnatal ontogeny, with size playing a major role as an integrating factor.

The nasal region plays a key role in shaping the facial complex, during infancy as well as throughout adolescence and adulthood, but does not develop divergently between the two species.

Within modern humans, ontogenetic trajectories diverge among different age classes, indicating that different modes of change occur during growth and development and not only among different human populations (Viðarsdóttir et al., 2002).

Divergence of facial trajectories is for the first time assessed for Neanderthals and modern humans, and regional differences underlying the divergence are investigated and described.

In addition, divergence of trajectories is reflected in different magnitudes of integration among facial regions of the two species, suggesting that differences in pathways of interactions during ontogeny may result in different morphologies and, potentially, different functionalities, which in turn, during ontogeny, might impact on cranial regional growth interactions and so morphology (O'Higgins et al., 2012). Further studies should clarify the different impacts of functional loadings at different ontogenetic stages and their influence on facial anatomy.

4.2 Limitations of the present study and implications for future research

By applying geometric morphometrics and multivariate analysis in this thesis the tempo and mode of interactions among cranial components have been described and detailed three-dimensional statistical models of craniofacial growth and development have been compared between modern humans and Neanderthals. One potential issue in this work arises because it is based on morphological analysis rather than *in vivo* experiments. Because causality and hierarchies are better studied once we can control some variables and keep track of changes derived from keeping those variables constant, data from *in vivo* experiments are essential to support any conclusion on modern human growth and development.

Limitations also arise from the availability of longitudinal ontogenetic data, of living (*H. sapiens*) and inevitably of fossil (*H. neanderthalensis*) material, as well as lack of information about those data (exact age and gender). Cross-sectional data can only give general insights and even though they cannot be gathered in fossils, longitudinal data in modern humans would be valuable additions to better contextualise the study of fossils

Further studies should focus on improving sample size and information. In addition, Finite Element Analyses (FEA) of crania to simulate the effects of masticatory system loadings at different stages of ontogeny could complement the current thesis by providing additional insights into how craniofacial growth and development are integrated through masticatory forces.

5.0 Supplementary Material

specimen	age_group	eruption pattern	age	known/estimated
HPN_001	younger subadult	No_teeth_erupted	0.5	e
HPN_002	younger subadult	No_teeth_erupted	0.5	e
HPN_004	younger subadult	No_teeth_erupted	0.5	e
HPN_005	younger subadult	No_teeth_erupted	0.5	e
HPN_006	younger subadult	No_teeth_erupted	0.5	e
HPN_007	younger subadult	No_teeth_erupted	0.5	e
Hum1175	younger subadult	No_teeth_erupted	0.5	e
SCH2___	younger subadult	No_teeth_erupted	0.5	e
SCH26mo	younger subadult	No_teeth_erupted	0.5	e
UCL_3__	younger subadult	No_teeth_erupted	0.5	e
UCL_C34	younger subadult	No_teeth_erupted	0.5	e
UCLA23D	younger subadult	No_teeth_erupted	0.5	e
SCH36__	younger subadult	M1dec_erupted	2	e
SCH13__	younger subadult	M1_in_crypt	4	e
SCH5___	younger subadult	M1_in_crypt	4	e
UCL_A23	younger subadult	M1_in_crypt	4	e
SCH13cs	younger subadult	M1_erupting	5.5	e
UCL-56_	younger subadult	M1_erupting	5.5	e
H-I001_	younger subadult	M1_erupting	5.5	e
UCL-A06	Older subadult	M1_erupted	6	e
UCL_159	Older subadult	M1_erupted	6	e
SCH20__	Older subadult	M1_erupted	6	e
SCH366_	Older subadult	M1_erupted	6	e
SCH7___	Older subadult	M1_erupted	6	e
SCH156y	Older subadult	I1_in_crypt	6.5	e
UCLA23M	Older subadult	I1_erupting	7.5	e
SCH4_8y	Older subadult	I2_in_crypt	8	e
SCH39fl	Older subadult	Premolars_in_crypt	9.5	e
SCH7_8y	Older subadult	M2_in crypt	10	e
SCH7sin	Older subadult	M2_in_crypt	10	e
SCH258y	Older subadult	M2_in_crypt	10	e
SCH13bm	Older subadult	M2_erupting	11.5	e
SCH13ri	Older subadult	M2_erupting	11.5	e
SCH3610	Older subadult	M2_erupting	11.5	e
SCH-27_	Older subadult	M2_erupting	11.5	e
UCLCDJu	Older subadult	M2_erupting	11.5	e
UCLF279	Older subadult	C_erupting	11	e
SCH1-12	Older subadult	M2_erupted	12	e
SCH31__	Older subadult	M2_erupted	12	e
SCH7fex	Older subadult	C_erupted	12	e
SCH6_18	Adult	M3_erupting	18.5	e
SCH3020	Adult	M3_erupted	19	k
SCH39fe	Adult	M3_erupted	19	k
SCH39le	Adult	M3_erupted	19	k

SCH39fr	Adult	M3_erupted	19	k
VA019__	Adult	M3_erupted	20	k
VA007__	Adult	M3_erupted	20	k
VA024__	Adult	M3_erupted	20	k
ANAT800	Adult	M3_erupted	23.5	e
ULAC013	Adult	M3_erupted	23.5	e
ULAC016	Adult	M3_erupted	23.5	e
VA001__	Adult	M3_erupted	23.5	e
VA002__	Adult	M3_erupted	23.5	e
VA003__	Adult	M3_erupted	23.5	e
VA004__	Adult	M3_erupted	23.5	e
VA012__	Adult	M3_erupted	23.5	e
VA013__	Adult	M3_erupted	23.5	e
VA014__	Adult	M3_erupted	23.5	e
VA017__	Adult	M3_erupted	23.5	e
VA020__	Adult	M3_erupted	23.5	e
VA021__	Adult	M3_erupted	23.5	e
VA022__	Adult	M3_erupted	23.5	e
VA025__	Adult	M3_erupted	23.5	e
VA030__	Adult	M3_erupted	23.5	e
VA050__	Adult	M3_erupted	23.5	e
VA051__	Adult	M3_erupted	23.5	e
VA052__	Adult	M3_erupted	23.5	e
VA053__	Adult	M3_erupted	23.5	e

Table S1. Human sample with description of stage of dental development, age and repository, for a total of 68 specimens. When the age was not known, it was estimated, up to a maximum of 23.5 years, when full dental maturity is reached (AlQahtani et al., 2010).

Fossil specimen	Courtesy of	Type	Age range
Mezmaiskaya 1	Dr. Gunz, Prof. Hublin, Prof. Maureille	Surface reconstruction from CT-scan	0 to 5.5
Le Moustier 2	Dr. Gunz, Prof. Hublin, Prof. Maureille	Surface reconstruction from CT-scan	0 to 5.5
Pech De L'Aze	Prof. Balzeau, Prof. Bahuchet, Prof. Grimaud-Hervé and Musee de l'Homme, Paris	Micro CT-scan	0 to 5.5
Roc De Marsal	NESPOS Archive, Prof. Macchiarelli, Dr. Mazurier, and Dr. Volpato, University of Poitiers	CT-scan	0 to 5.5
La Quina 18	La Sapienza University, Prof. Manzi	Photogrammetry of cast	6 to 18
La Chapelle	Natural History Museum,Paris	CT-scan	+18
La Ferassie	Natural History Museum, Paris	CT-scan	+18
Guattari	NESPOS Archive, Dr. Bondioli, Pigorini Museum, Rome	CT-scan	+18
Saccopastore1	La Sapienza University, Prof. Manzi	CT-scan	+18
Saccopastore2	La Sapienza Universit, Prof. Manzi	CT-scan	+18
Gibraltar1	Dr. Kruzinsky and the Natural History Museum, London	CT-scan	+18
Amud1	Morphosource	Surface scan from cast	+18

Table S2. List of Neanderthal specimens and age class. The age range was estimated from literature (Martín-González et al., 2012).

ID	1st measurement	2nd measurement	3rd measurement	Mean volume	Mean percentage error
VA001	13063.53	13635.49	12766.94	13155.32	2.43%
VA002	30722.56	30129.38	30628.29	30493.41	0.80%
VA003	19871.02	19342.4	19784.52	19665.98	1.10%
VA004	12568.25	13093.85	12373.45	12678.52	2.18%
VA007	30791.27	29950.45	30673.25	30471.65	1.14%
HI001	10241.26	9414.84	10189.4	9948.5	3.58%
HPN006	232.49	271.19	296.04	266.57	8.52%
UCL-A06	2972.27	3400.23	3640.49	2860.3	6.99%
UCL-F279	7958.4	8362.21	8665.71	8328.77	2.96%

Table S3. Repeated measurements of nine arbitrarily chosen specimens, mean volume and average percentage of deviation from the mean volume. Minimum deviation from the mean (VA002) 0.80%, maximum deviation from the mean (HPN006) 8.53%, total average error 3.3% (results carried out by Anna Lucas during herMSc).

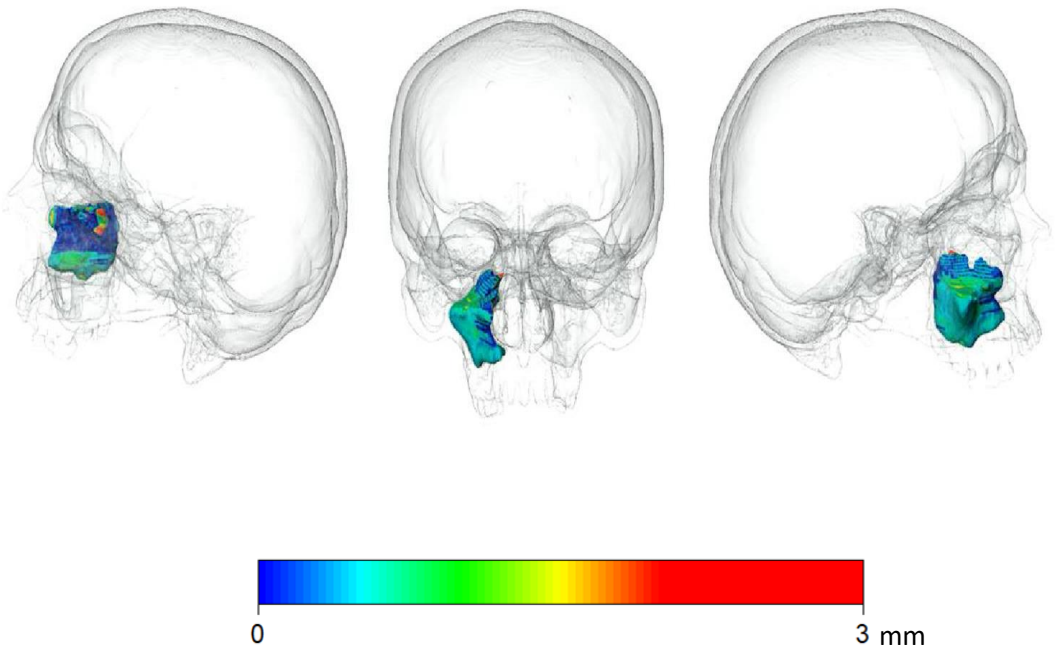

Figure S1. Colourmap mesh distance seen from medial (right), anterior (middle), and lateral (right) view indicating the surface distance (mm) between a semi-automatically segmented sinus and a sinus segmented using the R tool "ast-3d". Red indicates a mesh distance ≥ 2mm (results carried out by Anna Lucas during her MSc).

Landmarks Right/Left	Osteometric name	Description
1	Glabella	Most anterior point in the mid-sagittal plane at the lower margin of the frontal bone
2	Bregma	Intersection of coronal and sagittal sutures
3,4	Jugale	Intersection of temporal and frontal processes of the zygomatic bone
5,6	Frontomalare ant.	Most anterior point on the frontozygomatic suture
7,8	Zygoorbitale	Intersection of lower margin of the orbit and zygomaticomaxillar suture
9,10	Zygomaxilare	Most inferior point on the zygomaticomaxillar suture
11	Nasion	Most anterior point of the nasofrontal suture in the mid-sagittal plane
12	Rhinion	Midline point at inferior free end of the internasal suture
13,14	Alare	Most lateral point at the margin of the nasal aperture
15	Subspinale	Lowest point on the inferior margin of the nasal aperture in the mid-sagittal plane

16,17	Dacryon	Point on the medial border of the orbit where frontal, lacrimal and maxilla meet
18	Alveolar	Most anterior point on the alveolar portion of the premaxilla between the upper central incisors
19,20	-	Internal side of the last teeth
21,22	-	Root of maxillary arch
23,24	Zygotemporal suture R	Suture between zygomatic and temporal bones (superior and inferior, right)
25,26	Zygotemporal suture L	Suture between zygomatic and temporal bones (superior and inferior, left)
27	Incisive foramen	Most internal point of the incisive foramen
28	Staurion	Intersection of the sut. palatina mediana and sut. palatina transversa
29	Alveolon	Intersection of the midline of the palate and the line connecting the posterior borders of the alveolar crests
30,31	-	Inferolateral choanal corner
32,33	-	Superior margin of choana
34,35	Superior orbital fissure	Most external point of the superior fissure

36,37	Inferior orbital fissure	Most external point of the inferior orbital fissure
38,39	-	The point where the sagittal plane translated to the most external point of the frontal process of the zygomatic bone meets the coronal suture
40,41	Pterion	The region where the coronal suture meets the sphenoid bone
42,43	Frontotemporale	On the shortest distance between the temporal lines on the orbital torus
44,45	Frontomalare post.	Most posterior point on the frontozygomatic suture
46,47	-	Most inferior point on the zygomatic process
48,49	Orbital superior	Highest point on the orbital outline
50,51	-	Lateral point of the spheno-occipital synchondrosis
52	Basion	Anterior mid-sagittal margin of the foramen magnum
53,54	-	Most lateral point at the margin of the foramen magnum

55	Opisthion	Posterior mid-sagittal margin of the foramen magnum
56,57	Porion	Upper margin of each ear canal
58,59	PM points	Most posterior point on the mandibular body
60,61,62,63,64,65	Incisors, canines,molars	External alveolus at I2, C, last visible tooth
66	Opisthocranion	The most posterior point of the occipital bone along the midsagittal plane
67,68	Asterion	Where the lambdoid, parieto-mastoid, and occipito-mastoid sutures meet
69	Lambda	Point of meeting of the sagittal and the lambdoid suture
70	Inion	Midpoint of the external occipital protuberance
71,72,73,74	Posterior zygomatic root	Superior and inferior limits of the most posterior part of the zygomatic arch superior and inferior (right and left)
75,76	Mastoid process	Lower point of the mastoid process

77,78	Nasal floor	Antero-posterior midpoint along the nasal floor (Left,Right)
79,80,81,82,83,84	Occipital condyles	Most superior, external and inferior margin of the occipital condyles
85	Sella turcica	Central midpoint on the sella turcica
86,87	Infraorbital foramen	
88,89	P2	External alveolus at P2

Table S4. Landmark configuration applied to the modern human ontogenetic sample.

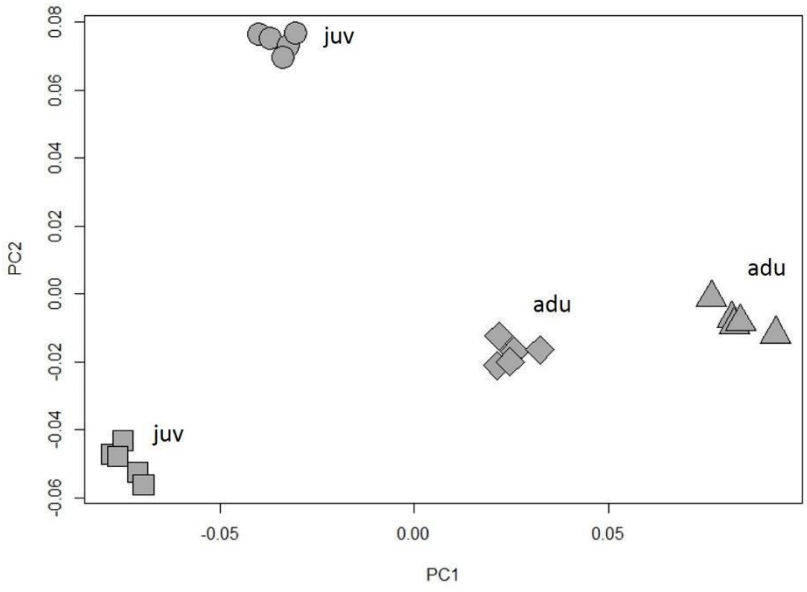

Figure S2. Principal Component Analysis of four modern human specimens landmarked in 5 different occasions showing the intraobserver error.

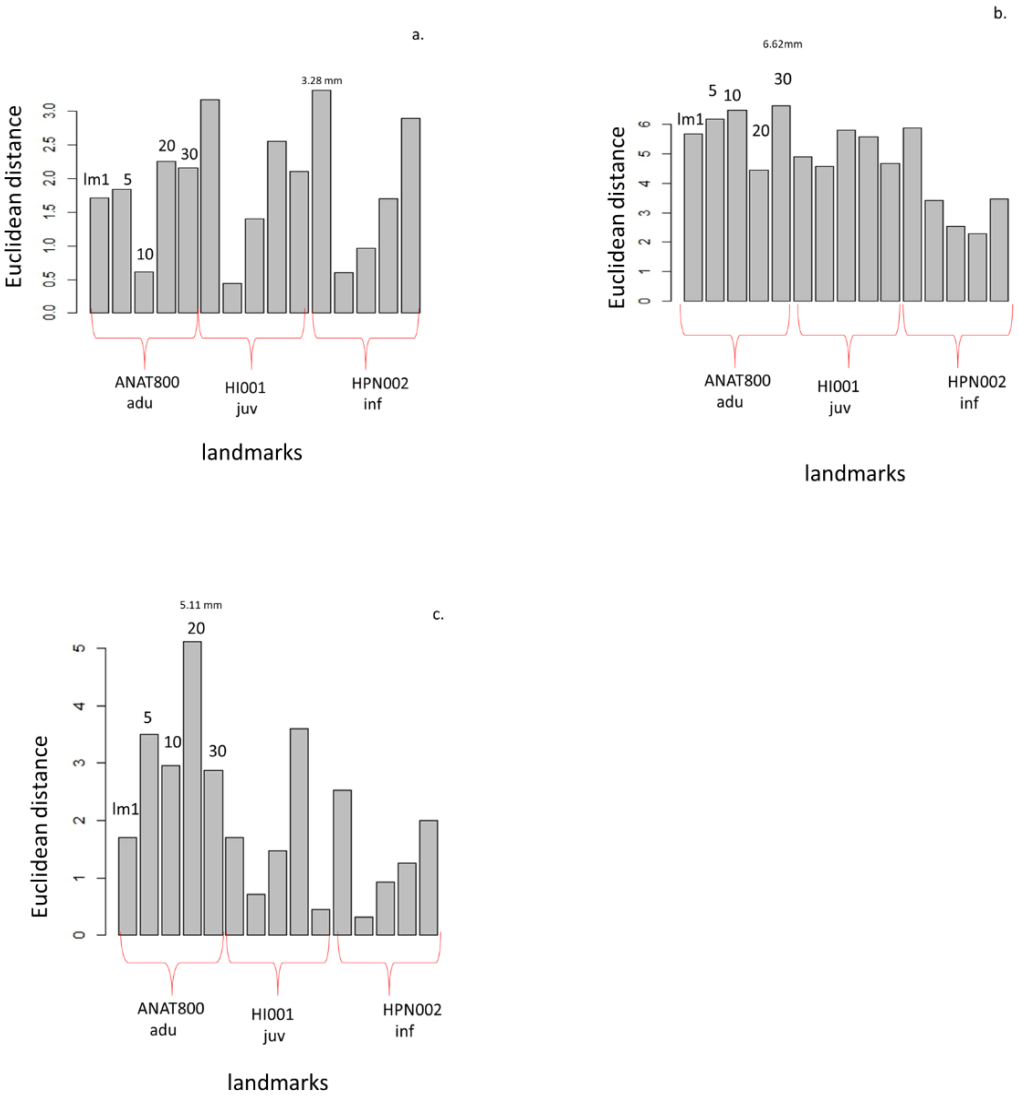

Figure S3. Accuracy test to compare the performance of TPS (a), geometric mean substitution (b) and regression (c). Five randomly chosen landmarks (lm 1, 5, 10, 20, 30) were removed from three specimens (ANAT800, HI001, HPN002) and estimated using the three methods. Then, the euclidean distance (in mm) between each of the original landmarks and the estimated ones was calculated for each individual and plotted.

6.0 Bibliography

Ackermann, R.R., 2002. Patterns of covariation in the hominoid craniofacial skeleton: implications for paleoanthropological models. *Journal of Human Evolution*, 43(2), pp.167-187.

Ackermann, R.R., 2005. Ontogenetic integration of the hominoid face. *Journal of Human Evolution*, *48*(2), pp.175-197.

Ackermann, R.R., 2009. Morphological integration and the interpretation of fossil hominin diversity. *Evolutionary Biology*, 36(1), pp.149-156.

Ackermann, R.R. and Cheverud, J.M., 2004. Detecting genetic drift versus selection in human evolution. *Proceedings of the National Academy of Sciences*, *101*(52), pp.17946-17951.

Ackermann, R.R. and Krovitz, G.E., 2002. Common patterns of facial ontogeny in the hominid lineage. *The Anatomical Record: Advances in Integrative Anatomy and Evolutionary Biology*, 269(3), pp.142-147.

Adams, D. C., 2016. Evaluating modularity in morphometric data: challenges with the RV coefficient and a new test measure. *Methods in Ecology and Evolution*, 7(5), 565-572.

Adams, D.C., Rohlf, F.J. and Slice, D.E., 2004. Geometric morphometrics: ten years of progress following the 'revolution'. *Italian Journal of Zoology*, *71*(1), pp.5-16.

Adibelli, Z.H., Songu, M. and Adibelli, H., 2011. Paranasal sinus development in children: A magnetic resonance imaging analysis. *American Journal of Rhinology & Allergy*, *25*(1), pp.30-35.

Aiello, L.C. and Andrews, P., 2000. The Australopithecines in review. *Human Evolution*, *15*(1-2), pp.17-38.

Aiello, L. and Dean, C., 1990. *An introduction to human evolutionary anatomy*. 1st ed. Cambridge: Academic Press.

Al Dayeh, A.A., Rafferty, K.L., Egbert, M. and Herring, S.W., 2013. Real-time monitoring of the growth of the nasal septal cartilage and the nasofrontal suture. *American Journal of Orthodontics and Dentofacial Orthopedics*, *143*(6), pp.773-783.

Alfaqeeh, S.A., Gaete, M. and Tucker, A.S., 2013. Interactions of the tooth and bone during development. *Journal of Dental Research*, *92*(12), pp.1129-1135.

Allen, M.P., 1997. Partial regression and residualized variables. *Understanding Regression Analysis*, pp.86-90.

AlQahtani, S.J., Hector, M.P. and Liversidge, H.M., 2010. Brief communication: the London atlas of human tooth development and eruption. *American Journal of Physical Anthropology*, *142*(3), pp.481-490.

Anton, S.C., 1989. Intentional cranial vault deformation and induced changes of the cranial base and face. *American Journal of Physical Anthropology*, *79*(2), pp.253-267.

Anzelmo, M., Ventrice, F., Barbeito-Andrés, J., Pucciarelli, H.M. and Sardi, M.L., 2015. Ontogenetic changes in cranial vault thickness in a modern sample of *Homo sapiens*. *American Journal of Human Biology*, 27(4), pp.475-485.

Arat, Z.M., Türkkahraman, H., English, J.D., Gallerano, R.L. and Boley, J.C., 2010. Longitudinal growth changes of the cranial base from puberty to adulthood: A Comparison of Different Superimposition Methods. *The Angle Orthodontist*, *80*(4), pp.725-732.

Arbour, J.H. and Brown, C.M., 2014. Incomplete specimens in geometric morphometric analyses. *Methods in Ecology and Evolution*, *5*(1), pp.16-26.

Baab, K.L., 2013. The impact of superimposition choice in geometric morphometric approaches to morphological integration. *Journal of Human Evolution*, *65*, pp.689-92.

Babula, W.J., Smiley, G.R. and Dixon, A.D., 1970. The role of the cartilaginous nasal septum in midfacial growth. *American Journal of Orthodontics and Dentofacial Orthopedics*, *58*(3), pp.250-263.

Barbeito-Andrés, J., Anzelmo, M., Ventrice, F., Pucciarelli, H.M. and Sardi, M.L., 2016. Morphological integration of the orbital region in a human ontogenetic sample. *The Anatomical Record: Advances in Integrative Anatomy and Evolutionary Biology*, *299*(1), pp.70-80.

Barbeito-Andrés, J., Ventrice, F., Anzelmo, M., Pucciarelli, H.M. and Sardi, M.L., 2015. Developmental covariation of human vault and base throughout postnatal ontogeny. *Annals of Anatomy-Anatomischer Anzeiger*, *197*, pp.59-66.

Barrett, J.F. and Keat, N., 2004. Artifacts in CT: recognition and avoidance. *Radiographics*, *24*(6), pp.1679-1691.

Bastir, M., 2008. A systems-model for the morphological analysis of integration and modularity in human craniofacial evolution. *Journal of Anthropological Science*, *86*, pp.37-58.

Bastir, M. and Rosas, A., 2004. Facial heights: evolutionary relevance of postnatal ontogeny for facial orientation and skull morphology in humans and chimpanzees. *Journal of Human Evolution*, 47(5), pp.359-381.

Bastir, M. and Rosas, A., 2005. Hierarchical nature of morphological integration and modularity in the human posterior face. *American Journal of Physical Anthropology*, *128*(1), pp.26-34.

Bastir, M. and Rosas, A., 2006. Correlated variation between the lateral basicranium and the face: a geometric morphometric study in different human groups. *Archives of Oral Biology*, *51*(9), pp.814-824.

Bastir, M. and Rosas, A., 2009. Mosaic evolution of the basicranium in *Homo* and its relation to modular development. *Evolutionary Biology*, 36(1), pp.57-70.

Bastir, M. and Rosas, A., 2016. Cranial base topology and basic trends in the facial evolution of *Homo*. *Journal of Human Evolution*, *91*, pp.26-35.

Bastir, M., Martínez, D.G., Recheis, W., Barash, A., Coquerelle, M., Rios, L., Peña-Melián, Á., Río, F.G. and O'Higgins, P., 2013. Differential growth and development of the upper and lower human thorax. *PloS one*, *8*(9).

Bastir, M., O'Higgins, P. and Rosas, A., 2007. Facial ontogeny in Neanderthals and modern humans. *Proceedings of the Royal Society B: Biological Sciences*, *274*(1614), pp.1125-1132.

Bastir, M., Rosas, A. and Kuroe, K., 2004. Petrosal orientation and mandibular ramus breadth: Evidence for an integrated petroso-mandibular developmental unit. *American Journal of Physical Anthropology*, 123(4), pp.340-350.

Bastir, M., Rosas, A. and O'Higgins, P., 2006. Craniofacial levels and the morphological maturation of the human skull. *Journal of Anatomy*, *209*(5), pp.637-654.

Bastir, M., Rosas, A. and Sheets, H.D., 2005. The morphological integration of the hominoid skull: a partial least squares and PC analysis with implications for European Middle Pleistocene mandibular variation. In Slice, D. (ed.), *Modern Morphometrics in Physical Anthropology*, pp. 265-284. Boston: Springer.

Bastir, M., Rosas, A., Lieberman, D.E. and O'Higgins, P., 2008. Middle cranial fossa anatomy and the origin of modern humans. *The Anatomical Record: Advances in Integrative Anatomy and Evolutionary Biology*, *291*(2), pp.130-140.

Bastir, M., Rosas, A., Stringer, C., Cuétara, J.M., Kruszynski, R., Weber, G.W., Ross, C.F. and Ravosa, M.J., 2010. Effects of brain and facial size on basicranial form in human and primate evolution. *Journal of Human Evolution*, *58*(5), pp.424-431.

Bates, K.T., Falkingham, P.L., Rarity, F., Hodgetts, D., Purslow, A. and Manning, P.L., 2010. Application of high-resolution laser scanning and photogrammetric techniques to data acquisition, analysis and interpretation in palaeontology. *The International Archives of the Photogrammetry, Remote Sensing and Spatial Information Sciences*, *38*(6), pp. 230-245.

Baume, L.J., 1961. The postnatal growth activity of the nasal cartilage septum. *Helvetica Odontologica Acta*, *5*, pp.9.

Baykul, T., Doğru, H., Yasan, H. and Aksoy, M.Ç., 2006. Clinical impact of ectopic teeth in the maxillary sinus. *Auris Nasus Larynx*, *33*(3), pp.277-281.

Behrents, R.G., 1975. *Growth in the aging craniofacial skeleton*. 1st ed. Michigan: University of Michigan.

Berger, A.J. and Kahn, D., 2012. Growth and development of the orbit. *Oral and Maxillofacial Surgery Clinics*, *24*(4), pp.545-555.

Bienvenu, T., Guy, F., Coudyzer, W., Gilissen, E., Roualdès, G., Vignaud, P. and Brunet, M., 2011. Assessing endocranial variations in great apes and humans using 3D data from virtual endocasts. *American Journal of Physical Anthropology*, *145*(2), pp.231-246.

Blackith, R.E. and Reyment, R.A., 1971. *Multivariate morphometrics*. London-New York: Academic Press.

Blaney, S.P.A., 1990. Why paranasal sinuses? *The Journal of Laryngology & Otology*, *104*(9), pp.690-693.

Blanton, P.L. and Biggs, N.L., 1969. Eighteen hundred years of controversy: the paranasal sinuses. *American Journal of Anatomy*, *124*(2), pp.135-147.

Bolk, L., 1909. On the position and displacement of the foramen magnum in the primates. *Verh Akad Wet Amst*, 12, pp.362-377.

Bookstein, F.L., 1982. Foundations of morphometrics. *Annual Review of Ecology and Systematics*, *13*(1), pp.451-470.

Bookstein, F.L., 1989. Principal warps: Thin-plate splines and the decomposition of deformations. *Transactions on Pattern Analysis and Machine Intelligence*, *11*(6), pp.567-585.

Bookstein, F.L., 1991. Thin-plate splines and the atlas problem for biomedical images. In *Biennial International Conference on Information Processing in Medical Imaging*, pp. 326-342. Berlin: Springer.

Bookstein, F.L., 1996a. Combining the tools of geometric morphometrics. *Advances in Morphometrics*, 284(1), pp. 131-151.

Bookstein, F.L., 1996b. Landmark methods for forms without landmarks: localizing group differences in outline shape. In *Proceedings of the Workshop on Mathematical Methods in Biomedical Image Analysis*, pp. 279-289. San Francisco: IEEE.

Bookstein, F.L., 1997. *Morphometric tools for landmark data: geometry and biology*. 1st ed. Cambridge: Cambridge University Press.

Bookstein, F.L., 1998. A hundred years of morphometrics. *Acta Zoologica Academiae Scientiarum Hungaricae*, *44*(1-2), pp.7-59.

Bookstein, F.L., Gunz, P., Mitteroecker, P., Prossinger, H., Schaefer, K. and Seidler, H., 2003. Cranial integration in Homo: singular warps analysis of the midsagittal plane in ontogeny and evolution. *Journal of Human Evolution*, *44*(2), pp.167-187.

Bookstein, F.L., Sampson, P.D., Streissguth, A.P. and Connor, P.D., 2001. Geometric morphometrics of corpus callosum and subcortical structures in the fetal-alcohol-affected brain. *Teratology*, *64*(1), pp.4-32.

Bookstein, F.L., Schäfer, K., Prossinger, H., Seidler, H., Fieder, M., Stringer, C., Weber, G.W., Arsuaga, J.L., Slice, D.E., Rohlf, F.J. and Recheis, W., 1999. Comparing frontal cranial profiles in archaic and modern *Homo* by morphometric analysis. *The Anatomical Record: Advances in Integrative Anatomy and Evolutionary Biology*, *257*(6), pp.217-224.

Bourne, R., 2010. *Fundamentals of digital imaging in medicine*. 1st ed. Berlin: Springer Science & Business Media.

Brenner, D.J. and Hall, E.J., 2007. Computed tomography—an increasing source of radiation exposure. *New England Journal of Medicine*, *357*(22), pp.2277-2284.

Broadbent, B.H., Broadbent, B.H. and Golden, W.H., 1975. *Bolton Standards of Dentofacial Developmental Growth (p. 47)*. St. Louis: Mosby.

Brodie, A.G., 1941. On the growth pattern of the human head. From the third month to the eighth year of life. *American Journal of Anatomy*, 68(2), pp.209-262.

Bromage, T.G., 1989. Ontogeny of the early hominid face. *Journal of Human Evolution*, 18(8), pp.751-773.

Brooker, C., 2009. *Mosby's Dictionary of Medicine, Nursing and Health Professions UK Edition E-Book*. London: Elsevier Health Sciences.

Brown, C.M., Arbour, J.H. and Jackson, D.A., 2012. Testing of the effect of missing data estimation and distribution in morphometric multivariate data analyses. *Systematic Biology*, *61*(6), pp.941-954.

Bruner, E., 2007. Cranial shape and size variation in human evolution: structural and functional perspectives. *Child's Nervous System*, *23*(12), pp.1357-1365.

Bruner, E., 2010. Morphological differences in the parietal lobes within the human genus: a neurofunctional perspective. *Current Anthropology*, 51(S1), pp.S77-S88.

Bruner, E., 2015. Functional craniology and brain evolution. In Bruner, E. (ed.), *Human Paleoneurology*, pp. 57-94. Cham: Springer.

Bruner, E., Amano, H., de la Cuétara, J.M. and Ogihara, N., 2015. The brain and the braincase: a spatial analysis on the midsagittal profile in adult humans. *Journal of Anatomy*, *227*(3), pp.268-276.

Bruner, E. and Jeffery, N., 2007. Extracting functional, phylogenetic and structural data from the subcortical brain: an exploratory geometric morphometric survey. *Journal of Anthropological Science*, *85*, pp.125-138.

Bruner, E. and Manzi, G., 2006. Digital tools for the preservation of the human fossil heritage: Ceprano, Saccopastore, and other case studies. *Human Evolution*, *21*(1), pp.33-44.

Bruner, E. and Ripani, M., 2008. A quantitative and descriptive approach to morphological variation of the endocranial base in modern humans. *American Journal of Physical Anthropology*, 137(1), pp.30-40.

Buck, L.T., De Groote, I., Hamada, Y. and Stock, J.T., 2018. Humans preserve non-human primate pattern of climatic adaptation. *Quaternary Science Reviews*, *192*, pp.149-166.

Bugaighis, I., O'higgins, P., Tiddeman, B., Mattick, C., Ben Ali, O. and Hobson, R., 2010. Three-dimensional geometric morphometrics applied to the study of children with cleft lip and/or palate from the North East of England. *The European Journal of Orthodontics*, *32*(5), pp.514-521.

Bullmore, E., Horwitz, B., Honey, G., Brammer, M., Williams, S. and Sharma, T., 2000. How good is good enough in path analysis of fMRI data?. *NeuroImage*, 11(4), pp.289-301.

Bulygina, E., Mitteroecker, P. and Aiello, L., 2006. Ontogeny of facial dimorphism and patterns of individual development within one human population. *American Journal of Physical Anthropology*, *131*(3), pp.432-443.

Burns, K.R., 2013. *Forensic anthropology training manual*. 1st ed. London: Routledge.

Buschang, P.H., Baume, R.M. and Nass, G.G., 1983. A craniofacial growth maturity gradient for males and females between 4 and 16 years of age. *American Journal of Physical Anthropology*, 61(3), pp.373-381.

Butaric, L.N., 2015. Differential scaling patterns in maxillary sinus volume and nasal cavity breadth among modern humans. *The Anatomical Record: Advances in Integrative Anatomy and Evolutionary Biology*, *298*(10), pp.1710-1721.

Butaric, L.N. and Maddux, S.D., 2016. Morphological covariation between the maxillary sinus and midfacial skeleton among sub-Saharan and circumpolar modern humans. *American Journal of Physical Anthropology*, *160*(3), pp.483-497.

Buzi, C., Micarelli, I., Profico, A., Conti, J., Grassetti, R., Cristiano, W., Di Vincenzo, F., Tafuri, M.A. and Manzi, G., 2018. Measuring the shape: performance evaluation of a photogrammetry improvement applied to the Neanderthal skull Saccopastore 1. *Acta Imeko*, *7*(3), pp.79-85.

Cameron, D.W. and Groves, C.P., 2004. *Bones, stones and molecules:" Out of Africa" and human origins*. 1st ed. Cambridge: Academic Press.

Campbell, R. and Willmore, K.E., 2009. Morphological integration at 50: patterns and processes of integration in biological anthropology. *Evolutionary Biology*, 36(1), pp.1-4.

Caparros, M., Ruíz, C.B., Moigne, A.M. and Bohorquez, A.M., 2012. Did Neanderthals and carnivores compete for animal nutritional resources in the surroundings of the cave of Zafarraya?. *Journal of Taphonomy*, *10*.

Cardini, A., 2019. Integration and modularity in Procrustes shape data: is there a risk of spurious results?. *Evolutionary Biology*, *46*(1), pp.90-105.

Cardini, A. and Elton, S., 2008. Does the skull carry a phylogenetic signal? Evolution and modularity in the guenons. *Biological Journal of the Linnean Society*, *93*(4), pp.813-834.

Cardini, A. and Polly, P.D., 2013. Larger mammals have longer faces because of size-related constraints on skull form. *Nature Communications*, 4, p.2458.

Carlson, K.B., De Ruiter, D.J., DeWitt, T.J., McNulty, K.P., Carlson, K.J., Tafforeau, P. and Berger, L.R., 2016. Developmental simulation of the adult cranial morphology of Australopithecus sediba. *South African Journal of Science*, *112*(7-8), pp.1-9.

Carr, L.M., 1962. Eruption ages of permanent teeth. *Australian Dental Journal*, *7*(5), pp.367-373.

Chaiyasate, S., Baron, I. and Clement, P., 2007. Analysis of paranasal sinus development and anatomical variations: a CT genetic study in twins. *Clinical Otolaryngology*, *32*(2), pp.93-97.

Charsoula, A., Kaitartzis, C., Katsiba, D., Papadimitriou, A., Smponia, A., Xatzipanagiotidis, P. and Arvaniti, M., 2011, March. The ossification process of the occipital bone and normal variants: evaluation by Computed Tomography (CT). *European Congress of Radiology*.

Chatzigianni, A. and Halazonetis, D.J., 2009. Geometric morphometric evaluation of cervical vertebrae shape and its relationship to skeletal maturation. *American Journal of Orthodontics and Dentofacial Orthopedics*, *136*(4), pp.481-e1.

Chernoff, B. and Magwene, P.M., 1999. Morphological integration. *Morphological Integration*, pp.319-353.

Cheverud, J.M., 1982. Phenotypic, genetic, and environmental morphological integration in the cranium. *Evolution*, pp.499-516.

Cheverud, J.M., 1996. Developmental integration and the evolution of pleiotropy. *American Zoologist*, 36(1), pp.44-50.

Cheverud, J.M., Kohn, L.A., Konigsberg, L.W. and Leigh, S.R., 1992. Effects of fronto-occipital artificial cranial vault modification on the cranial base and face. *American Journal of Physical Anthropology*, *88*(3), pp.323-345.

Chhabra, A., Thawait, G.K., Soldatos, T., Thakkar, R.S., Del Grande, F., Chalian, M. and Carrino, J.A., 2013. High-resolution 3T MR neurography of the brachial plexus and its branches, with emphasis on 3D imaging. *American Journal of Neuroradiology*, *34*(3), pp.486-497.

Churchill, S.E., Shackelford, L.L., Georgi, J.N. and Black, M.T., 2004. Morphological variation and airflow dynamics in the human nose. *American Journal of Human Biology*, *16*(6), pp.625-638.

Clarke, R.J., 1977. A juvenile cranium and some adult teeth of early *Homo* from Swartkrant, Transvaal. *South African Journal of Science*, *73*(2), pp.46.

Clement, A.F., Hillson, S.W. and Aiello, L.C., 2012. Tooth wear, Neanderthal facial morphology and the anterior dental loading hypothesis. *Journal of Human Evolution*, *62*(3), pp.367-376.

Cobb, S.N. and O'Higgins, P., 2004. Hominins do not share a common postnatal facial ontogenetic shape trajectory. *Journal of Experimental Zoology Part B: Molecular and Developmental Evolution*, *302*(3), pp.302-321.

Collado, F., Bombard, A., Li, V.S., Juliard, K. and Weiner, Z., 2004. Ethnic variation of fetal nasal bone length between 11-14 weeks' gestation. *American Journal of Obstetrics & Gynecology*, *191*(6), pp.S146.

Conith, A. J., Lam, D. T., & Albertson, R. C., 2019. Muscle-induced loading as an important source of variation in craniofacial skeletal shape. *Genesis*, *57*(1), e23263.

Constantino, P.J., 2013. The “robust” australopiths. *Nature Education Knowledge*, *4*(1), p.592.

Couette, S. and White, J., 2010. 3D geometric morphometrics and missing-data. Can extant taxa give clues for the analysis of fossil primates?. *Comptes Rendus Palevol*, *9*(6-7), pp.423-433.

Couly, G., Creuzet, S., Bennaceur, S., Vincent, C. and Le Douarin, N.M., 2002. Interactions between Hox-negative cephalic neural crest cells and the foregut endoderm in patterning the facial skeleton in the vertebrate head. *Development*, 129(4), pp.1061-1073.

Cross, D.L. and McDonald, J.P., 2000. Effect of rapid maxillary expansion on skeletal, dental, and nasal structures: a postero-anterior cephalometric study. *The European Journal of Orthodontics*, 22(5), pp.519-528.

Cunningham, J.A., Rahman, I.A., Lautenschlager, S., Rayfield, E.J. and Donoghue, P.C., 2014. A virtual world of paleontology. *Trends in Ecology & Evolution*, *29*(6), pp.347-357.

Cupero, T.M., Middleton, C.E. and Silva, A.B., 2001. Effects of functional septoplasty on the facial growth of ferrets. A*rchives of Otolaryngology–Head & Neck Surgery*, 127(11), pp.1367-1369.

Davis, W.E., Templer, J. and Parsons, D.S., 1996. Anatomy of the paranasal sinuses. *Otolaryngologic Clinics of North America*, *29*(1), pp.57-74.

De Azevedo, S., González, M.F., Cintas, C., Ramallo, V., Quinto-Sánchez, M., Márquez, F., Hünemeier, T., Paschetta, C., Ruderman, A., Navarro, P. and Pazos, B.A., 2017. Nasal airflow simulations suggest convergent adaptation in Neanderthals and modern humans. *Proceedings of the National Academy of Sciences*, *114*(47), pp.12442-12447.

Dean, J.A. and Turner, E.G., 2016. Eruption of the teeth: local, systemic, and congenital factors that influence the process. In Dolan J., and Dumas J., (ed.), *McDonald and Avery's Dentistry for the Child and Adolescent*, pp. 349-374. Maryland: Mosby.

De Groote, M.A. and Fang, F.C., 1995. NO inhibitions: antimicrobial properties of nitric oxide. *Clinical Infectious Diseases*, 21, pp.S162-S165.

Delaire, J. and Precious, D., 1987. Interaction of the development of the nasal septum, the nasal pyramid and the face. *International Journal of Pediatric Otorhinolaryngology*, *12*(3), pp.311-326.

Dellepiane, M., Dell'Unto, N., Callieri, M., Lindgren, S. and Scopigno, R., 2013. Archeological excavation monitoring using dense stereo matching techniques. *Journal of Cultural Heritage*, *14*(3), pp.201-210.

Demes, B., 1987. Another look at an old face: biomechanics of the Neandertal facial skeleton reconsidered. *Journal of Human Evolution*, *16*(3), pp.297-303.

de Oliveira, F.B., Porto, A. and Marroig, G., 2009. Covariance structure in the skull of Catarrhini: a case of pattern stasis and magnitude evolution. *Journal of Human Evolution*, 56(4), pp.417-430.

Diewert, V.M., 1985. Development of human craniofacial morphology during the late embryonic and early fetal periods. *American Journal of Orthodontics*, *88*(1), pp.64-76.

Doi, K., 2007. Computer-aided diagnosis in medical imaging: historical review, current status and future potential. *Computerized medical imaging and graphics*, *31*(4-5), pp.198-211.

Drake, A.G. and Klingenberg, C.P., 2008. The pace of morphological change: historical transformation of skull shape in St Bernard dogs. *Proceedings of the Royal Society B: Biological Sciences*, *275*(1630), pp.71-76.

Dryden, I.L. and Mardia, K.V., 1992. Size and shape analysis of landmark data. *Biometrika*, *79*(1), pp.57-68.

Dryden, I.L. and Mardia, K.V., 1993. Multivariate shape analysis. *Sankhyā: The Indian Journal of Statistics, Series A*, pp.460-480.

Dryden, I.L. and Mardia, K.V., 1998. *Statistical analysis of shape.* 1st ed. Chichester: Wiley.

Duncan, O. D.,1966. Path analysis: Sociological examples. *American Journal of Sociology*, *72*(1), pp.1-16.

Duterloo, H.S. and Enlow, D.H., 1970. A comparative study of cranial growth in *Homo* and *Macaca*. *American Journal of Anatomy*, *127*(4), pp.357-367.

Enlow, D.H., 1966. A comparative study of facial growth in *Homo* and *Macaca*. *American Journal of Physical Anthropology*, *24*(3), pp.293-307.

Enlow, D.H., 1975. *The plan of the human face. Handbook of Facial Growth*. 1st ed. Philadelphia: WB Saunders Company.

Enlow, D.H., 1990. *Facial growth*. 1st ed. Philadelphia: WB Saunders Company.

Enlow, D.H. and Hans, M.G., 1996. *Essentials of facial growth*. 1st ed. Philadelphia: WB Saunders Company.

Enlow, D.H. and Moyers, R.E., 1971. 1 Growth and Architecture of the Face. *The Journal of the American Dental Association*, *82*(4), pp.763-774.

Enlow, D.H. and Moyers, R.E., 1982. *Handbook of facial growth*. 1st ed. Philadelphia: WB Saunders Company.

Erdur, O., Ucar, F.I., Sekerci, A.E., Celikoglu, M. and Buyuk, S.K., 2015. Maxillary sinus volumes of patients with unilateral cleft lip and palate. International journal of pediatric otorhinolaryngology, 79(10), pp.1741-1744.

Escaravage Jr, G.K. and Dutton, J.J., 2013. Age-related changes in the pediatric human orbit on CT. *Ophthalmic Plastic & Reconstructive Surgery*, 29(3), pp.150-156.

Esteve-Altava, B., Diogo, R., Smith, C., Boughner, J. C., & Rasskin-Gutman, D., 2015. Anatomical networks reveal the musculoskeletal modularity of the human head. *Scientific Reports*, *5*, pp.8298.

Esteve-Altava, B., & Rasskin-Gutman, D., 2014. Beyond the functional matrix hypothesis: a network null model of human skull growth for the formation of bone articulations. Journal of anatomy, 225(3), 306-316.

Evans, C., Marton, T., Rutter, S., Anumba, D.O., Whitby, E.H. and Cohen, M.C., 2009. Cranial vault defects: the description of three cases that illustrate a spectrum of anomalies. *Pediatric and Developmental Pathology*, 12(2), pp.96-102.

Evin, A., Souter, T., Hulme-Beaman, A., Ameen, C., Allen, R., Viacava, P., Larson, G., Cucchi, T. and Dobney, K., 2016. The use of close-range photogrammetry in zooarchaeology: Creating accurate 3D models of wolf crania to study dog domestication. *Journal of Archaeological Science: Reports*, *9*, pp.87-93.

Evteev, A.A. and Grosheva, A.N., 2019. Nasal cavity and maxillary sinuses form variation among modern humans of Asian descent. *American Journal of Physical Anthropology,* 169(3), pp.513-525.

Evteev, A., Anikin, A. and Satanin, L., 2018. Midfacial growth patterns in males from newborn to 5 years old based on computed tomography. *American Journal of Human Biology*, *30*(4), p.e23132.

Evteev, A., Cardini, A.L., Morozova, I. and O'Higgins, P., 2014. Extreme climate, rather than population history, explains mid-facial morphology of Northern Asians. *American Journal of Physical Anthropology*, *153*(3), pp.449-462.

Falkingham, P.L., 2012. Acquisition of high resolution three-dimensional models using free, open-source, photogrammetric software. *Palaeontologia Electronica*, *15*(1), p.15.

Farkas, L.G., Posnick, J.C., Hreczko, T.M. and Pron, G.E., 1992. Growth patterns in the orbital region: a morphometric study. *The Cleft Palate-Craniofacial Journal*, 29(4), pp.315-318.

Fehrenbach, M.J. and Herring, S.W., 1997. Spread of dental infection. *Practical Hygiene*, *6*, pp.13-19.

Feldkamp, L.A., Goldstein, S.A., Parfitt, M.A., Jesion, G. and Kleerekoper, M., 1989. The direct examination of three-dimensional bone architecture *in vitro* by computed tomography. *Journal of Bone and Mineral Research*, *4*(1), pp.3-11.

Ferros, I., Mora, M.J., Obeso, I.F., Jimenez, P. and Martinez-Insua, A., 2015. The nasomaxillary complex and the cranial base in artificial cranial deformation: relationships from a geometric morphometric study. *European Journal of Orthodontics*, *37*(4), pp.403-411.

Franciscus, R.G., 1999. Neandertal nasal structures and upper respiratory tract "specialization". *Proceedings of the National Academy of Sciences*, 96(4), pp.1805-1809.

Franciscus, R.G., 2002. Neanderthals. In Pagel, M. (ed.), *Encyclopedia of Evolution*. Oxford: Oxford University Press, pp. 493e497.

Freidline, S.E., Gunz, P., Harvati, K. and Hublin, J.J., 2012. Middle Pleistocene human facial morphology in an evolutionary and developmental context. *Journal of Human Evolution*, *63*(5), pp.723-740.

Furuta, M., 2001. Measurement of orbital volume by computed tomography: especially on the growth of the orbit. Japanese journal of ophthalmology, 45(6), pp.600-606.

Gannon, P.J., Doyle, W.J., Ganjian, E., Marquez, S., Gnoy, A., Gabrielle, H.S. and Lawson, W., 1997. Maxillary sinus mucosal blood flow during nasal vs tracheal respiration. *Archives of Otolaryngology–Head & Neck Surgery*, *123*(12), pp.1336-1340.

Garib, D.G., Yatabe, M.S., Ozawa, T.O. and da Silva Filho, O.G., 2010. Alveolar bone morphology under the perspective of the computed tomography: defining the biological limits of tooth movement. *Dental Press Journal of Orthodontics*, *15*(5), pp.192-205.

German, R.Z., 2004. The ontogeny of sexual dimorphism: the implications of longitudinal vs. cross-sectional data for studying heterochrony in mammals. *Cambridge Studies in Biological and Evolutionary Anthropology*, pp.11-23.

Gharaibeh, W.S., Rohlf, F.J., Slice, D.E. and DeLisi, L.E., 2000. A geometric morphometric assessment of change in midline brain structural shape following a first episode of schizophrenia. *Biological psychiatry*, *48*(5), pp.398-405.

Gkantidis, N. and Halazonetis, D.J., 2011. Morphological integration between the cranial base and the face in children and adults. *Journal of Anatomy*, *218*(4), pp.426-438.

Godinho, R.M. and O'Higgins, P., 2018. The biomechanical significance of the frontal sinus in Kabwe 1 (*Homo heidelbergensis*). *Journal of Human Evolution*, *114*, pp.141-153.

Godinho, R.M., Spikins, P. and O'Higgins, P., 2018. Supraorbital morphology and social dynamics in human evolution. *Nature Ecology & Evolution*, *2*(6), pp.956-961.

Goergen, M.J., Holton, N.E. and Grünheid, T., 2017. Morphological interaction between the nasal septum and nasofacial skeleton during human ontogeny. *Journal of Anatomy*, *230*(5), pp.689-700.

Goel, N., Yadav, A. and Singh, B.M., 2016, November. Medical image processing: a review. In *2016 Second International Innovative Applications of Computational Intelligence on Power, Energy and Controls with their Impact on Humanity (CIPECH)*, pp. 57-62.

Goerres, G.W., Hany, T.F., Kamel, E., von Schulthess, G.K. and Buck, A., 2002. Head and neck imaging with PET and PET/CT: artefacts from dental metallic implants. *European Journal of Nuclear Medicine and Molecular Imaging*, *29*(3), pp.367-370.

González-José, R., Van der Molen, S., González-Pérez, E. and Hernandez, M., 2004. Patterns of phenotypic covariation and correlation in modern humans as viewed from morphological integration. *American Journal of Physical Anthropology*, *123*(1), pp.69-77.

Gonzalez, P.N., Perez, S.I. and Bernal, V., 2010. Ontogeny of robusticity of craniofacial traits in modern humans: a study of South American populations. *American Journal of Physical Anthropology*, 142(3), pp.367-379.

Goodall, C., 1991. Procrustes methods in the statistical analysis of shape. *Journal of the Royal Statistical Society: Series B (Methodological)*, *53*(2), pp.285-321.

Gorza, L. and Thevissen, P., 2019. Prevalence of morphological variations of the maxillary sinus in panoramic radiographs of caucasian individuals. In *71 AAFS Annual Scientific Meeting*, pp. 706-706, Baltimore.

Goswami, A., and Polly, P. D.,2010. Methods for studying morphological integration and modularity. *The Paleontological Society Papers*, *16*, pp.213-243.

Gould, S.J. and Lewontin, R.C., 1979. The spandrels of San Marco and the Panglossian paradigm: a critique of the adaptationist programme. *Proceedings of the Royal Society of London. Series B. Biological Sciences*, *205*(1161), pp.581-598.

Gower, J.C., 1975. Generalized procrustes analysis. *Psychometrika*, *40*(1), pp.33-51.

Grahe, K., 1931. Experimental study of development of the nasal sinuses. *Acta Oto-Laryngologica*, *15*, p.141.

Grauer, D., Cevidanes, L. S., Styner, M. A., Ackerman, J. L., & Proffit, W. R.,2009. Pharyngeal airway volume and shape from cone-beam computed tomography: relationship to facial morphology. *American Journal of Orthodontics and Dentofacial Orthopedics*, 136(6), pp.805-814.

Gray, H., 2009. *Gray's anatomy: with original illustrations by Henry Carter*. 1st ed. London: Arcturus Publishing.

Gray, H. and Lewis, W.H., 2000. *Anatomy of the human body*. 20th ed. Philadelphia: Lea & Febiger.

Grine, F.E., 1981. Trophic differences between 'gracile' and 'robust' australopithecines: A scanning electron microscope analysis of occlusal events. *South African Journal of Science*, *77*(5), pp.203-230.

Grymer, L.F. and Bosch, C., 1997. The nasal septum and the development of the midface. A longitudinal study of a pair of monozygotic twins. *Rhinology*, *35*(1), pp.6-10.

Grymer, L.F., Hilberg, O., Pedersen, O.F. and Rasmussen, T.R., 1991. Acoustic rhinometry: values from adults with subjective normal nasal patency. *Rhinology*, *29*(1), pp.35-47.

Grymer, L.F., Pedersen, O.F., Hilberg, O. and Elbrønd, O., 1989. Acoustic rhinometry: evaluation of the nasal cavity with septal deviations, before and after septoplasty. *The Laryngoscope*, *99*(11), pp.1180-1187.

Gunz, P. and Mitteroecker, P., 2013. Semilandmarks: a method for quantifying curves and surfaces. *Hystrix, the Italian Journal of Mammalogy,* 24: 103–109.

Gunz, P., Mitteroecker, P. and Bookstein, F.L., 2005. Semilandmarks in three dimensions. In *Modern Morphometrics in Physical Anthropology*, pp. 73-98. Springer, Boston, MA.

Gunz, P., Mitteroecker, P., Neubauer, S., Weber, G.W. and Bookstein, F.L., 2009. Principles for the virtual reconstruction of hominin crania. *Journal of Human Evolution*, *57*(1), pp.48-62.

Gunz, P., Neubauer, S., Golovanova, L., Doronichev, V., Maureille, B., & Hublin, J. J., 2012. A uniquely modern human pattern of endocranial development. Insights from a new

cranial reconstruction of the Neandertal newborn from Mezmaiskaya. *Journal of human evolution*, *62*(2), 300-313.

Gunz, P., Neubauer, S., Maureille, B. and Hublin, J.J., 2010. Brain development after birth differs between Neanderthals and modern humans. *Current Biology*, *20*(21), pp.21-22.

Gupta, M., Agrawal, A., Veeraraghavan, A. and Narasimhan, S.G., 2011, June. Structured light 3D scanning in the presence of global illumination. In *CVPR 2011*, pp. 713-720.

Gupta, P., Tripathi, T., Singh, N., Bhutiani, N., Rai, P. and Gopal, R., 2020. A review of genetics of nasal development and morphological variation. *Journal of Family Medicine and Primary Care*, *9*(4), p.1825.

Hajeer, M.Y., Ayoub, A.F. and Millett, D.T., 2004. Three-dimensional assessment of facial soft-tissue asymmetry before and after orthognathic surgery. *British Journal of Oral and Maxillofacial Surgery*, *42*(5), pp.396-404.

Hall, B.K. and Precious, D.S., 2013. Cleft lip, nose, and palate: the nasal septum as the pacemaker for midfacial growth. *Oral surgery, oral medicine, oral pathology and oral radiology*, *115*(4), pp.442-447.

Hallgrimsson, B., Jamniczky, H., Young, N.M., Rolian, C., Parsons, T.E., Boughner, J.C. and Marcucio, R.S., 2009. Deciphering the palimpsest: studying the relationship between morphological integration and phenotypic covariation. *Evolutionary Biology*, *36*(4), pp.355-376.

Hallgrimsson, B., Lieberman, D.E., Liu, W., Ford-Hutchinson, A.F. and Jirik, F.R., 2007. Epigenetic interactions and the structure of phenotypic variation in the cranium. *Evolution & Development*, *9*(1), pp.76-91.

Hallgrimsson, B., Willmore, K., Dorval, C. and Cooper, D.M., 2004. Craniofacial variability and modularity in macaques and mice. *Journal of Experimental Zoology Part B: Molecular and Developmental Evolution*, 302(3), pp.207-225.

Harding, R. and Bocking, A.D. eds., 2001. *Fetal growth and development*. Cambridge: University Press.

Hartman, C., Holton, N., Miller, S., Yokley, T., Marshall, S., Srinivasan, S. and Southard, T., 2016. Nasal septal deviation and facial skeletal asymmetries. *The Anatomical Record: Advances in Integrative Anatomy and Evolutionary Biology*, 299(3), pp.295-306.

Harvati, K., 2010. Neanderthals. *Evolution: Education and Outreach*, *3*(3), pp.367-376.

Harvati-Papatheodorou, K., 2013. Neanderthals. In Begun, D. R. (ed.), *A Companion to Paleoanthropology*, pp.538-556. New Jersey: Wiley-Blackwell.

Heiland, M., Schulze, D., Rother, U. and Schmelzle, R., 2004. Postoperative imaging of zygomaticomaxillary complex fractures using digital volume tomography. *Journal of Oral and Maxillofacial Surgery*, *62*(11), pp.1387-1391.

Hein, G., Weiss, C., Lehmann, G., Niwa, T., Stein, G. and Franke, S., 2006. Advanced glycation end product modification of bone proteins and bone remodelling: hypothesis and preliminary immunohistochemical findings. *Annals of the Rheumatic Diseases*, *65*(1), pp.101-104.

Hendrikse, J.L., Parsons, T.E. and Hallgrímsson, B., 2007. Evolvability as the proper focus of evolutionary developmental biology. *Evolution & Development*, *9*(4), pp.393-401.

Herring, S.W., 2008. Mechanical influences on suture development and patency. In Rice, D.P (ed.) *Craniofacial sutures* (Vol. 12, pp. 41-56). London: Karger Publishers.

Heuzé, Y., Martínez-Abadías, N., Stella, J.M., Senders, C.W., Boyadjiev, S.A., Lo, L.J. and Richtsmeier, J.T., 2012. Unilateral and bilateral expression of a quantitative trait: asymmetry and symmetry in coronal craniosynostosis. J*ournal of Experimental Zoology Part B: Molecular and Developmental Evolution*, 318(2), pp.109-122.

Higham, T., Compton, T., Stringer, C., Jacobi, R., Shapiro, B., Trinkaus, E., Chandler, B., Gröning, F., Collins, C., Hillson, S. and O'Higgins, P., 2011. The earliest evidence for anatomically modern humans in northwestern Europe. *Nature*, *479*(7374), pp.521-524.

Highmore, N.,1961. *Corporis humani disquisitio anatomica*. 1st ed. Oxford: Broun.

Hollander, M., Wolfe, D.A. and Chicken, E., 2013. *Nonparametric statistical methods* (Vol. 751). John Wiley & Sons.

Holton, N.E. and Franciscus, R.G., 2008. The paradox of a wide nasal aperture in cold-adapted Neandertals: a causal assessment. *Journal of Human Evolution*, *55*(6), pp.942-951.

Holton, N.E., Franciscus, R.G., Marshall, S.D., Southard, T.E. and Nieves, M.A., 2011. Nasal septal and premaxillary developmental integration: implications for facial reduction in *Homo*. *The Anatomical Record: Advances in Integrative Anatomy and Evolutionary Biology*, *294*(1), pp.68-78.

Holton, N.E., Piche, A. and Yokley, T.R., 2018. Integration of the nasal complex: Implications for developmental and evolutionary change in modern humans. *American Journal of Physical Anthropology*, *166*(4), pp.791-802.

Holton, N.E., Yokley, T.R. and Butaric, L., 2013. The morphological interaction between the nasal cavity and maxillary sinuses in living humans. *The Anatomical Record: Advances in Integrative Anatomy and Evolutionary Biology*, *296*(3), pp.414-426.

Holton, N.E., Yokley, T.R. and Figueroa, A., 2012. Nasal septal and craniofacial form in European-and African-derived populations. *Journal of Anatomy*, *221*(3), pp.263-274.

Holton, N.E., Yokley, T.R. and Franciscus, R.G., 2011. Climatic adaptation and Neandertal facial evolution: A comment on Rae et al., 2011. *Journal of Human Evolution*, *5*(61), pp.624-627.

Honn, M. and Goz, G., 2007. Reference values for craniofacial structures in children 4 to 6 years old: review of the literature. *Journal of Orofacial and Orthopedics*, 68(3), pp.170-182.

Hounsfield, G.N., 1973. Computerized transverse axial scanning (tomography): Part 1. Description of system. *The British Journal of Radiology*, *46*(552), pp.1016-1022.

Howe, A.M., Hawkins, J.K. and Webster, W.S., 2004. The growth of the nasal septum in the 6–9 week period of foetal development—warfarin embryopathy offers a new insight into prenatal facial development. *Australian Dental Journal*, 49(4), pp.171-176.

Howerton Jr., W.B. and Mora, M.A., 2008. Advancements in digital imaging: what is new and on the horizon? *The Journal of the American Dental Association*, *139*, pp.S20-S24.

Hublin, J.J., Neubauer, S. and Gunz, P., 2015. Brain ontogeny and life history in Pleistocene hominins. *Philosophical Transactions of the Royal Society B: Biological Sciences*, *370*(1663), p.20140062.

Hunter, W.S., Baumrind, S. and Moyers, R.E., 1993. An inventory of United States and Canadian growth record sets: preliminary report. *American Journal of Orthodontics and Dentofacial Orthopedics*, 103(6), pp.545-555.

Hutton, T.J., Buxton, B.F., Hammond, P. and Potts, H.W., 2003. Estimating average growth trajectories in shape-space using kernel smoothing. *Transactions on Medical Imaging*, 22(6), pp.747-753.

Jeffery, N. and Spoor, F., 2004. Ossification and midline shape changes of the human fetal cranial base. *American Journal of Physical Anthropology*, *123*(1), pp.78-90.

Jiang, C., Yin, N., Zheng, Y. and Song, T., 2015. Characteristics of maxillary morphology in unilateral cleft lip and palate patients compared to normal subjects and skeletal class III patients. *Journal of Craniofacial Surgery*, 26(6), pp.e517-e523.

Jin, S.W., Sim, K.B. and Kim, S.D., 2016. Development and growth of the normal cranial vault: an embryologic review. *Journal of Korean Neurosurgical Society*, *59*(3), p.192.

Joe, B., 1991. Construction of three-dimensional Delaunay triangulations using local transformations. *Computer Aided Geometric Design*, 8(2), pp.123-142.

Jolliffe, I.T., 1986. *Principal Component Analysis*. 1st ed. New York: Springer.

Jung, R.E. and Haier, R.J., 2007. The Parieto-Frontal Integration Theory (P-FIT) of intelligence: converging neuroimaging evidence. *Behavioral and Brain Sciences*, *30*(2), p.135.

Karaplis, A.C., 2008. Embryonic development of bone and regulation of intramembranous and endochondral bone formation. In J. Bilezekian, L. Raisz and G. Rodan (ed.), *Principles of Bone Biology*, pp. 53-84. Cambridge: Academic Press.

Katina, S., Bookstein, F.L., Gunz, P. and Schaefer, K., 2007. Was it worth digitizing all those curves? A worked example from craniofacial primatology. *American Journal of Physical Anthropology*, *44*, p.140.

Katz, D. and Friess, M., 2014. 3D from standard digital photography of human crania—a preliminary assessment. *American Journal of Physical Anthropology*, *154*(1), pp.152-158.

Katz, S., Tal, A. and Basri, R., 2007. Direct visibility of point sets. *Transactions on Graphics*, 26(3), pp.24-es.

Kelley, P., Hopper, R. and Gruss, J., 2007. Evaluation and treatment of zygomatic fractures. *Plastic and Reconstructive Surgery*, *120*(7), pp.5S-15S.

Kendall, D.G., 1984. Shape manifolds, procrustean metrics, and complex projective spaces. *Bulletin of the London Mathematical Society*, *16*(2), pp.81-121.

Kent, J.T. and Mardia, K.V., 2001. Shape, Procrustes tangent projections and bilateral symmetry. *Biometrika*, *88*(2), pp.469-485.

Kiliaridis, S., Kjellberg, H., Wenneberg, B. and Engström, C., 1993. The relationship between maximal bite force, bite force endurance, and facial morphology during growth: A cross-sectional study. *Acta Odontologica Scandinavica*, *51*(5), pp.323-331.

Kim, H.J., Yoon, H.R., Kim, K.D., Kang, M.K., Kwak, H.H., Park, H.D., Han, S.H. and Park, C.S., 2002. Personal-computer-based three-dimensional reconstruction and simulation of maxillary sinus. *Surgical and Radiologic Anatomy*, *24*(6), pp.392-398.

Kim, I. S., Lee, M. Y., Lee, K. I., Kim, H. Y., & Chung, Y. J.,2008. Analysis of the development of the nasal septum according to age and gender using MRI. *Clinical and Experimental Otorhinolaryngology*, *1*(1), 29, pp.75-85.

Kim, Y.M., Rha, K.S., Weissman, J.D., Hwang, P.H. and Most, S.P., 2011. Correlation of asymmetric facial growth with deviated nasal septum. *The Laryngoscope*, *121*(6), pp.1144-1148.

Klingenberg, C.P., 2008. Morphological integration and developmental modularity. *Annual Review of Ecology, Evolution, and Systematics*, 39, pp.115-132.

Klingenberg, C.P., 2009. Morphometric integration and modularity in configurations of landmarks: tools for evaluating a priori hypotheses. *Evolution & Development*, *11*(4), pp.405-421.

Klingenberg, C.P., 2013. Cranial integration and modularity: insights into evolution and development from morphometric data. *Hystrix, the Italian Journal of Mammalogy*, *24*(1), pp.43-58.

Klingenberg, C.P., 2016. Size, shape, and form: concepts of allometry in geometric morphometrics. *Development Genes and Evolution*, *226*(3), pp.113-137.

Klingenberg, C.P. and Marugán-Lobón, J., 2013. Evolutionary covariation in geometric morphometric data: analyzing integration, modularity, and allometry in a phylogenetic context. *Systematic Biology*, *62*(4), pp.591-610.

Klingenberg, C.P. and Zaklan, S.D., 2000. Morphological integration between developmental compartments in the Drosophila wing. *Evolution*, *54*(4), pp.1273-1285.

Kohn, L.A.P., Leigh, S.R., Jacobs, S.C. and Cheverud, J.M., 1993. Effects of annular cranial vault modification on the cranial base and face. *American Journal of Physical Anthropology*, *90*(2), pp.147-168.

Kopher, R.A. and Mao, J.J., 2003. Suture growth modulated by the oscillatory component of micromechanical strain. *Journal of Bone and Mineral Research*, *18*(3), pp.521-528.

Koppe, T., Nagai, H. and Alt, K.W., 1999. The paranasal sinuses of higher primates. *Berlin: Quintessence*.

Koski, K., 1968. Cranial growth centers: Facts or fallacies? *American Journal of Orthodontics*, *54*(8), pp.566-583.

Krennmair, G., Ulm, C. and Lugmayr, H., 1997. Maxillary sinus septa: incidence, morphology and clinical implications. *Journal of Cranio-Maxillofacial Surgery*, *25*(5), pp.261-265.

Krimmel, M., Breidt, M., Bacher, M., Müller-Hagedorn, S., Dietz, K., Bülthoff, H., Reinert, S. and Kluba, S., 2015. Three-dimensional normal facial growth from birth to the age of 7 years. *Plastic and Reconstructive Surgery*, *136*(4), pp.490e-501e.

Krovitz, G.E., 2003. Shape and growth differences between Neandertals and modern humans: grounds for a species-level distinction?. *Cambridge Studies in Biological and Evolutionary Anthropology*, pp.320-342.

Kuroe, K., Rosas, A. and Molleson, T., 2004. Variation in the cranial base orientation and facial skeleton in dry skulls sampled from three major populations. *The European Journal of Orthodontics*, *26*(2), pp.201-207.

Kuykendall, K.L. and Rae, T.C., 2008. Presence of the maxillary sinus in fossil Colobinae (Cercopithecoides williamsi) from South Africa. *The Anatomical Record: Advances in Integrative Anatomy and Evolutionary Biology*, *291*(11), pp.1499-1505.

Kvinnsland, S., 1974. Partial resection of the cartilaginous nasal septum in rats; its influence on growth. *The Angle Orthodontist*, *44*(2), pp.135-140.

Lacruz, R.S., Bromage, T.G., O'Higgins, P., Arsuaga, J.L., Stringer, C., Godinho, R.M., Warshaw, J., Martínez, I., Gracia-Tellez, A., De Castro, J.M.B. and Carbonell, E., 2015. Ontogeny of the maxilla in Neanderthals and their ancestors. *Nature Communications*, *6*(1), pp.1-6.

Lacruz, R.S., Stringer, C.B., Kimbel, W.H., Wood, B., Harvati, K., O'Higgins, P., Bromage, T.G. and Arsuaga, J.L., 2019. The evolutionary history of the human face. *Nature Ecology & Evolution*, *3*(5), pp.726-736.

Landes, C.A., Bitsakis, J., Diehl, T. and Bitter, K., 2002. Introduction of a three-dimensional anthropometry of the viscerocranium. Part I: measurement of craniofacial development and establishment of standard values and growth functions. *Journal of Cranio-Maxillofacial Surgery*, 30(1), pp.18-24.

Latham, R.A., 1970. Maxillary development and growth: the septo-premaxillary ligament. *Journal of Anatomy*, 107(Pt 3), p.471.

Latham, R.A. and Burston, W.R., 1964. The effect of unilateral cleft of the lip and palate on maxillary growth pattern. *British Journal of Plastic Surgery*, *17*, pp.10-17.

Latham, R.A. and Burston, W.R., 1966. The postnatal pattern of growth at the sutures of the human skull. A histological survey. *The Dental Practitioner and Dental Record*, *17*(2), p.61.

Lawson, W., Patel, Z.M. and Lin, F.Y., 2008. The development and pathologic processes that influence maxillary sinus pneumatization. *The Anatomical Record: Advances in Integrative Anatomy and Evolutionary Biology*, *291*(11), pp.1554-1563.

Lele, S.R. and Richtsmeier, J.T., 1991. Euclidean distance matrix analysis: A coordinate-free approach for comparing biological shapes using landmark data. *American Journal of Physical Anthropology*, *86*(3), pp.415-427.

Lele, S.R. and Richtsmeier, J.T., 2001. *An invariant approach to statistical analysis of shapes*. 1st ed. Philadelphia: CRC Press.

Levine, R.A., Garza, J.R., Wang, P.T., Hurst, C.L. and Dev, V.R., 2003. Adult facial growth: applications to aesthetic surgery. *Aesthetic Plastic Surgery*, 27(4), pp.265-268.

Liao, Y.F., Huang, C.S., Liou, J.W., Lin, W.Y. and Ko, W.C., 1998. Premaxillary size and craniofacial growth in patients with cleft lip and palate. *Changgeng Yi Xue Za Zhi*, 21(4), pp.391-396.

Lieberman, D.E., 1998. Sphenoid shortening and the evolution of modern human cranial shape. *Nature*, *393*(6681), pp.158-162.

Lieberman, D.E., 2008. Speculations about the selective basis for modern human craniofacial form. *Evolutionary Anthropology: Issues, News, and Reviews*, *17*(1), pp.55-68.

Lieberman, D.E., 2011. *The evolution of the human head*. 1st ed. Cambridge: Harvard University Press.

Lieberman, D.E., Hallgrímsson, B., Liu, W., Parsons, T.E. and Jamniczky, H.A., 2008. Spatial packing, cranial base angulation, and craniofacial shape variation in the mammalian skull: testing a new model using mice. *Journal of Anatomy*, *212*(6), pp.720-735.

Lieberman, D.E., Krovitz, G.E. and McBratney-Owen, B., 2004. Testing hypotheses about tinkering in the fossil record: the case of the human skull. *Journal of Experimental Zoology Part B: Molecular and Developmental Evolution*, *302*(3), pp.284-301.

Lieberman, D.E., McBratney, B.M. and Krovitz, G., 2002. The evolution and development of cranial form in *Homo sapiens*. *Proceedings of the National Academy of Sciences*, *99*(3), pp.1134-1139.

Lieberman, D.E., Pearson, O.M. and Mowbray, K.M., 2000. Basicranial influence on overall cranial shape. *Journal of Human Evolution*, *38*(2), pp.291-315.

Likus, W., Bajor, G., Gruszczyńska, K., Baron, J., Markowski, J., Machnikowska-Sokołowska, M., Milka, D. and Lepich, T., 2014. Cephalic index in the first three years of life: study of children with normal brain development based on computed tomography. *The Scientific World Journal*, *2014*.

Lorkiewicz-Muszyńska, D., Kociemba, W., Rewekant, A., Sroka, A., Jończyk-Potoczna, K., Patelska-Banaszewska, M. and Przystańska, A., 2015. Development of the maxillary sinus from birth to age 18. Postnatal growth pattern. *International Journal of Pediatric Otorhinolaryngology*, *79*(9), pp.1393-1400.

Luhmann, T., Robson, S., Kyle, S. and Harley, I., 2007. *Close range photogrammetry*. 1st ed. Hoboken: Wiley.

Maddux, S.D. and Butaric, L.N., 2017. Zygomaticomaxillary Morphology and Maxillary Sinus Form and Function: How Spatial Constraints Influence Pneumatization Patterns among Modern Humans. *The Anatomical Record: Advances in Integrative Anatomy and Evolutionary Biology*, *300*(1), pp.209-225.

Mah, P., Reeves, T.E. and McDavid, W.D., 2010. Deriving Hounsfield units using grey levels in cone beam computed tomography. *Dentomaxillofacial Radiology*, *39*(6), pp.323-335.

Makedonska, J., 2014. New insights into the phenotypic covariance structure of the anthropoid cranium. *Journal of anatomy*, *225*(6), pp.634-658.

Mansoor, A., Bagci, U., Foster, B., Xu, Z., Papadakis, G.Z., Folio, L.R., Udupa, J.K. and Mollura, D.J., 2015. Segmentation and image analysis of abnormal lungs at CT: current approaches, challenges, and future trends. *RadioGraphics*, *35*(4), pp.1056-1076.

Marcus, L.F. and Corti, M., 1996. Overview of the new, or geometric morphometrics. In *Advances in morphometrics*, pp. 1-13. Springer, Boston, MA.

Mardia, K.V., Kent. J.T and Bibby, J. M., 1979. *Multivariate Analysis*. 1st ed. New York: Academic Press.

Marroig, G., Shirai, L.T., Porto, A., de Oliveira, F.B. and De Conto, V., 2009. The evolution of modularity in the mammalian skull II: evolutionary consequences. *Evolutionary Biology*, 36(1), pp.136-148.

Marquez, E.J., 2008. A statistical framework for testing modularity in multidimensional data. *Evolution: International Journal of Organic Evolution*, *62*(10), pp.2688-2708.

Marquez, S., 2008. The paranasal sinuses: the last frontier in craniofacial biology. *The Anatomical Record: Advances in Integrative Anatomy and Evolutionary Biology*, *291*(11), pp.1350-1361.

Marquez, S., Gannon, P.J., Lawson, W., Reidenberg, J.S. and Laitman, J.T., 2002, January. Were Neanderthals full of" NO" gas? The relationship between paranasal sinus morphology and nitric oxide production. In *American Journal of Physical Anthropology*, pp. 107-107.

Márquez, S., Pagano, A.S., Delson, E., Lawson, W. and Laitman, J.T., 2014. The nasal complex of Neanderthals: an entry portal to their place in human ancestry. *The Anatomical Record: Advances in Integrative Anatomy and Evolutionary Biology*, *297*(11), pp.2121-2137.

Martínez-Abadías, N., Esparza, M., Sjøvold, T., González-José, R., Santos, M. and Hernández, M., 2009. Heritability of human cranial dimensions: comparing the evolvability of different cranial regions. *Journal of Anatomy*, *214*(1), pp.19-35.

Martínez-Abadías, N., Esparza, M., Sjøvold, T., González-José, R., Santos, M., Hernández, M. and Klingenberg, C.P., 2012. Pervasive genetic integration directs the evolution of human skull shape. *Evolution: International Journal of Organic Evolution*, *66*(4), pp.1010-1023.

Martínez-Abadías, N., Heuzé, Y., Wang, Y., Jabs, E.W., Aldridge, K. and Richtsmeier, J.T., 2011. FGF/FGFR signaling coordinates skull development by modulating magnitude of morphological integration: evidence from Apert syndrome mouse models. *PLoS One*, *6*(10), pp.1-9.

Martín-González, J.A., Mateos, A., Goikoetxea, I., Leonard, W.R. and Rodríguez, J., 2012. Differences between Neandertal and modern human infant and child growth models. *Journal of Human Evolution*, *63*(1), pp.140-149.

Mavrodi, A. and Paraskevas, G., 2013. Evolution of the paranasal sinuses' anatomy through the ages. *Anatomy & Cell Biology*, *46*(4), pp.235-238.

Mays, S., 2012. Nasal septal deviation in a mediaeval population. *American Journal of Physical Anthropology*, *148*(3), pp.319-326.

McCarthy, R.C., 2001. Anthropoid cranial base architecture and scaling relationships. *Journal of Human Evolution*, *40*(1), pp.41-66.

McCarthy, R. C., 2004. *Constraints on primate craniofacial growth and architecture*. 1st ed. Washington: The George Washington University.

McCollum, M.A., 1999. The robust australopithecine face: a morphogenetic perspective. *Science*, 284(5412), pp.301-305.

McIntosh, A.R., Bookstein, F.L., Haxby, J.V. and Grady, C.L., 1996. Spatial pattern analysis of functional brain images using partial least squares. *Neuroimage*, *3*(3), pp.143-157.

McPherron, S.P., Gernat, T. and Hublin, J.J., 2009. Structured light scanning for high-resolution documentation of in situ archaeological finds. *Journal of Archaeological Science*, *36*(1), pp.19-24.

McLaughlin, C.R., 1949. Absence of the septal cartilage with retarded nasal development. *British Journal of Plastic Surgery*, 2(1), pp.61-64.

Meehan, M., Teschner, M. and Girod, S., 2003. Three-dimensional simulation and prediction of craniofacial surgery. *Orthodontics & Craniofacial Research*, *6*, pp.102-107.

Mehra, P. and Murad, H., 2004. Maxillary sinus disease of odontogenic origin. *Otolaryngologic Clinics of North America*, *37*(2), pp.347-364.

Mellion, Z.J., Behrents, R.G. and Johnston Jr, L.E., 2013. The pattern of facial skeletal growth and its relationship to various common indexes of maturation. *American Journal of Orthodontics and Dentofacial Orthopedics*, 143(6), pp.845-854.

Mettler Jr, F.A., Wiest, P.W., Locken, J.A. and Kelsey, C.A., 2000. CT scanning: patterns of use and dose. *Journal of Radiological Protection*, *20*(4), p.353.

Mitchell, R.J., 2001. Path analysis. D*esign and Analysis of Ecological Experiments*. Oxford University Press, Oxford, UK, pp.217-234.

Mitteroecker, P. and Bookstein, F., 2008. The evolutionary role of modularity and integration in the hominoid cranium. *Evolution: International Journal of Organic Evolution*, *62*(4), pp.943-958.

Mitteroecker, P. and Gunz, P., 2009. Advances in geometric morphometrics. *Evolutionary Biology*, *36*(2), pp.235-247.

Mitteroecker, P., Gunz, P., Bernhard, M., Schaefer, K. and Bookstein, F.L., 2004. Comparison of cranial ontogenetic trajectories among great apes and humans. *Journal of Human Evolution*, *46*(6), pp.679-698.

Mitteroecker, P., Gunz, P., Windhager, S. and Schaefer, K., 2013. A brief review of shape, form, and allometry in geometric morphometrics, with applications to human facial morphology. *Hystrix, the Italian Journal of Mammalogy*, *24*(1), pp.59-66.

Mondin, V., Rinaldo, A. and Ferlito, A., 2005. Management of nasal bone fractures. *American Journal of Otolaryngology*, 26(3), pp.181-185.

Mooney, M.P., Siegel, M.I., Kimes, K.R. and Todhunter, J., 1989. A test of two midfacial growth models using path analysis of normal human fetal material. *The Cleft Palate Journal*, *26*(2), pp.93-9.

Moss, M.L., 1968. A theoretical analysis of the functional matrix. *Acta Biotheoretica*, *18*(1-4), pp.195-202.

Moss, M.L., 1997. The functional matrix hypothesis revisited. 4. The epigenetic antithesis and the resolving synthesis. *American Journal of Orthodontics and Dentofacial Orthopedics*, *112*(4), pp.410-417.

Moss, M.L. and Salentijn, L., 1969. The primary role of functional matrices in facial growth. *American Journal of Orthodontics*, 55(6), pp.566-577.

Moss, M.L. and Young, R.W., 1960. A functional approach to craniology. *American Journal of Physical Anthropology*, *18*(4), pp.281-292.

Moss, M.L., Bromberg, B.E., Song, I.G. and Eisenman, G., 1968. The passive role of nasal septal cartilage in mid-facial growth. *Plastic and Reconstructive Surgery*, *41*(6), pp.536-542.

Mowbray, K., 2005. Surface bone histology of the occipital bone in humans and chimpanzees. *The Anatomical Record: Advances in Integrative Anatomy and Evolutionary Biology Part B: The New Anatomist: An Official Publication of the American Association of Anatomists*, *283*(1), pp.14-22.

Musumeci, G., Castrogiovanni, P., Coleman, R., Szychlinska, M.A., Salvatorelli, L., Parenti, R., Magro, G. and Imbesi, R., 2015. Somitogenesis: From somite to skeletal muscle. *Acta Histochemica*, *117*(4-5), pp.313-328.

Nahhas, R.W., Valiathan, M. and Sherwood, R.J., 2014. Variation in timing, duration, intensity, and direction of adolescent growth in the mandible, maxilla, and cranial base: The Fels longitudinal study. *The Anatomical Record: Advances in Integrative Anatomy and Evolutionary Biology*, *297*(7), pp.1195-1207.

Neaux, D., Gilissen, E., Coudyzer, W. and Guy, F., 2015. Implications of the relationship between basicranial flexion and facial orientation for the evolution of hominid craniofacial structures. *International Journal of Primatology*, *36*(6), pp.1120-1131.

Neaux, D., Guy, F., Gilissen, E., Coudyzer, W. and Ducrocq, S., 2013. Covariation between midline cranial base, lateral basicranium, and face in modern humans and chimpanzees: a 3D geometric morphometric analysis. *The Anatomical Record: Advances in Integrative Anatomy and Evolutionary Biology*, *296*(4), pp.568-579.

Neeser, R., Ackermann, R.R. and Gain, J., 2009. Comparing the accuracy and precision of three techniques used for estimating missing landmarks when reconstructing fossil hominin crania. *American Journal of Physical Anthropology*, *140*(1), pp.1-18.

Negus, S.V., 1957. The function of the paranasal sinuses. *AMA Archives of Otolaryngology*, *66*(4), pp.430-442.

Negus, V.E. and Street, H., 1954. The function of the paranasal sinuses. *Acta Oto-Laryngologica*, *44*(5-6), pp.408-426.

Neubauer, S., Gunz, P. and Hublin, J.J., 2009. The pattern of endocranial ontogenetic shape changes in humans. *Journal of Anatomy*, *215*(3), pp.240-255.

Nicolae, C., Nocerino, E., Menna, F. and Remondino, F., 2014. Photogrammetry applied to problematic artefacts. *The International Archives of Photogrammetry, Remote Sensing and Spatial Information Sciences*, *40*(5), p.451.

Nie, X., 2005. Cranial base in craniofacial development: developmental features, influence on facial growth, anomaly, and molecular basis. *Acta Odontologica Scandinavica*, *63*(3), pp.127-135.

Nikitiuk, D.B., 1983. Forms and factors of the variability of paranasal sinuses. *Arkhiv Anatomii, Gistologii i Embriologii*, 85(9), pp.60-67.

Niven, L., Steele, T.E., Finke, H., Gernat, T. and Hublin, J.J., 2009. Virtual skeletons: using a structured light scanner to create a 3D faunal comparative collection. *Journal of Archaeological Science*, *36*(9), pp.2018-2023.

Noback, M.L., Harvati, K. and Spoor, F., 2011. Climate-related variation of the human nasal cavity. *American journal of physical anthropology*, *145*(4), pp.599-614.

Nuñez-Castruita, A., López-Serna, N. and Guzmán-López, S., 2012. Prenatal development of the maxillary sinus: a perspective for paranasal sinus surgery. *Otolaryngology-Head and Neck Surgery*, *146*(6), pp.997-1003.

O'Connor, C.F., Franciscus, R.G. and Holton, N.E., 2005. Bite force production capability and efficiency in Neandertals and modern humans. *American Journal of Physical Anthropology*, *127*(2), pp.129-151.

O'Higgins, P., 1997. Methodological issues in the description of forms. *Fourier Descriptors and Their Applications in Biology*, pp.74-105.

O'Higgins, P., 2000. The study of morphological variation in the hominid fossil record: biology, landmarks and geometry. *The Journal of Anatomy*, *197*(1), pp.103-120.

O'Higgins, P., and Cohn, M.J., 2000. Development, Growth and Evolution. Implications for the study of the Hominid Skeleton. *Linnean Society Symposium Series*, (vol 20, pp. 271).

O'Higgins, P. and Dryden, I.L., 1992. Studies of craniofacial development and evolution. *Archaeology in Oceania*, *27*(3), pp.105-112.

O'Higgins, P. and Dryden, I.L., 1993. Sexual dimorphism in hominoids: further studies of craniofacial shape differences in Pan, Gorilla and Pongo. *Journal of Human Evolution*, *24*(3), pp.183-205.

O'Higgins, P., Bastir, M. and Kupczik, K., 2006. Shaping the human face. *International Congress Series* (Vol. 1296, pp. 55-73).

O'Higgins, P., Weber, G.W., Baverstock, H., Proa, M., Dunn, J. and Fornai, C., 2012. *Manuals for the EVAN Toolbox*. Vienna: University of Vienna Press.

Olsen, A., 2014. Bezier: Bezier Curve and Spline Toolkit. *R Package Version*, *1*.

Olson, E.C. and Miller, R.L., 1999. *Morphological integration*. 1st ed. Chicago: University of Chicago Press.

Opperman, L.A., 2000. Cranial sutures as intramembranous bone growth sites. *Developmental dynamics: an official publication of the American Association of Anatomists*, *219*(4), pp.472-485.

Opperman, L.A., Gakunga, P.T. and Carlson, D.S., 2005, December. Genetic factors influencing morphogenesis and growth of sutures and synchondroses in the craniofacial complex. *Seminars in Orthodontics*, Vol. 11 (4), pp.199-208.

Pajares, F. and Miller, M.D., 1994. Role of self-efficacy and self-concept beliefs in mathematical problem solving: A path analysis. *Journal of Educational Psychology*, *86*(2), pp.193.

Paoloni, V., Lione, R., Farisco, F., Halazonetis, D.J., Franchi, L. and Cozza, P., 2017. Morphometric covariation between palatal shape and skeletal pattern in class II growing subjects. E*uropean Journal of Orthodontics*, 39(4), pp.371-376.

Pilbeam, D. and Gould, S.J., 1974. Size and scaling in human evolution. *Science*, *186*(4167), pp.892-901.

Piras, P., Profico, A., Pandolfi, L., Raia, P., Di Vincenzo, F., Mondanaro, A., Castiglione, S. and Varano, V., 2020. Current options for visualization of local deformation in modern shape analysis applied to paleobiological case studies. *Frontiers in Earth Science*, *8*, pp.66.

Pirinen, S., 1995. Endocrine regulation of craniofacial growth. *Acta Odontologica Scandinavica*, *53*(3), pp.179-185.

Pirinen, S., Majurin, A., Lenko, H.L. and Koski, K., 1994. Craniofacial features in patients with deficient and excessive growth hormone. *Journal of Craniofacial Genetics and Developmental Biology*, *14*(3), pp.144-152.

Ponce de Leon, M.S.P. and Zollikofer, C.P., 2001. Neanderthal cranial ontogeny and its implications for late hominid diversity. *Nature*, *412*(6846), pp.534-538.

Ponce de Leon, M.S.P., Golovanova, L., Doronichev, V., Romanova, G., Akazawa, T., Kondo, O., Ishida, H. and Zollikofer, C.P., 2008. Neanderthal brain size at birth provides insights into the evolution of human life history. *Proceedings of the National Academy of Sciences*, 105(37), pp.13764-13768.

Pool, C., Shokri, T., Vincent, A., Wang, W., Kadakia, S. and Ducic, Y., 2020, May. Prosthetic Reconstruction of the Maxilla and Palate. In *Seminars in Plastic Surgery,* Vol. 34(2), pp. 114-119. New York: Thieme Medical Publishers.

Porto, A., de Oliveira, F.B., Shirai, L.T., De Conto, V. and Marroig, G., 2009. The evolution of modularity in the mammalian skull I: morphological integration patterns and magnitudes. *Evolutionary Biology*, 36(1), pp.118-135.

Porto, A., Shirai, L.T., de Oliveira, F.B. and Marroig, G., 2013. Size variation, growth strategies, and the evolution of modularity in the mammalian skull. *Evolution*, *67*(11), pp.3305-3322.

Precious, D. and Delaire, J., 1987. Balanced facial growth: a schematic interpretation. *Oral Surgery, Oral Medicine, Oral Pathology*, *63*(6), pp.637-644.

Profico, A., Bellucci, L., Buzi, C., Di Vincenzo, F., Micarelli, I., Strani, F., Tafuri, M.A. and Manzi, G., 2019. Virtual anthropology and its application in cultural heritage studies. *Studies in Conservation*, *64*(6), pp.323-336.

Profico, A., Piras, P., Buzi, C., Di Vincenzo, F., Lattarini, F., Melchionna, M., Veneziano, A., Raia, P. and Manzi, G., 2017. The evolution of cranial base and face in Cercopithecoidea and Hominoidea: Modularity and morphological integration. *American Journal of Primatology*, *79*(12), p.22721.

Profico, A., Schlager, S., Valoriani, V., Buzi, C., Melchionna, M., Veneziano, A., Raia, P., Moggi-Cecchi, J. and Manzi, G., 2018. Reproducing the internal and external anatomy of fossil bones: Two new automatic digital tools. *American Journal of Physical Anthropology*, *166*(4), pp.979-986.

Profico, A., Veneziano, A., Melchionna, M., Piras, P. and Raia, P., 2015. Arothron: R functions for geometric morphometrics analyses. *R Package Version*, *314*(1.0).

Pujol, A., Rissech, C., Ventura, J. and Turbón, D., 2016. Ontogeny of the male femur: Geometric morphometric analysis applied to a contemporary Spanish population. *American Journal of Physical Anthropology*, *159*(1), pp.146-163.

Pun, T., 1980. A new method for grey-level picture thresholding using the entropy of the histogram. *Signal processing*, *2*(3), pp.223-237.

R Core Team, 2019. *RStudio: integrated development for R*. Boston. Available at http://www. rstudio. com.

Radlanski, R. J., and Renz, H., 2006. Genes, forces, and forms: mechanical aspects of prenatal craniofacial development. *Developmental dynamics: an official publication of the American Association of Anatomists*, *235*(5), pp.1219-1229.

Radulesco, T., Michel, J., Mancini, J., Dessi, P. and Adalian, P., 2018. Sex estimation from human cranium: forensic and anthropological interest of maxillary sinus volumes. *Journal of Forensic Sciences*, 63(3), pp.805-808.

Rae, T.C., 2008. Paranasal pneumatization in extant and fossil Cercopithecoidea. *Journal of Human Evolution*, *54*(3), pp.279-286.

Rae, T.C. and Koppe, T., 2000. Isometric scaling of maxillary sinus volume in hominoids. *Journal of Human Evolution*, *38*(3), pp.411-423.

Rae, T.C. and Koppe, T., 2004. Holes in the head: evolutionary interpretations of the paranasal sinuses in catarrhines. *Evolutionary Anthropology: Issues, News, and Reviews: Issues, News, and Reviews*, *13*(6), pp.211-223.

Rae, T.C., Hill, R.A., Hamada, Y. and Koppe, T., 2003. Clinal variation of maxillary sinus volume in Japanese macaques (*Macaca fuscata*). *American Journal of Primatology*, *59*(4), pp.153-158.

Rae, T.C., Koppe, T. and Stringer, C.B., 2011a. The Neanderthal face is not cold adapted. *Journal of Human Evolution*, *60*(2), pp.234-239.

Rae, T.C., Koppe, T. and Stringer, C.B., 2011b. Hyperpneumatized Neanderthals? Reply to Holton et al., 2011. *Journal of Human Evolution*, *61*(5), pp.628-629.

Raff, R.A., 2012. *The shape of life: genes, development, and the evolution of animal form*. 1st ed. Chicago: University of Chicago Press.

Rak, Y., 1986. The Neanderthal: a new look at an old face. *Journal of Human Evolution*, *15*(3), pp.151-164.

Rak, Y., 2014. *The australopithecine face*. 1st ed. New York: Academic Press.

Ramanojam, S., Halli, R., Hebbale, M. and Bhardwaj, S., 2013. Ectopic tooth in maxillary sinus: case series. *Annals of Maxillofacial Surgery*, *3*(1), p.89.

Ravosa, M.J., 1988. Browridge development in Cercopithecidae: a test of two models. *American Journal of Physical Anthropology*, 76(4), pp.535-555.

Razi, T., Niknami, M. and Ghazani, F.A., 2014. Relationship between Hounsfield unit in CT scan and gray scale in CBCT. *Journal of Dental Research, Dental Clinics, Dental Prospects*, *8*(2), pp.107.

Rengier, F., Mehndiratta, A., Von Tengg-Kobligk, H., Zechmann, C.M., Unterhinninghofen, R., Kauczor, H.U. and Giesel, F.L., 2010. 3D printing based on imaging data: review of

medical applications. *International Journal of Computer Assisted Radiology and Surgery*, *5*(4), pp.335-341.

Rhoton Jr, A.L., 2002. The anterior and middle cranial base. *Neurosurgery*, *51*, pp.1-273.

Ricciardelli, E.J., 1995. Embryology and anatomy of the cranial base. *Clinics in Plastic Surgery*, *22*(3), pp.361-372.

Rice, D.P., 2008. *Craniofacial Sutures: Development, Disease and Treatment*. 1st ed. Basel: Karger Medical and Scientific Publishers.

Richtsmeier, J.T., Aldridge, K., DeLeon, V.B., Panchal, J., Kane, A.A., Marsh, J.L., Yan, P. and Cole III, T.M., 2006. Phenotypic integration of neurocranium and brain. *Journal of Experimental Zoology Part B: Molecular and Developmental Evolution*, *306*(4), pp.360-378.

Richtsmeier, J.T. and De Leon, V.B., 2009. Morphological integration of the skull in craniofacial anomalies. *Orthodontics & Craniofacial Research*, *12*(3), pp.149-158.

Richtsmeier, J.T. and Flaherty, K., 2013. Hand in glove: brain and skull in development and dysmorphogenesis. *Acta Neuropathologica*, *125*(4), pp.469-489.

Richtsmeier, J.T., Cheverud, J.M. and Lele, S., 1992. Advances in anthropological morphometrics. *Annual Review of Anthropology*, *21*(1), pp.283-305.

Richtsmeier, J.T., Cheverud, J.M., Danahey, S.E., Corner, B.D. and Lele, S., 1993a. Sexual dimorphism of ontogeny in the crab-eating macaque (*Macaca fascicularis*). *Journal of Human Evolution*, *25*(1), pp.1-30.

Richtsmeier, J.T., Corner, B.D., Grausz, H.M., Cheverud, J.M. and Danahey, S.E., 1993b. The role of postnatal growth pattern in the production of facial morphology. *Systematic Biology*, *42*(3), pp.307-330.

Riolo, M.L., 1974. *An atlas of craniofacial growth: cephalometric standards from the University School Growth Study, the University of Michigan*. Michigan: University of Michigan Press.

Ripamonti, U., Richter, P.W., Nilen, R.W.N. and Renton, L., 2008. The induction of bone formation by smart biphasic hydroxyapatite tricalcium phosphate biomimetic matrices in the non-human primate *Papio ursinus*. *Journal of Cellular and Molecular Medicine*, *12*(6b), pp.2609-2621.

Ritman, E.L., 2002. Molecular imaging in small animals—roles for micro-CT. *Journal of Cellular Biochemistry*, *87*(S39), pp.116-124.

Robinson, J.T., 1954. Prehominid dentition and hominid evolution. *Evolution*, *8*(4), pp.324-334.

Robinson, H.E., Zerlin, G.K. and Passy, V., 1982. Maxillary sinus development in patients with cleft palates as compared to those with normal palates. *The Laryngoscope*, *92*(2), pp.183-187.

Rohlf, F.J., 1999. Shape statistics: Procrustes superimpositions and tangent spaces. *Journal of Classification*, *16*(2), pp.197-223.

Rohlf, F.J., 2000. On the use of shape spaces to compare morphometric methods. *Hystrix: the Italian Journal of Mammalogy*, 11(1).

Rohlf, F.J. and Marcus, L.F., 1993. A revolution in morphometrics. *Trends in Ecology & Evolution*, *8*(4), pp.129-132.

Rohlf, F.J. and Slice, D., 1990. Extensions of the Procrustes method for the optimal superimposition of landmarks. *Systematic Biology*, *39*(1), pp.40-59.

Rohrich, R.J., Love, E.J., Byrd, H.S. and Johns, D.F., 2000. Optimal timing of cleft palate closure. *Plastic and Reconstructive Surgery*, 106(2), pp.413-421.

Rolian, C., 2014. Genes, development, and evolvability in primate evolution. *Evolutionary Anthropology: Issues, News, and Reviews*, 23(3), pp.93-104.

Rosano, G., Taschieri, S., Gaudy, J.F., Lesmes, D. and Del Fabbro, M., 2010. Maxillary sinus septa: a cadaveric study. *Journal of Oral and Maxillofacial Surgery*, 68(6), pp.1360-1364.
Roth, V.L. and Mercer, J.M., 2000. Morphometrics in development and evolution. *American Zoologist*, *40*(5), pp.801-810.

Rosas, A. and Bastir, M., 2002. Thin-plate spline analysis of allometry and sexual dimorphism in the human craniofacial complex. *American Journal of Physical Anthropology*, 117(3), pp.236-245.

Rosas, A. and Martinez-Maza, C., 2010. Bone remodeling of the *Homo heidelbergensis* mandible; the Atapuerca-SH sample. *Journal of Human Evolution*, 58(2), pp.127-137.

Roseman, C. C., Weaver, T. D., & Stringer, C. B., 2011. Do modern humans and Neandertals have different patterns of cranial integration? *Journal of Human Evolution*, *60*(6), 684-693.

Ross, C. and Henneberg, M., 1995. Basicranial flexion, relative brain size, and facial kyphosis in *Homo sapiens* and some fossil hominids. *American Journal of Physical Anthropology*, *98*(4), pp.575-593.

Ross, C.F. and Ravosa, M.J., 1993. Basicranial flexion, relative brain size, and facial kyphosis in nonhuman primates. *American Journal of Physical Anthropology*, *91*(3), pp.305-324.

Ross, C.F., Henneberg, M., Ravosa, M.J. and Richard, S., 2004. Curvilinear, geometric and phylogenetic modeling of basicranial flexion: is it adaptive, is it constrained? *Journal of Human Evolution*, 46(2), pp.185-213.

Rozzi, F.V.R. and De Castro, J.M.B., 2004. Surprisingly rapid growth in Neanderthals. *Nature*, *428*(6986), pp.936-939.

Rudasill, K.M. and Rimm-Kaufman, S.E., 2009. Teacher–child relationship quality: The roles of child temperament and teacher–child interactions. *Early Childhood Research Quarterly*, 24(2), pp.107-120.

Ryan, K.G., Auerbach, B. and Butaric, L., 2019. Modularity and Integration of the Sphenoid Body in Human Cranial Variation: The Confluence of Functional Matrices. *The FASEB Journal,* 33(1_supplement), pp.612-20.

Sadler J., 2018. C*apturing morphology*. Master thesis (unpublished), Hull York Medical School York (UK).

Sahin, G., Klimek, L., Mullol, J., Hörmann, K., Walther, L.E. and Pfaar, O., 2011. Nitric oxide: a promising methodological approach in airway diseases. *International Archives of Allergy and Immunology*, *156*(4), pp.352-361.

Sahni, D. and Jit, I., 2005. Time of closure of cranial sutures in northwest Indian adults. *Forensic Science International*, *148*(2-3), pp.199-205.

Sandikcioglu, M., Mølsted, K. and Kjær, I., 1994. The prenatal development of the human nasal and vomeral bones. *Journal of Craniofacial Genetics and Developmental Biology*, *14*(2), pp.124-134.

Sapirstein, P., 2016. Accurate measurement with photogrammetry at large sites. *Journal of Archaeological Science*, *66*, pp.137-145.

Sardi, M.L. and Rozzi, F.V.R., 2012. Different cranial ontogeny in Europeans and Southern Africans. *PLoS One*, *7*(4), p.e35917.

Sardi, M.L., Ventrice, F. and Ramírez Rozzi, F., 2007. Allometries throughout the late prenatal and early postnatal human craniofacial ontogeny. *The Anatomical Record: Advances in Integrative Anatomy and Evolutionary Biology*, 290(9), pp.1112-1120.

Sarnat, B.G., 1982. Eye and orbital size in the young and adult. *Ophthalmologica*, 185(2), pp.74-89.

Schlager, S., 2017. Morpho and Rvcg–Shape Analysis in R: R-Packages for geometric morphometrics, shape analysis and surface manipulations. In Zheng, G., Li, S., Szekely, G., (ed.), *Statistical Shape and Deformation Analysis*, pp. 217-256. Cambridge: Academic Press.

Schmidle, G., Rieger, M., Klauser, A.S., Thauerer, M., Hoermann, R. and Gabl, M., 2014. Intraosseous rotation of the scaphoid: assessment by using a 3D CT model—an anatomic study. *European Radiology*, *24*(6), pp.1357-1365.

Schultz, A.H., 1942. Conditions for balancing the head in primates. *American Journal of Physical Anthropology*, *29*(4), pp.483-497.

Scott, J.H., 1954. The growth of the human face. *Proceedings of the Royal Society of Medicine*, 47(2), 91-100.

Scott, J.H., 1956. Growth at facial sutures. *American Journal of Orthodontics*, *42*(5), pp.381-387.

Scott, J.H., 1962. The growth of the cranio-facial skeleton. *Irish Journal of Medical Science*, *37*(6), pp.276-286.

Scuderi, A.J., Harnsberger, H.R. and Boyer, R.S., 1993. Pneumatization of the paranasal sinuses: normal features of importance to the accurate interpretation of CT scans and MR images. *American Journal of Roentgenology*, *160*(5), pp.1101-1104.

Shapiro, G.G., Furukawa, C.T., Pierson, W.E., Gilbertson, E. and Bierman, C.W., 1986. Blinded comparison of maxillary sinus radiography and ultrasound for diagnosis of sinusitis. *Journal of Allergy and Clinical Immunology*, *77*(1), pp.59-64.

Sharan, A. and Madjar, D., 2008. Maxillary sinus pneumatization following extractions: a radiographic study. *International Journal of Oral & Maxillofacial Implants*, *23*(1), pp.48-56.

Shea, B.T., 1977. Eskimo craniofacial morphology, cold stress and the maxillary sinus. *American Journal of Physical Anthropology*, *47*(2), pp.289-300.

Shea, J.J., 1936. Morphologic characteristics of the sinuses. *Archives of Otolaryngology*, *23*(4), pp.484-487.

Sicher, H. and DuBrul, L.E., 1949. *Oral Anatomy*. 1st ed. Maryland Heights: Mosby Co. St. Louis.

Siegel, M.I. and Sadler, D., 1981. Nasal septum resection and craniofacial growth in a chimpanzee animal model: implications for cleft palate surgery. *Plastic and Reconstructive Surgery*, 68(6), pp.849-853.

Sijbers, J. and Postnov, A., 2004. Reduction of ring artefacts in high-resolution micro-CT reconstructions. *Physics in Medicine & Biology*, *49*(14), pp.247-253.

Silveira, A.M., Fishman, L.S., Subtelny, J.D. and Kassebaum, D.K., 1992. Facial growth during adolescence in early, average and late maturers. *The Angle Orthodontist*, 62(3), pp.185-190.

Singh, G.D., Levy-Bercowski, D. and Santiago, P.E., 2005. Three-dimensional nasal changes following nasoalveolar molding in patients with unilateral cleft lip and palate: geometric morphometrics. *The Cleft Palate-Craniofacial Journal*, *42*(4), pp.403-409.

Singh, N., Harvati, K., Hublin, J.J. and Klingenberg, C.P., 2012. Morphological evolution through integration: a quantitative study of cranial integration in *Homo, Pan, Gorilla and Pongo*. *Journal of Human Evolution*, *62*(1), pp.155-164.

Sistiaga, A., Mallol, C., Galván, B. and Summons, R.E., 2014. The Neanderthal meal: a new perspective using faecal biomarkers. *PloS one*, *9*(6), pp.10145.

Slice, D.E., 2007. Geometric morphometrics. *Annual Review of Anthropology*, *36(271),* pp. 261-281.

Slizewski, A. and Semal, P., 2009. Experiences with low and high cost 3D surface scanner. *Quartär*, *56(1)*, pp.131-138.

Smith, A.S., Estroff, J.A., Barnewolt, C.E., Mulliken, J.B. and Levine, D., 2004. Prenatal diagnosis of cleft lip and cleft palate using MRI. *American Journal of Roentgenology*, 183(1), pp.229-235.

Smith, H.F., 2009. Which cranial regions reflect molecular distances reliably in humans? Evidence from three-dimensional morphology. *American Journal of Human Biology*, *21*(1), pp.36-47.

Smith, M.W., Carrivick, J.L. and Quincey, D.J., 2016. Structure from motion photogrammetry in physical geography. *Progress in Physical Geography*, *40*(2), pp.247-275.

Smith, T.M., Toussaint, M., Reid, D.J., Olejniczak, A.J. and Hublin, J.J., 2007. Rapid dental development in a middle Paleolithic Belgian Neanderthal. *Proceedings of the National Academy of Sciences*, 104(51), pp.20220-20225.

Sneath, P.H. and Sokal, R.R., 1962. Numerical taxonomy. *Nature*, *193*(4818), pp.855-860.

Sokal, R.R., 1958. Quantification of systematic relationships and of phylogenetic trends. *Proceedings of the Tenth International Congress of Entomology*, *1*, pp.409-415.

Spassov, A., Toro-Ibacache, V., Krautwald, M., Brinkmeier, H. and Kupczik, K., 2017. Congenital muscle dystrophy and diet consistency affect mouse skull shape differently. *Journal of Anatomy*, *231*(5), pp.736-748.

Sperber, G.H., Sperber, S.M. and Guttmann, G.D., 2010. *Craniofacial embryogenetics and development*. 2nd ed. Raleigh: PMPH-USA.

Spoor, C.F., Zonneveld, F.W. and Macho, G.A., 1993. Linear measurements of cortical bone and dental enamel by computed tomography: applications and problems. *American Journal of Physical Anthropology*, *91*(4), pp.469-484.

Stage, F.K., Carter, H.C. and Nora, A., 2004. Path analysis: An introduction and analysis of a decade of research. *The Journal of Educational Research*, 98(1), pp.5-13.

Strauss, R.E. and Bookstein, F.L., 1982. The truss: body form reconstructions in morphometrics. *Systematic Biology*, *31*(2), pp.113-135.

Streiner, D.L., 2005. Finding our way: an introduction to path analysis. *The Canadian Journal of Psychiatry*, 50(2), pp.115-122.

Stringer, C., 2002. Modern human origins: progress and prospects. *Philosophical Transactions of the Royal Society of London. Series B: Biological Sciences*, 357(1420), pp.563-579.

Stringer, C.B., Hublin, J.J. and Vandermeersch, B., 1984. The origin of anatomically modern humans in Western Europe. *The Origins of Modern Humans: a World Survey of the Fossil Evidence*, pp.51-135.

Sun, Z., 2007. Multislice CT angiography in abdominal aortic aneurysm treated with endovascular stent grafts: evaluation of 2D and 3D visualisations. *Biomedical Imaging and Intervention Journal*, *3*(4), pp.20-30.

Sun, Z., Lee, E. and Herring, S.W., 2004. Cranial sutures and bones: growth and fusion in relation to masticatory strain. *The Anatomical Record: Advances in Integrative Anatomy and Evolutionary Biology Part A: Discoveries in Molecular, Cellular, and Evolutionary Biology: An Official Publication of the American Association of Anatomists*, *276*(2), pp.150-161.

Sutton, M., Rahman, I. and Garwood, R., 2016. Virtual palaeontology—an overview. *The Paleontological Society Papers*, *22(1)*, pp.1-20.

Suwa, G., 1989. The premolar of KNM-WT 17000 and relative anterior to posterior dental size. *Journal of Human Evolution*, *18*(8), pp.795-799.

Tallman, M., 2016. Shape Ontogeny of the Distal Femur in the Hominidae with Implications for the Evolution of Bipedality. *PloS One*, 11(2), pp. e0148371.

Thiagarajan, B. and Ulaganathan, V., 2013. Fracture nasal bones. *Otolaryngology Online Journal*, *3*(1.5), pp.1-16.

Thompson, J.A., 1917. *On growth and form.* 1st ed. Cambridge: Cambridge University Press.

Tillier, A.M., 1995. Neanderthal ontogeny: A new source for critical analysis. *Anthropologie (1962-)*, pp.63-68.

Toennies, K.D., 2017. *Guide to medical image analysis*. 1st ed. London: Springer London.

Toro-Ibacache, V., Muñoz, V.Z. and O'Higgins, P., 2016. The relationship between skull morphology, masticatory muscle force and cranial skeletal deformation during biting. *Annals of Anatomy-Anatomischer Anzeiger*, 203, pp.59-68.

Trinkaus, E., 1987. The Neandertal face: evolutionary and functional perspectives on a recent hominid face. *Journal of Human Evolution*, *16*(5), pp.429-443.

Trinkaus, E., Athreya, S., Churchill, S., Demeter, F., Henneberg, M., Kondo, O., Manzi, G., Maureille, B. and Trinkaus, E., 2006. Modern human versus Neanderthal evolutionary distinctiveness. *Current Anthropology*, 47(4), pp.597-620.

Tzou, C.H.J. and Frey, M., 2011. Evolution of 3D surface imaging systems in facial plastic surgery. *Facial Plastic Surgery Clinics*, *19*(4), pp.591-602.

Underwood, A.S., 1910. An inquiry into the anatomy and pathology of the maxillary sinus. *Journal of Anatomy and Physiology*, *44*(Pt 4), p.354.

Van Der Straeten, C., 2013. The use of magnetic resonance imaging (MRI) to evaluate hip resurfacing. In De Smet, Campbell, Van Der Straeten (ed.), *The Hip Resurfacing Handbook*, pp. 242-252. Cambridge: Woodhead Publishing.

Van, J.L., Van, G.Z., Howard, C.V., Verwoerd-Verhoef, H.L., Van, D.V. and Verwoerd, C.D., 1996. Growth characteristics of the human nasal septum. *Rhinology*, *34*(2), pp.78-82.

Verhoeven, G., 2011. Taking computer vision aloft–archaeological three-dimensional reconstructions from aerial photographs with photoscan. *Archaeological prospection*, *18*(1), pp.67-73.

Verwoerd, C.D. and Verwoerd-Verhoef, H.L., 2007. Rhinosurgery in children: basic concepts. *Facial Plastic Surgery*, *23*(04), pp.219-230.

Vetter, U., Helbing, G., Pirsig, W., Heinze, E., Gammert, C. and Landolt, A., 1985. Human nasal septal cartilage: local distribution of different enzyme activities in healthy adults and acromegalic patients. *The Laryngoscope*, *95*(4), pp.469-473.

Vetter, U., Pirsig, W. and Heinze, E., 1984. Postnatal growth of the human septal cartilage: preliminary report. *Acta Oto-Laryngologica*, 97(1-2), pp.131-136.

Viðarsdóttir, U.S. and Cobb, S., 2004. Inter-and intra-specific variation in the ontogeny of the hominoid facial skeleton: testing assumptions of ontogenetic variability. *Annals of Anatomy, 186*(5-6), pp.423-428.

Viðarsdóttir, U.S., O'Higgins, P. and Stringer, C., 2002. A geometric morphometric study of regional differences in the ontogeny of the modern human facial skeleton. *Journal of Anatomy*, *201*(3), pp.211-229.

Villmoare, B.A., Dunmore, C., Kilpatrick, S., Oertelt, N., Depew, M.J. and Fish, J.L., 2014. Craniofacial modularity, character analysis, and the evolution of the premaxilla in early African hominins. *Journal of Human Evolution*, *77*, pp.143-154.

Von Cramon-Taubadel, N. and Smith, H.F., 2012. The relative congruence of cranial and genetic estimates of hominoid taxon relationships: Implications for the reconstruction of hominin phylogeny. *Journal of Human Evolution*, *62*(5), pp.640-653.

Von Cramon-Taubadel, N., Frazier, B.C. and Lahr, M.M., 2007. The problem of assessing landmark error in geometric morphometrics: theory, methods, and modifications. *American Journal of Physical Anthropology*, *134*(1), pp.24-35.

Wagner, G.P., Pavlicev, M. and Cheverud, J.M., 2007. The road to modularity. *Nature Reviews Genetics*, 8(12), pp.921-931.

Wallace, J.A., Barrett, M.J., Brown, T., Brace, C.L., Howells, W.W., Koritzer, R.T., Sakura, H., Stloukal, M., Wolpoff, M.H. and Žlábek, K., 1975. Did La Ferrassie I use his teeth as a tool?[and comments and reply]. *Current Anthropology*, *16*(3), pp.393-401.

Wang, Q., Wright, B.W., Smith, A., Chalk, J. and Byron, C.D., 2010. Mechanical impact of incisor loading on the primate midfacial skeleton and its relevance to human evolution. *The Anatomical Record: Advances in Integrative Anatomy and Evolutionary Biology, 293*(4), pp.607-617.

Weaver, T.D., 2009. The meaning of Neandertal skeletal morphology. *Proceedings of the National Academy of Sciences*, *106*(38), pp.16028-16033.

Weaver, T.D., Roseman, C.C. and Stringer, C.B., 2007. Were neandertal and modern human cranial differences produced by natural selection or genetic drift? *Journal of Human Evolution*, *53*(2), pp.135-145.

Weber, G.W., 2014. Another link between archaeology and anthropology: virtual anthropology. *Digital Applications in Archaeology and Cultural Heritage*, *1*(1), pp.3-11.

Weber, G.W. and Bookstein, F.L., 2011. *Virtual anthropology: a guide to a new interdisciplinary field.* 1st ed. Vienna: Springer.

Weickenmeier, J., Fischer, C., Carter, D., Kuhl, E. and Goriely, A., 2017. Dimensional, geometrical, and physical constraints in skull growth. *Physical Review Letters*, *118*(24), pp.248101.

Wexler, M.R. and Sarnat, B.G., 1965. Rabbit snout growth after dislocation of nasal septum. *Archives of Otolaryngology*, *81*(1), pp.68-71.

Whitbeck, M. and Guo, H., 2006. Multiple Landmark Warping Using Thin-plate Splines. *Image Processing and Computer Vision*, *6*, pp.256-263.

Wilderman, A., VanOudenhove, J., Kron, J., Noonan, J.P. and Cotney, J., 2018. High-resolution epigenomic atlas of human embryonic craniofacial development. *Cell Reports*, *23*(5), pp.1581-1597.

Willekens, I., Buls, N., Lahoutte, T., Baeyens, L., Vanhove, C., Caveliers, V., Deklerck, R., Bossuyt, A. and de Mey, J., 2010. Evaluation of the radiation dose in micro-CT with optimization of the scan protocol. *Contrast Media & Molecular Imaging*, *5*(4), pp.201-207.

Williams, R., 2015. *Intro to path analysis*. Paris: University of Notre Dame.

Wilson, D. B. (1979). Embryonic development of the head and neck: part 3, the face. *Head & Neck Surgery*, 2(2), pp.145-153.

Wong, K.K., Filatov, S. and Kibblewhite, D.J., 2010. Septoplasty retards midfacial growth in a rabbit model. *The Laryngoscope*, *120*(3), pp.450-453.

Wright, S., 1921. Outlined the theory of path analysis on the basis of standardized partial regression analysis. *Annals of Mathematical Statistics*, *5*, pp.161-215.

Wright, S., 1934. The method of path coefficients. *The Annals of Mathematical Statistics*, 5(3), pp.161-215.

Wroe, S., Parr, W.C., Ledogar, J.A., Bourke, J., Evans, S.P., Fiorenza, L., Benazzi, S., Hublin, J.J., Stringer, C., Kullmer, O. and Curry, M., 2018. Computer simulations show that Neanderthal facial morphology represents adaptation to cold and high energy demands, but not heavy biting. *Proceedings of the Royal Society B: Biological Sciences*, *285*(1876), pp.20180085.

Yokley, T.R., 2006. *The functional and adaptive significance of anatomical variation in recent and fossil human nasal passages*. Doctoral dissertation, Duke University, North Carolina.

Young, W.F., 1960. The Influence of Growth of the Teeth and Nasal System on Growth of the Face. *Transactions of the European Orthodontic Society*, 36, pp.385-388.

Zarrinkelk, H.M., Throckmorton, G.S., Ellis III, E. and Sinn, D.P., 1995. A longitudinal study of changes in masticatory performance of patients undergoing orthognathic surgery. *Journal of Oral and Maxillofacial Surgery*, *53*(7), pp.777-782.

Zelditch, M.L., 1987. Evaluating models of developmental integration in the laboratory rat using confirmatory factor analysis. *Systematic Zoology*, *36*(4), pp.368-380.

Zelditch, M.L., Swiderski, D.L. and Sheets, H.D., 2012. *Geometric morphometrics for biologists: a primer*. 1st ed. New York: Academic Press.

Zelop, C.M., Milewski, E., Brault, K., Benn, P., Borgida, A.F. and Egan, J.F., 2005. Variation of fetal nasal bone length in second-trimester fetuses according to race and ethnicity. *Journal of Ultrasound in Medicine*, *24*(11), pp.1487-1489.

Zollikofer, C.P. and DeLeón, M.S.P., 2002. Visualizing patterns of craniofacial shape variation in *Homo sapiens*. *Proceedings of the Royal Society of London. Series B: Biological Sciences*, *269*(1493), pp.801-807.

Zollikofer, C.P. and De Leon, M.S.P., 2010. The evolution of hominin ontogenies. *Seminars in Cell & Developmental Biology* (Vol. 21, No. 4, pp. 441-452).

Zollikofer, C.P., De Leon, M.S.P., Schmitz, R.W. and Stringer, C.B., 2008. New insights into mid-late Pleistocene fossil hominin paranasal sinus morphology. *The Anatomical Record: Advances in Integrative Anatomy and Evolutionary Biology*, *291*(11), pp.1506-1516.

Zollikofer, C.P., Bienvenu, T. and De Leon, M.S.P., 2017. Effects of cranial integration on hominid endocranial shape. *Journal of Anatomy*, *230*(1), pp.85-105.

Zuckerkandl, E., Lichtwitz, L. and Garnault, P., 1895. *Anatomie normale et pathologique des fosses nasales*. 1st ed. Paris: Masson.